הטכניון מכון טכנולוגי לישראל
הפקולטה להנדסה אוירונוטית

TECHNION Israel Institute of Technology
Department of Aeronautical Engineering

(NASA-CR-163934) ACTIVE CONTROLS FOR FLUTTER SUPPRESSION AND GUST ALLEVIATION IN SUPERSONIC AIRCRAFT Final Report (Technion - Israel Inst. of Tech.) 269 p HC A12/MF A01 CSCL 01C G3/08 N81-17097 Unclas 41353

ACTIVE CONTROLS FOR FLUTTER SUPPRESSION AND GUST ALLEVIATION IN SUPERSONIC AIRCRAFT

by

E. NISSIM

FINAL REPORT
(1977-1980)
GRANT NSG-7373

November 1980

ACTIVE CONTROLS FOR FLUTTER SUPPRESSION AND GUST ALLEVIATION IN SUPERSONIC AIRCRAFT

E. NISSIM

Department of Aeronautical Engineering

Technion - Israel Institute of Technology

Haifa, Israel

FINAL REPORT

GRANT NSG 7373 monitored by Mr. I. Abel of NASA,

Langley Research Center

General Outline of the Report

Most of the results pertaining to the work performed under the above grant had already been published. The list of these publications is given in the following (copies of which are included in the present report):

1) Nissim, E. and Lottati, I.: Active Controls for Flutter Suppression and Gust Alleviation in Supersonic Aircraft. Journal of Guidance and Control, Vol. 3, No. 4, July - Aug. 1980.
2) Nissim, E. and Lottati, I.: On Single-Degree-of Freedom Flutter Induced by Active Controls. Journal of Guidance and Control, Vol. 2, No. 4, Sept.-Oct. 1979.
3) Nissim, E.: Flutter Suppression and Gust Alleviation Using Active Controls - Review of Developments and Applications Based on the Aerodynamic Energy Concept. Proceedings of the XI Congress of the International Council of the Aeronautical Sciences, Sept. 1978.

There is no intention in the present report to repeat results appearing in the above-mentioned publications

During the course of the grant, its scope had been extended to cover some work done on active controls on the modified YF-17 flutter model. The results of this effort are summarized in two attached reports. The first report relates to the basic derivation of a suitable control law. The second report relates to the discrepencies found between analysis and wind tunnel tests and shows that they originate from the lack of proper implementation of the desired control law. These reports which are attached herein are the following:

ARTICLE NO. 79-0792R

Active Controls for Flutter Suppression and Gust Alleviation in Supersonic Aircraft

E. Nissim* and I. Lottati†
Technion—Israel Institute of Technology, Haifa, Israel

Application is made in the present paper of the recently developed relaxed aerodynamic energy concept and synthesis techniques to the definition of appropriate active control systems for the low-speed flutter model of the B-2707-300 supersonic cruise airplane. The effectiveness of the resulting activated systems is analytically tested for flutter suppression, wing root bending moment alleviation, and ride control (fuselage accelerations). The results obtained indicate that considerable increase in flutter speeds can be obtained by the various control systems, using a single trailing-edge control. In all cases, the flutter suppression control system led to a substantial reduction in both wing root bending moments and in fuselage and wing accelerations.

Introduction

THEORETICAL analyses and wind tunnel tests of a low-speed flutter model (1/20 scale) of the B-2707-300 airplane (Fig 1), were conducted under the supersonic transport (SST) Follow-on Program—Phase II.[1] Reference 1 states that "two constraints of the airplane made a flutter-free design unusually difficult: 1) the relatively low payload/total weight ratio made additional structural weight or mass balance particularly distasteful, and 2) any arrangement of lifting surface planforms, thickness, or major mass relocation (e.g., nacelles) degraded the delicate cruise economy or c.g. balance." Because of this flutter dilemma, considerable efforts were directed towards the development of an active flutter suppression system with the objective of improving the flutter speeds of the SST airplane.

Reference 1 shows that the developed flutter suppression system yields only minor improvements in flutter speeds (9.4% increase with activated inboard ailerons, 3.2% increase with activated outboard ailerons, and 11.3% increase with activated inboard and outboard ailerons). The purpose of the present work is to apply the recently developed relaxed energy concept[2] and synthesis techniques[3] to the definition of an appropriate active control system for flutter suppression. The effectiveness of the resulting activated system is then analytically tested for flutter suppression, root bending moment alleviation, and ride control (fuselage and wing accelerations).

Previous analytical applications of the relaxed energy concept for flutter suppression involved the BQM-34E/F drone aircraft[3,4] (with a research supercritical wing) and the YF-17 fighter aircraft[5] (suppression of three different configurations of wing store flutter). The present work supplements the applications to include supersonic type cruise aircraft and is also the first one to investigate the effectiveness of the flutter suppression system (as obtained through the use of the relaxed energy concept), not only for flutter suppression but also for gust alleviation and ride control.

Description of SST Model and Mathematical Representation

Description of the SST Model

Figure 1 shows the general layout of the B-2707-300 low-speed flutter model. As can be seen it is possible to activate the two trailing-edge (t.e.) ailerons and the horizontal stabilizer. In Ref. 1, activation of the two ailerons was attempted for purpose of flutter suppression and activation of the horizontal stabilizer (with geared elevator) was attempted for purpose of rigid-body stability augmentation. In the present work, activation of the outboard aileron only will be attempted. This follows the results of a previous investigation[6] which showed that for flutter suppression, the activated system should be located as near the tip of the wing as possible. The outboard aileron measures 13.4% of the wing semi-span and 26% of the wing chord. Its mid-span line is located around 72% of the wing semi-span.

Equations of Motion and Their Solution

The equations of motion are formulated and solved (for both flutter suppression and gust alleviation problems) following identical lines as outlined in Refs. 3-5, 7. The flutter results are presented by root locus type plots taking the dynamic pressure Q_D as a parameter. The gust alleviation and ride control results are obtained from a continuous gust program, using unit rms gust input based on a Von Kármán gust spectrum.

Control Law

The general form of the control law employed in this work was established in Ref 2 using the relaxed energy approach.

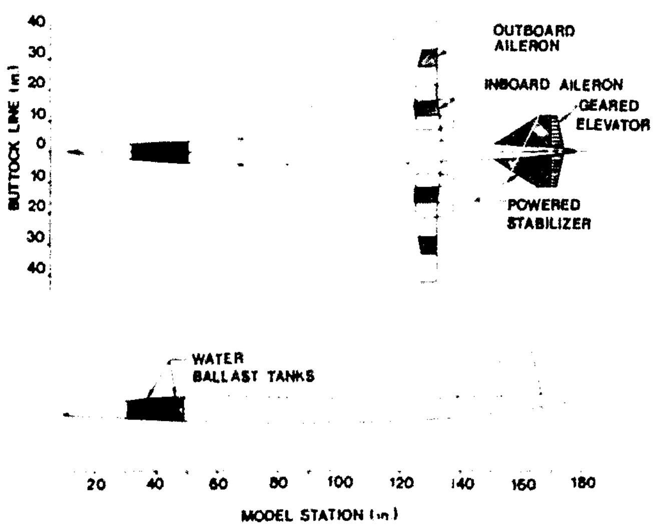

Presented as Paper 79-0792 at the AIAA/ASME 20th Structures and Structural Dynamics Conference, St. Louis, Mo., April 4-6, 1979; submitted April 26, 1979; revision received Sept. 5, 1979.

Index categories: Guidance and Control; Structural Design; Aeroelasticity and Hydroelasticity.

*Professor, Dept. of Aeronautical Engineering. Member AIAA.

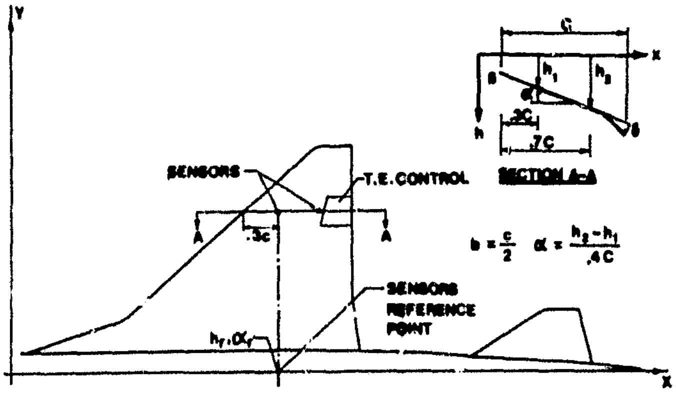

Fig. 2 Geometrical description of the active control system.

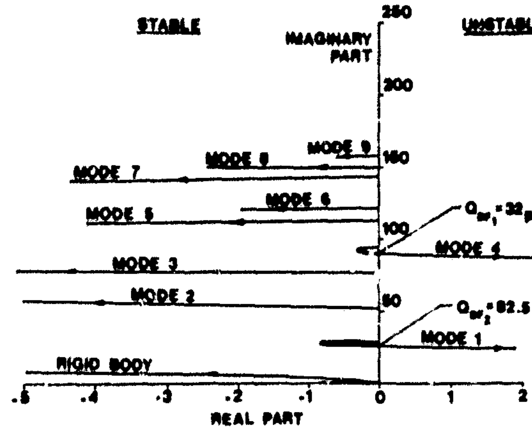

Fig. 3 Open-loop root locus plot at $M = 0.2$.

The control law for the t.e. control surface is given by the following general form:

$$\delta = -1.86(\alpha_l - \alpha_r) + R_T \lfloor 4 \quad 2.8 \rfloor \begin{Bmatrix} \dfrac{h_l - h_r}{b} \\ \alpha_l - \alpha_r \end{Bmatrix} \tag{1}$$

where δ is the deflection of the t.e. control surface (see Fig. 2) and where h_l, α_l denote the translation and rotation of the 30% chord point of the control surface mid-span section, respectively (see Fig. 2). The parameters h_r and α_r similarly denote the translation and rotation of a reference point located along the center line of the fuselage and b denotes the semi-chord length at the control surface mid-span section (see Fig. 5). R_T is defined by the following expression (see also Refs. 2, 3):

$$R_T = \frac{a_1 S^2}{S^2 + 2\zeta_1 \omega_{n_1} S + \omega_{n_1}^2} + \frac{a_2 S^2}{S^2 + 2\zeta_2 \omega_{n_2} S + \omega_{n_2}^2} \tag{2}$$

The parameters α_i, ζ_i, ω_{n_i} are all positive and their values determined by an optimization program based on the gust response of the aircraft under consideration following the method of Ref. 3.

Mathematical Model

The equations of motion, included two rigid-body modes (plunge and pitch) and nine symmetric elastic modes. The generalized aerodynamic forces were computed using the Doublet-Lattice method. The generalized inertia and elastic matrices for the flutter model were supplied by the aircraft manufacturing company together with the mode shapes. The t.e. control was assumed to be mass balanced.

Objectives

The following objectives were set for the present work:

1) To define control systems for different values of assumed maximum flight dynamic pressure (with $M = 0.2$) to determine whether an upper bound exists for flutter speed (while activating a single t.e. control).

2) To check the effectiveness of the resulting flutter suppression systems in reducing the wing root bending moments (b.m.) and in reducing the accelerations of the aircraft due to continuous gust inputs.

3) To spot check the effectiveness for flutter suppression of a control system, as defined in objective 1, above, at a higher Mach number, such as $M = 0.9$.

Presentation and Discussion of Results

The presentation and discussion of results will be grouped under three major headings involving flutter suppression, gust alleviation and ride control characteristics.

Flutter Suppression Systems

The effectiveness of the activated t.e. control system can only be assessed by comparison with the open-loop system. The open-loop root locus plots for $M = 0.2$ and $M = 0.9$ are presented in Figs. 3 and 4. It can be seen that for $M = 0.2$, two flutter dynamic pressures (Q_{DF}) exist: the first with $Q_{DF} = 32$ psf (for zero structural damping g) and $\omega_F = 89.7$ rad/s, and the second with $Q_{DF} = 82.5$ psf (for $g = 0$) and $\omega_F = 25.1$ rad/s. Similarly, for $M = 0.9$, three flutter speeds exist with the following values (for $g = 0$): $Q_{DF} = 33$ psf with $\omega_F = 81.8$ rad/s, $Q_{DF} = 74.5$ psf with $\omega_F = 21.8$ rad/s, and $Q_{DF} = 78.5$ psf with $\omega_F = 68.7$ rad/s. Since some of the above flutter branches represent mild flutter instabilities the values of Q_{DF} for the cases where $g = 0.015$ and $g = 0.03$ are included in a summarizing table (Table 1). It is interesting to note that the lowest value of Q_{DF} increases from $Q_{DF} = 32$ psf at $M = 0.2$ and $g = 0$ to $Q_{DF} = 51$ psf at $M = 0.2$ and $g = 0.03$. For $M = 0.9$ the corresponding values of Q_{DF} vary from $Q_{DF} = 33$ psf when $g = 0$ to $Q_{DF} = 37$ psf when $g = 0.03$, thus indicating the existence of a more violent flutter.

Determination of the Control Law Parameters

The control law parameters are determined through the use of an optimization program which minimizes the root mean square rms deflection rates of the control surface due to a unit rms gust input based on the Von Kármán gust spectrum. This procedure is described in detail in Ref. 3.

The optimization was performed at two different flight dynamic pressures: at $Q_D = 75$ psf and at $Q_D = 89$ psf, while maintaining $M = 0.2$. The optimization procedure yields the following optimal control laws:

For $Q_D = 75$ psf

$$\delta = \left[\lfloor 0 \quad -1.86 \rfloor + \left(\frac{0.5S^2}{S^2 + 2 \times 1 \times 34.4S + (34.4)^2} + \frac{3.33S^2}{S^2 + 2 \times 0.5 \times 100.6S + (100.6)^2} \right) \lfloor 4 \quad 2.8 \rfloor \right] \cdot \begin{Bmatrix} \dfrac{h_l - h_r}{b} \\ \alpha_l - \alpha_r \end{Bmatrix} \tag{3}$$

with

$\dot{\delta}_{rms} = 14.37$ deg/s/ft/s

$\delta_{rms} = 0.236$ deg/ft/s

Table 1 Summary of flutter results

	Open-loop		Closed-loop control law I		Closed-loop control law II
	$M=0.2$	$M=0.9$	$M=0.2$	$M=0.9$	$M=0.2$
Flutter Q_D, psf					
$g=0$	32	33	84 (163%)[a]	76 (130%)[a]	89 (178%)[a]
$g=0.015$	42	35	88 (110%)[a]	77 (120%)[a]	91 (117%)[a]
$g=0.03$	51	37	91 (78%)[a]	78 (110%)[a]	94 (84%)[a]
Max. value[b] of δ_{rms}, deg/s/fT/s					
$g=0$		...	14.37	10.90	23.81
$g=0.015$	...	...	11.89	10.54	18.72
$g=0.03$		...	10.92	10.24	16.17
Max. value[b] of δ_{rms}, deg/ft/s					
$g=0$	...		0.236	0.262	0.789
$g=0.015$		...	0.200	0.248	0.609
$g=0.03$		...	0.186	0.238	0.515

[a] % increase in Q_D due to activation of the outboard t.e. control.
[b] Up to dynamic pressure of Q_D optimization.

For $Q_D = 89$ psf

$$\delta = \left\{ \begin{bmatrix} 0 & 1.86 \end{bmatrix} + \left(\frac{0.8S^2}{S^2 + 2\times 0.5\times 20S + (20)^2} + \frac{1.62S^2}{S^2 + 2\times 0.5\times 100S + (100)^2} \right) \begin{bmatrix} 4 & 2.8 \end{bmatrix} \right\} \cdot \begin{Bmatrix} \dfrac{h_1 - h_2}{b} \\ \alpha_1 - \alpha_2 \end{Bmatrix} \tag{4}$$

with

$\delta_{rms} = 23.81$ deg/s/ft/s

$\delta_{rms} = 0.789$ deg/ft/s

ORIGINAL PAGE IS
OF POOR QUALITY

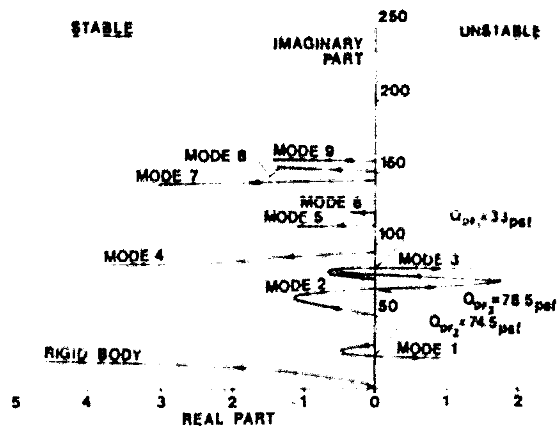

Fig. 4 Open-loop root locus plot at $M=0.9$.

The control law given by Eq. (3) will be referred to as control law I, whereas the one given by Eq. (4) will be referred to as control law II. The meaning of the different parameters of the control laws, Eqs. (3) and (4), is explained in Refs. 2 and 3. There is no intention to repeat the various details herein except for the statement that the above results show that for minimum control rates, maximum damping is introduced around the frequency of 100 rad/s whereas the minimum flutter frequency is around 90 rad/s. A secondary damping concentration is introduced by the above control laws at frequencies which vary with the optimization Q_D. For $Q_D = 75$ psf the frequency is around 34 rad/s whereas for $Q_D = 89$ psf the frequency is around 20 rad/s. Both frequencies relating to the secondary damping concentration are in the neighborhood of the frequency relating to the second open-loop flutter branch located around 25 rad/s.

Closed-Loop Performance

The effectiveness of the above control laws in flutter suppression at $M = 0.2$ is shown in Figs. 5 and 6. As can be seen, the flutter branch relating to $Q_{DF} = 32$ psf and $\omega = 89.7$ rad/s (for the open-loop case) is suppressed and yields no flutter up to the maximum dynamic pressure used for the root locus plots (that is up to $Q_D = 120$ psf). On the other hand, the flutter branch associated with the open-loop values of $Q_{DF} = 82.5$ psf and $\omega = 25.1$ rad/s is only slightly affected by the activated t.e. system. For control law I, the value of Q_{DF} associated with this branch is increased to $Q_{DF} = 84$ psf and for control law II to $Q_{DF} = 89$ psf (with $g = 0$ in both cases). The attempts to increase the values of this flutter branch beyond $Q_{DF} = 90$ psf were not successful. This result is interesting since the relaxed energy approach does not ensure the suppression of flutter in all cases, due to the fact that it does not turn all the aerodynamic energy eigenvalue positive (in the case of the activated t.e. alone system). For a l.e.-t.e. system the suppression of flutter is ensured since all the aerodynamic energy eigenvalues assume positive values. Table 1 supplements the abovementioned results to include the effects of structural damping on the flutter speeds.

If we disregard the increase in flutter speed of each flutter branch and view the overall increase in flutter speed of the SST model, we arrive at the following conclusions: 1) the largest increase in flutter speed is for $g = 0$, yielding an increase of 67%, whereas the smallest increase in flutter speed is for $g = 0.03$, yielding an increase of 33%. 2) The variation of the overall flutter speed of the system with the dynamic pressure at which the optimization of the control parameters is performed is very small. This is illustrated in Fig. 7 where it can also be seen that the maximum flutter dynamic pressure is obtained when Q_{DF} is equal to the value of the optimization Q_D (that is around 90 psf). Finally, control law I was tested for flutter at $M = 0.9$ yielding the value of $Q_{DF} = 76$ psf for $g = 0$ and $Q_{DF} = 78$ psf for $g = 0.03$ (see Fig. 8).

Figure 9 shows a comparison between the results obtained in the present work and those reported in Ref. 1. As can be seen, the closed-loop flutter speeds obtained herein are

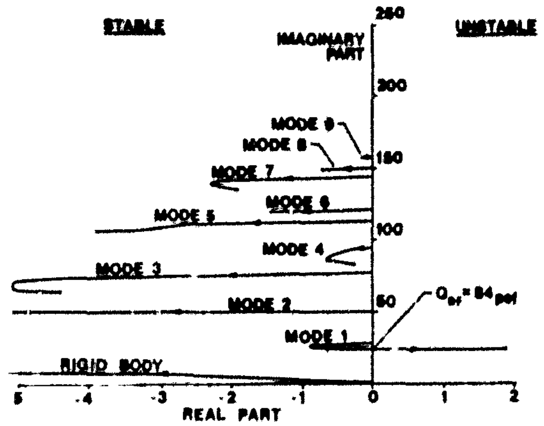

Fig. 5 Closed-loop root locus plot at $M = 0.2$, using control law I.

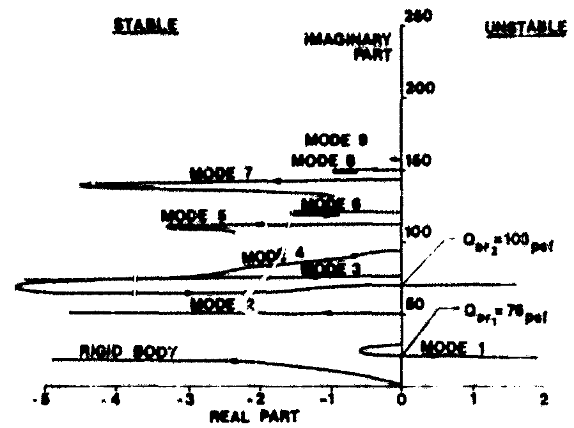

Fig. 8 Closed-loop root locus plot at $M = 0.9$, using control law I.

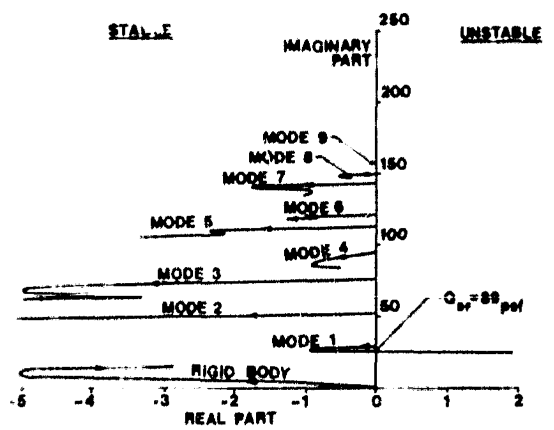

Fig. 6 Closed-loop root locus plot at $M = 0.2$, using control law II.

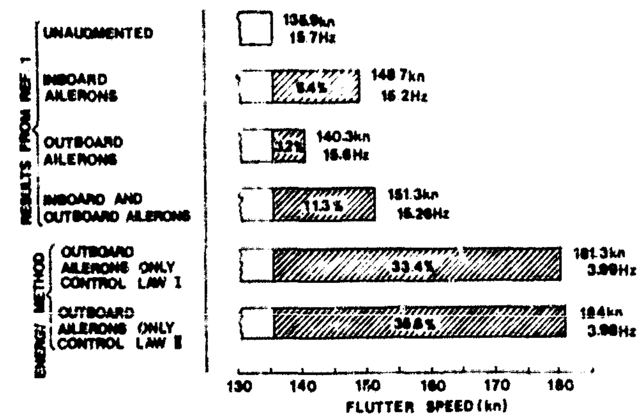

Fig. 9 Comparison between various results for the SST model at $M = 0.2$.

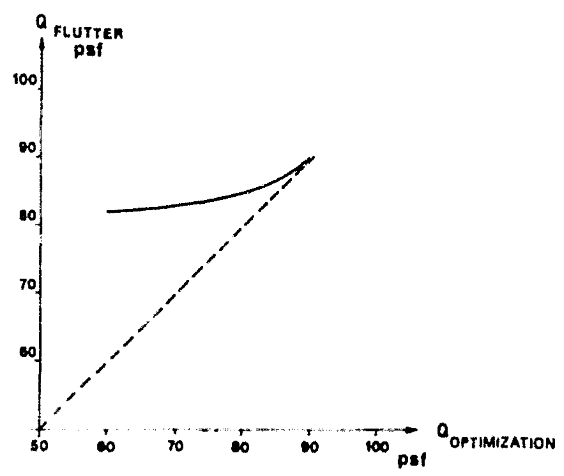

Fig. 7 Variation of flutter dynamic pressure with dynamic pressure at which optimization is performed at $M = 0.2$ ($g = 0$).

substantially more effective than those reported in Ref. 1 for the same SST flutter model with $g = 0.03$ and $M = 0.2$.

Control Surface Activity

The activity of the t.e. control (due to the different control laws) at the various flight dynamic pressures is shown in Figs. 10 and 11 for various values of g. It can be seen that control law II requires about 3.3 times as large rms control deflections as control law I, whereas rms control rates are larger by about 66% compared with control law I. Hence control law I appears to be better especially when considering that the difference between the overall flutter speeds due to those two control laws is small. Figure 12 shows that the control surface activity of control law I at $M = 0.9$ is smaller than the activity at $M = 0.2$

Wing Root Bending Moment Alleviation

The quantitative effect of the activated t.e. system on the rms wing root bending moment (b.m.) is meaningful only for flight speeds which are below the open loop flutter speeds. For speeds above the open-loop flutter speed the nonactivated rms wing root b.m. must clearly assume infinite values. Therefore, for flight speeds which lie between the open- and closed-loop flutter speeds the alleviation must therefore be infinite since the closed-loop system clearly yields finite rms values of b.m. The results to be presented herein will therefore relate to a range of dynamic pressures up to 32 psf which represents the open-loop value of Q_{DF} for $g = 0$ and $M = 0.2$. No attempt will be made to change the above value of g or the above value of M. Figure 13 shows the variation with flight dynamic pressure of the rms bending moment ratio, defined as the ratio between the closed-loop and open-loop rms b.m. [denoted as $(b.m.)/(b.m.)_0$] for the abovementioned two control laws. Figure 14 shows the variation with Q_D of the ratio between the peak open- and closed-loop values of the b.m. as obtained from a PSD plot, an example of which is shown in Fig. 15 (with $Q_D = 26$ psf using control law I). As can be seen, the alleviation in peak bending moments is much larger than the alleviation in rms b.m. at comparable values of Q_D. It is also interesting to note that control law II is more effective in reducing peak values of b.m. and relatively ineffective (that is, yields only minor improvements over the results obtained from control law I) in reducing rms b.m. values. Hence, the increase in the control activity associated with control law II, although ineffective for flutter suppression appears to be effective for peak b.m. alleviation.

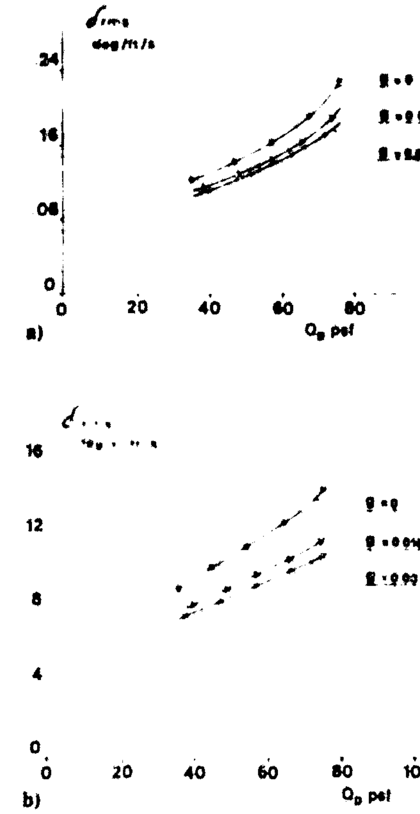

Fig. 10 Variation of control surface activity with dynamic pressure (for various values of structural damping) at $M = 0.2$, using control law I ($g = 0$): a) control surface deflection, b) control surface rate.

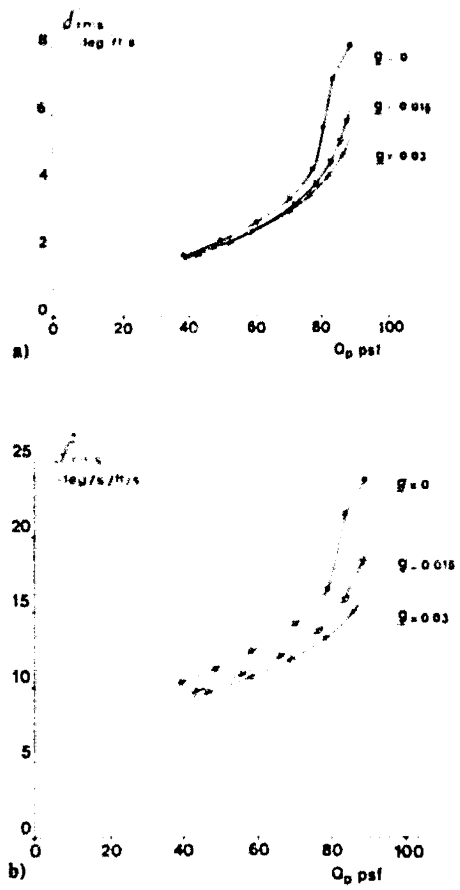

Fig. 11 Variation of control surface activity with dynamic pressure (for various values of structural damping) at $M = 0.2$, using control law II ($g = 0$): a) control surface deflection, b) control surface rate.

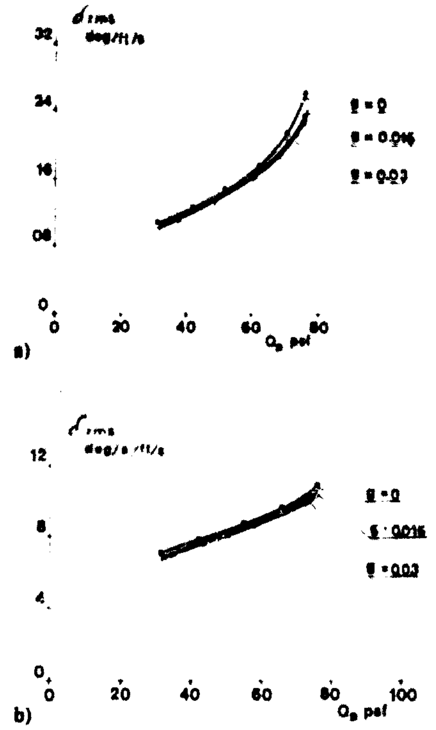

Fig. 12 Variation of control surface activity with dynamic pressure (for various values of structural damping) at $M = 0.9$, using control law II ($g = 0$): a) control surface deflection, b) control surface rate.

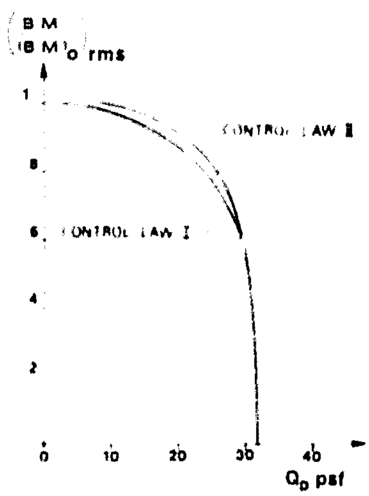

Fig. 13 Variation of rms wing root bending moment ratio with flight dynamic pressure at $M = 0.2$ ($g = 0$).

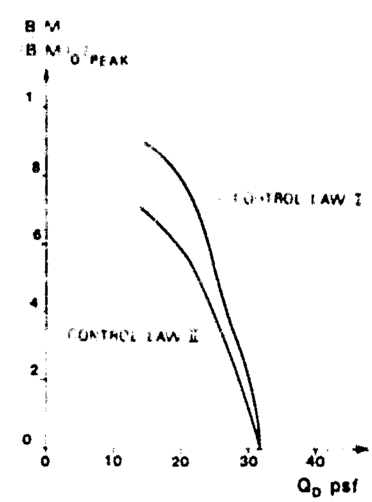

Fig. 14 Variation of peak wing root bending moment ratio with flight dynamic pressure at $M = 0.2$ ($g = 0$).

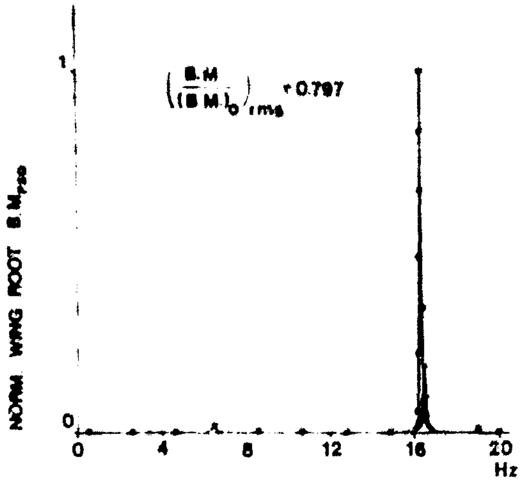

Fig. 15 PSD representation of normalized wing root bending moment at $M = 0.2$ and $Q_D = 26$ psf, using control law I.

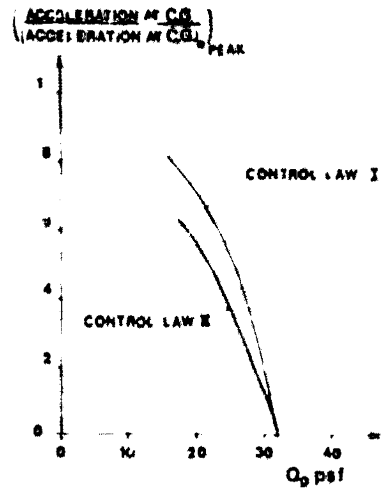

Fig. 17 Variation of peak acceleration ratio at c.g. with flight dynamic pressure at $M = 0.2$ ($g = 0$).

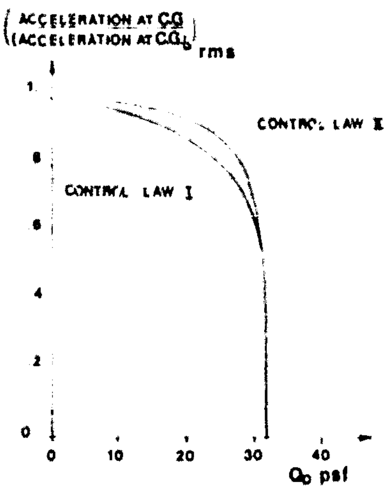

Fig. 16 Variation of rms acceleration ratio at c.g. with flight dynamic pressure at $M = 0.2$ ($g = 0$).

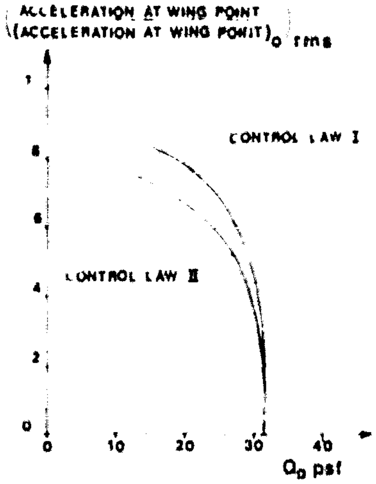

Fig. 18 Variation of rms acceleration ratio at wing point with flight dynamic pressure at $M = 0.2$ ($g = 0$).

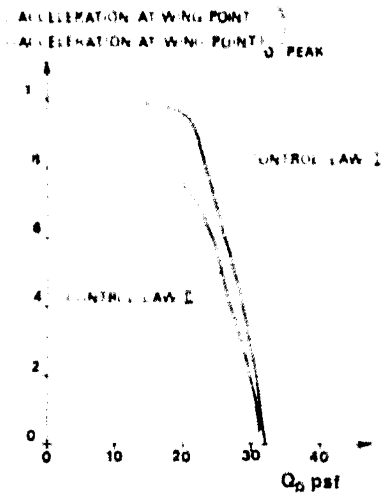

Fig. 19 Variation of peak acceleration ratio at wing point with flight dynamic pressure at $M = 0.2$ ($g = 0$).

Acceleration Alleviation

For reasons similar to those given in the case of the b.m. alleviation, the acceleration alleviation is relevant for flight speeds up to the open-loop flutter speed. Here again, only the case relating to $g = 0$ and $M = 0.2$ will be treated. Figure 16 shows the variation of the rms acceleration ratio (defined as the ratio between the closed-loop and open-loop rms accelerations) at the center of gravity (c.g.) of the SST model. Figure 17 shows the variation of the peak acceleration ratio at c.g. The results here are similar to those obtained for the b.m. ratio, that is, the activated systems are much more effective in reducing peak c.g. acceleration than in reducing rms accelerations at c.g. Similarly, control law II is relatively more effective in reducing peak c.g. accelerations than in reducing rms accelerations (compared with control law I).

The variation with Q_D of the rms acceleration ratio for a point on the wing located at the midchord of the midspan section of the outboard control surface (to be referred to as the wing point) is shown in Fig. 18. The ratio between the peak accelerations at the above point with and without activation of the control surface is shown in Fig. 19 as a function of Q_D. As can be seen, the activated t.e. system is effective in reducing both the rms and the peak values of the accelerations at the above wing point. Here, control law II is substantially more effective than control law I in reducing both the peak acceleration ratio (similar to previously discussed cases) and the rms acceleration ratio (unlike previous cases where the difference was small).

Conclusions

The application of the relaxed aerodynamic energy method coupled with the previously developed synthesis techniques yields effective flutter suppression systems when applied to the SST flutter model. The effectiveness of the control laws obtained herein substantially exceed the effectiveness of similar systems designed by classical methods as reported in Phase II of the SST Technology Follow-on Program. The application treated in this work follows two successful applications relating to the BQM-34E/F drone aircraft (DAST Program) and to the VF-17 external store flutter suppression program, as mentioned earlier in this paper. The beneficial effects of the flutter suppression system on both gust alleviation and ride control problems are in agreement with a previous work involving combined l.e.-t.e. control systems based on the original formulation of the aerodynamic energy method.

Cases can be envisaged where the effectiveness of the t.e. control system, based on the relaxed energy method, will be of doubtful nature. Such a case was encountered in this work when trying to increase the flutter speed associated with the second flutter branch. It is however felt that when such cases do arise, an alternative location of the activated control surface might prove to overcome this difficulty. Alternatively, a combined l.e.-t.e. control system might be attempted. Finally, it might be worth noting that the control surface activity as obtained from the derived control laws in the present application is within present-day technology capability.

Acknowledgments

The work reported herein is a part of a study supported by NASA through its Aeroelasticity Branch at the Langley Research Center (under Grant NSG 7373). The numerical data for the 2707-300 airplane was supplied by the Boeing Company.

References

[1] Gregory, R.A., Ryneveld, A.D., and Imes, R.S., "SST Technology Follow-On Program-Phase II—A Low Speed Model Analysis and Demonstration of Active Control Systems for Rigid-Body and Flexible Mode Stability," Boeing Commercial Airplane Company, Seattle, Wash. Rept No. FAA-SS-73-18, June 1974.

[2] Nissim, E., "Recent Advances in Aerodynamic Energy Concept for Flutter Suppression and Gust Alleviation Using Active Controls," NASA TN D-8519, Sept. 1977.

[3] Nissim, E. and Abel, I., "Development and Application of an Optimization Procedure for Flutter Suppression using the Aerodynamic Energy Concept," NASA TP1137, Feb. 1978.

[4] Nissim, E. "Comparative study Between two Different Active Flutter Suppression Systems," Journal of Aircraft, Vol 15, Dec. 1978, pp. 843-848.

[5] Nissim, E. and Lottati, I., "Active External Store Flutter Suppression in the YF-17 Flutter Model," *Journal of Guidance and Control*, Vol. 2, Sept.-Oct. 1979, pp. 395-401.

[6] Nissim, E., Caspi, A., and Lottati, I., "Application of the Aerodynamic Energy Concept to Flutter Suppression and Gust Alleviation by Use of Active Controls," NASA TN D-8212, June 1976.

[7] Sevart, F.D., "Development of Active Flutter Suppression Wind Tunnel Testing Technology," AFFDL-TR-74-126, 1975.

[8] Pratt, K.G., "Response of Flexible Airplanes to Atmospheric Turbulence. Performance and Dynamics of Aerospace Vehicles," NASA SP-258, March 1971, pp. 439-503.

[9] Nissim, E., "Flutter Suppression Using Active Controls Based on the Concept of Aerodynamic Energy," NASA TN D-6199, March 1971.

ARTICLE NO. 79-4115

On Single-Degree-of-Freedom Flutter Induced by Activated Controls

E. Nissim* and I. Lottati†
Technion - Israel Institute of Technology, Haifa, Israel

It is shown that activation of the trailing-edge control of an airfoil leads to single-degree-of-freedom type instabilities which span over a very wide region of reduced frequencies k, including high values of k (unlike the nonactivated system). These instabilities are shown to be sensitive to changes in pitching axis location, control deflection phase angle, and values of the reduced frequency. These sensitivities of the single-degree-of-freedom system cause the activated airfoil to be potentially sensitive to changes in flight conditions, and may be the source of the many difficulties encountered in suppressing classical multi-degree-of-freedom flutter by means of active controls. The results presented herein relate to zero Mach number and to a 20% trailing-edge control surface.

Nomenclature

b = semichord length
C = control gain [see Eqs. (1) and (8)]
h = displacement of the quarter chord point, positive downward
I = torsional moment of inertia per unit span
Im( ) = the imaginary part of ( )
k = reduced frequency $= \omega b/v$
K = structural stiffness
L = aerodynamic lift force, positive downward
M = aerodynamic pitching moment, positive nose up
L_h, M_h = oscillatory lift and moment coefficients due to plunging oscillation
L_α, M_α = oscillatory lift and moment coefficients due to pitching oscillation
L_δ, M_δ = oscillatory lift and moment coefficients due to control oscillation
R_δ = cross moment of inertia (between torsional and control rotation degree of freedom)
v = flight velocity
$x_4 b$ = distance of pitching axis from the midchord point, positive downstream
α = angle of attack
δ = deflection of the trailing edge control surface, positive downward
ω = frequency of oscillation
ψ = phase angle between α and δ or h and δ [see Eqs. (1) and (8)]
ρ = air density

Subscripts

R = real part of the associated parameter
I = imaginary part of the associated parameter

Introduction

THE classical aeroelastic dynamic instability, known as flutter, is a result of the interaction of two or more structural degrees of freedom. Each of the fluttering degrees of freedom is stable in the absence of the remaining degrees of freedom. Single degree of freedom type flutter instabilities are normally associated with either nonlinear aerodynamics or separated flows.[2] There exists, however, a single degree of freedom type of flutter instability which is based on linear aerodynamics,[1] and comes about when an airfoil oscillates in pitch around an axis located in the vicinity of its leading edge at very low values of reduced frequency k. This instability is known to originate from a negative aerodynamic damping term caused by the unsteady nature of the oscillating flow. This latter pitching instability is, however, of academic nature only, due to the very low values of reduced frequency k required for its existence. In all other cases (having somewhat higher value of k), the aerodynamic damping matrices due to structural oscillations, are known to be always of positive definite nature.

Recent technological advances in automatic control technology have promoted a considerable number of investigations regarding the effects of active controls on problems of flutter suppression and gust alleviation.[4-7] An active control system on a lifting surface, such as a wing, is designed to actuate a control surface in response to oscillations of the wing in a manner which stabilizes the system. Hence the activated control surface introduces considerable changes in the aerodynamic forces acting on the system. Since the determination of stability boundaries for multi degree of freedom fluttering system using active controls can be carried out numerically for specific examples only, and since the results obtained normally lack in generality, it is proposed to investigate in the present paper the existence of instability boundaries involving activated single-degree-of-freedom systems. Such single-degree-of-freedom instability boundaries can serve to indicate the regions of definite instabilities in any activated multi-degree-of freedom system, but they clearly fail to indicate the regions of stability for such systems. These simplifed instability boundaries can, therefore, help to define possible regions of stability in complex systems and promote some physical understanding of a complex problem.

Mathematical Model

The airfoil is assumed to oscillate in pitch around an axis located at $x_4 b$ from its midchord point (positive direction of displacements and forces are shown in Fig. 1). The trailing edge control surface deflection is assumed to be driven by a control law of the form:

$$\delta = C\alpha e^{i\psi} \tag{1}$$

Received June 23, 1978; revision received Sept. 15, 1978. Reprints of this article may be ordered from AIAA Special Publications, 1290 Avenue of the Americas, New York, N.Y. 10019. Order by Article No. at top of page. Member price $2.00 each, nonmember, $3.00 each. Remittance must accompany order.

Index category: Aeroelasticity and Hydroelasticity.

*Professor, Dept. of Aeronautical Engineering. Member AIAA.
†Aeronautical Engineer, Dept. of Aeronautical Engineering.

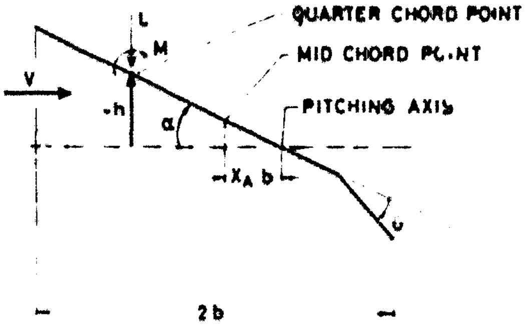

Fig. 1 Description of the two-dimensional oscillating single-degree-of-freedom system.

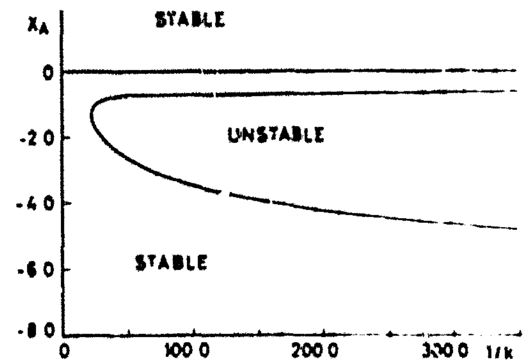

Fig. 2 Instability boundary for the nonactivated single-degree-of-freedom pitching oscillation at $M=0$.

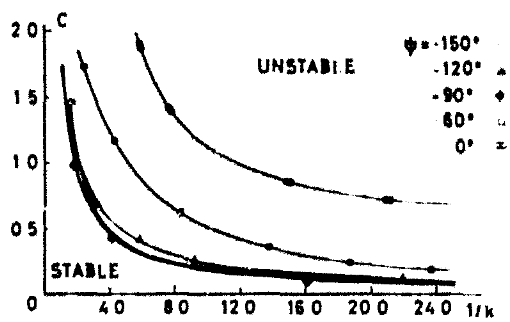

Fig. 3 Instability boundaries for activated system.

where C denotes the control gain and ψ the phase angle between α and δ. In the absence of structural damping, the equation of motion in the pitching degree of freedom assumes the form

$$I\ddot{\alpha}+K\alpha+R_{\alpha}\ddot{\delta}=-L(x_A+0.5)b+M \tag{2}$$

where I, R_{α}, K are inertia, cross-inertia, and stiffness terms, respectively, and L, M are given by[7]

$$L=\pi\rho b^3\omega^2\left[L_h\frac{h}{b}+L_{\alpha}\alpha+L_{\delta}\delta\right] \tag{3a}$$

$$M=\pi\rho b^4\omega^2\left[M_h\frac{h}{b}+M_{\alpha}\alpha+M_{\delta}\delta\right] \tag{3b}$$

The coordinate h refers to the displacement of the quarter-chord point (positive downward). L_h, M_h, L_α, M_α, L_δ, and M_δ are complex aerodynamic coefficients which depend on k and on the Mach number. For further definition of the notation, see Fig. 1.

Ignoring the inertia coupling with the control surface (R_α), and substituting Eqs. (1) and (3) into Eq. (2) and rearranging, the following equation is obtained using the relation $h/b=-(x+0.50\alpha)$:

$$I\ddot{\alpha}+\{K-\pi\rho b^4\omega^2[(x_A+0.5)^2L_h-(x_A+0.5)$$
$$\times(L_\alpha+L_\delta Ce^{i\psi}+M_h)+M_\alpha+M_\delta Ce^{i\psi}]\}\alpha=0 \tag{4}$$

Remembering that the values of the various aerodynamic derivatives are complex, that I, K are real and positive, and assuming the system to be statically stable, we obtain [from Eq. (4)] the following condition for dynamic instability:

$$\mathrm{Im}[(x_A+0.5)^2L_h-(x_A+0.5)(L_\alpha+L_\delta Ce^{i\psi}+M_h)$$
$$+M_\alpha+M_\delta Ce^{i\psi}]>0 \tag{5}$$

where Im denotes "imaginary part of." It is interesting to note that Eq. (5) contains aerodynamic terms only. For any constant value of Mach number, instability boundaries can therefore be plotted using Eq. (5), for various values of reduced frequency k, of pitching axis locations x_A, of control gains C, and of phase angle ψ.

For the limiting case of pure bending oscillations of an activated control system (with mass balanced control surface), the following equation of motion is obtained:

$$B\ddot{h}+kh=L \tag{6}$$

where

$$L=\pi\rho b^3\omega^2(L_h h/b+L_\delta\delta) \tag{7}$$

Assuming the control law

$$\delta=C(h/b)e^{i\psi} \tag{8}$$

and substituting Eqs. (7) and (8) into Eq. (6), the following condition for dynamic instability in pure bending is obtained:

$$\mathrm{Im}[L_h+L_\delta Ce^{i\psi}]>0 \tag{9}$$

In this case, the instability boundaries (Eq. 9) are functions of k, C, and ψ only (for any given constant value of Mach number)

Presentation and Discussion of Results

The instability boundaries for the single-degree-of-freedom, nonactivated system will first be presented for purposes of subsequent comparison with the activated system. The pure bending instability boundaries of the activated system will then be presented in the form of C vs $1/k$ for various values of ψ. Finally, the pitching instability boundaries of the activated system will be presented in a series of graphs. Each graph relates to a constant value of C and the boundaries are presented in the form x_A vs $1/k$ for various values of ψ. The Mach number is kept equal to zero throughout this work. The system is assumed to have a 20% chord trailing-edge control surface. The aerodyanmic derivativs are computed using analytical expression following the method of Ref. 7.

Instability Boundary for the Unactivated System

Figure 2 shows the unstable region caused by pitching oscillation as a function of the pitching axis location x_A and $1/k$. It can be seen that instability starts around the value of $1/k>25$ or $k<0{,}04$. Furthermore, the critical location of the pitching axis is around the leading edge (that is, $x_A\approx-1$). The instability boundary in Fig. 2 has been known for many years[3] and it has little practical value due to the very low values of k associated with this instability.

Instability Boundaries for the Activated, Pure Bending Oscillation

Figure 3 shows the instability boundaries C vs $1/k$ for various values of phase angle ψ. The unstable region lies above the various curves, whereas the stable region lies below them. The gain C is made to vary between 0 and 2 and the angle ψ is varied between 0 and ± 180 deg. For negative values of C (i.e., $-2<C<0$), the instability curves shown in Fig. 3 have the form of their reflection (about the abscissa) with the values of ψ changed to $(\psi+180$ deg). This point will be discussed further in a subsequent section of this paper.

It is very interesting to note that:

1) Activated single-degree-of-freedom bending instability occurs over a very wide range of values of k (not necessarily low values of k).

2) Phase angle changes between 0 and -90 deg promote the instability, with $\psi=-90$ deg as the most critical angle. The instability subsides as ψ is further changed toward $\psi=-180$ deg. Positive values of phase angles (0 deg $<\psi<180$ deg) do not show any instabilities within the positive range of values of C, as shown in Fig. 3.

Instability Boundaries for the Activated Pitching Oscillation

Figures 4-11 present the instability boundaries of the activated system. Each figure relates to a different fixed value of gain C and shows the effects of the pitching axis location x_A and the reduced frequency k on the instability boundaries. A careful study of the figures shows that:

1) The instability boundaries cover a very wide range of k values, including a high value of k.

2) The instability regions increase as the gain C is increased.

3) The largest instability regions are obtained for phase angle of $\psi=\pm 90$ deg, with instabilities for both values starting with $C=0.5$.

4) The least unstable location of the pitching axis lies around the midchord region (i.e., $x_A \approx 0$).

5) The phase angles ψ which maintain stability throughout the various values of C and x_A lie in the first quadrant within $0<\psi<30$ deg (that is, in the region of $\psi \approx 15$ deg).

6) A second range of values of ψ which maintains stability, except for large values of C (that is, $C>1.8$), lies in the third quadrant around $\psi=-180$ deg. For $C=2$ and $\psi=180$ deg, the region of instability is very narow (around the midchord region).

7) For $0<\psi<180$ deg, two distinct regions of instability often occur (see, for example, Figs. 7-11), with one region located at very high values of k (that is, at very low values of $1/k$).

8) The shapes of the instability regions vary considerably with the reduced frequency k. Hence, the employment of unsteady aerodynamics is essential for activated flutter analysis.

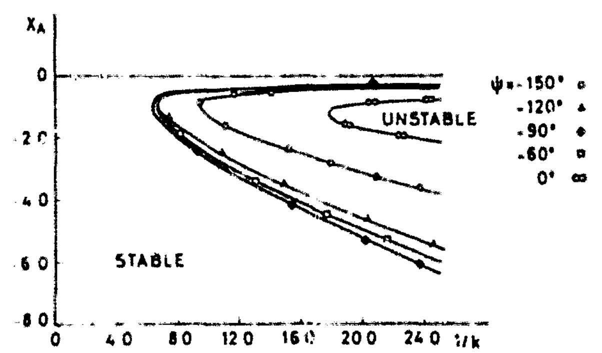

Fig. 4 Instability boundaries for activated system with control gain value of $C=0.30$.

Closed-Form Expressions of the Effects of Control Surface on the Stability Boundaries

It has been shown that in the absence of control surface rotation, single-degree-of-freedom instability can only occur for pitching oscillations provided $1/k>25$ (see Fig. 2). Since the remaining figures presented in this paper (i.e., Figs. 3-11) cover the range of $0<1/k<25$, it follows that instability boundaries within this latter region must be brought about by the detrimental effects of control surface rotation. These detrimental effects can be isolated from Eqs. (5) and (9) to yield closed-form expressions. A study of these expressions

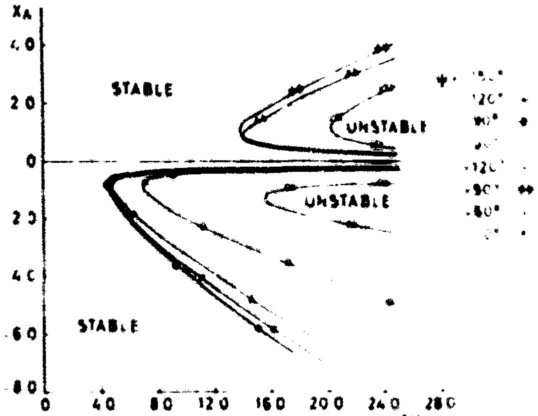

Fig. 5 Instability boundaries for activated system with control gain value of $C=0.50$.

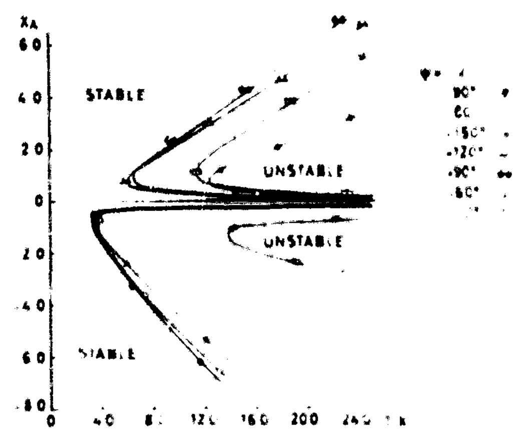

Fig. 6 Instability boundaries for activated system with control gain value of $C=0.75$.

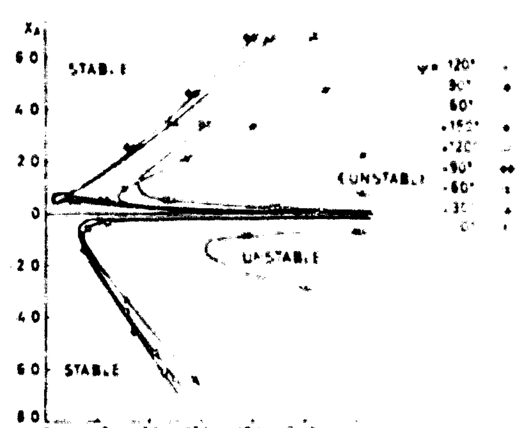

Fig. 7 Instability boundaries for activated system with control gain value of $C=1.00$.

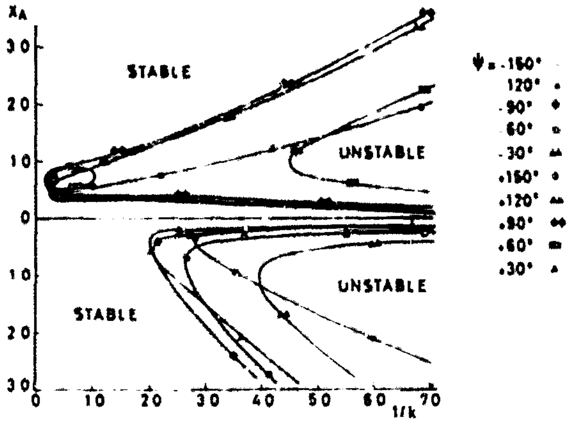

Fig. 8 Instability boundaries for activated system with control gain value of $C = 1.25$.

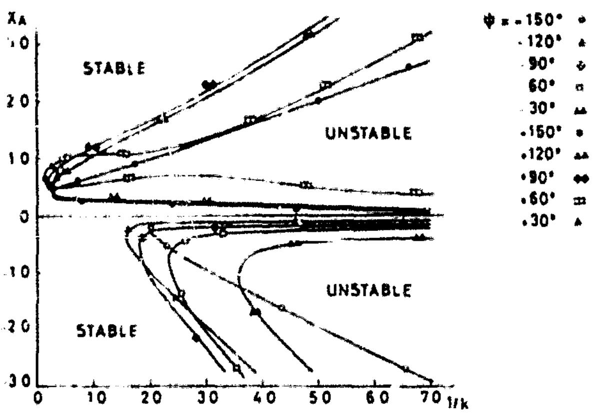

Fig. 9 Instability boundaries for activated system with control gain value of $C = 1.50$.

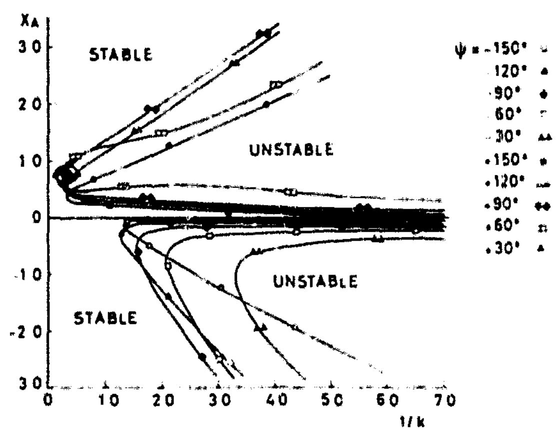

Fig. 10 Instability boundaries for activated system with control gain value of $C = 1.75$.

can shed some additional light on the effects of the different parameters and especially on the role of the phase angle ψ.

Control Surface Effects in Pure Bending Oscillations

Equation (9) shows that control surface rotation is destabilizing when

$$\mathrm{Im}(CL_\delta e^{i\psi}) > 0$$

or, alternatively, when

$$C[L_{\delta_R}\sin\psi + L_{\delta_I}\cos\psi] > 0 \qquad (10)$$

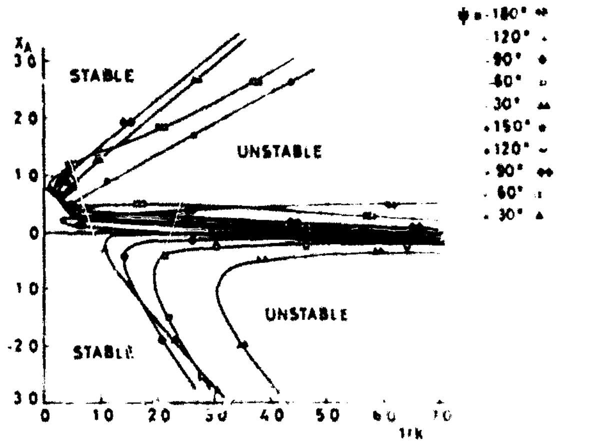

Fig. 11 Instability boundaries for activated system with control gain value of $C = 2.00$.

where the added subscripts R and I denote, respectively, the real and imaginary parts of the associated parameters (i.e., L_δ in the preceding case).

The value of L_{δ_R} is about one order of magnitude larger than L_{δ_I} over most of the $1/k$ range (that is, $1/k > 1.5$). Hence, instability is largest around $|\psi| = 90$ deg for the preceding $1/k$ range. Equation (10) also shows how the real and imaginary parts of the control surface lift coefficient are turned into a pure bending damping coefficient through the phase angle ψ and control gain C. It is worth noting that the following identity:

$$C[L_{\delta_R}\sin\psi + L_{\delta_I}\cos\psi] = -C[L_{\delta_R}\sin(\psi + 180\ \mathrm{deg}) + L_{\delta_I}\cos(\psi + 180\ \mathrm{deg})] \qquad (11)$$

implies that instability boundaries with positive gain values may be replaced by identical boundries with negative gain values, provided the corresponding values of the phase angle ψ are increased by 180 deg (as already noted earlier in this work). It may also be observed that the destabilizing effect of the control surface rotation is directly proportional to the control gain C.

Control Surface Effects in Pure Pitching Oscillations

The destabilizing effects of the control surface during pitching oscillations can easily be isolated from Eq. (5) to yield

$$\mathrm{Im}\{Ce^{i\psi}[M_\delta - (x_4 + 0.5)L_\delta]\} > 0$$

or, alternatively,

$$C\{[M_{\delta_R} - (x_4 + 0.5)L_{\delta_R}]\sin\psi + [M_{\delta_I} - (x_4 + 0.5)L_{\delta_I}]\cos\psi\} > 0 \qquad (12)$$

Here again the control surface aerodynamic coefficients are transformed into main surface damping coefficients through the phase angle ψ and control gain C. The inequality expressed by Eq. (12) depends not only on the relative values of L_{δ_R}, L_{δ_I}, M_{δ_R}, M_{δ_I} (which vary with k) but also on the pitching axis location x_4 which, in turn, affects the damping of the main surface through the remaining terms in Eq. (5). Hence, the effects of the various parameters on the instability boundaries are of complex nature. Even the dominance of M_{δ_R} over M_{δ_I} is limited to a lower reduced frequency range ($1/k$ greater than about 4) than the corresponding one associated with the L_δ coefficient. Hence, for $1/k > 4$, the widest instability will occur when $|\psi| \approx 90$ deg. Figure 11, for example, illustrates this point and also shows that at the lower range of $1/k$ values, the widest instability regions occur with values of $|\psi| \neq 90$ deg.

Some Remarks on Flutter Suppression of Activated Systems

It can be seen that for almost any chosen phase angle, there exists a region of pitching axis locations for which single-degree-of-freedom instability exists. This implies that an activated trailing edge control may stabilize a mode whose pitching axis lies outside the unstable region and yet may lead to a severe instability of another mode whose pitching axis falls within the unstable region. Similar sensitivities to changes in phase angles can also be observed (keeping the pitching axis location x_4 constant), especially in the low region of $1/k$ or high region of k. These facts make stabilization both difficult and also very sensitive to modal and phase angle changes. It is well known that activated flutter suppression systems have a tendency to be sensitive to changes in flight conditions and flight configurations, in addition to their possible adverse effects on initially stable modes. It is, therefore, very possible that this sensitivity essentially originates from the aforementioned single degree of freedom instabilities rather than from the more complex multi degree of freedom flutter.

It is also well known that the classical bending torsion type of flutter is caused by the skew symmetric components of the real part of the generalized aerodynamic matrix.[4] It can be shown that symmetry in the preceding matrix can be achieved at $C \approx 1.85$ and $\psi = 180$ deg for $k = 0.1$ or if $C \approx 2$ and $\psi = 180$ deg for $k = 0.5$. Therefore, classical flutter will not occur for values of C equal to those just specified (dependent on k). Hence, from classical flutter point of view, ψ should lie in the third quadrant, around $\psi = 180$ deg. As already noted, the region of $\psi \approx 180$ deg leads to single-degree-of-freedom type instability for values of $C > 1.8$ and is inferior to the first quadrant values from the point of view of the single degree of freedom type instability. Hence, if C is limited to a value of $C < 1.8$ and $\psi = 180$ deg, no single degree of freedom flutter will occur, but classical flutter may occur. If, on the other hand, C is given the value of 1.85 or larger depending on k, no classical bending-torsion flutter can occur, but a single degree of freedom instability will take place. Hence, a system may exist (having x_4 around the midchord region), for which stabilization by means of activated trailing-edge control surface is impossible. The stabilization of such systems can only be achieved if modal changes are introduced that cause the pitching axis to shift from the midchord region. These results are in agreement with those obtained by the use of the aerodynamic energy concept.[8]

Conclusions

It has been shown that activation of the trailing edge control of an airfoil leads to single degree of freedom type instabilities which span over a very wide region of reduced frequencies k, including high values of k (unlike the nonactivated system). The origin of these instabilities lies in the introduction by the control surface of negative aerodynamic damping forces. This implies that aerodynamic damping forces must never be neglected while performing flutter analysis of activated control systems (unlike many instances in nonactivated flutter problems). Futhermore, since the instability boundaries vary considerably with the reduced frequency k, oscillatory aerodynamic coefficients must always be used in active control flutter analysis. The sensitivities of the activated single degree of freedom system to changes in pitching axis location, control deflection phase angle, and values of the reduced frequency cause the activated airfoil to be potentially sensitive to changes in flight conditions and may be the source of the many difficulties encountered in suppressing flutter by means of active controls. Since incompressible flow has been assumed throughout this paper, it is felt that further work is required to determine the possible effects of compressibility on the single degree of freedom instability reported herein.

Acknowledgments

This work is part of a study supported by NASA under Grant NSG 7373.

References

[1] Rauscher, M., "Model Experiments on Flutter at the Massachusetts Institute of Technology," *Journal of the Aeronautical Sciences*, Vol. 3, March 1936, pp. 171-172.

[2] Krzywoblocki, M.Z., "Investigation of the Wing-Wake Frequency with Application of the Strouhal Number," *Journal of the Aeronautical Sciences*, Vol. 12, Jan. 1945, pp. 51-62.

[3] Runyan, H.L., Cunningham, H.J., and Watkins, C.E., "Theoretical Investigation of Several Types of Single Degree of Freedom Flutter," *Journal of Aeronautical Sciences*, Vol. 19, Feb. 1952, pp. 101-110.

[4] Nissim, E., "Flutter Suppression Using Active Controls Based on the Concept of Aerodynamic Energy," NASA TN D-6199, March 1971.

[5] Topp, L.J., "Potential Performance Gains by Use of a Flutter Suppression System," Paper 7-B3, 1971 Joint Automatic Control Conference, St. Louis, Mo., Aug. 1971.

[6] Roger, K.L., Hodges, G.E., and Felt, L., "Active Flutter Suppression—A Flight Test Demonstration," AIAA Paper 74-402, Structures, Structural Dynamics and Materials Conference, Las Vegas, Nev., April 1974.

[7] Smilg, B. and Wasserman, L.S., "Application of Three Dimensional Flutter Theory to Aircraft Structures," ACTR No. 4798, Material Div., U.S. Army Air Corps, July 9, 1942.

[8] Nissim, E., "Recent Advances in Aerodynamic Energy Concept for Flutter Suppression and Gust Alleviation Using Active Controls," NASA TN D-8519, Sept. 1977.

FLUTTER SUPPRESSION AND GUST ALLEVIATION USING ACTIVE CONTROLS - REVIEW OF DEVELOPMENTS AND APPLICATIONS BASED ON THE AERODYNAMIC ENERGY CONCEPT

E. Nissim
Department of Aeronautical Engineering
Technion - Israel Institute of Technology
Haifa, Israel

Abstract

The paper presents the current state-of-the-art of the aerodynamic energy concept. The latest applications of the relaxed energy concept, most of which are as yet unpublished, are also presented in this paper. These applications include the suppression of external-store flutter of three different configurations of the YF-17 flutter model, using single trailing-edge (T.E.) control surface activated by single, fixed gain, control law. Also included are some initial results regarding the suppression of flutter of the 1/20 scale, low speed wind-tunnel model, of the Boeing 2707-300 supersonic transport, using an activated T.E. control surface. Additional results regarding comparative study between activated leading-edge - T.E. and T.E. alone control systems are also presented together with a review of previously published formulations and applications.

Introduction

The ability of the aerodynamic control surfaces to promote flutter instabilities has been known for many decades. Classical books in the field of Aeroelasticity[1] include considerable material to this effect under such headings as "bending-aileron flutter" or "torsion-aileron flutter". These control surface induced flutter instabilities are traditionally overcome by reducing the deflections of the control surfaces by mass balancing of the control surfaces. It seems therefore reasonable to assume that this ability of the aerodynamic control surfaces to promote flutter could be reversed by appropriate control of their deflection, so as to combat the main lifting surface flutter instability, such as the wing bending-torsion flutter. Indeed, to put it differently, the origin of flutter lies in the nature of the oscillatory aerodynamic forces which permit the transfer of energy from the airstream to the wing. This flow of energy could be controlled, in principle, by modifying the aerodynamic forces through appropriate deflections of the control surfaces. The implementation of this approach requires, therefore, a rapidly responding control system which is actuated by the motion of the main surface and which leads to an appropriate deflection of the control surface.

The introduction of such activated control surfaces is not limited to problems of flutter suppression. Their potential applications span over a wide class of problems related to the improvement of performance of aircraft. The recent technological advances made in the field of control systems and the increased reliability of control system components, brought about by the space program, have paved the way for the incorporation of increasingly sophisticated control systems in aircraft. In his AIAA Von Karman Lecture[2], I.E. Garruck states: "A major current trend which will play a dominant role in research, development, and practice during the years ahead is the union of modern control technology and aeroelasticity; for example, in control configured vehicles (CCV)... Although aeroelasticians and control specialists have in the past usually gone their separate ways and both fields have become quite sophisticated, in the last few years there have been attempts at real cooperation and adaptation to each other's methods so that important information has been published." Among the numerous proposed applications in CCV are: relaxed aerodynamic stability, gust and maneuver load allevation (with fatigue damage reduction through modal suppression), ride quality control, flutter suppression, taxi load alleviation and automatic control of variable geometry. As could be expected some of the proposed applications have recently come to fruition: An active control system has been installed on the B-52 aircraft[3,4] to control the response of the rigid body mode and one elastic mode (first aft body bending) to gust inputs. Flutter suppression by active controls has been demonstrated in flight[5] on the B-52 airplane (the mild flutter instability was induced by an added ballast tank). Other applications relating to the control of the rigid body modes have been incorporated in several military development areas, including the YF-16 aircraft. Applications relating to the suppression of external store flutter are currently under way for the F4 airplane.[6,7] In addition, a number of feasibility studies have been made to assess the merits (in terms of weight saving and of performance increase) of applications of active control technology to aircraft[8-13] Some of these studies were supplemented by comprehensive wind-tunnel validation programs.[14,15]

As can be seen, the use of active controls spans a wide class of problems. However, one of the major difficulties which characterizes the introduction of active control systems into elastic structures lies in the tendency of the activated systems to be very sensitive to system changes caused by the different flight conditions (such as flight speed, flight altitude, flight duration and type of mission). This sensitivity implies that a control system which is optimized at one flight condition may either show consierable degradation, or even give rise to adverse effects at other flight conditions.

The aerodynamic energy concept was formulated[16] in an attempt to define active control systems which do not exhibit such sensitivities to changing flight conditions. There is no intention to present herein a review of the extensive literature in the field of active control of aeroelastic response, nor is there any intention to review the different approaches and methods available for synthesis. Attempt will only be made in the present paper to review the developments of the aerodynamic energy approach, together with its applications, to problems of flutter suppression and gust alleviation (with emphasis on flutter suppression problems). Whenver possible, comparisons will be made between results obtained by the aerodynamic energy method and those obtained by other methods such as classical or modern control theory.

The Aerodynamic Energy Approach

Basic Concept

The aerodynamic energy concept was developed primarily for problems of flutter suppression using active controls. It hinges on the idea that since flutter instabilities originate from the nature of the aerodynamic forces, the roots of their suppression should clearly lie in the ability to modify these forces. The above idea can be implemented provided the following problem can successfully be treated: Given a fluttering system and given a control surface which can be activated, what should be the relationship between the oscillation of the system and the deflection of the control surface (normally referred to as "control law") that will ensure the necessary changes in the aerodynamic forces. This problem has been treated in refs. 16, 17. Major points relating to analysis and results are presented in the following section

The Energy Analysis

Let the n equations

$$\{F\} = -\omega^2[B + \pi\rho b^4 s(A_R + i\,A_I)]\{q\}+[E]\{q\} \quad (1)$$

represent the equations of motion of n structural modes with r activated controls, where at flutter

$$\{F\} = 0$$

and where ω represents the frequency of oscillation; $[B]$, the mass matrix; $[A_R]$ and $[A_I]$, the real and imaginary parts of the aerodynamic matrix, respectively; $[E]$, the stiffness matrix; ρ, the density of the fluid; s, reference length; b, a reference semichord length; and $\{q\}$, the response vector. The matrices in equation (1) can be partitioned into square matrices (n x n) relating to the structural modes (subscripted by s) and rectangular matrices (n x r) relating to control surface couplings (subscripted by c). After partitioning the matrices, equation (1) becomes

$$\{F\} = \Big[-\omega^2\big[[B_s \vdots B_c]+\pi\rho b^4 s([A_{R,s} \vdots A_{R,c}] + i[A_{I,s} \vdots A_{I,c}])\big] + [E_s \vdots E_c]\Big]\begin{Bmatrix} q \\ q_c \end{Bmatrix} \quad (2)$$

Assume a control law of the form

$$\{q_c\} = [T]\ \{q\} \quad (3)$$

where $[T]$ is a (r x n) matrix representing the transfer functions of the control law, and assume that no elastic couplings exist between structural modes and control deflections, thus causing $[E_c]=0$. It can be shown(16,17) that the work P done by the system on its surrounding per cycle can be written as

$$P = \frac{\pi^2\rho b^4 s\omega^2}{2}\lfloor q_R - iq_I \rfloor\ [U]\ \{q_R + iq_I\} \quad (4)$$

where

$$[U] = -\Big([A_{I,s}]+[A_{I,s}]^T+[A_{I,c}][T]+[T^*]^T[A_{I,c}]^T\Big) + i\Big([A_{R,s}]-[A_{R,s}]^T+[A_{R,c}][T]-[T^*]^T[A_{R,c}]^T + \frac{[B_c]\ [T] - [T^*]^T\ [B_c]^T}{\pi\rho b^4 s}\Big) \quad (5)$$

and where

$$\{q\} = \{q_0\}e^{i\omega t} = \{q_R + iq_I\}e^{i\omega t} \quad (6)$$

The sign of P determines stability, and therefore it is advantageous to convert equation (4) to a more convenient form. It can be shown(16,17) that P can be reduced to the form

$$P = \tfrac{1}{2}\pi^2\rho b^4\omega^2 s\Big(\lfloor\xi_R\rfloor\ [\ ^{\backslash}\lambda_{\backslash}]\{\xi_R\} + \lfloor\xi_I\rfloor[\ ^{\backslash}\lambda_{\backslash}]\{\xi_I\}\Big) \quad (7)$$

or alternatively

$$P = \tfrac{1}{2}\pi^2\rho b^4\omega^2 s\Big[\lambda_1\ (\xi^2_{R,1}+\xi^2_{I,1}) + \lambda_2(\xi^2_{R,1}+\xi^2_{I,2}) + \ldots + \lambda_n(\xi^2_{R,n} + \xi^2_{I,n})\Big] \quad (8)$$

where $[\ ^{\backslash}\lambda_{\backslash}]$ is a diagonal matrix of the eigenvalues λ_i necessarily real, of the Hermitian matrix $[U]$ (as given by eqn (5)), and where the vectors $\{\xi_R\}$ and $\{\xi_I\}$ are defined by the transformation

$$\{q_0\} = [Q_R + iQ_I]\ \{\xi_R + i\xi_I\} \quad (9)$$

The matrix $[Q_R + iQ_I]$ is a square modal matrix of the principal eigenvectors.

Discussion of Energy Concept

The work per cycle P done by the system on its surroundings has a direct bearing on the stability of the system. If P is positive, the system is dissipative, and therefore stable. If P is negative, the system is unstable because work is done by the surroundings on the system. Equation (8) shows that if all the eigenvalues λ_i of the system are positive, the system is stable regardless of the motions represented by the generalized energy coordinates ξ. If one or more of the λ eigenvalues is negative, the system is potentially unstable. Its ultimate stability is determined by the relative values of the terms ξ and λ. If the ξ values make the positive eigenvalues dominate the right-hand side of equation (8), the work P is positive and the system is stable. If, on the other hand, the ξ values make the negative terms dominate eqn. (8), P is negative and the system is unstable. Hence, the requirement for all λ's to be positive is a sufficient but not a necessary condition for stability.

For mass-balanced control surfaces ($[B_c]=0$, the eigenvalues λ obtained from $[U]$ (Eq. (5)) are dependent only on the aerodynamic properties of the system and the activated control law (matrix $[T]$). In the case of mass-balanced surfaces, the eigenvalues are referred to as aerodynamic eigenvalues. These latter eigenvalues are, in general, functions of the reduced frequency k and Mach number M. If mass unbalance is a fixed quantity in the system, the eigenvalues λ also depend on the fluid density ρ in addition to their dependence on k and M. Note that instability at zero airspeed can be brought about only through these mass unbalance terms. All the results presented in this paper relate to mass-balanced control systems only and therefore, aerodynamic eigenvalues are obtained from the following [U] matrix

$$[U] = -\left\{[A_{I,s}]+[A_{I,s}]^T+[A_{I,s}][T]+[T^*][A_{I,c}]^T\right\}$$

$$+\, i\left\{[A_{R,s}]-[A_{R,s}]^T+[A_{R,c}][T]-[T^*]^T[A_{R,c}]^T\right\} \quad (10)$$

It may be recalled that the energy approach, in its original development[16], sought to determine the matrix [T] to render all the aerodynamic eigenvalues (of matrix [U] eq. (10)) large and positive. This requirement regarding the aerodynamic eigenvalues insures both the stability of the system (since P is always positive) and its insensitivity to various flight conditions (which manifest themselves in the form of changing values of λ and changing values of the system responses ξ).

Generalized Model

The energy approach has been formulated for a general n degree of freedom system. Therefore, the energy concept can be applied to any problem. The results of such application, however, will be specific for the system considered since the generalized aerodynamic forces depend not only on the system geometry but also on its structural natural modal responses. If, however, the energy concept is applied to a two dimensional strip, the aerodynamic matrices are independent of geometry and responses of the system. As a result, the aerodynamic eigenvalues are independent of any specific system and are only functions of k, M, and the transfer function matrix [T]. Therefore, if [T] is defined using a two-dimensional strip as a model, these [T] values are applicable to any three-dimensional wing within the limitations of strip theory; thus, the model is generally applicable. Sketch (a) illustrates the generalized model considered, and the arrows indicate positive displacements and rotations.

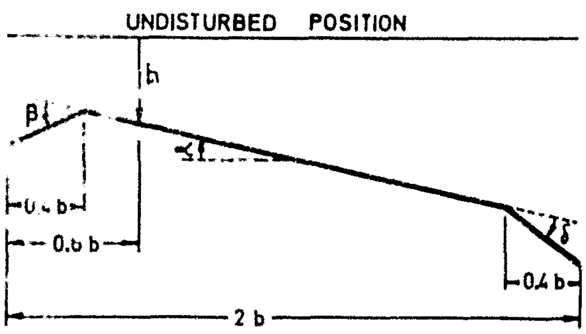

Sketch (a)

Analysis of the Generalized Model

The motion of the generalized two-dimensional model is defined by two parameters: the displacement h of the 30 per cent chord point and the rotation α about this point. Two control surfaces are assumed to be available for activation: a 20 per cent chord trailing-edge (T.E.) control and a 20 per cent chord leading-edge (L.E.) control. Two aerodynamic eigenvalues, λ_{min} and λ_{max} are obtained using this model. The analysis and results which accompanied the original derivation of the energy concept,[16] employed a transfer function matrix of the form

$$[T] = [C] + i\,[G] \qquad (11)$$

The matrices [C] and [G] were assumed to have constant values (in eqn (11)) thus making the subsequent mechanization of the control law difficult. The matrix [T] was determined numerically by an optimization program which required λ_{min} to be positive and large over a wide range of k values. This was achieved by maximizing the area under the curve λ_{min} vs 1/k using the C_{ij} and G_{ij} terms as parameters.

It should be stressed at this stage that the generalized two-dimensional model adopted herein serves only to indicate, on the basis of the strip theory, whether energy is dissipated or absorbed by the partial span strip where the activated controls are installed. Therefore, in order to suppress flutter with a minimum number of activated partial span strips, one should aim at dissipating enough energy in the activated strip, so as to compensate for any energy input by the nonactivated portions of the wing. One should therefore attempt not only to turn λ_{min} positive but also to cause λ_{min} to assume large (and positive) values.

Results of the Original Formulation of the Energy Concept

Typical results obtained with M=0 using the procedure just described[16] are presented in Fig. 1 for the unactivated system, in Fig. 2 for the activated T.E. control and in Fig. 3 for the activated combined L.E.-T.E. control system (for further details see ref. 16). The optimized values of the transfer functions [C] and [G] for these two types of activated systems are given by

a) For the T.E. Control system

$$[C]_{opt} = \begin{bmatrix} 0 & 0 \\ -0.35 & -1.9 \end{bmatrix}; \quad [G]_{opt} = \begin{bmatrix} 0 & 0 \\ 0.35 & 0.1 \end{bmatrix} \qquad (11a)$$

b) For the combined L.E.-T.E. Control system

$$[C]_{opt} = \begin{bmatrix} 0.5 & 1.0 \\ -0.05 & -1.7 \end{bmatrix}; \quad [G]_{opt} = \begin{bmatrix} -0.5 & 1.0 \\ 0.45 & 0.2 \end{bmatrix} \qquad (11b)$$

The following points emerging from these figures are worth noting:

1) The value of λ_{min} for the inactivated system (fig. 1) is negative throughout the range of k $(0.0128 \leq k \leq 19.5)$ and the value of λ_{max} is positive throughout this same range. Furthermore, the absolute values of $|\lambda_{min}|$ and $|\lambda_{max}|$ are of the same order of magnitude.

2) The values of λ_{min} for the T.E. system (Fig. 2) is only marginally positive (except at high k values) and is highly sensitive to off-design values. The values of C_{22} which improve λ_{min} cause λ_{max} to deteriorate appreciably.

3) The optimum values of λ_{min} for the combined L.E.-T.E. control system (Fig. 3) is large and positive over the whole range of $1/k$. The off-design sensitivity is greatly reduced as compared with the T.E. control system. Here again, the values of C_{22} which improve λ_{min} cause λ_{max} to deteriorate.

The results presented in ref. 16 indicate the following additional important points:

4) Systems having two sensors (to determine both h and α) are superior to any single-sensor system.

5) Mach number effects are beneficial for the whole k range for the L.E.-T.E. system (fig. 4) whereas the T.E. system shows minor improvements except for the very low range of k values where some deterioration takes place.

6) The values of λ_{min} (and λ_{max}) for the L.E.-T.E. control system could be increased considerably by the simultaneous increase of all the G_{ij} terms by a constant factor $\omega/\omega_r>1$ (see fig. 5). The T.E. control system showed a deterioration in λ_{min} accompanied by a considerable improvement in λ_{max} when such an increase in its G_{ij} terms was attempted (see ref. 16). Thus, the control law for the L.E.-T.E. system could be brought to the following convenient form

$$\{\beta\} = [C]\begin{Bmatrix} h/b \\ \alpha \end{Bmatrix} + \frac{1}{\omega_r}[G]\begin{Bmatrix} \dot{h}/b \\ \dot{\alpha} \end{Bmatrix} \qquad (12)$$

where ω_r is a reference frequency which maintains the non-dimensional nature of eqn. (12). Clearly, the mechanization of this latter control law is much simpler than the one given by eqn. (11).

The above results led to the conclusion that the L.E.-T.E. control system, driven by two sensors, is the most effective system for purposes of flutter suppression. For this reason the L.E.-T.E. system was chosen for testing the effectiveness of active controls in the early applications of the energy method. However, before proceeding to these applications, a few points should be mentioned regarding the physical significance of the optimized control laws (see sketches (b) and (c)). The optimized L.E.-T.E. control law will be chosen for this

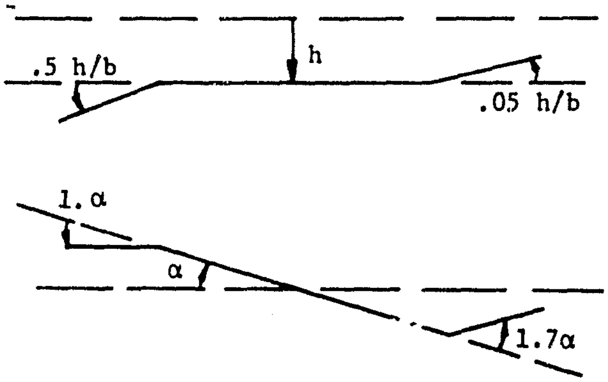

Sketch (b)

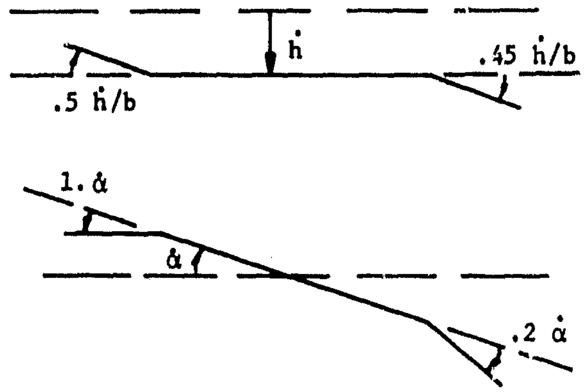

Sketch (c)

purpose since it includes the essential features of the two control surfaces employed by the generalized model.

It is interesting to note that the main effect of the in-phase deflections of the control surfaces is to counteract any lift building up; that is, the lift increase due to the angle of attack α is opposed by the forces created by the deflections of the L.E. and T.E. control surfaces. Furthermore, the out-of-phase control deflections increase the damping forces. It can therefore be seen that flutter suppression is achieved by both reducing the energy input into the system and increasing the dissipation of energy.

Early Applications of the Aerodynamic Energy Concept

The first application of the results produced by the aerodynamic energy concept was made using a SST type wing for which detailed analysis using at least 10 degrees of freedom already existed[18]. The application was carried out by members of the Boeing Wichita division under contract to the Langley Research Center. The wing configuration is indicated in Fig. 6. Flutter control was achieved using several independent stripwise units each of which consisted of combined L.E.-T.E. control surfaces having 20% chord each and activated by sensors located at 30% and 70% chord locations, (using a control law as given by eqn (11)). The results, employing M=0.9 lifting surface aerodynamics, supplemented by strip theory for the control strips, indicated that the use of T.E. controls alone would increase the flutter speed by only a few per cent (~ 5%) while the use of the combined L.E.-T.E. systems yielded with outboard segment A alone an 11% increase, with mid segment B alone - 28% increase, and with inboard segment C alone - 21% increase in the flutter speed. The combined use of B and C led to an increase in flutter speed not specifically determined but noted to be in excess of 41% of the original speed. A root locus plot corresponding to this case is shown in Fig. 7. A corresponding experimental exploratory study[15] was undertaken in the Langley Transonic Dynamics Tunnel using a simplified version of a proposed supersonic transport wing design (Fig. 8). The active flutter suppression method, based on the aerodynamic energy criterion, was verified experimentally using three different control laws (as defined by eqn (11)). The first two control laws utilized both leading edge and trailing-edge active control surfaces, whereas the third control law required only a single

T.E. control surface. At Mach number 0.9 the experimental results demonstrated increases in flutter dynamic pressure from 12.5 per cent with a L.E.-T.E. active control system to 30 per cent with active T.E. control. The mechanization of the L.E. control has met with great difficulties due to what is now believed to be a control induced instability caused by the mass unbalanced L.E. control. As a result of this instability of the L.E. control (which was present even at zero airspeeds) activation of the L.E. control could only be attained at M=0.9. Nevertheless, two important points follow this essentially experimental study (15).

1) An active flutter suppression system was demonstrated successfully, using L.E. and T.E. control surfaces, to suppress flutter on a model in a wind tunnel.

2) Irrespective of the difficulties encountered in the mechanization of the L.E. control, it is still significant to note that a single L.E. control yielded satisfactory results in suppressing flutter over the entire range of Mach numbers tested.

Somewhat different analytical applications (19,20) using a somewhat different control law, of the type given by eqn (12), with ω_r acting as a control parameter (the smaller ω_r is, the more effective the active controls become), were made on two different types of subsonic aircraft using a discrete gust approach(20) based on aerodynamic strip theory. These aircraft are the twin-boom, twin turboprop Arava 101 transport (maximum mass 6800 Kg, see Fig. 9) and the Westwind, twinjet business transport (maximum mass 9400 Kg) which is a modified version of the Rockwell Jet Commander (Fig. 10). The wing on each aircraft was divided into [illegible] equally spaced strips as shown in Fig. 11: Each strip could accommodate a pair of active controls (that is, 20% chord L.E.-T.E. controls). The strips located along the horizontal tail were allowed spans equal to one third and one tenth of the horizontal tail semispan of the Arava and Westwind aircraft respectively. The best locations for a single activated system along the span of the wing were determined for bending-moment alleviation, reduction in fuselage accelerations, and flutter suppression. Reference 19 deals with step gust inputs whereas reference 20 deals with 1-cos shape gust with peak values following the requirements of the federal aviation authorities.

The simultaneous treatment of flutter suppression and gust alleviation problems follows as a natural consequence of the control law derived by the use of the aerodynamic energy which, as already mentioned earlier, acts to reduce the energy input into the system and increase the dissipation of energy.

The main points emerging from this application (20) are briefly summarized by the following points:

1) A single activated strip located at the outboard region of the wing promotes negative bending moments (M_b) at the root of the wing during upgust conditions (see Fig. 12). These negative bending moments are caused by the restraining forces exerted by the activated strip, at its outboard location, as a result of the upward motion of the airplane caused by the upgust forces. For similar reasons, an activated strip located at the root region of the wing promotes increase in bending moments during upgust conditions (see Fig. 13).

To overcome these difficulties, the control law was modified to activate the control surfaces using the elastic contributions of the motion. In mathematical terms, h and α in the control law were replaced by $(h-h_r)$ and $(\alpha-\alpha_r)$ where the subscript r refers to a reference point around the root of the wing. This reference point is chosen in such a manner so as to "filter out" all the rigid body contributions to the control inputs. The results following the introduction of the above changes into the control law (referred to in ref. 20 as the extended control law) are shown in Fig. 14. As can be noted, the effects of the extended control law on the maximum values of the root bending moment are indeed dramatic. The best location of the activated strip for maximum bending-moment reductions is in the tip region of the wing but inboard of the tip strip.

2) The optimum strip location for maximum increase in the flutter speed is at the wing tip strip. Furthermore, the effectiveness of the activated strip is greatly increased by the introduction of the extended control law. Flutter speeds could easily be increased by more than 70% of the open loop flutter speeds.

3) The optimum strip location for maximum reductions in fuselage accelerations is at the root strip location for the ordinary control law (Fig. 15). The extended control law yields better results with optimum strip location at the inboard region of the wing (but clearly not on the reference strip, see Fig. 16).

In summarizing the results of the above application(20), it may be stated that the extended control law, which is based on the wing elastic deformations only, presents a major step forward in problems of flutter suppression and gust alleviation. It leads to almost complete decoupling between the rigid body responses, elastic responses, and the activated control forces. As a result, major improvements in performance are obtained. For this reason, free flying wind tunnel models might show greatly reduced performance as compared with clamped models unless some form of an extended control law is used.

The above applications have shown that the energy concept produces effective activated systems. There were indications, however, that the derived control laws could be improved and that the mechanization of the L.E. control was more involved than that of the T.E. control. Furthermore, some of the control laws (such as the one defined by eqn (11)) were difficult to realize. This led to an investigation aimed at avoiding the use of the L.E. control while maintaining the effectiveness of the activated system. The results of this investigation are described in the following section.

Active Flutter Suppression Using Trailing-Edge and Tab Control Surfaces

As already stated earlier in this paper, the L.E. control may present some control problems since it carries relatively large aerodynamic hinge moments. Furthermore, there has been some reluctance to introduce a L.E. control due to its possible detrimental effects on the general aerodynamic characteristics of the wing. The activated T.E.-tab combination, if effective for flutter suppression, could alleviate the difficulties associated with the L.E.-T.E. system. It is shown (21) that an 8% chord tab should be chosen for a 20% chord T.E. control. The results obtained[21] for the variations of λ_{min} with 1/k show that the T.E.-tab system activated by both linear and rotational sensors, has a flutter suppression performance comparable to the L.E.-T.E. system. The main advantage of the T.E.-tab system over the L.E.-T.E. system lies in the lower actuator torque requirements, whereas its main disadvantage lies in its relatively higher control surface rotations. Applications pertaining to the T.E.-tab system were not further pursued in view of the progress made regarding the activation of T.E. alone control system. Some details regarding these developments are presented in the following section.

Relaxation of the Energy Concept

Objective and Formulation of Relaxed Conditions

The energy approach, in its original development[16], sought to determine the matrix [T] so as to render all the aerodynamic eigenvalues large and positive. This requirement regarding the aerodynamic eigenvalues ensures both the stability of the system (since P will always be positive) and its insensitivity to the various flight conditions. Since the derived control laws are of general nature and do not take into consideration any specific property of the analysed system, it is possible to argue that the limitations concerning the potentials of the T.E. control system to perform effectively as flutter suppressor is inherent in the above formulation of the problem. Assume that other methods of stabilization exist, or can be devised, and that all we wish to ensure is the insensitivity of the stabilized system to changes in flight conditions. The implications of such an approach on the energy concept involve the relaxation of the requirement that all the aerodynamic eigenvalues must be large and positive. Assume, therefore, that such a relaxation is now introduced which permits some of the aerodynamic eigenvalues to be negative. Stability can only be achieved under these conditions by modifying the responses of the system so as to render the responses associated with the positive eigenvalues to be the dominant ones. This latter requirement forms a necessary condition for stability but does not ensure, in itself, the insensitivity of the resulting stabilized system to the various flight conditions. In order to ensure that this relaxed stability requirement yields a system which shows only small sensitivities to the changing flight conditions the absolute values of the negative aerodynamic eigenvalues must always be made much smaller than those eigenvalues associated with the dominant responses of the stabilized system. For the generalized two-dimensional model adopted in this work, two aerodynamic eigenvalues, λ_{min} and λ_{max} are obtained. In the original derivation of the aerodynamic energy concept, λ_{min} was required to be positive and large. In the relaxed energy approach,[17] λ_{min} is permitted to be negative provided

$$\lambda_{min} = \text{near maximum value (may be negative)}$$
$$\lambda_{max} \gg \lambda_{min} \tag{13}$$

and provided that these relations are maintained for all flight conditions. The above two requirements regarding λ_{min} and λ_{max} will be referred to as the "relaxed energy requirements". As can be noted, the above relaxation is made possible by abandoning the sufficiency condition for stability in the original formulation while maintaining its insensitivity to changes in flight conditions. It is worth noting that since the dissipation of energy by the activated strip depends both on λ_{min} and on λ_{max}, the importance of λ_{max} should not be overlooked even when λ_{min} is positive and large. Considerable improvements in the potential performance of the activated control system may result, if changes in the control gains are permitted which lead to small degradations in λ_{min}, provided these degradations are accompanied by large increases in λ_{max}. This implies that while determining the optimum values of the transfer function matrix [T] we seek to optimize not only the area under the λ_{min} vs 1/k curve but also the weighted addition of the area under the λ_{max} vs 1/k curve, so as to satisfy eqns (13). Convenient ways of performing the above optimization of the [T] matrix are described in ref. 17.

In addition to the above relaxation of the energy concept, two other major changes were introduced in ref. 17:

1) Unlike the original derivation, only realizable transfer functions were considered

2) The influence on the target function of the very low frequency portion of the λ vs 1/k curves was reduced by both an appropriate redefinition of the aerodynamic eigenvalues and the reduction of the k range from

$$0.0128 \le k \le 19.5$$

as used during the original derivation,[16] to

$$0.04 \le k \le 3.5$$

The redefintion of the aerodynamic eigenvalues involves the inclusion of the frequency effects into these aerodynamic eigenvalues. Hence, eqn (8) was modified to the form

$$P = \tfrac{1}{2}\pi^2\rho b^2 V^2 s \left| \bar\lambda_1(\xi_{R,1}^2 + \xi_{I,1}^2) + \bar\lambda_2(\xi_{R,2}^2 + \xi_{I,2}^2) + \dots + \bar\lambda_n(\xi_{R,n}^2 + \xi_{I,n}^2) \right| \tag{14}$$

yielding the following relation between the λ's

$$\bar\lambda_i = k^2\lambda_i \tag{15}$$

Hence, at the low range of k values, the newly defined eigenvalues are smaller than the originally defined eigenvalues by a factor of k^2. These changes permit the giving of more weight to the intermediate frequencies during the optimization process.

<u>Optimization Results</u>[17]:

The variation of the non activated $\bar{\lambda}$'s with $1/k$ is shown in Fig. 17. It is interesting to compare these $\bar{\lambda}$ with their λ counterparts in Fig. 1 and to note the large changes in the shape of the curves.

Two types of optimized transfer functions were derived.[17] The first type is referred to as the damping type transfer function (D.T.T.F.) and it assumes the following optimum values for $[T]$.

$$[T] = \begin{bmatrix} 0. & 0. \\ 0. & -1.86 \end{bmatrix} + ik \begin{bmatrix} a_L & 0 \\ 0 & a_T \end{bmatrix} \begin{bmatrix} -4. & 4. \\ 4. & 3.2 \end{bmatrix} \quad (16)$$

where a_L and a_T are positive free parameters. These free parameters were introduced as a result of the unbounded behaviour of the target function with respect to increase of these parameters. The transfer function for the T.E. alone system is obtained from eqn (16) by letting $a_L=0$.

The second type of optimized transfer function is referred to as the localized damping type transfer function (L.D.T.T.F.) and it assumes the following optimum values for $[T]$

$$[T] = \begin{bmatrix} 0. & 0. \\ 0. & -1.86 \end{bmatrix} + R \begin{bmatrix} a_L & 0 \\ 0 & a_T \end{bmatrix} \begin{bmatrix} -4. & 4. \\ 4. & 2.8 \end{bmatrix} \quad (17)$$

where once again a_L and a_T are positive free parameters (which follow the unbounded nature of the target function with increase of these parameters) and R is given by

$$R = \frac{(ik)^2}{(ik)^2 + 2\zeta k_n (ik) + k_n^2} \quad (18)$$

where both ζ and k_n are positive constants. Fig. 18 shows the variation of $\bar{\lambda}_{min}$ vs $1/k$ and $\bar{\lambda}_{max}$ vs $1/k$ at various Mach numbers using the optimized D.T.T.F., as defined by eqn (16) with $a_L=0$ (that is, T.E. only control system) and $a_T=25$. The corresponding curves using the L.D.T.T.F. defined by eqns (17,18) are shown in Fig. 19 using the values of $a_L=0$, $a_T=1$, $\zeta=0.5$ and $k_n=0.2$. It can be seen that the results corresponding to the D.T.T.F. (Fig. 18) satisfy the relaxed energy requirements (as expressed by eqn (13)) over the whole range of k's investigated. The L.D.T.T.F. yields results (Fig. 19) which satisfy the relaxed energy requirements only around the peak region of the curves. The location of this peak region (along the $1/k$ axis) is around $1/k_n$ and the width of the curves (in addition to their height) are controlled by the parameter ζ. In addition, stiffness terms are introduced as R varies with k. These terms vanish when $k=0$ and therefore do not affect the static behaviour of the system. They, however, can be used to change the response of of the system, if necessary, so as to ensure stabilization. In general, several R values can be used, having different values of k_n, ζ and a's, if greater flexibility in the $\bar{\lambda}$ distributions (with k) is required while using the L.D.T.T.F. (see ref. 22). For the L.E.-T.E. systems, large improvements in the values of $\bar{\lambda}_{min}$ are obtained (see ref. 17) with almost negligible effects on the values of $\bar{\lambda}_{max}$ (as compared with the T.E. alone control system).

The working forms of the above transfer functions are simplified to the following forms for purposes of subsequent applications:-

For the D.T.T.F. matrix $[T]$ is given by

$$[T] = \begin{bmatrix} 0 & 0 \\ 0 & -1.86 \end{bmatrix} + i\frac{\omega}{\omega_R} \begin{bmatrix} a_L & \\ & a_T \end{bmatrix} \begin{bmatrix} -4. & 4. \\ 4. & 3.2 \end{bmatrix} \quad (19)$$

where ω_R is a reference frequency, normally chosen as the open-loop flutter frequency. For the L.D.T.T.F., matrix $[T]$ is given by

$$[T] = \begin{bmatrix} 0. & 0. \\ 0. & -1.8 \end{bmatrix} + \begin{bmatrix} (R_{L,1}\, a_{L,1} + R_{L,2}\, a_{L,2}) & 0 \\ 0 & (R_{T,1}\, a_{T,1} + R_{T,2}\, a_{T,2}) \end{bmatrix} \cdot \begin{bmatrix} -4. & 4. \\ 4. & 2.8 \end{bmatrix} \quad (20)$$

where

$$R_j = \frac{(i\omega)^2}{(i\omega)^2 + 2\zeta_j \omega_{n,j}(i\omega) + (\omega_{n,j})^2} \quad (21)$$

It can be seen that both transfer functions include parameters which can only be determined in connection with the system considered. The L.D.T.T.F. has more parameters for determination and has more potential regarding possible changes in the responses of the system. It is generally considered to be preferable to the D.T.T.F. On the other hand, the D.T.T.F. has less such parameters and, therefore, their values are much easier to determine.

<u>Analytical Applications of the Relaxed Energy Approach</u>

An optimization procedure was developed[22] for the determination of the various free parameters (that exist in the above transfer functions) so as to minimize control surface response to continuous gust inputs over a wide range of flight conditions. Most applications relate to T.E. alone control systems in an attempt to determine their effectiveness for flutter suppression. Extended type control laws (driven by the elastic responses of the system) were exclusively employed in all applications.

The first application of the above optimization procedure using the newly defined transfer functions was made to a violent wing flutter case of a drone aircraft[29] selected by the National Aeronautics and Space Administration for flight research programs aimed at validating active control system concepts. A plan view drawing of the flight vehicle-research wing combination is shown in Fig. 20. Guided by previous results[20], the T.E. control surface was placed as near to the tip of each wing as was structurally possible (Fig. 21). All the aerodynamic forces were computed using unsteady lifting surface doublet lattice method. The design objective of the flutter suppression system was to provide a 20% increase in flutter speed (to be demonstrated in flight) above that of the basic wing. Although detailed results regarding this case appear in ref. 22, preference will be given here to the results appearing in ref. 23 since they include comparisons with results obtained using classical control system synthesis. Table 1 presents a summary of the calculated flutter characteristics. It can be seen that both the classical and the energy methods achieve the objective set for the flutter suppression system (with somewhat higher flutter speed values using the energy method). Figure 22 shows comparisons of control surface rates and displacements. As can be seen, the maximum values for the rates (and displacements) using the energy method are around 20% lower than those produced by the classical method. In their discussion of results the authors state (23): "Two major differences result in the application of these methods. The first difference is in establishing the form, gains, and break frequencies of the shaping filter. In the classical method, this process is a function of previous experience coupled with results of analysis for the particular system being studied and in general cannot be extended to other problems. In the aerodynamic energy method, on the other hand, a fixed form of the shaping filter is given with free parameters available to fit this form to the dynamic characteristics of the system being considered. The second difference is the manner in which the gust analysis is used. In the classical method the gust is used to evaluate rates and deflections of the control system after preliminary design of the shaping filter is complete. If the rates or deflections are beyond the capability of the control system then an iterative process including changes to the shaping filter and possibly the control surface size is begun. This process is continued until both the stability and gust response requirements are met. In the energy method, the fixed form of the shaping filter allows the gust to act as a driver in establishing the free parameters which in turn permits the minimization of control surface activity while maintaining stability."

A second application has recently been made to the YF-17 flutter model[24] with the object of suppressing the external store flutter of three different store configurations using a T.E. alone control surface. The geometrical description of the active control system is shown in Fig. 23. Note that the T.E. control surface spans only 7 per cent of each wing. The description of the three configurations is given in Table 2 and the results of the optimization procedure are given in Table 3. These latter results relate to M=0 and V=98 m/s and were obtained using a dynamic pressure Q_D which is twice the value (determined arbitrarily in the absence of a definition of the desired flight envelope) of the minimum flutter dynamic pressure, corresponding to configuration B. A L.D.T.T.F. was employed and its free parameters were determined using configuration B. The resulting control law was maintained fixed during applications to configurations A and C The significance of these results is threefold:

1) A single control law with fixed gains is employed for all configurations

2) Very large increases in flutter dynamic pressures are obtained for all configurations

3) The effectiveness of the activated control system is maintained over the whole range of flight conditions (thus providing yet another confirmation regarding the potential of the relaxed energy concept).

It may also be worth noting that although the open loop configruation B is most critical from flutter considerations, the largest control surface activity corresponds to configuration C. This activity can be reduced by increasing the span of the control surface ($\sim$ 7%) employed in this application.

A single application of a L.E.-T.E. control system has recently been made using the previously described drone aircraft.[25] It is shown that the L.E.-T.E. control system yields a closed loop system with flutter speeds which are higher than those of the T.E. alone system. In addition the activity of each of the control surfaces in the L.E.-T.E. system is much lower than that corresponding to the T.E. alone system. If, however, the performance of the two systems is judged on the basis of the maximum control surface activity (corresponding to the desired 44% increase in the flutter dynamic pressure) rather than on the maximum flutter speed, and if we further require that the performance of a system with two control surfaces be compared only with systems having two control surfaces (in this case a comparison between L.E.-T.E. and T.E.-T.E. systems) one finds that the performance of the L.E.-T.E. control system is comparable to the performance of the T.E. alone system, with slight advantage to the latter system. Although this finding may be of specific nature and need not necessarily hold true for other applications, it is of importance since it shows that a T.E. alone control system can yield results which compare favourably with a L.E.-T.E. control system.

It is not unintentional that we choose to close the circle of applications by returning to the first example which served to test the potentials of the aerodynamic energy method - that is the application relating to the Boeing's supersonic transport. Comparison is now made between the results reported in reference 26, and which forms Phase II of the SST technology follow-on program, and those obtained through the use of the relaxed energy concept[27]. These results relate to the full span 1/20 scale low-speed model of the Boeing 2707-300 supersonic transport. Figure 24 shows the general configuration of the model. It can be seen that two T.E. control surfaces are available for activation. The application based on classical control methods[26] attempted the activation of both control surfaces whereas the application based on the energy approach (27) attempted the activation of the outboard aileron only (based on experience gained from previous applications (20)). These results, which were obtained using lifting surface unsteady aerodynamics, are presented in Fig. 25. As can be seen, the energy method yeilds an increase in flutter speed of 33% using the outboard aileron only (and L.D.T.T.F.) whereas the classical method yields an increase in flutter speed of 11.3% only, using both outboard and inboard ailerons. Furthermore, the energy method yields the following control surface activity of the outboard aileron, at a speed which is 16% above the inactivated flutter speed

$$\dot{\delta}_{RMS} = 25.3 \ \text{deg/s/m/s}$$

$$\delta_{RMS} = 0.33 \ \text{deg/m/s}$$

These activities are not considered to be excessive. It should be noted that flutter speeds could further be increased by specifying higher flight dynamic pressures when using the gust optimization program.

Remarks on Applications using Modern Control Theory

The author of this paper is unaware of any major comparative studies between designs based on the aerodynamic energy method and those based on modern control theory. Some use has, however, been made of the aerodynamic energy control law (eqns (11b), (12)) as derived for the L.E.-T.E. system in the original formulation of the energy concept in connection with some work which employed optimal control methods[28]. The above control law was applied[28] to a two dimensional subsonic strip, with specified actuator dynamics included in the analysis. The results showed that the plunge and pitch modes were stabilized throughout the range of parameter investigated whereas the leading-edge control mode was unstable throughout this range. Such a condition can arise if one considers the control laws of the form given by eqn (3) to correspond to the command deflections rather than to the actual deflections. It should therefore be stressed that control surface dynamics should be compensated in all applications employing the energy control laws so as to cause the transfer function matrix [T] to relate between the structural oscillations and the actual control surface deflections. It is worth mentioning the results which correspond to the above mentioned two dimensional strip as obtained through the use of optimal control theory [28]. It will be appropriate, however, to make a brief introduction to the method used.

The linear optimal control theory requires[29] the equations of motion of the system to be brought to the following form

$$\{\dot{X}\} = [A]\{X\} + [B]\{u\} \qquad (22)$$

where $\{X\}$ represents the N state variables, $[A]$ (of order $N \times N$) the plant (or system) matrix; $[B]$ (of order $N \times m$) the control distribution matrix; and $\{u\}$ (of order m) the control input vector. Both the matrices [A] and [B] (eqn 22) are constant for a given Mach number, given flight velocity and given flight altitude. Optimal control theory requires the minimization of the performance index (PI), with equations (22) used as constraints, where PI is given by

$$PI = \int_0^\infty \left(\lfloor X \rfloor [Q]\{X\} + \lfloor u \rfloor [P]\{u\}\right) dt \qquad (23)$$

and where $[Q]$ is either positive definite or positive semidefinite, and $[P]$ is always required to be positive definite. The problem now remains of selecting the weighting matrices [Q] and [P]. For the minimization of {u}, [Q] is chosen as [Q]=0. The resulting optimized control law, which is of the form

$$\{u\} = [T]\{X\} \qquad (24)$$

where the T_{ij} terms are constants, causes all the stable open-loop eigenvalues to remain unchanged while the open-loop unstable eigenvalues are reflected about the $i\omega$ axis (that is, the sign of the real part of the unstable roots is reversed). This result (see also ref. 31) permits application of the "pole placement" method for the determination of the matrix [T]. Application of the above optimal control method was made to the two dimensional strip example using a T.E. only control system[28]. The stabilized closed-loop system was found to become unstable below the open loop flutter speed, thus showing the importance of the sensitivity of the activated system to off-design conditions. The above system with two control surfaces was eventually stabilized by reflecting the unstable flutter eigenvalue about a line parallel to the $i\omega$ axis and crossing the real axis of the root locus plot at a value of 5 rads/sec. Such a reflection is arbitrary and is not, in itself, a result of application of optimal control considerations. It can thus be seen that off-design considerations forces the designer to compromise for a suboptimal system. The aerodynamic energy concept introduces these compromises in a consistent manner whereas other methods deal with this problem in an ad hoc arbitrary fashion.

An additional point which is worth noting relates to the inclusion of the actuator dynamics in the plant equations (22). It is felt that such inclusion[28,30] is limiting since parameters relating to control surface dynamics can be changed if necessary so as to reduce control surface activity. The exclusion of control surface dynamics from the energy synthesis considerations should therefore be viewed as promoting efficiency rather than as a limitation. The form of the various R's (eqn (18)) associated with the L.D.T.T.F. have the form of an actuator transfer function. It is therefore possible to view the values of the optimized R's as representing the desired actuator dynamics. These latter values clearly indicate the changes that need to be introduced into the existing actuator.

As a final remark, it is interesting to note that the determination of the control law using the energy concept meets none of the difficulties which characterize the optimal control approach such as problems associated with aerodynamic modeling, state augmentation and eventually, the state vector identification for purposes of implementation of the control law. The use of the continuous gust program for the minimization of the control surface activity using the energy method presents absolutely no aerodynamic modeling or state augmentation problems. Similarly, the relationship between the control surface deflection and the response of the wing at a specified location (see eqn (12) as an example) presents no need for state vector identification (this is similar to the I.L.A.F. concept developed in reference 8).

Concluding Remarks

The paper presents the current state-of-the-art of the aerodynamic energy concept. Many of the applications relating to the relaxed energy method have not yet been published. It is felt that the relaxed energy method, coupled with the gust response optimization procedure yields effective control systems for the suppression of flutter. These systems may consist of either L.E.-T.E. or T.E. alone control surfaces. These activated systems may also be used for gust load alleviation and ride control (if appropriately located) as shown in one of the early applications. There remains to extend the method to the supersonic flight regime and to test the possible advantages of deriving control laws based on the system's generalized matrices (somewhat along the lines of ref. (31) using the relaxed energy approach) rather than on the generalized two-dimensional strip model.

Further substantiation of results is needed using both wind tunnel models and flight test programs before attempting to incorporate some flutter suppression systems in either existing or future aircraft.

Acknowledgement

All the work performed by the author in the field of active controls was supported by NASA-Langley Research Center, through grants and through NRC Research Associateships. The author wishes to express his sincere thanks and appreciation for this support and for the continued encouragement given by the NASA (Langley) Aeroelasticity Branch throughout the years.

References

1. Bisplinghoff, R.L., Ashley, H. and Halfman, R.L.: Aeroelasticity, Addison-Wesley Publishing Co., 1955.

2. Garrick, I.E.: Aeroelasticity - Frontiers and Beyond. J. Aircraft, September 1976.

3. Dempster, J.B. and Roger, K.L.: Evaluation of B-52 Structural Response to Random Turbulence with Stability Augmentation Systems. J. Aircraft, Nov-Dec, 1967.

4. Dempster, J.B. and Arnold, J.I.: Flight Test Evaluation of an Advanced Stability Augmentation System for the B-52 Aircraft. AIAA Paper No. 68-1068, Oct. 1968.

5. Roger, K.L. Hodges, G.E. and Felt, L.: Active Flutter Suppression - A Flight Test Demonstration. AIAA Paper No. 74-402, Apr. 1974.

6. Perisho, C.H., Triplett, W.E., and Mykytow, W.J.: Design Considerations for an Active Suppression System for Fighter Wing/Store Flutter. AGARD-CP-175, Apr. 1975.

7. Honlinger, H., and Lotze, A.: Active Suppression of Aircraft Flutter. To be presented at the ICAS Conference, Lisbon, Sept. 1978.

8. Wykes, J.H., and Mori, A.S.: Techniques and Results of an Analytical Investigation Into Controlling the Structural Modes of Flexible Aircraft. AIAA Symposium on Structural Dynamics and Aeroelasticity, Aug.-Sept. 1965.

9. Wykes, J.H. and Mori, A.S.: An Analysis of Flexible Aircraft Structure Mode Control. AFFDL-TR-65-190, Pt. I, U.S. Air Force, June 1966.

10. Topp, L.J.: Potential Performance Gains by Use of a Flutter Suppression System. Paper No. 7-B3, 1971 Joint Automatic Control Conference (St. Louis, Mo.), Aug. 1971.

11. Thompson, G.O., and Kass, G.J.: Active Flutter Suppression - An Emerging Technology, J. Aircraft Mar. 1972.

12. Many Authors: Impact of Active Control Technology on Airplane Design. AGARD CPP-157, Oct. 1974.

13. Many Authors: Active Control Systems for Load Alleviation, Flutter Suppression, and Ride Control. AGARD AG175, 1974.

14. Redd, L.T., Gilman, J., Jr., Cooley D.E. and Sevart, F.D.: Wind-Tunnel Investigation of a B-52 Model Flutter Suppression System. J. Aircraft, Nov. 1974.

15. Sandford, M.C., Abel, I. and Gray, D.L.: Transonic Study of Active Flutter Suppression Based on an Energy Concept. NASA TR R450, Dec. 1975.

16. Nissim, E.: Flutter Suppression Using Active Controls Based on the Concept of Aerodynamic Energy. NASA TN D-6199, Mar. 1971.

17. Nissim, E.: Recent Advances in Aerodynamic Energy Concept for Flutter Suppression and Gust Alleviation Using Active Controls. NASA TN D-8519, Sept. 1977.

18. Garrick, I.E.: Perspectives in Aeroelasticity. Fifth Theodore von Karman Memorial Lecture. Israel Journal of Technology, 1972.

19. Nissim, E.: Flutter Suppression and Gust Alleviation Using Active Controls. TAE Rep. No. 198 - Technion, Israel Inst. Technol., 1974 (Available as NASA CR-138658).

20. Nissim, E., Caspi, A., and Lottati, I.: Application of the Aerodynamic Energy Concept to Flutter Suppression and Gust Alleviation by Use of Active Controls. NASA TN D-8212.

21. Nissim, E.: Active Flutter Suppression Using Trailing-Edge and Tab Control Surfaces. J. AIAA, June, 1976.

22. Nissim, E., and Abel, I.: Development and Application of an Optimization Procedure for Flutter Suppression Using Active Controls. NASA TP 1137, Feb. 1978.

23. Abel, I., Perry, B. III, and Murrow, H.N.: Synthesis of Active Controls for Flutter Suppression on a Flight Research Wing. AIAA Paper 77-1062, Guidance and Control Conference, Aug. 1977.

24. Nissim, E., and Lottati, I.: Active Controls for the Suppression of External Store Flutter in the YF-17 Flutter Model. Submitted for publication in J. Aircraft.

25. Nissim, E.: Comparative Study Between Two Different Flutter Suppression Systems. To be published in J. Aircraft.

26. Gregory, R.A., Ryneveld, A.D., and Imes, R.S.: SST Technology Follow-On Program - Phase II: A Low Speed Model Analysis and Demonstration of Active Control Systems for Rigid Body and Flexible Mode Stability. Report No. FAA - SS-73-18, June 1974.

27. Nissim, E.: Study of Active Control Systems for Application to Supersonic Cruise Aircraft To be published.

28. Edward, J.W., Breakwell, J.V. and Bryson, A.E. Jr.: Active Flutter Control Using Generalized Unsteady Aerodynamic Theory. AIAA Paper No. 77-1061 Guidance and Control Conference, Aug. 1977.

29. Schultz, D.G. and Melsa, J.L.: State Functions and Linear Control Systems. McGraw-Hill Book Co., 1967.

30. Turner, M.R.: Active Flutter Suppression. AGARD-CP-175, Apr. 1975.

31. Pinnamaneni, R. and Stearman, R.O.: Design and Analysis of Flutter Suppression Systems Through the Use of Active Controls. AFOSR-TR-75-0964, Jan. 1975.

* * *

Table 1: Summary of Calculated Flutter Characteristics of Drone Research Vehicle.

Mach number	Basic wing (No control) Dyn press kPa	Basic wing (No control) Freq Hz	Closed-loop Classical Dyn press kPa	Closed-loop Classical Freq Hz	Closed-loop Energy Dyn press kPa	Closed-loop Energy Freq Hz
0[illegible]	[illegible]	[illegible]6.9	43.[illegible]	8.[illegible]	46.9	8.3
0.8	26.[illegible]	18.0	*NF	-	*NF	-
[illegible]	[illegible]	19.[illegible]	*NF	-	*NF	-

*No flutter to sea level dynamic pressure

Table 2: Description of the Three Wing/Store Configurations of YF-17

Description \ Config.		A	B	C
Tip launch rail		Aim-9E(flex)	Empty	Empty
W.S.1.543 Pylon		Not instal.	Aim-7s(rig)	Aim-9E(rig)
W.S.1.052 Pylon		Aim-7(rig)	Not instal.	Not instal.
ω_{n1}	(HZ)	6.5377	5.12[illegible]4	7.0099
ω_{n2}	"	11.0111	7.5891	11.9223
ω_{n3}	"	13.3887	14.5104	14.9007
ω_{n4}	"	15.9500	16.2730	25.5323
ω_{n5}	"	24.3176	36.8006	38.2069
ω_{n6}	"	38.2780	38.5456	41.3348
ω_{n7}	"	44.4797	43.0960	46.9919

$\omega_{n,i}$ (HZ) natural frequency of the i^{th} elastic mode.

Table 3: Summary of Results: Three wing/store configurations of YF-17 with activated outboard T.E. control using I.D.T.T.F. and V = 98 m/s

	Basic Wing (no control)		CLOSED - LOOP							
STRUCT. DAMPING	g = 0		g = 0				g = 0.015		g = 0.03	
CONFIG.	Flutter Dyn. Press. kPa	Freq. rad/s	Flutter Dyn. Press. kPa	Freq. rad/s	Max* RMS Control Rate deg/s/m/s	Max* RMS Control Rotation deg/m/s	Max* RMS Control Rate deg/s/m/s	Max* RMS Control Rotation deg/m/s	Max* RMS Control Rate deg/s/m/s	Max* RMS Control Rotation deg/m/s
A	3.64	80	8.91	10	83	2.39	72	2.23	65	2.10
B	2.63	43	8.95 8.95	10 37	161	4.17	87	2.53	68	2.17
C	4.31	65	8.52	10	156	3.15	121	2.69	104	2.49

* Values relate to flights up to dyn. press. of 5.26 kPa

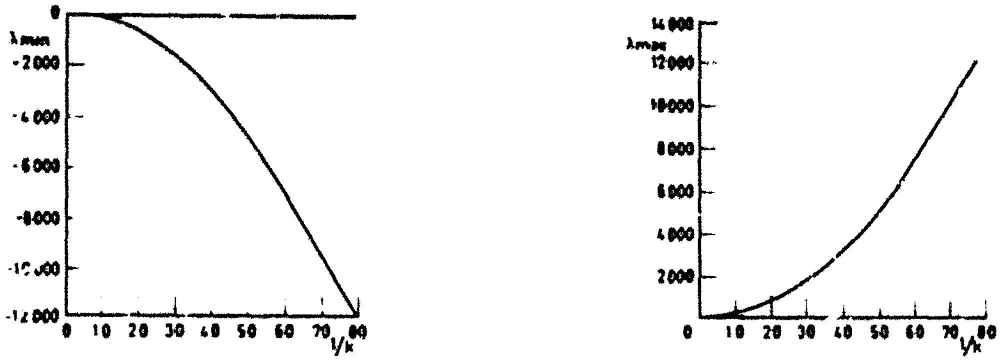

(a) λ_{min} (b) λ_{max}

Fig. 1. λ_{min} and λ_{max} vs 1/k. Wing strip with no control surfaces.

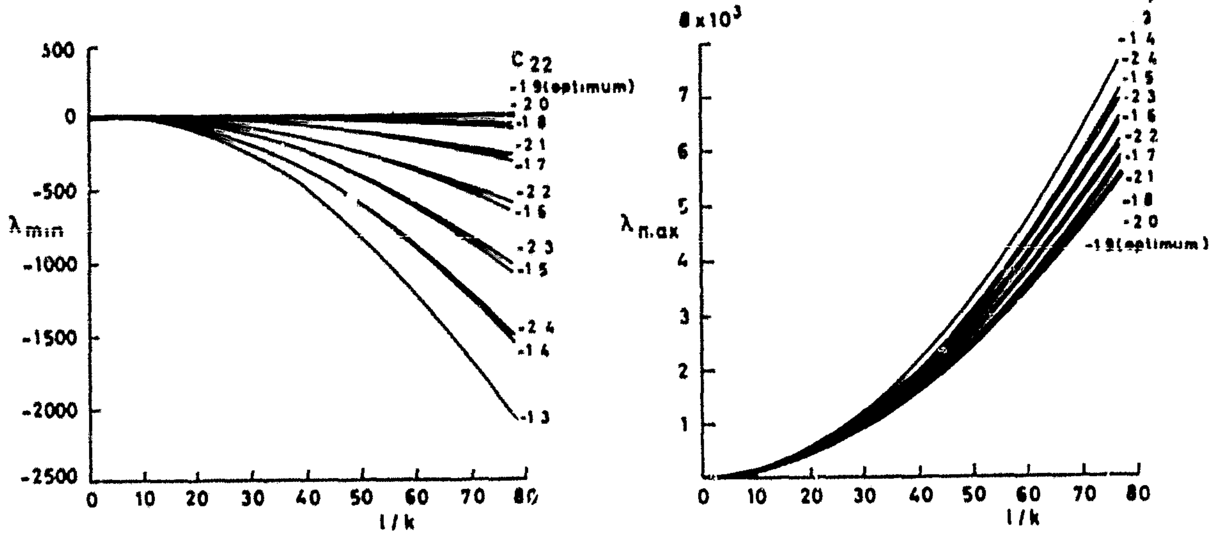

(a) λ_{min} (b) λ_{max}

Fig. 2. λ_{min} and λ_{max} vs 1/k for various values of C_{22}. Wing strip with T.E. control using eqns (11) (11a).

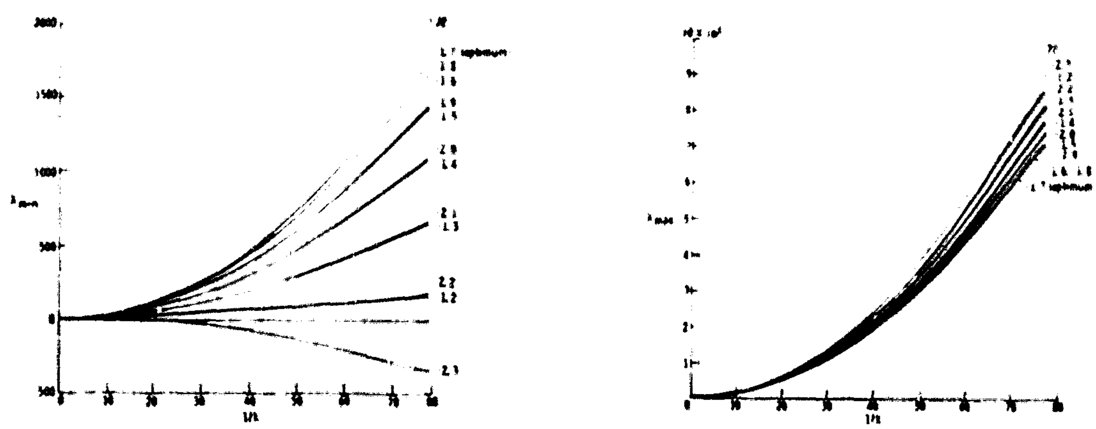

(a) λ_{min} (b) λ_{max}

Fig. 3. λ_{min} and λ_{max} vs 1/k for various values of C_{22}. Wing strip with L.E.-T.E. controls using eqns (11), (11b).

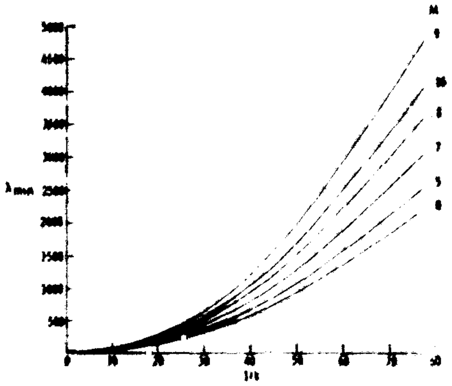

Fig. 4. λ_{min} vs 1/k at various Mach numbers. Wing strip with L.E.-T.E. controls using eqns (11), (11b).

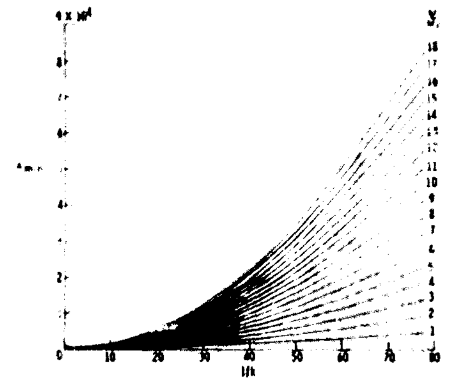

Fig. 5. λ_{min} vs 1/k for various values of ω/ω_r. Wing strip with L.E.-T.E. controls using eqns (11b), (12).

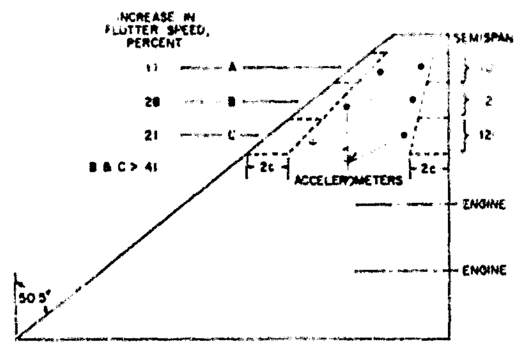

Fig. 6. Effectiveness of L.E.-T.E. system as flutter suppressor for SST type wing with engines.

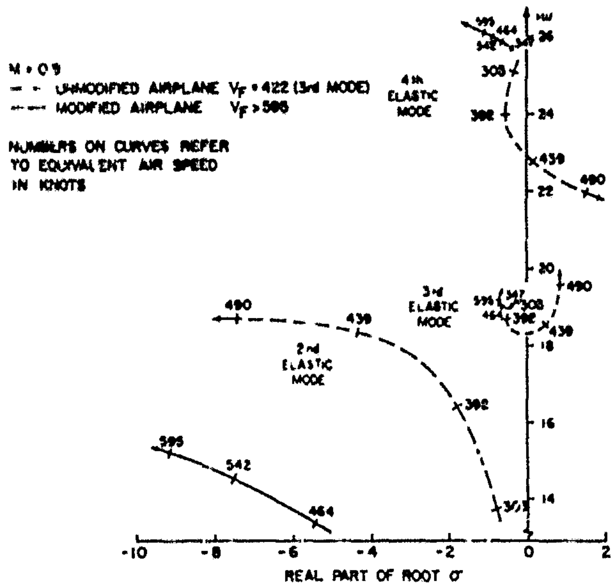

Fig. 7. Root locus plot comparing the unmodified airplane with modified one for combined case B and C of Fig. 6.

Fig. 8. Experimental wing for flutter suppression shown mounted in the Langley transonic dynamic tunnel.

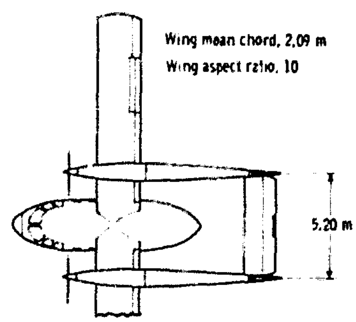

Fig. 9. Plan view of Arava STOL Transport.

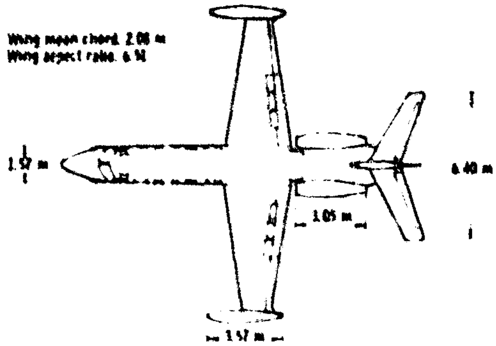

Fig. 10. Plan view of Westwind business jet transport.

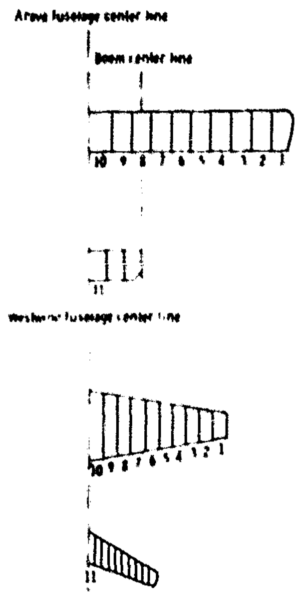

Fig. 11. Strip allocations along wing and horizontal tail of Arava and Westwind aircraft.

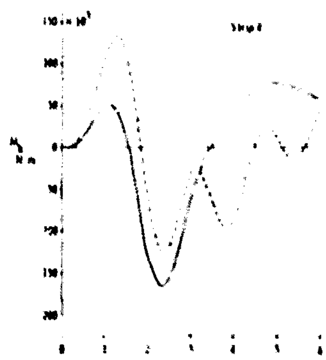

Fig. 12. Variation with time of wing root bending moment. Westwind transport with activated L.E.-T.E. system at strip 4 and with δ_{max}=0.5 rad.

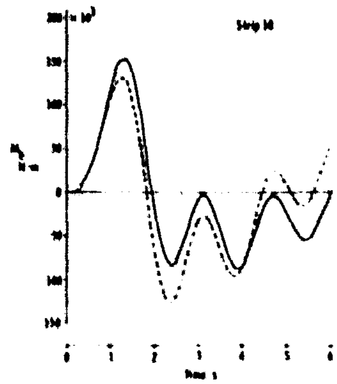

Fig. 13. Variation with time of wing root bending moment. Westwind transport with activated L.E.-T.E. system at strip 10 and with δ_{max}=0.5 rad.

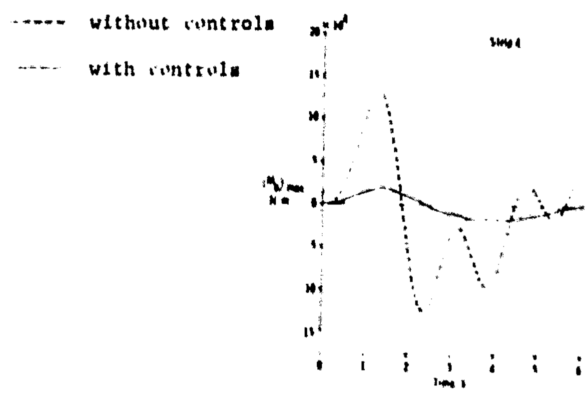

Fig. 14. Variation with time of wing root bending moment. Westwind transport with activated L.E.-T.E. system at strip 4 and with δ_{max}=0.5 rad. (using extended control law).

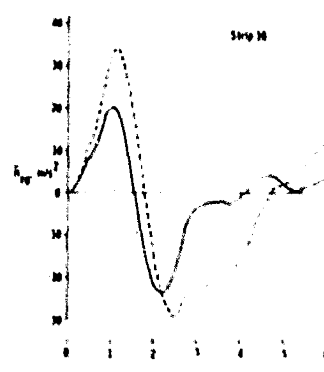

Fig. 15. Variation with time of linear acceleration at center of gravity. Westwind transport with activated L.E.-T.E. system at strip 10 and with δ_{max}=0.5 rad.

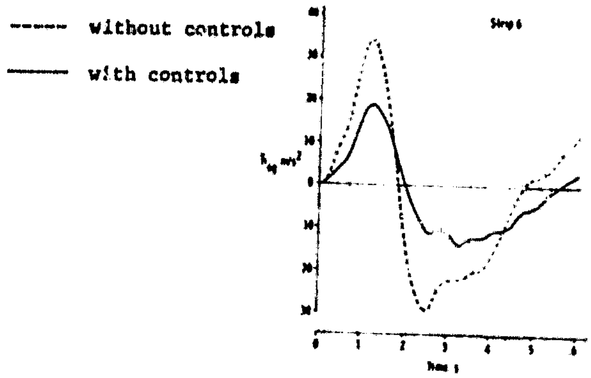

Fig. 16. Variation with time of linear acceleration at center of gravity. Westwind transport with activated L.E.-T.E. system at strip 6 and with δ_{max}=0.5 rad.(using extended control law).

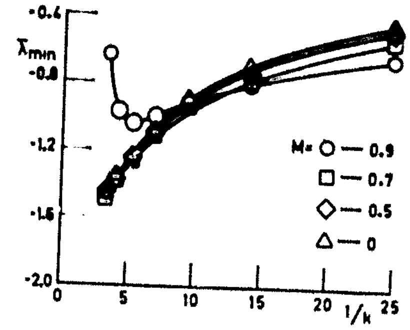

(a) $\bar{\lambda}_{min}$

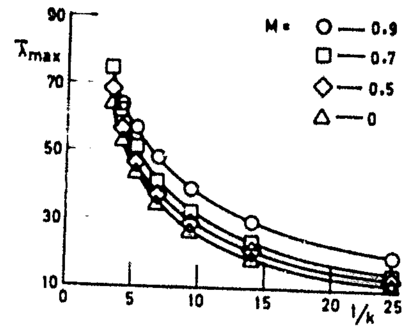

(b) $\bar{\lambda}_{max}$

Fig. 17. $\bar{\lambda}_{min}$ and $\bar{\lambda}_{max}$ vs 1/k at various Mach numbers. Wing strip with no control surfaces.

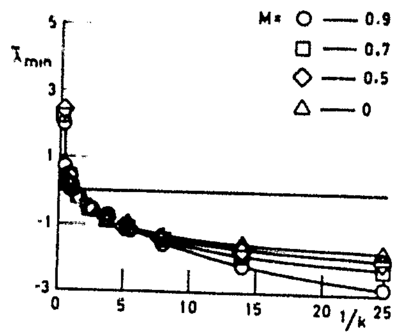

(a) $\bar{\lambda}_{min}$

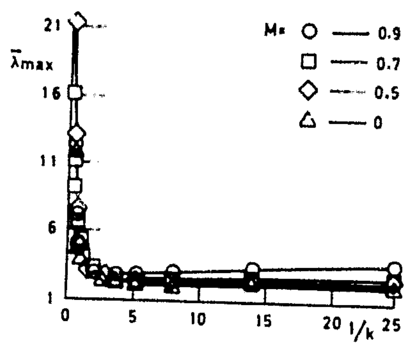

(b) $\bar{\lambda}_{max}$

Fig. 18. $\bar{\lambda}_{min}$ and $\bar{\lambda}_{max}$ vs 1/k at various Mach numbers. Wing strip with T.E. control using D.T.T.F.

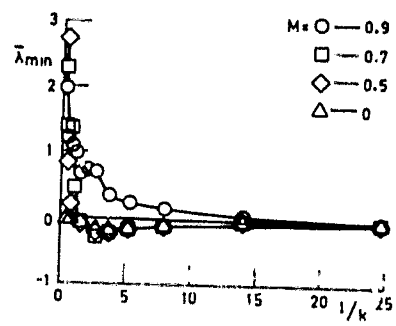

(a) $\bar{\lambda}_{min}$

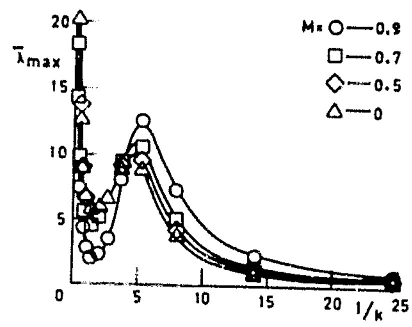

(b) $\bar{\lambda}_{max}$

Fig. 19. $\bar{\lambda}_{min}$ and $\bar{\lambda}_{max}$ vs 1/k at various Mach numbers. Wing strip with T.E. control using L.D.T.T.F.

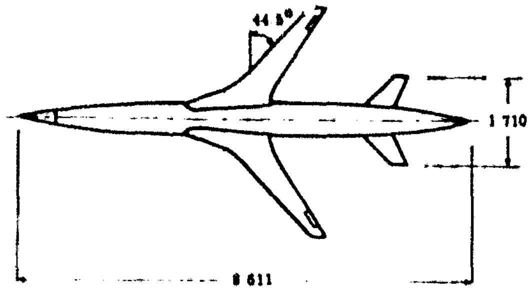

Fig. 20. Plan view of drone research vehicle (linear dimensions are in meters).

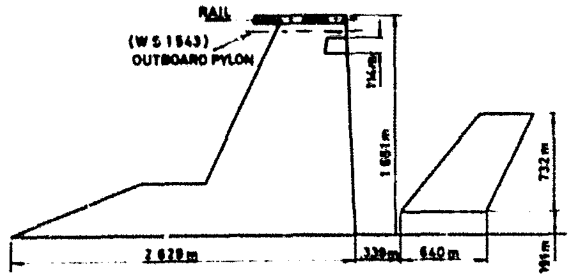

Fig. 23. Plan view (schematic) of YF-17 flutter model.

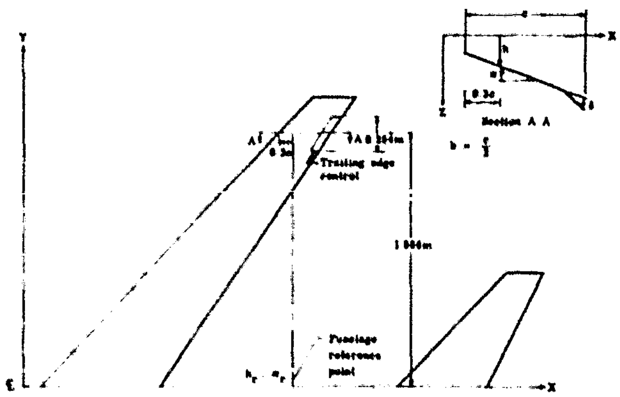

Fig. 21. Geometrical description of active control system for the drone vehicle.

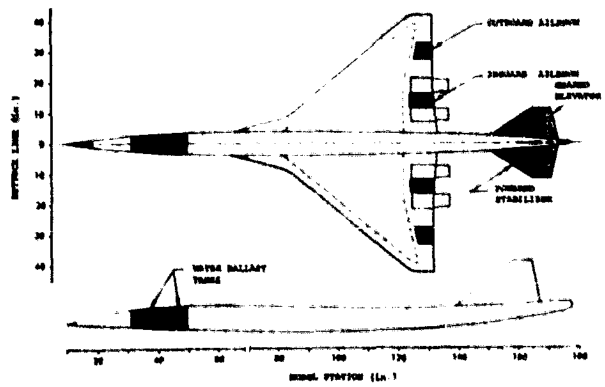

Fig. 24. General configuration of the SST model.

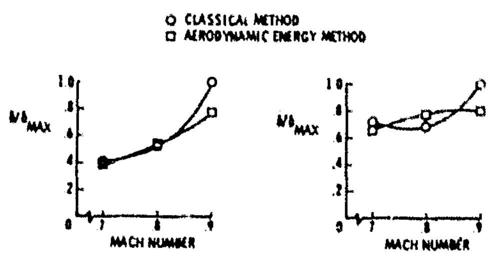

Fig. 22. Comparisons of control surface rates and displacements for the drone vehicle.

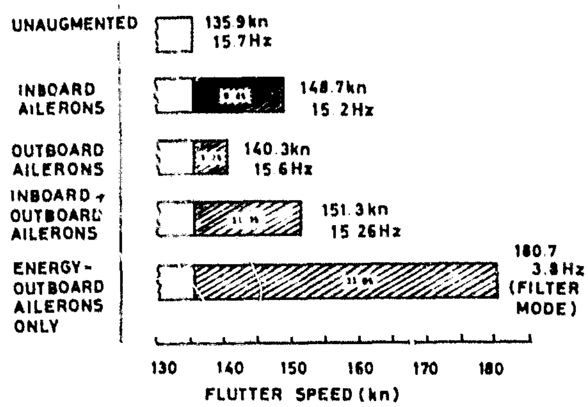

Fig. 25. Flutter results for the SST model.

ACTIVE EXTERNAL STORE FLUTTER SUPPRESSION IN THE MODIFIED YF-17 FLUTTER MODEL

by

E. Nissim* and I. Lottati**

Department of Aeronautical Engineering,
Technion - Israel Institute of Technology,
Haifa, Israel

* Professor

** Aeronautical Engineer

INTRODUCTION

The investigation reported in this work relates to the suppression of external store flutter in the YF-17 flutter model. Configuration B was specified for the above purpose with the objective of enabling the activated model to be tested in a wind tunnel at Mach number M = 0.8 and at dynamic pressures up to 69% above open loop flutter dynamic pressure. A schematic plan view of the model is shown in Fig. 1. Two control surfaces are available for activation: A leading-edge (L.E.) control and a trailing edge (T.E.) control. Control laws are defined in an attempt to meet the above mentioned objectives. No attempt is made, however, to get into the details associated with the mechanization of the control laws obtained.

Mathematical Model

The dynamic characteristics of the model were supplied by NASA. They included generalized masses, natural frequencies and mode shapes for 10 symmetric structural modes in addition to two rigid body modes. The generalized aerodynamic forces were computed using the Doublet-Lattice method with 126 boxes on each wing and 32 boxes on each half horizontal tail.

The formulation of the equations of motion and synthesis techniques[1] are based on the relaxed aerodynamic energy approach[2]. The general form of the control law employed was established in Ref. (2) and is given by the following expressions

$$\begin{Bmatrix} \beta \\ \delta \end{Bmatrix} = \left(\begin{bmatrix} 0 & 0 \\ 0 & -1.86 \end{bmatrix} + \begin{bmatrix} K_{L.E.} & 0 \\ 0 & K_{T.E.} \end{bmatrix} \begin{bmatrix} -4 & 4 \\ 4 & 2.8 \end{bmatrix} \right) \begin{Bmatrix} \dfrac{h_1 - h_r}{b} \\ \alpha_1 - \alpha_r \end{Bmatrix} \tag{1a}$$

where β and δ are the deflections of the L.E. and T.E. control surfaces, respectively, and where h_1, α_1 denote the translation and rotation of the 30 per cent chord point at the control surface mid span section respectively (see Fig. 1). The parameters h_r and α_r similarly denote the translation and rotation of a reference point located along the center line of the fuselage and b denotes the semi chord length at the control surface mid span section. The K's are given by the following expressions

$$K = \frac{a_1 s^2}{s^2 + 2\zeta_1 \omega_{n_1} s + \omega_{n_1}^2} + \frac{a_2 s^2}{s^2 + 2\zeta_2 \omega_{n_2} s + \omega_{n_2}^2} \tag{1b}$$

where $s = i\omega$ and where ω represents the frequency of oscillation. The parameters a_i, ζ_i, ω_{n_i} are all positive and their values determined by an optimization program based on the gust response of the model following the method of Ref. 1. The parameters in Eq. (1) will be subscripted by either L.E. or T.E. to indicate reference to either L.E. or T.E. control law transfer functions, respectively.

Presentation and Discussion of Results

The root locus plot for the open loop system, with the dynamic pressure Q_D acting as a parameter, is shown in Fig. 2. As can be seen the value of the dynamic pressure at flutter (Q_{D_F}) is equal to $Q_{D_F} = 84$ psf. with frequency $\omega = 36.6$ rad/s. Activation of the T.E. alone yielded only marginal results, indicating the need to relocate the control surface (see also Ref. 3). The L.E. alone yielded better results but since these results originate from changes in the responses associated with the energy eigenvectors and not from changes in the energy eigenvalues (as required by the relaxed energy approach), the work based on a L.E. alone system was not pursued. Hence, the work to be reported herein will relate to a combined L.E. - T.E. system (at $M = 0.8$).

The control laws derived from the energy approach neglected the effectis of control surface mass unbalance in an attempt to obtain generalized results. An activated system with mass-balanced control surfaces was therefore tested first. The synthesis technique yielded the following control law by specifying that the model should fly at a maximum dynamic pressure ($Q_{D_{max}}$) of 143 psf., and by attempting to minimize the control surface rates of the system:-

$$R_{T.E.} = \frac{1.62\ s^2}{s^2 + 2 \times 1 \times 4 \times s + (4)^2} + \frac{15.\ \ s^2}{s^2 + 2 \times 0.5 \times 57 \times s + (57)^2}$$

$$R_{L.E.} = \frac{4.07\ s^2}{s^2 + 2 \times 1 \times 41.5 \times s + (41.5)^2} \qquad (2)$$

with ($g = 0.$, structural damping)

$$\dot{\beta}_{rms} = 16.04 \text{ deg/s/ft/s}$$

$$\beta_{rms} = 0.31 \text{ deg/ft/s}$$

$$\dot{\delta}_{rms} = 15.21 \text{ deg/s/ft/s}$$

$$\delta_{rms} = 0.29 \text{ deg/ft/s}$$

The optimization was constrained to yield control surfaces with nearly equal values of control rates. The closed loop root locus plot for the above activated system is shown in Fig. 3. As can be seen, flutter has completely been suppressed up to a dynamic pressure of 200 psf (maximum value used in plotting all the root locus plots to be presented herein).

The introduction of control surface mass unbalance has modified the root-locus plot (Fig. 4) to such an extent that instabilities cover most of the flight dynamic pressures. A careful examination of the variation of R with frequency (Fig. 5) and its effects on the flutter speed has shown that the aerodynamic and inertial stability effects are not compatible. The gust optimization program was constrained to yield maximum aerodynamic damping around the flutter frequency only while minimizing the control activity at higher frequencies. This approach yields the following values for the control law parameters:

$$R_{T.E.} = \frac{1.88 \; s^2}{s^2 + 2 \times 0.16 \times 39.1 \times s + (39.1)^2}$$

$$R_{L.E.} = \frac{1.26 \; s^2}{s^2 + 2 \times 0.29 \times 38.8 \times s + (38.8)^2} \tag{3}$$

with (g = 0., structural damping)

$\dot{\delta}_{rms} = 14.66$ deg/s/ft/s

$\delta_{rms} = 0.44$ deg/ft/s

$\dot{\beta}_{rms} = 14.26$ deg/s/ft/s

$\dot{\beta}_{rms} = 0.4$ deg/ft/s

The root locus plot associated with the above control system is shown in Fig. 6. As can be seen, except for a small region of instability at very low values of Q_D (which is counteracted by normal structural damping) no flutter exists up to $Q_D = 200$ psf. The above control law will be referred to as control law I. The variation of the control surfaces activity with Q_D is shown in Fig. 7 and a sensitivity variation of the T.E. control rate activity (as an example) with the control parameters is shown in Fig. 8. Cancellation of the parameter $C_{21} = -1.86$ (eq. 1a) simplifies the control law and shows no effect on stability (figures not included).

A second alternative control law (to be referred to as control law II) was attempted by trying to match the flutter and inertial stability requirements at the various regions of frequency. This was done by using the synthesis technique[(1)] in the presence of a filter $\left(\frac{300}{s + 300}\right)$ which multiplies the transfer functions shown in Eq. (1a). The results for the control parameters are given by

$$R_{T.E.} = \frac{4\ s^2}{s^2 + 2 \times 0.43 \times 57.4 \times s + (57.4)^2}$$

$$R_{L.E.} = \frac{2.07\ s^2}{s^2 + 2 \times 0.5 \times 41.5 \times s + (41.5)^2} \qquad (4)$$

with (g = 0 , structural damping)

$\dot{\delta}_{rms}$ = 21.38 deg/s/ft/s

δ_{rms} = .51 deg/ft/s

$\dot{\beta}_{rms}$ = 19.35 deg/s/ft/s

β_{rms} = .52 deg/ft/s

The closed loop root locus plot is shown in Fig. 9. As can be seen, there is no flutter up to Q_D = 200 psf. The variation of the control surface activities with Q_D is shown, for control law II, in Fig. 10. A sensitivity variation of the T.E. control rate (as an example) with the control parameters is shown in Fig. 11. The cancellation of $C_{21} = -1.86$ introduces in this case a flutter instability, at Q_D = 145 psf (see Fig. 12). Therefore $C_{21} = -1.86$ has to be retained. This implies that the acceleration signals have to be integrated. Integrations of the form $\frac{1}{s+\varepsilon}$ and $\frac{1}{(s+\varepsilon)^2}$ had been tested in the region of $0.1 < \varepsilon < 1.$ and no visible effects could be detected on the root locus plots (figures not included).

The block diagrams for the above two control laws are presented in Figs. 13, 14.

Acknowledgement

The work reported herein is a part of a study supported by NASA through its Aeroelasticity Branch at the Langley Research Center (under Grant NSG 7373).

REFERENCES

1. Nissim, E.; and Abel, I.; "Development and application of an optimization procedure for flutter suppression using the aerodynamic energy concept", NASA TP 1137, Feb. 1978.

2. Nissim, E.; "Recent advances in aerodynamic energy concept for flutter suppression and gust alleviation using active controls," NASA TN D-8519, 1977.

3. Nissim, E.; and Lottati, I.; "Active external store flutter suppression in the YF-17 flutter model", to be published in J. Guidance and Control, May 1979.

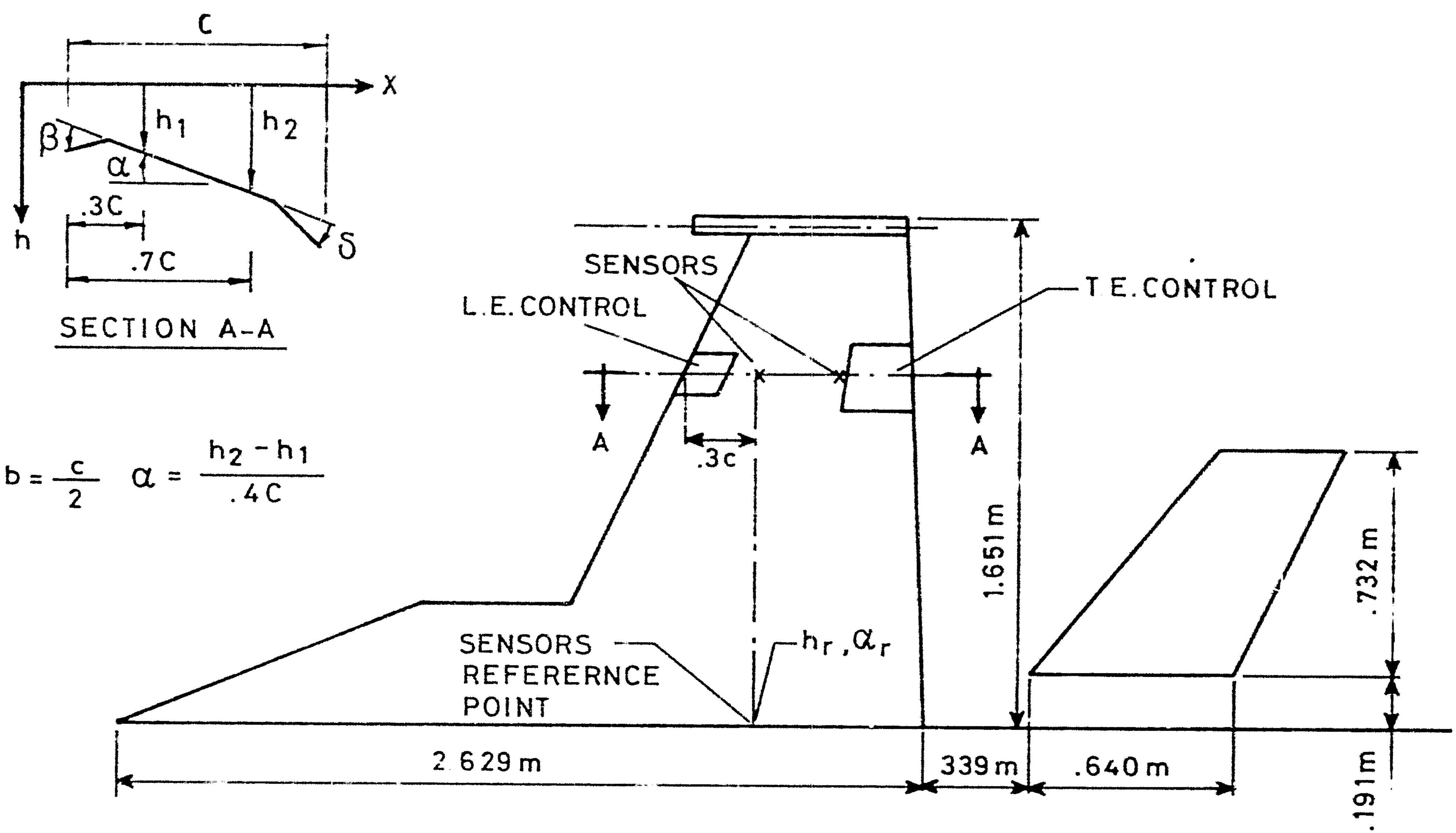

Figure 1: Plan view of YF-17 flutter model and geometrical description of the active control system

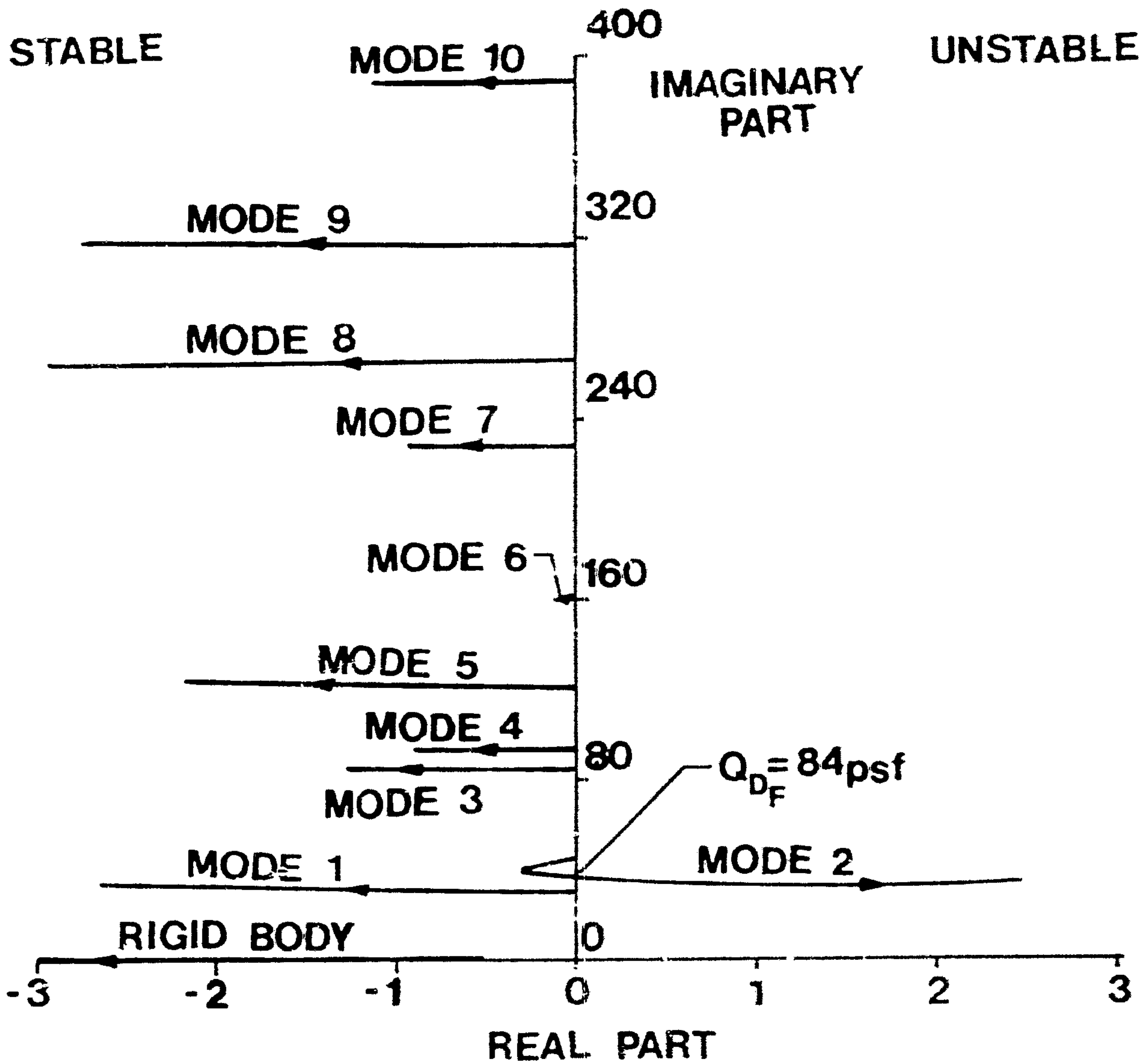

Figure 2: Open loop root locus plot (M = 0.8)

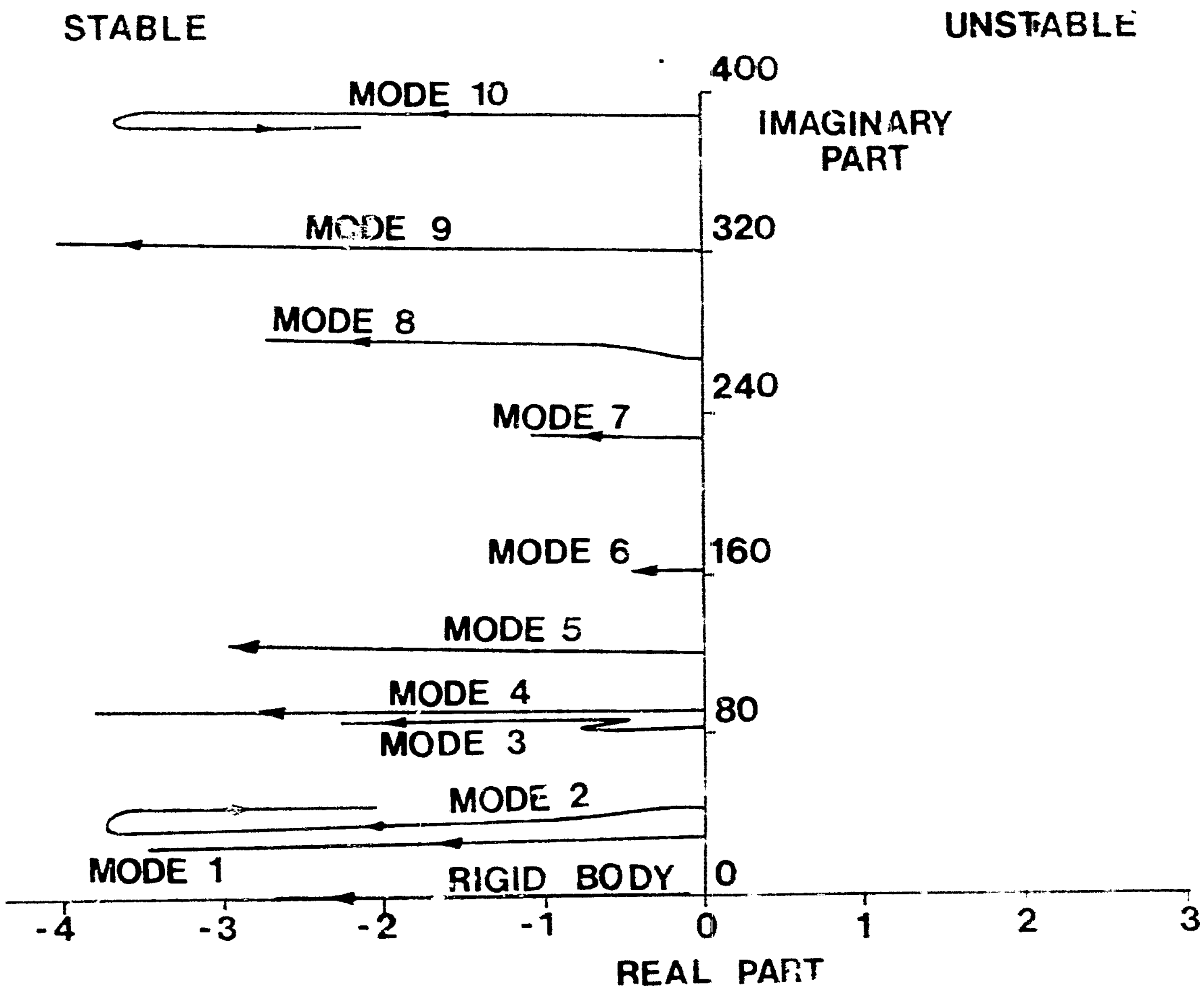

Figure 3: Closed loop root locus plot using control law obtained with mass balanced control surfaces (M = 0.8)

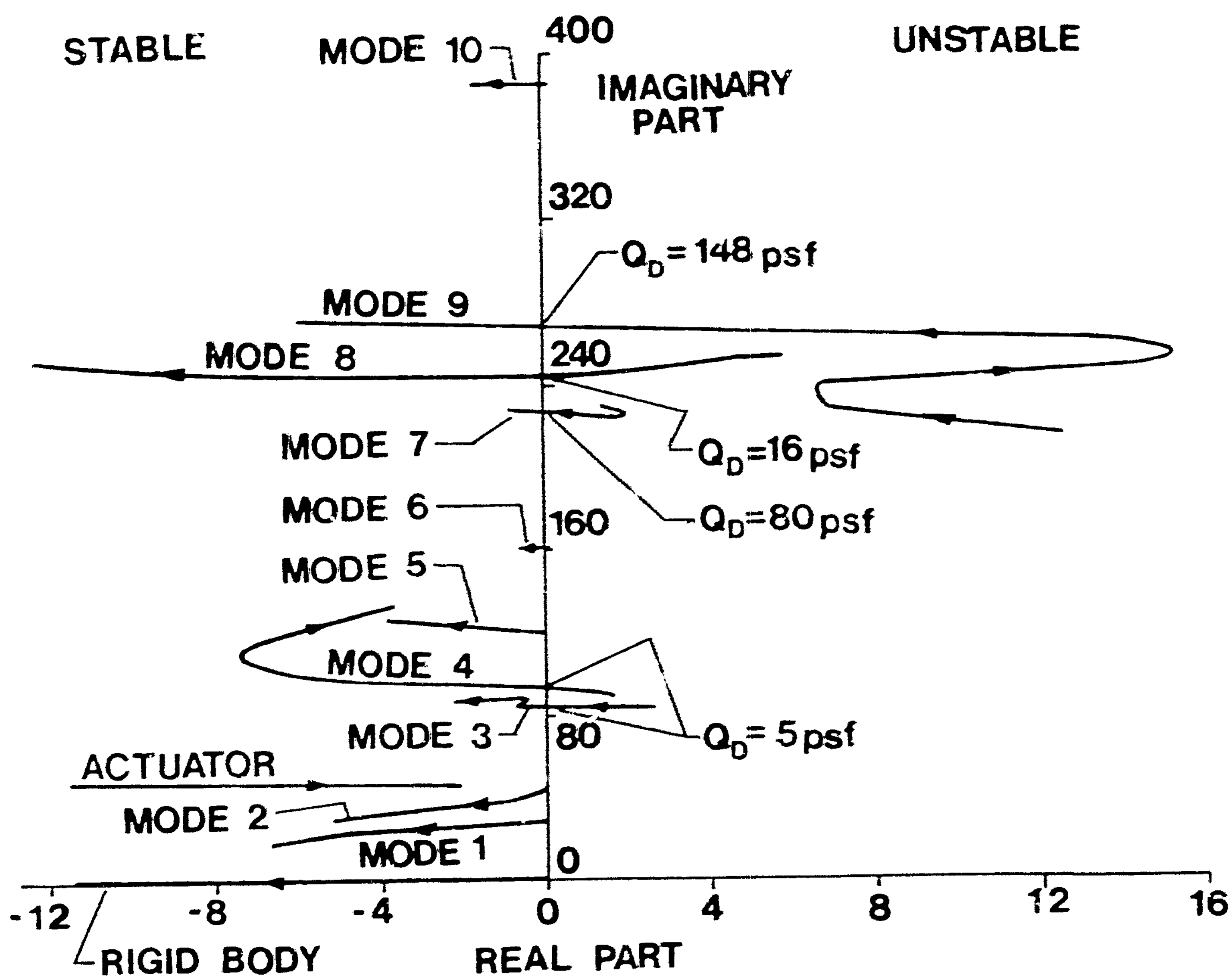

Figure 4: Closed loop root locus plot after introduction of control surfaces mass unbalance (using control law obtained for mass balanced system) at M = 0.8.

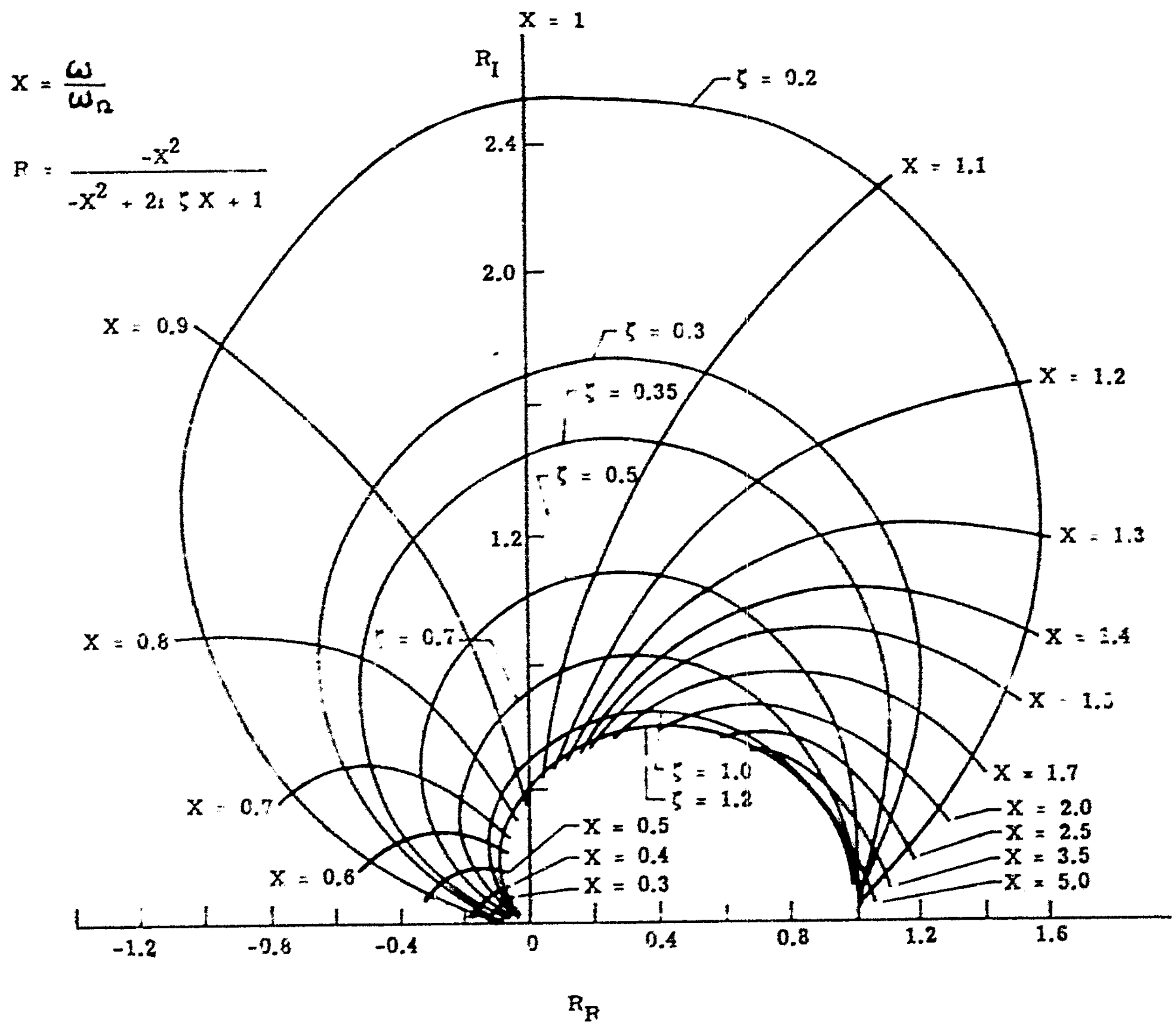

Figure 5: Variation of R with frequency

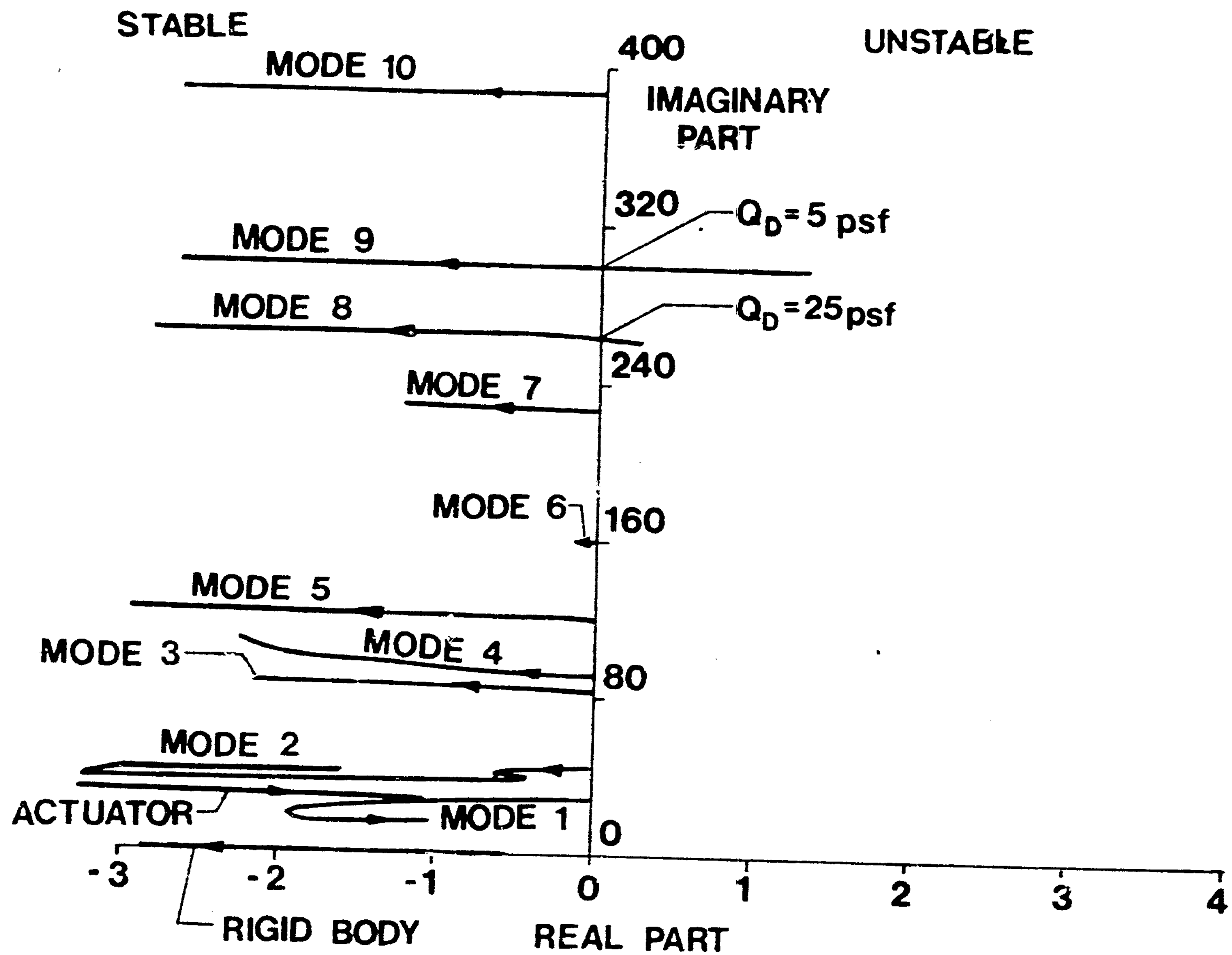

Figure 6: Closed loop root locus plot using control law I with unbalanced control surfaces (M = 0.8)

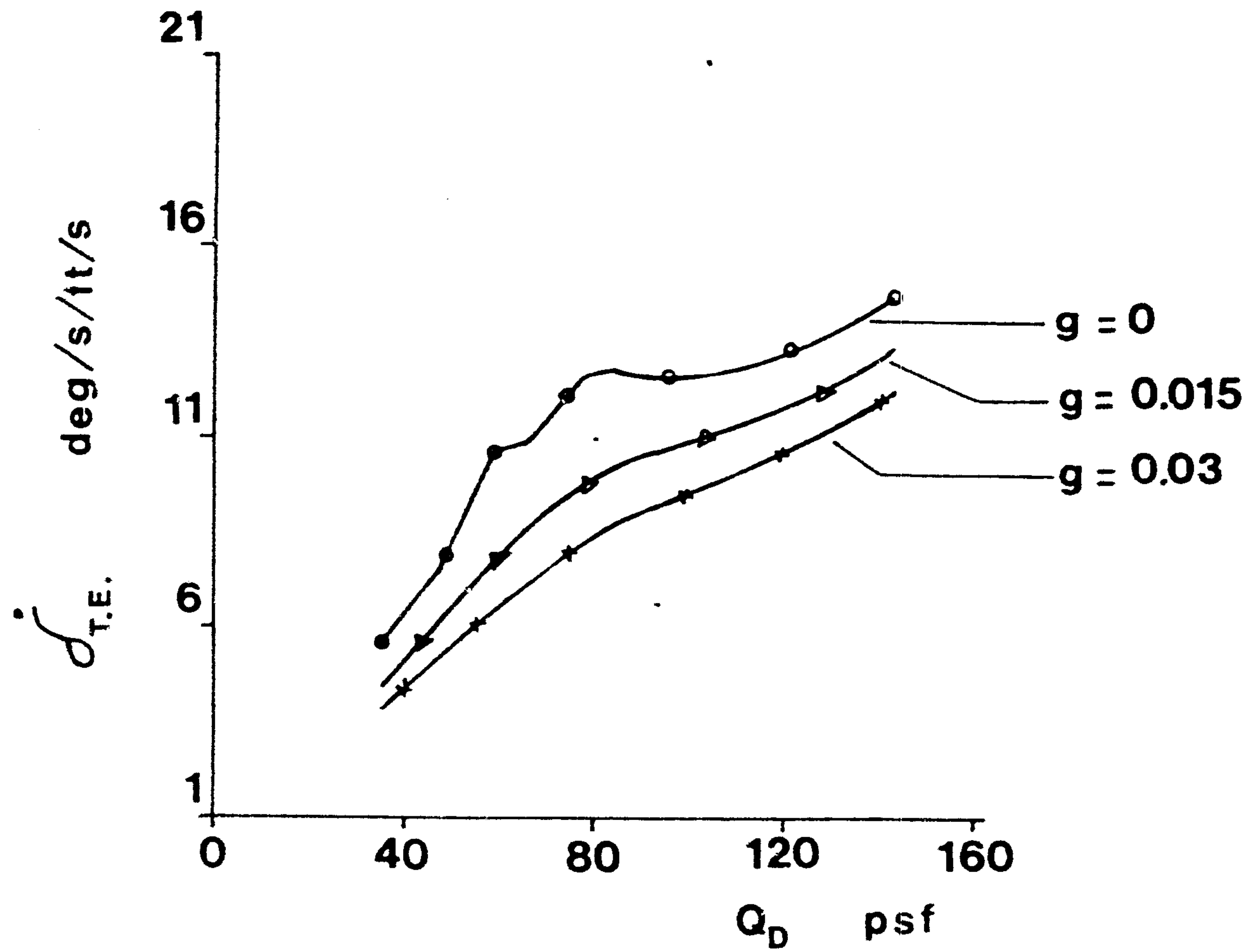

Figure 7a: T.E. control rate

Figure 7: Variation with Q_D of control surface activity, using control law I with unbalanced control surfaces (M = 0.8)

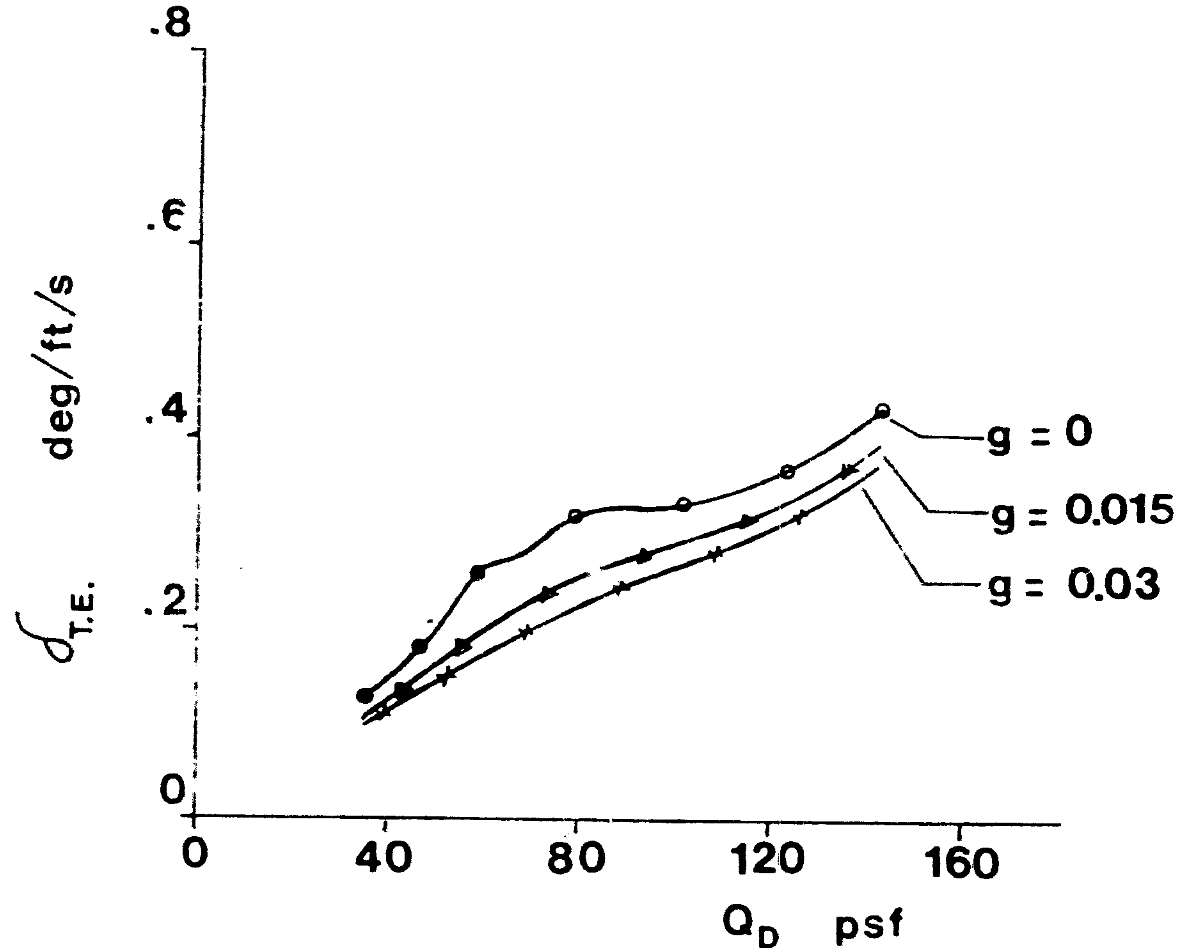

Figure 7b: T.E. control deflection

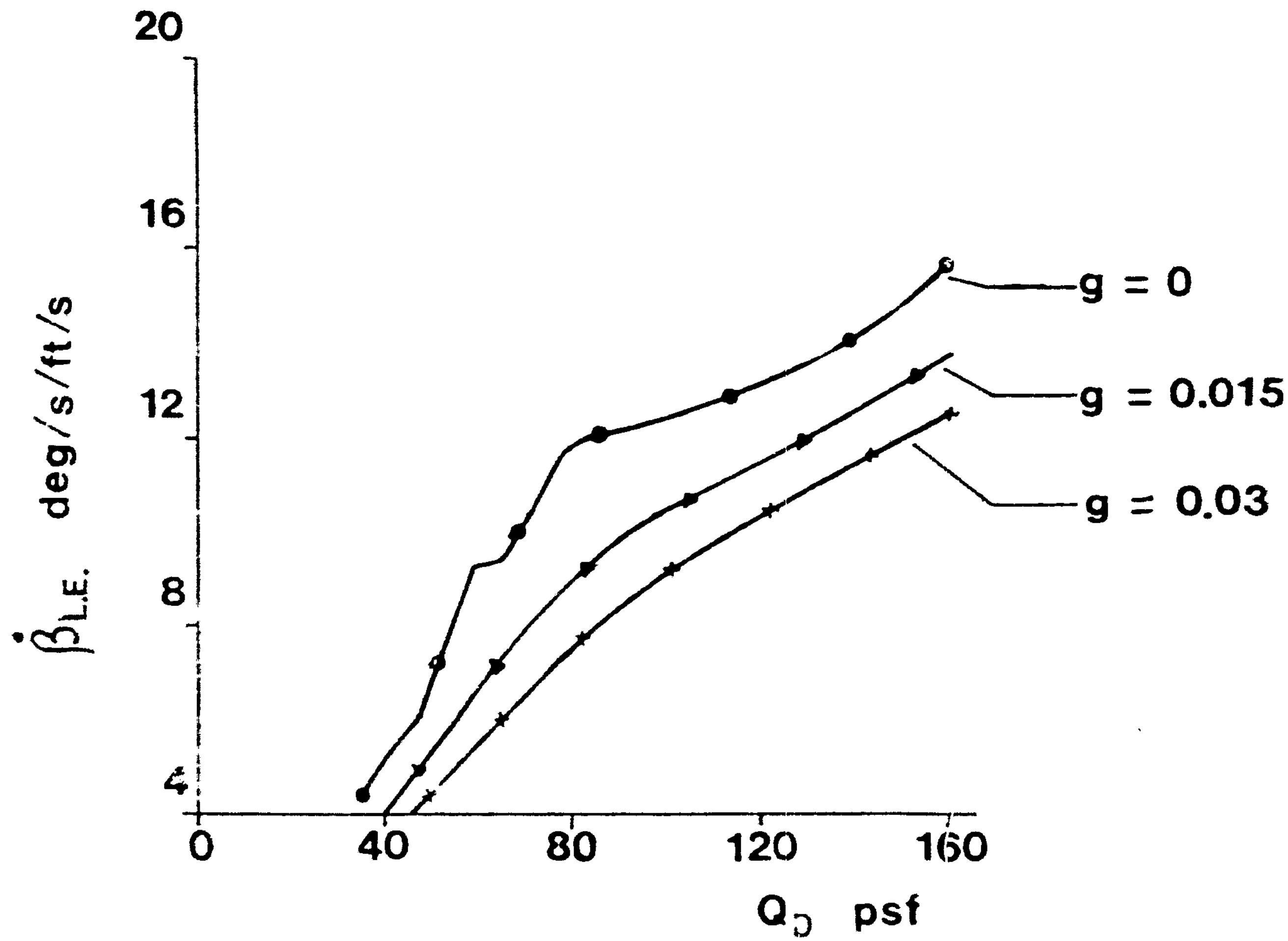

Figure 7c: L.E. control rate

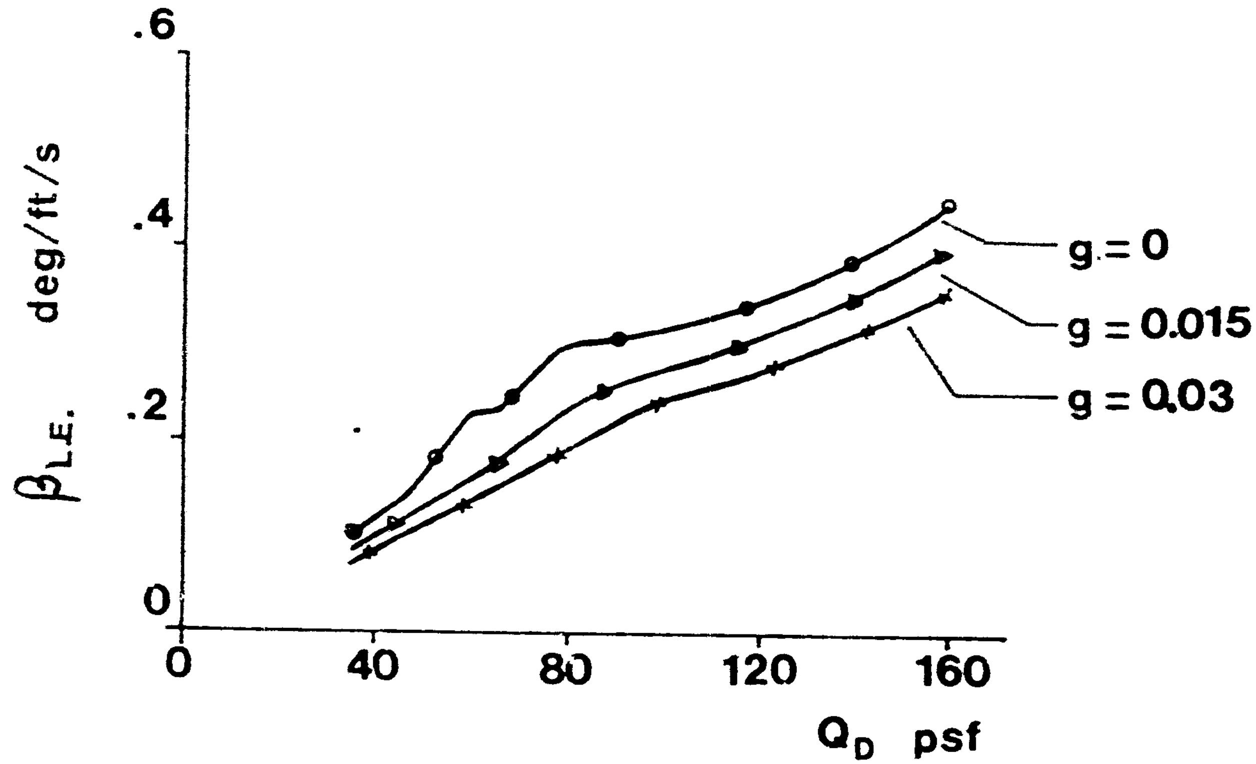

Figure 7d: L.E. control deflection

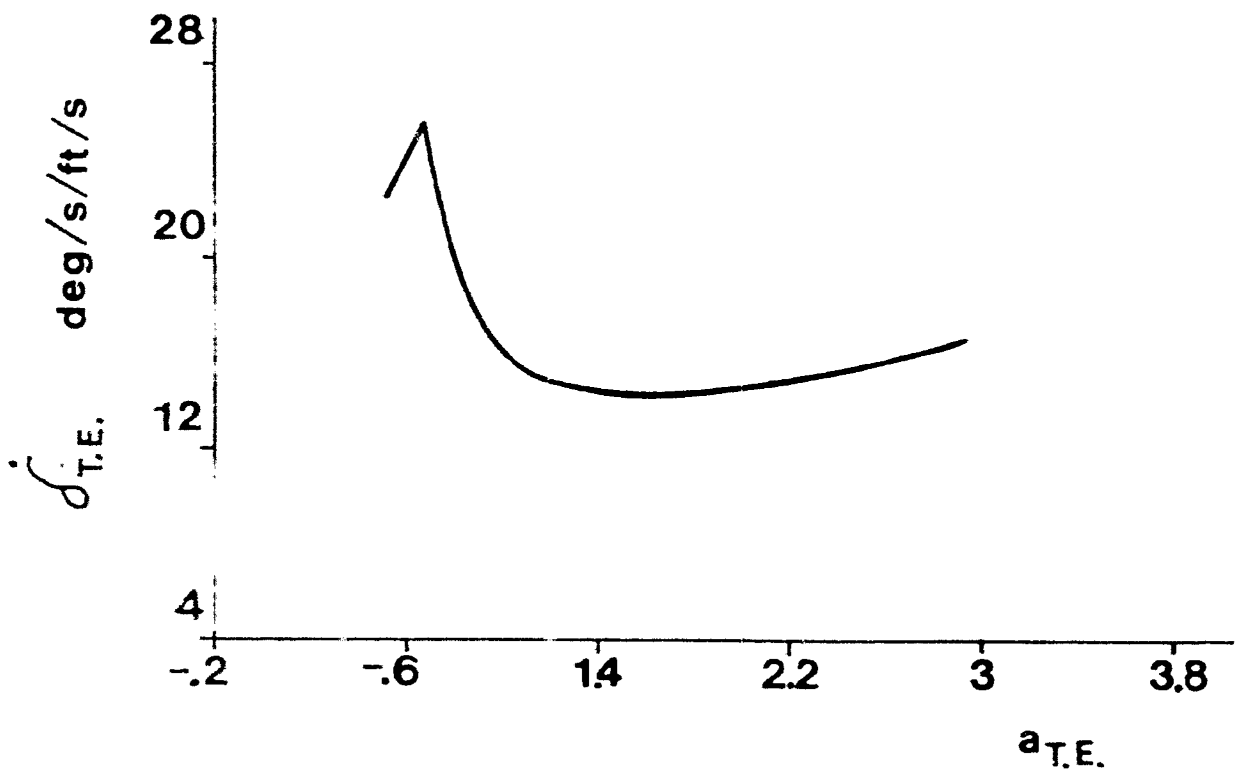

Figure 8a: Variation with $Q_{T.E.}$

Figure 8: Variation of T.E. control rate with control law parameters using control law I with Q_D = 1-3 psf (M = 0.8, unbalanced control surfa es)

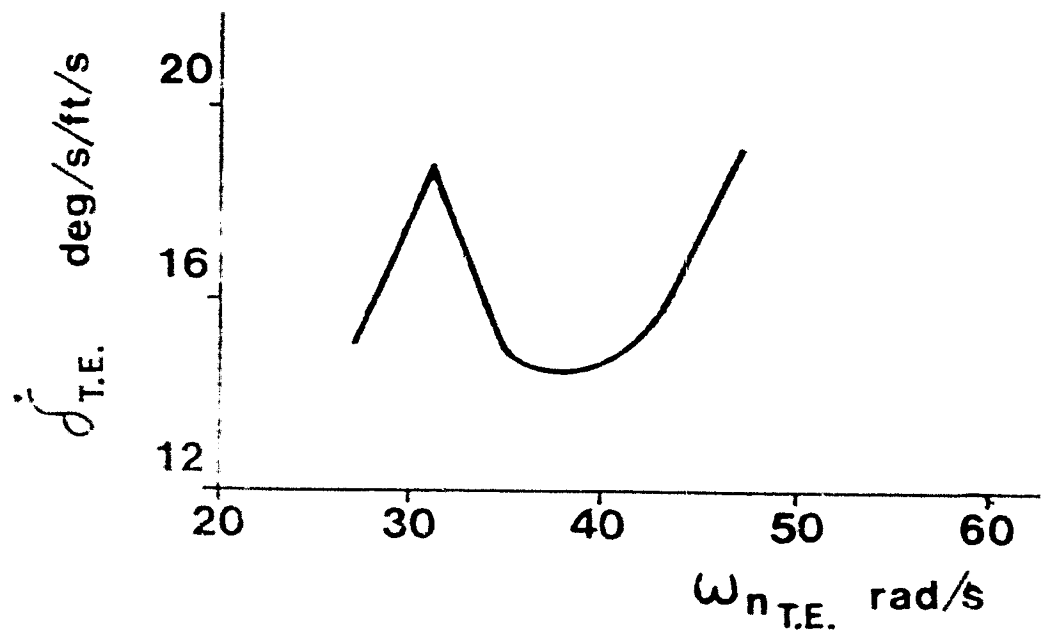

Figure 8b: Variation with $\omega_{n_{T.E.}}$

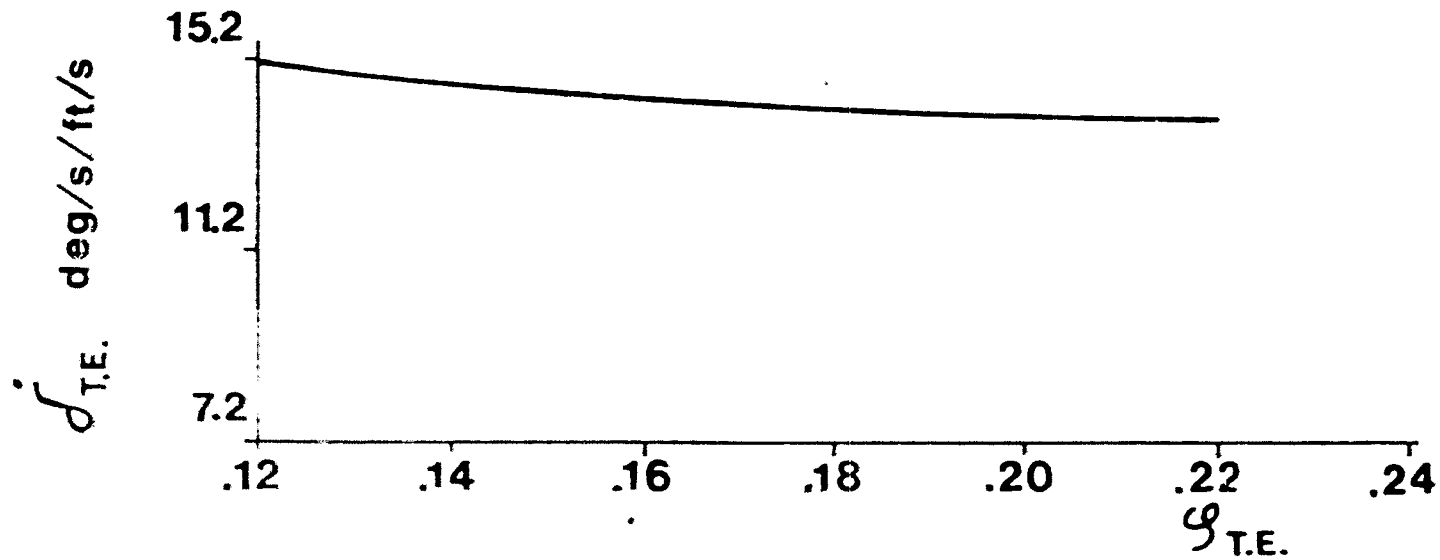

Figure 8c: Variation with $\zeta_{T.E.}$

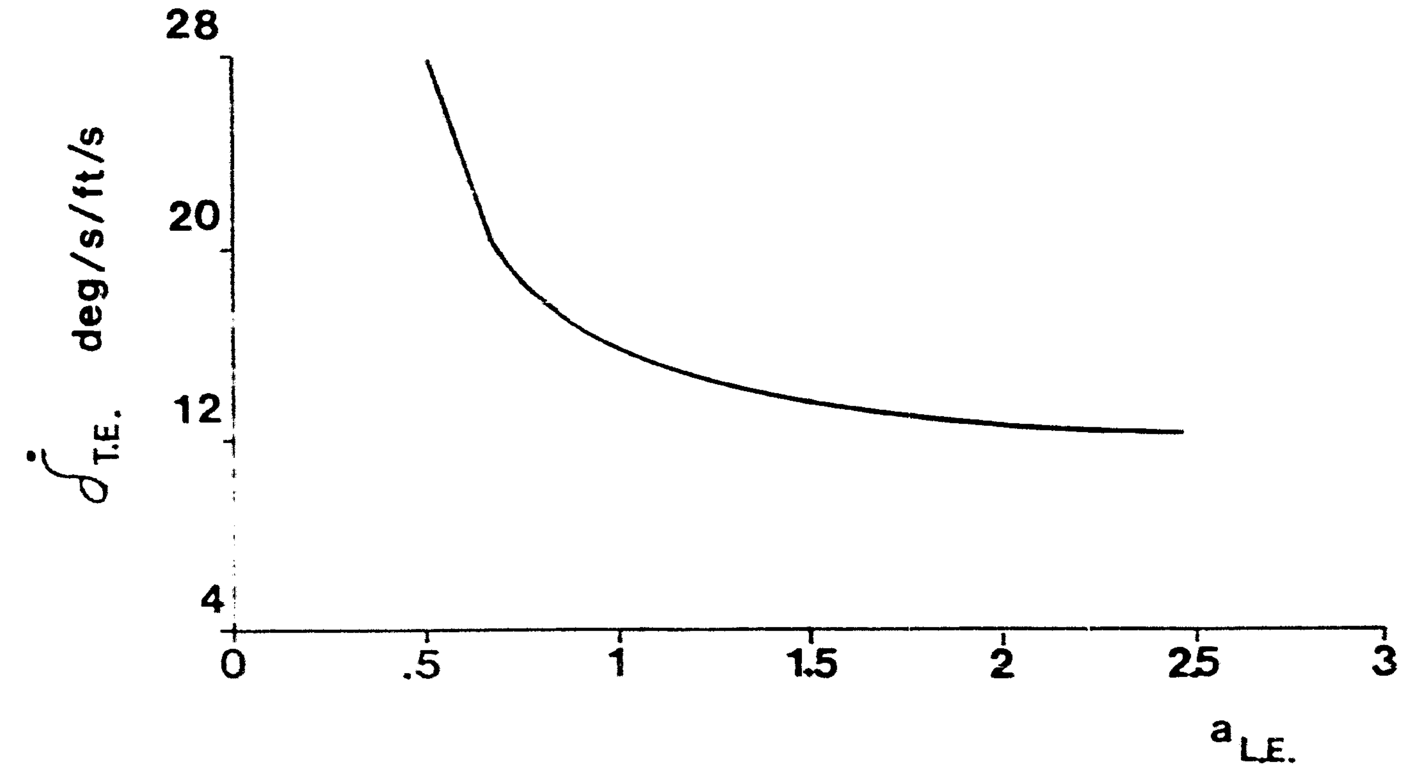

Figure 8d: Variation with $a_{L.E.}$

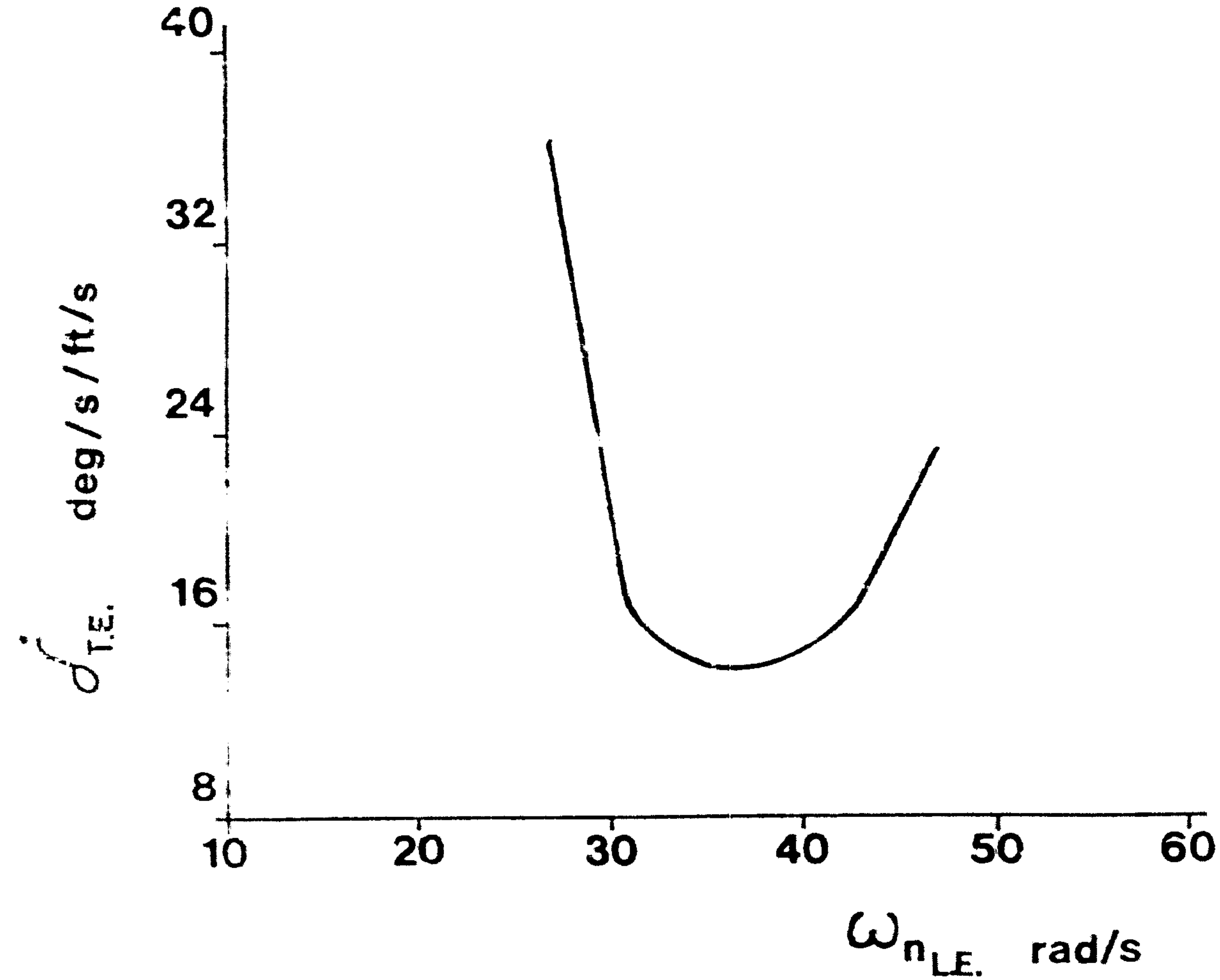

Fir :re 8e: Variation with $\omega_{n_{L.E.}}$

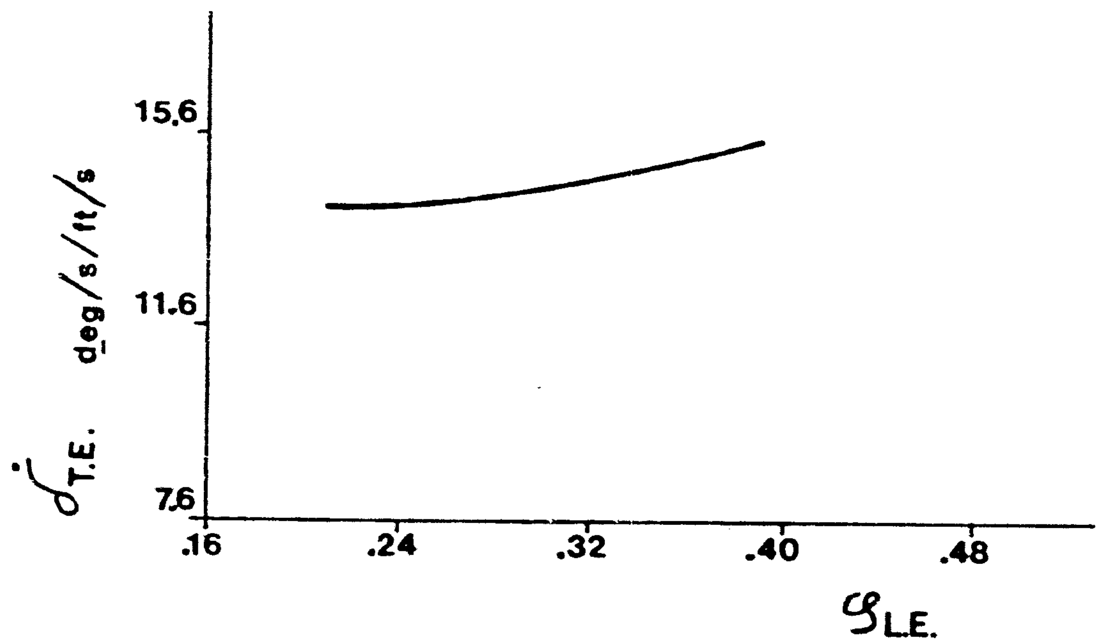

Figure 8f: Variation with $\varsigma_{L.E.}$

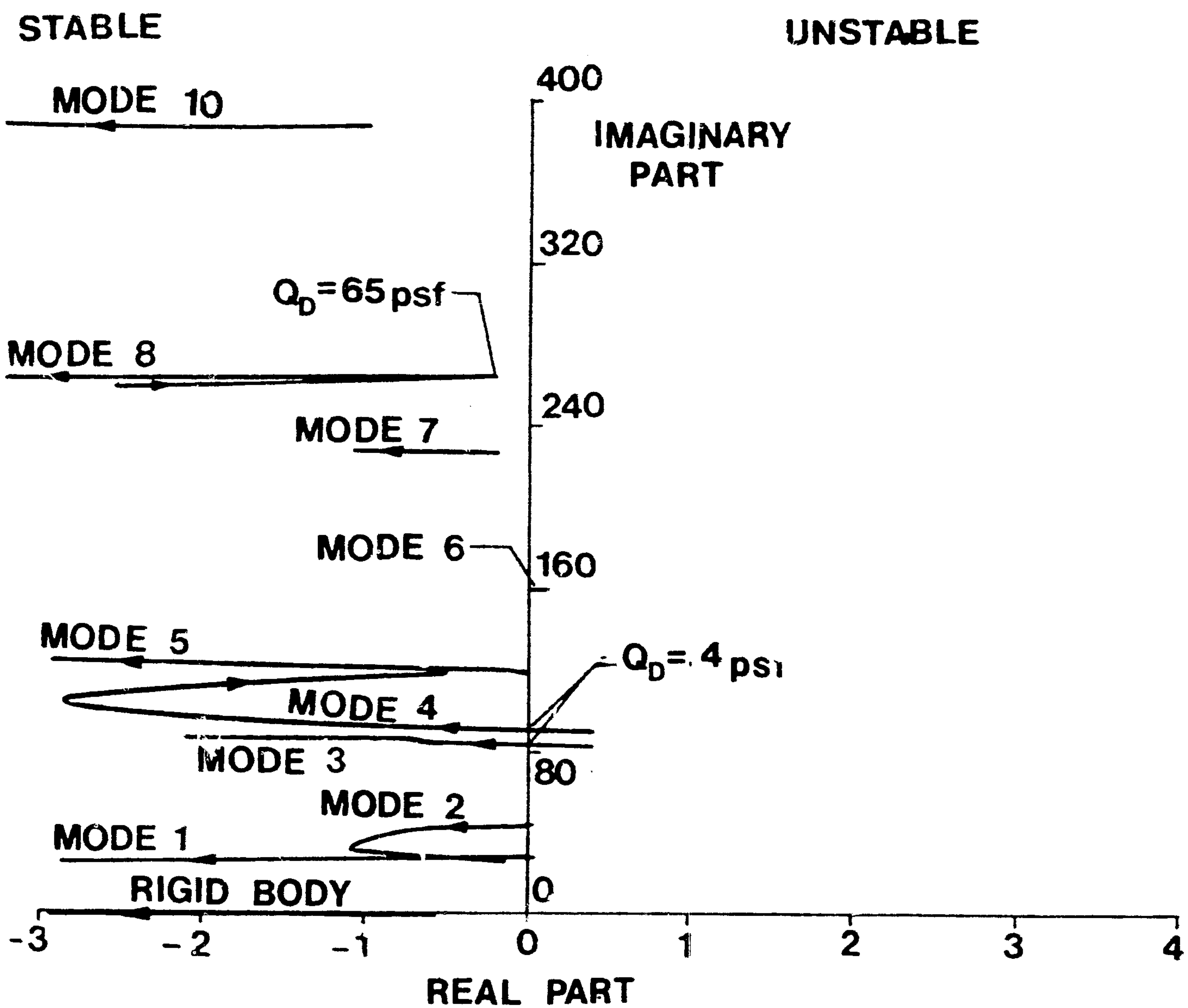

Figure 9: Closed loop root locus plot using control law II with unbalanced control surfaces (M = 0.8)

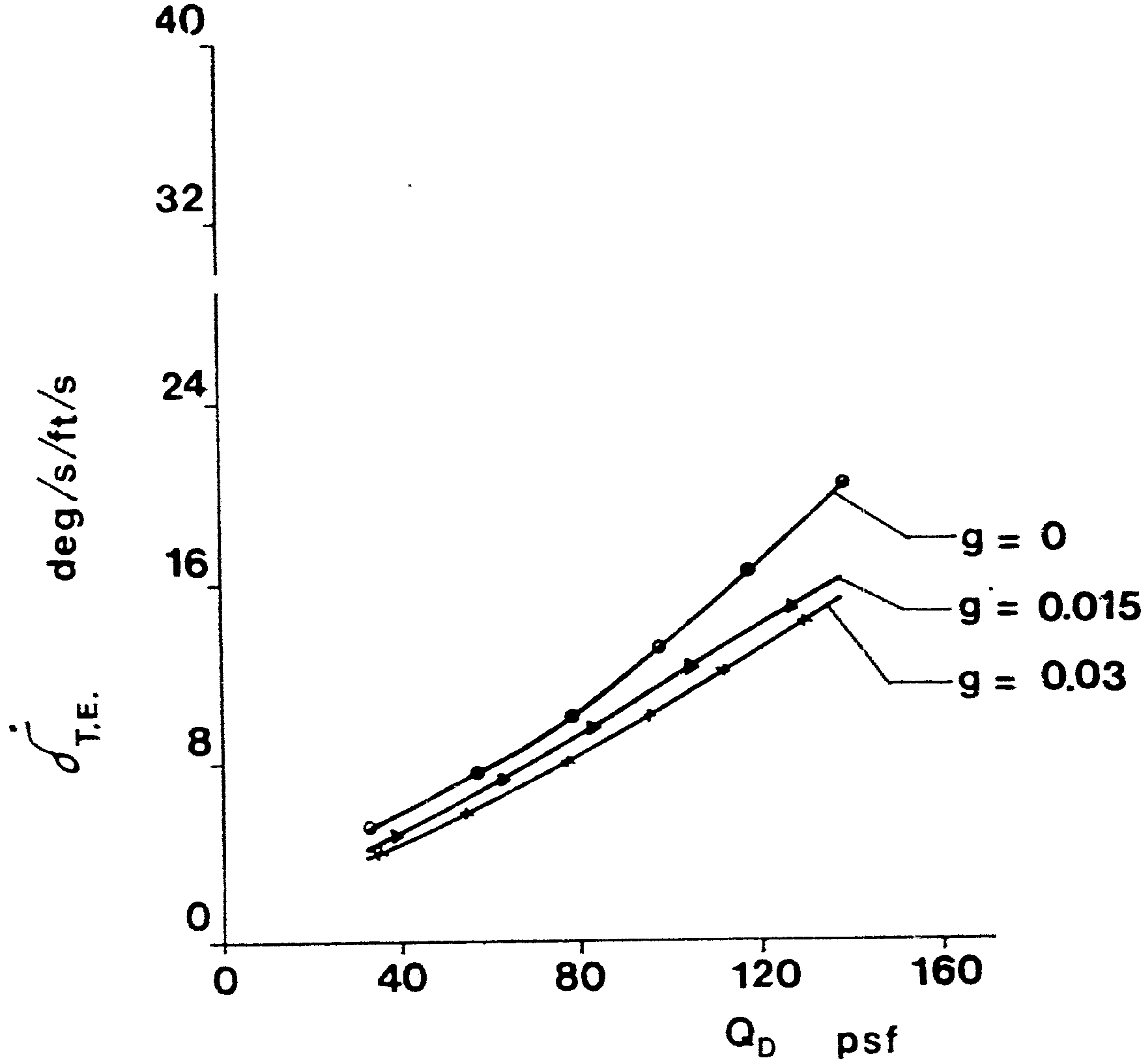

Figure 10a: T.E. control rate

Figure 10: Variation with Q_D of control surface activity, using control law II with unbalanced control surfaces (M = 0.8).

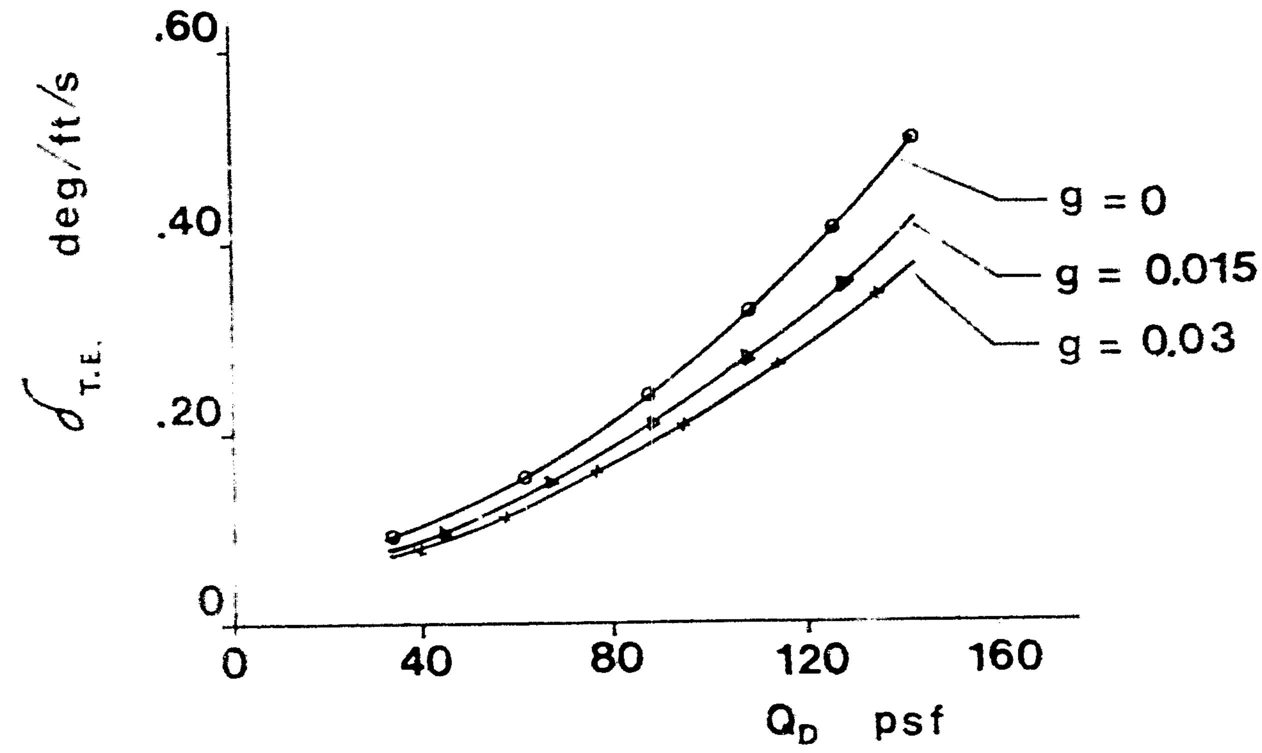

Figure 10b: T.F. control deflection

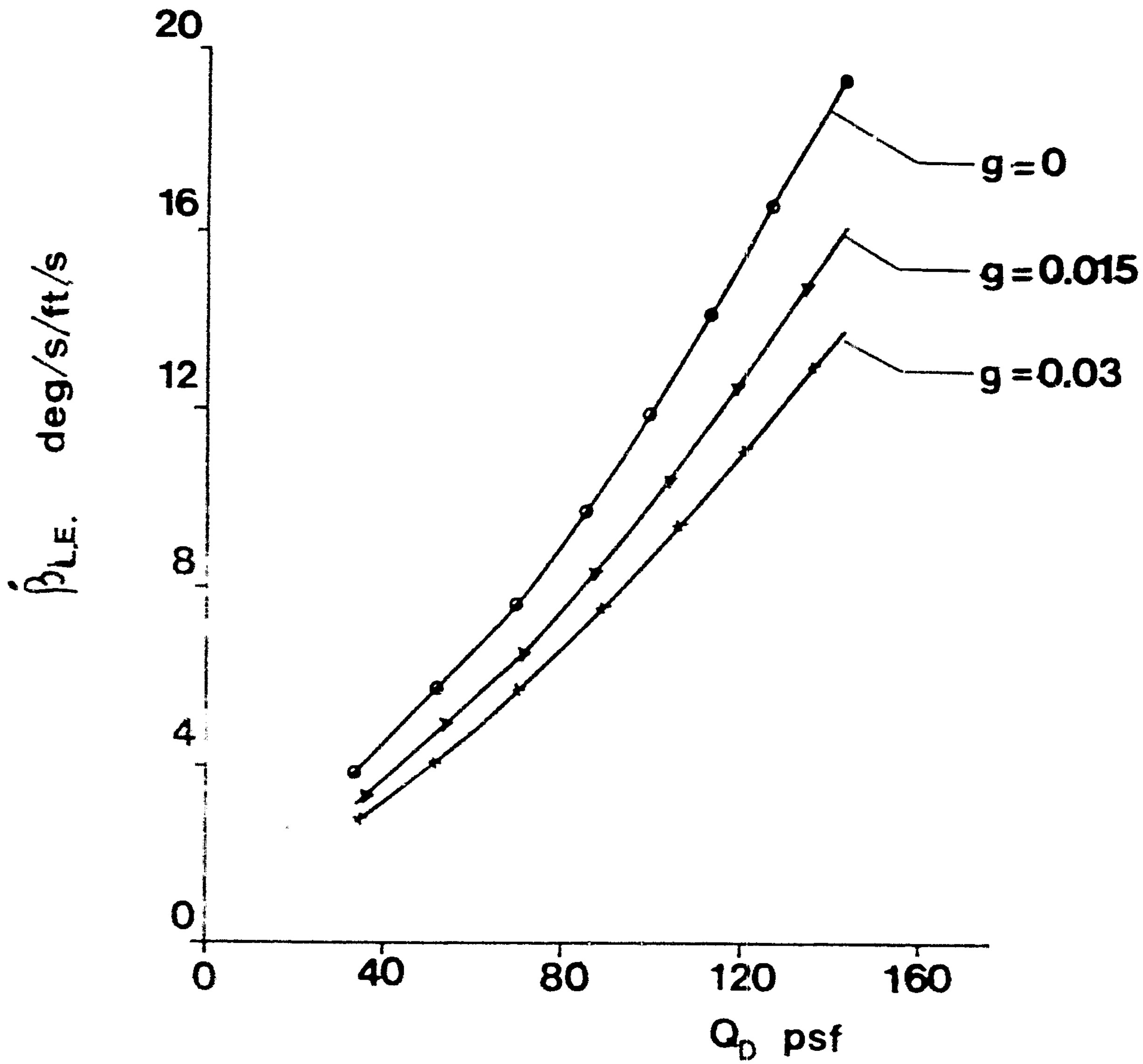

Figure 10c: L.E. control rate

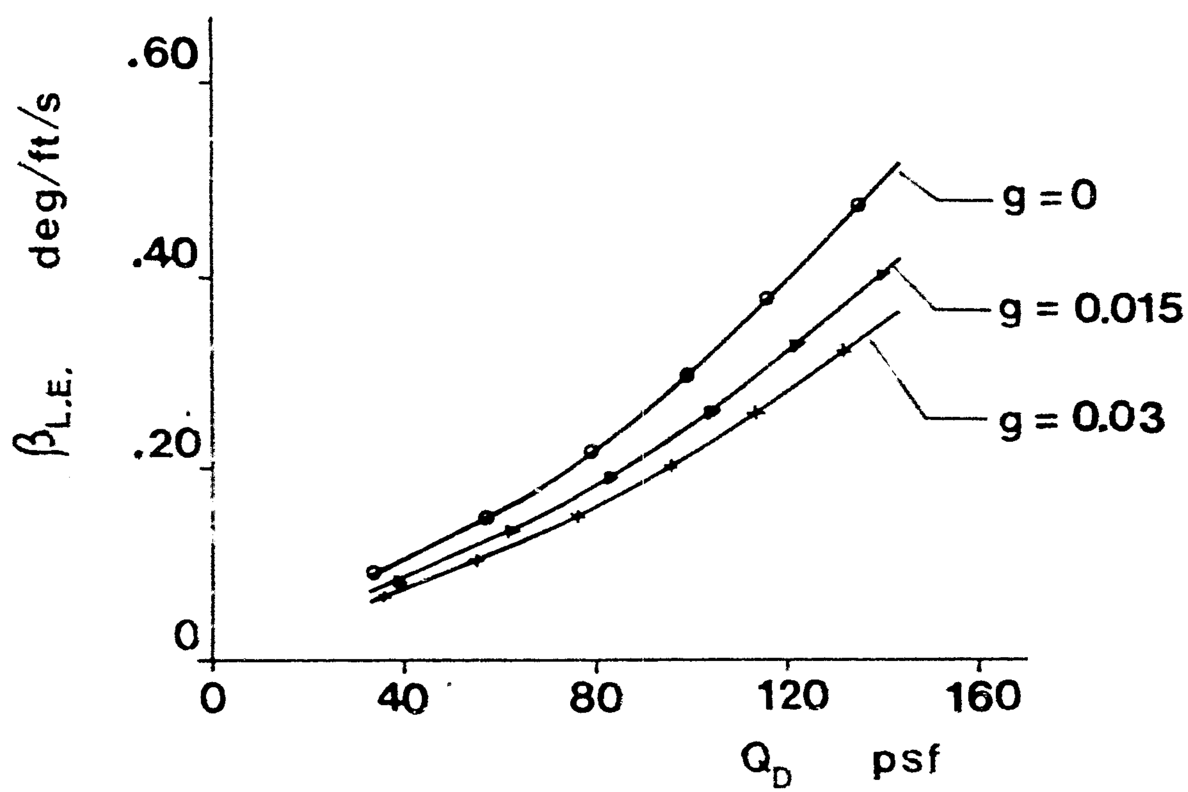

Figure 10d: L.E. control deflection

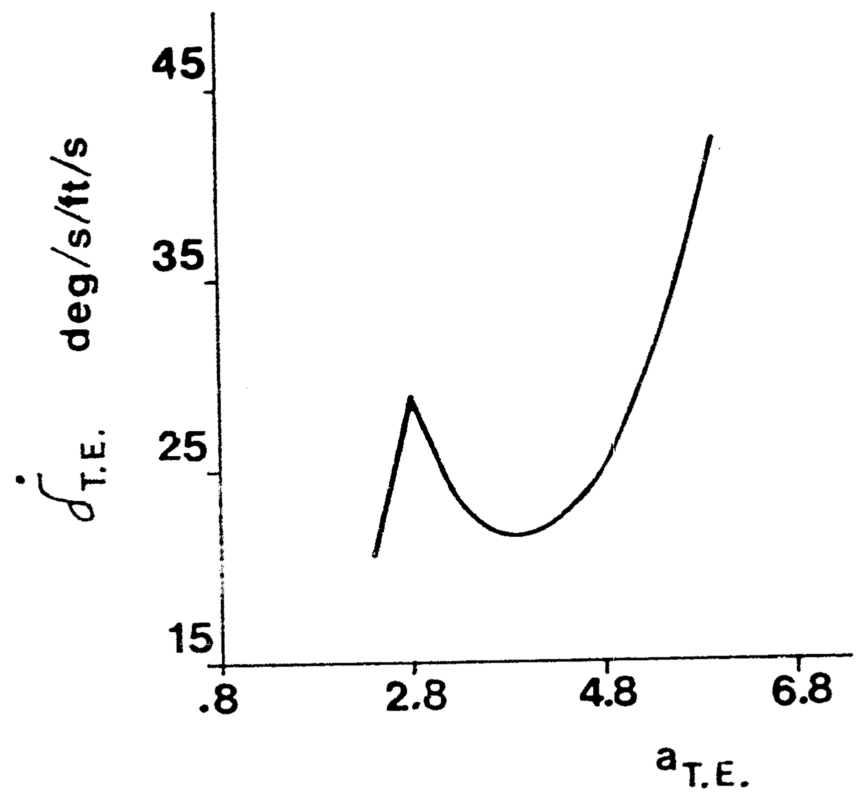

Figure 11a: Variation with $Q_{T.E.}$

Figure 11: Variation of T.E. control rate with control law parameters using control law II with Q_D = 143 psf (M = 0.8, unbalanced control surfaces).

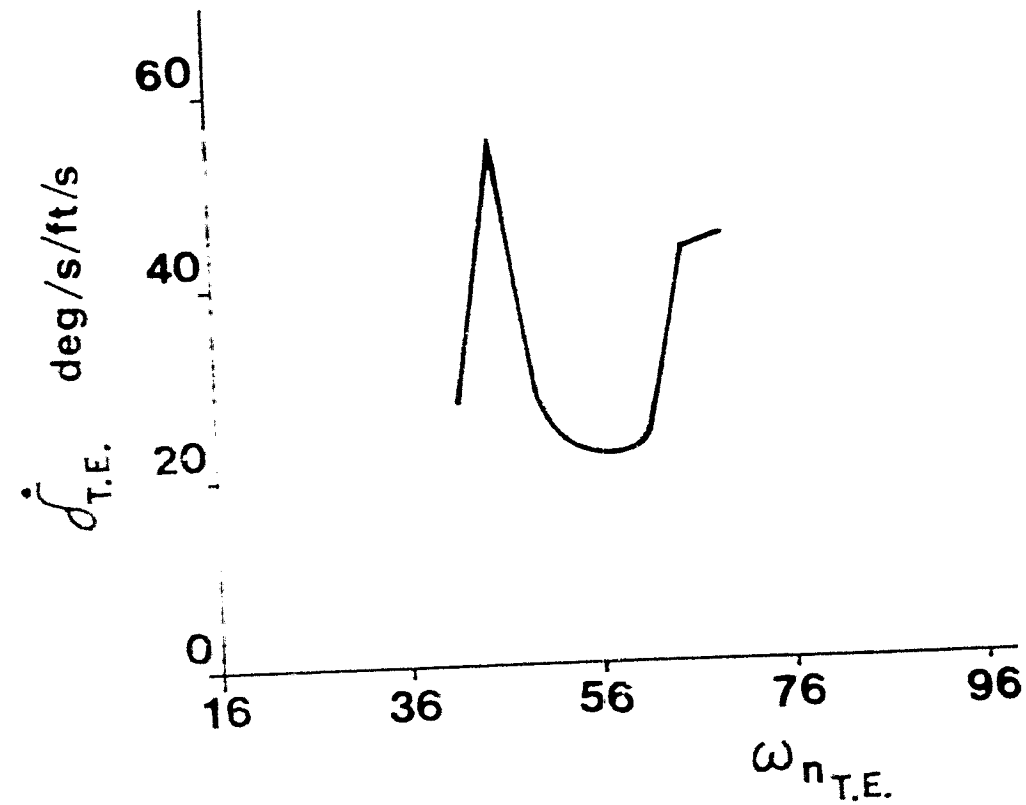

Figure 11 : Variation with $\omega_{n_{T.E.}}$

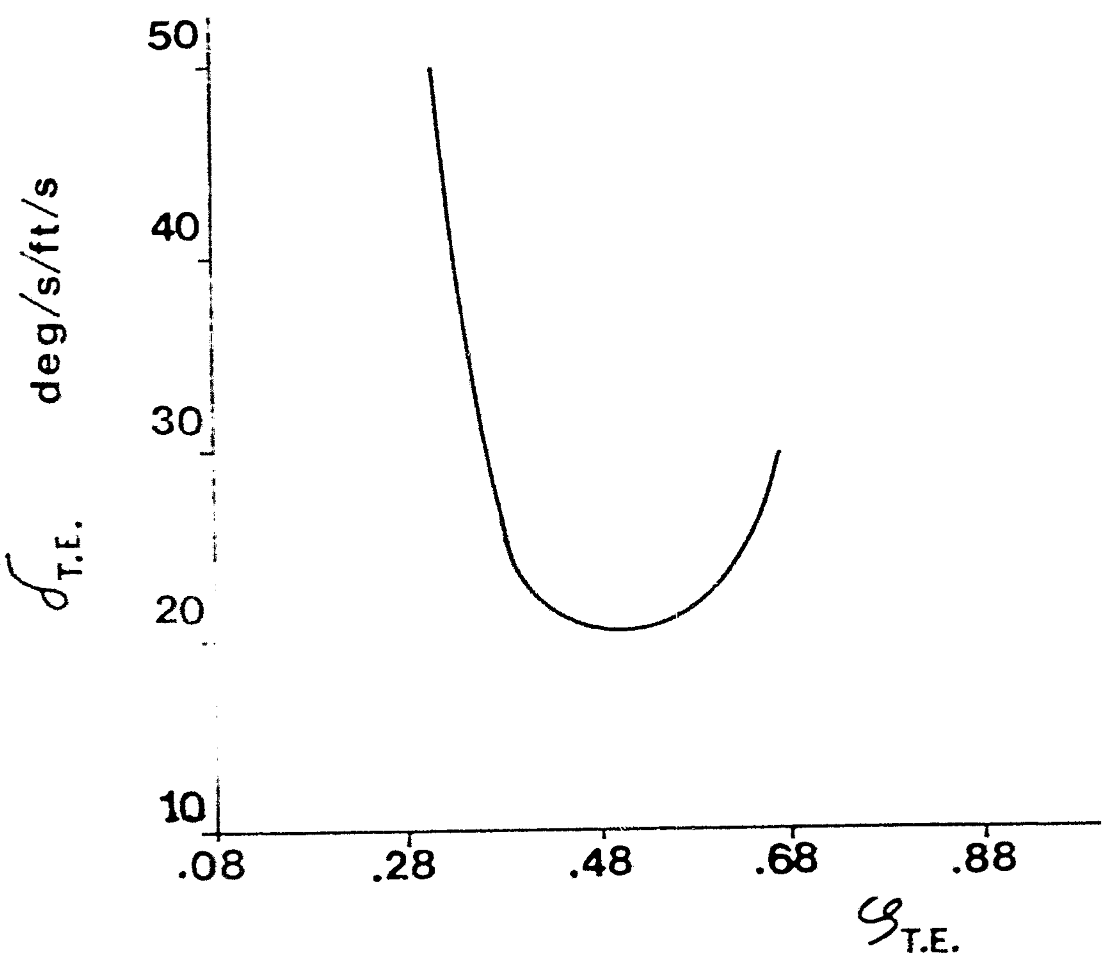

Figure 11c: Variation with $\varsigma_{T.E.}$

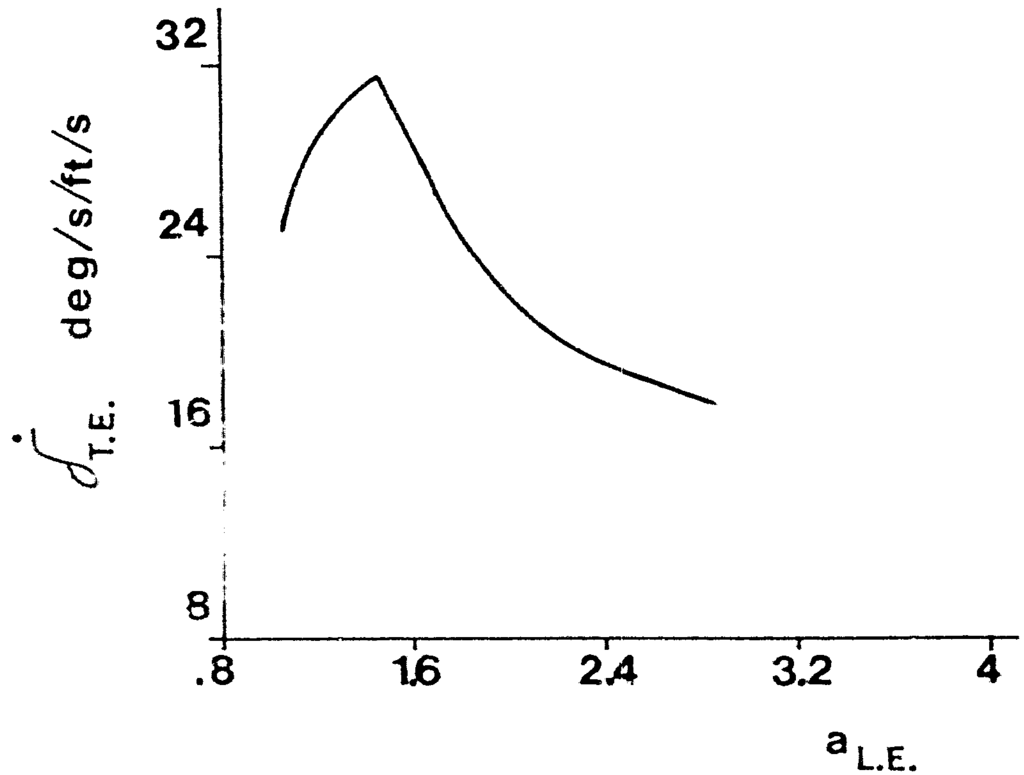

Figure 11d: Variation with $a_{L.E.}$

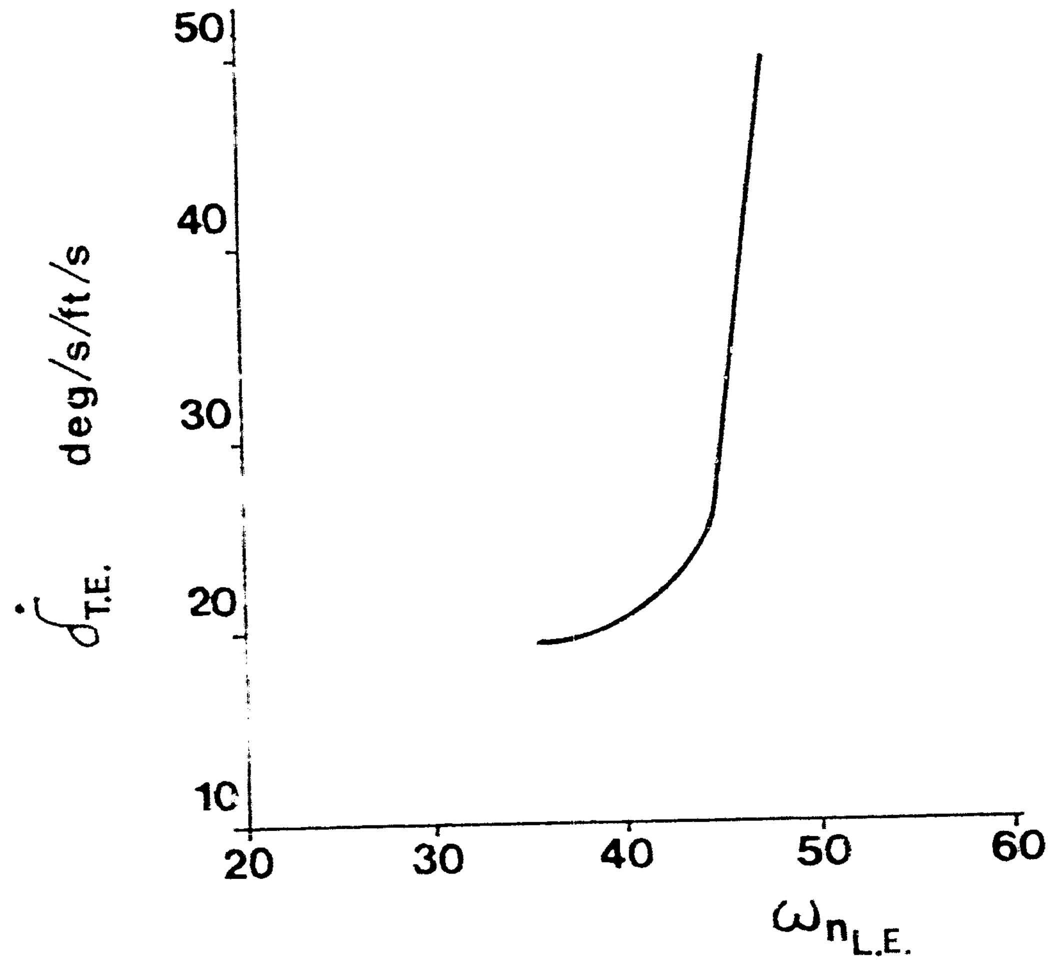

Figure 11e: Variation with $\omega_{n_{L.E.}}$

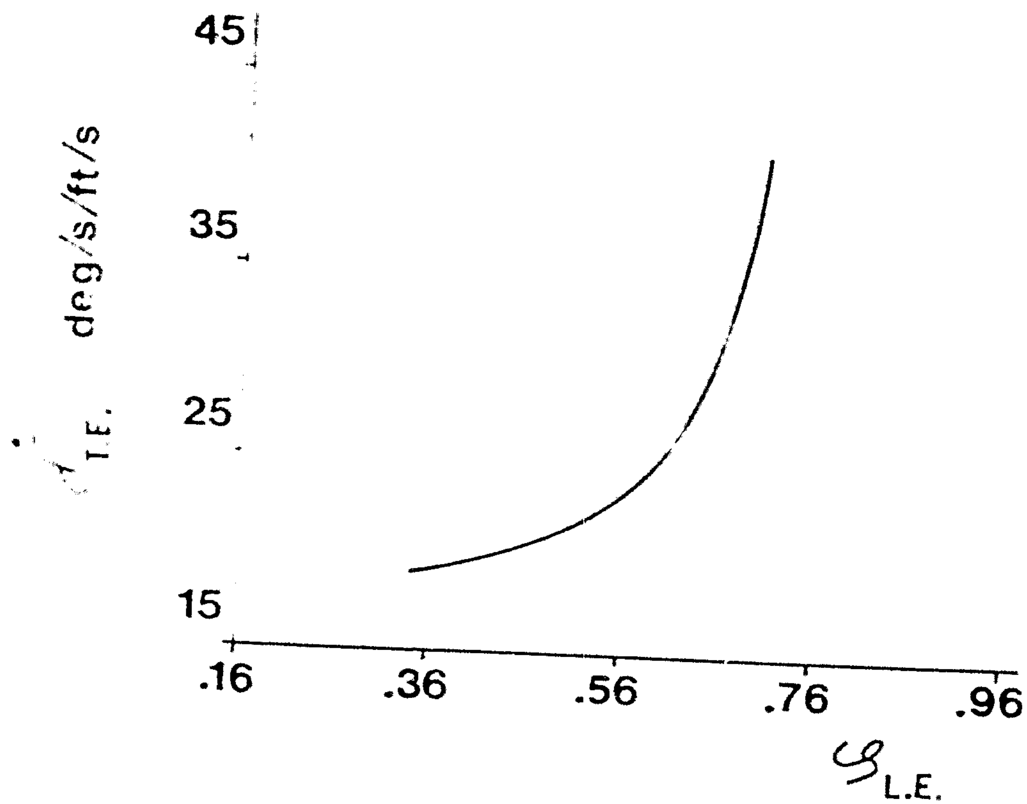

Figure [illegible] Variation with [illegible]

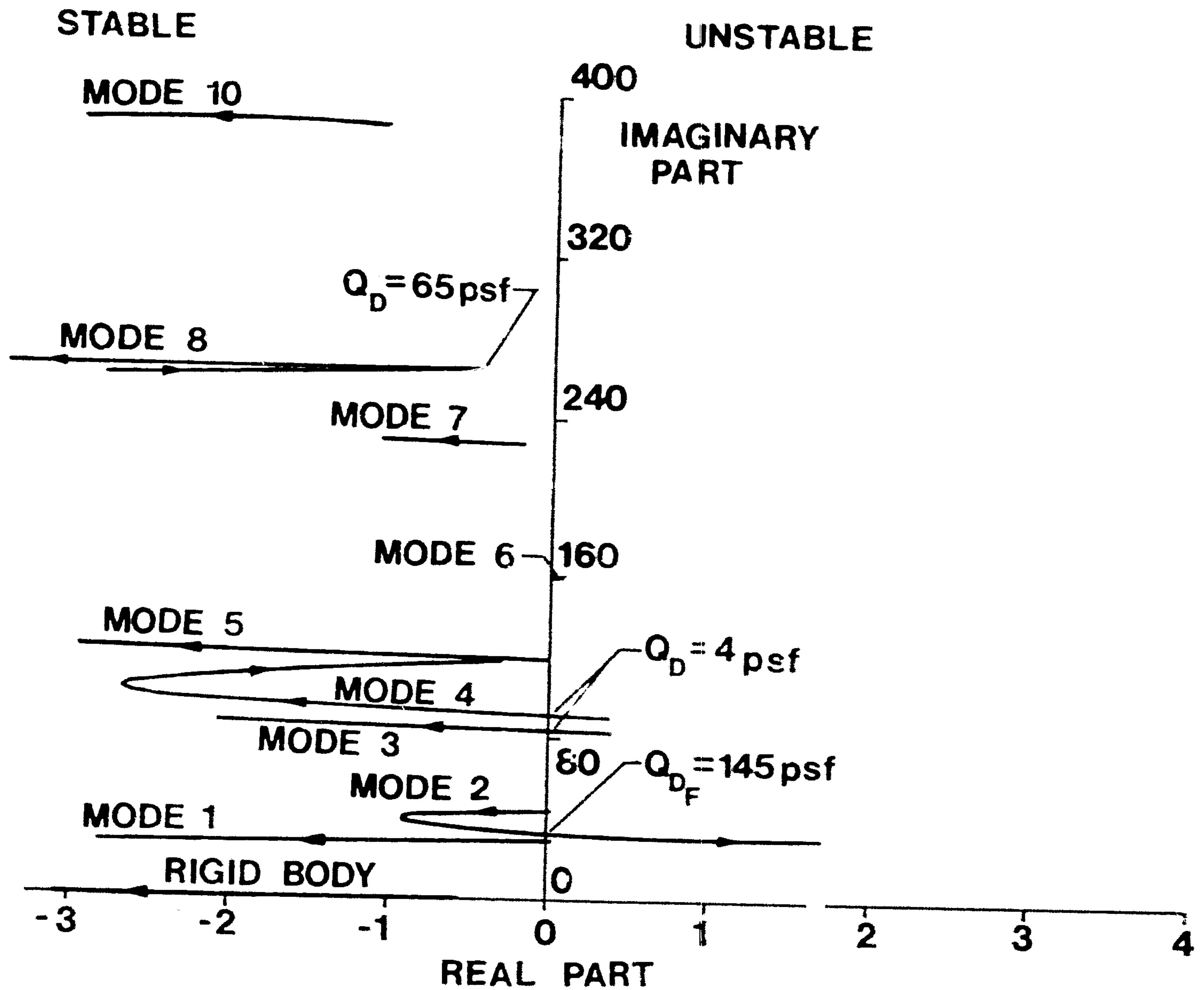

Figure 12: Closed loop root locus plot using control law II with unblanced control surfaces and with C2: = 0 (M = 0.8).

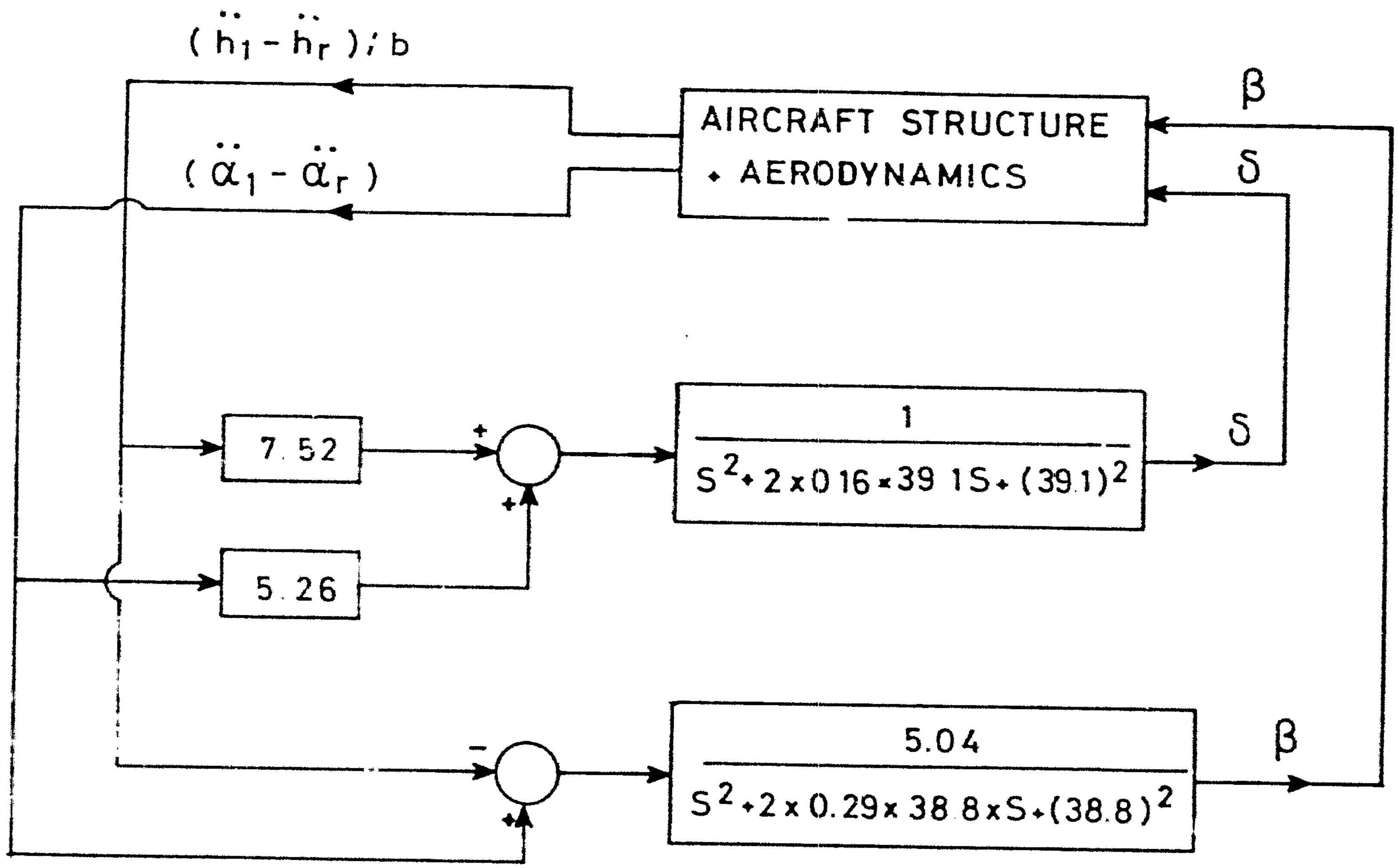

Figure 13: Block diagram representation of control law 1

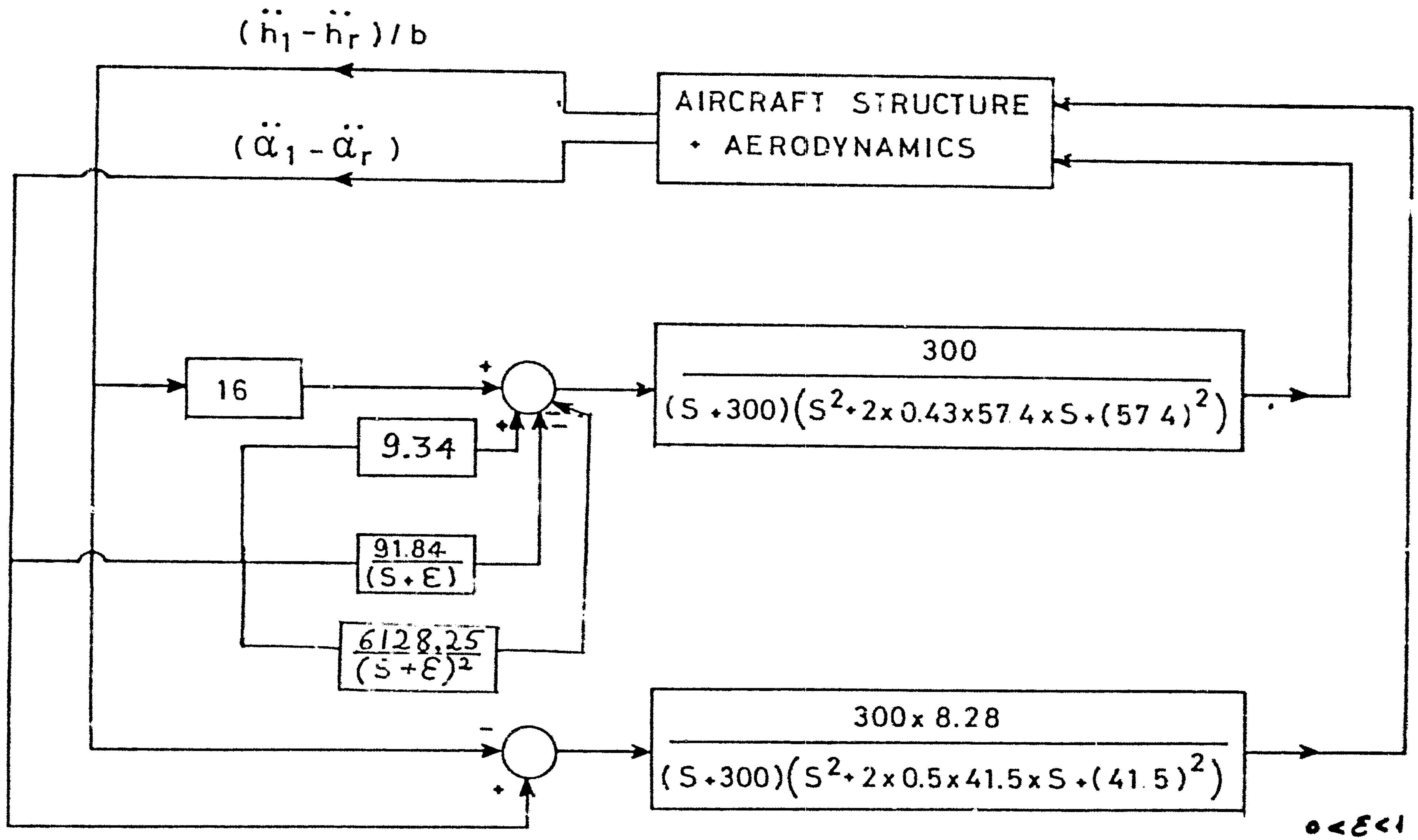

Figure 14: Block diagram representation of control law II (with [illegible]

ACTIVE EXTERNAL STORE FLUTTER SUPPRESSION IN THE MODIFIED YF-17 FLUTTER MODEL: ANALYSIS VS. WIND TUNNEL TESTS

by

E. Nissim* and I. Lottati**

Department of Aeronautical Engineering
Technion - Israel Institute of Technology,
Haifa, Israel

The work reported herein is a part of a study supported by NASA through its Aeroelasticity Branch at the Langley Research Center (under Grant NSG 7373).

----

* Professor

** Lecturer

INTRODUCTION

The investigation reported in this work relates to the suppression of external store flutter in the YF-17 flutter model. Configuration B was specified for the above purpose with the objective of enabling the activated model to be tested in a wind tunnel at Mach number $M = 0.8$ and at dynamic pressures up to 69% above the open loop flutter dynamic pressure. Two control laws were derived at an earlier stage of this work[1], and were shown to yield the desired flutter suppression capability through the activation of a combined leading-edge (L.E.) - Trailing-edge (T.E.) control system.

The mechanization of one of the derived control laws was carried out by Northrop and subsequently, the flutter stability augmented YF-17 model was tested in the Langley 16 ft transonic dynamic tunnel. The test results, as reported to the authors of the present work, showed no correlation with the analysis and the tunnel tests were discontinued at a dynamic pressure which was below the open loop flutter dynamic pressure.

The object of the present paper is to present a critical review of the analysis versus the test results and to indicate the sources of the discrepancies obtained. For convenience, some of the major result reported in Reference 1 will be presented herein once again.

ANALYTICAL RESULTS[1] - INITIAL MODEL

Background

The analytical results reported in Ref. 1 were based on a dynamic model supplied by NASA. It included generalized masses, natural frequencies and mode shapes for 10 symmetric structural modes and two rigid body modes. The generalized aerodynamic forces were computed using the Doublet-Lattice method with 126 boxes on each wing and 32 boxes on each half horizontal tail. The box allocation was identical to the one appearing in the Northrop report supplied to the authors of this paper.

The general form of the control laws is given by the following expression

$$\begin{Bmatrix}\beta\\ \delta\end{Bmatrix} = \left(\begin{bmatrix}0&0\\0&C_{22}\end{bmatrix} + \begin{bmatrix}R_{L.E.}&0\\0&R_{T.E.}\end{bmatrix}\begin{bmatrix}-4&4\\4&2.8\end{bmatrix}\right)\begin{Bmatrix}\dfrac{h_1-h_r}{b}\\ \alpha_1-\alpha_r\end{Bmatrix} \qquad (1)$$

where β and δ are the deflections of the L.E. and T.E. control surfaces, respectively, and where h_1 , α_1 denote the translation and rotation of the 30 percent chord point at the control surface mid-span section, respectively (see Fig. 1). The parameters h_r and α_r similarly denote the translation and rotation of a reference point located along the center line of the fuselage and b denotes the semi-chord length at the control surface mid span section. The R's represent transfer functions which are dependent on S where $S = i\omega$.

Open Loop Results:

The root locus plot for the open loop system, with the dynamic pressure Q_D acting as a parameter, is shown in Fig. 2. As can be seen, the value of the dynamic pressure at flutter (Q_{DF}) is equal to Q_{DF} = 84 PSF, with frequency ω = 36.6 rad/s.

Closed Loop Results:

Activation of the T.E. alone yielded only marginal improvements in Q_{DF}, indicating the need to relocate the control surface (see also Refs. 2,3). The L.E. alone yielded better results but since these results originated from changes in responses associated with the energy eigenvectors and not from changes in the energy eigenvalues (as required by the energy approach), the work based on a L.E. alone system was not persued. Hence, the work reported herein relates to a combined L.E.-T.E. system (at M = 0.8).

Two closed loop L.E.-T.E. control laws were derived and presented in Ref. 1. They are presented once again in the following for sake of completeness.

Control Law 1:

In this control law $C_{22} = 0$ and the R's appearing in Eq.(1) are given by

$$R_{T.E.} = \frac{1.88\ S^2}{S^2 + 2 \times 0.16 \times 39.1 \times S + (39.1)^2} \tag{2}$$

$$R_{L.E.} = \frac{1.26\ S^2}{S^2 + 2 \times 0.29 \times 38.8 \times S + (38.8)^2} \tag{2}$$

The root locus plot associated with the above control system is shown in Fig. 3, (assuming zero structural damping, $g = 0$). As can be seen, except for a small region of instability at very low values of Q_D (which is counteracted by normal structural damping), no flutter exists up to $Q_D = 200$ psf. The maximum control activity (at $Q_D = 143$ psf, corresponding to the highest specified Q_D) is given by (for $g=0$)

$$\dot{\delta}_{rms} = 14.86 \text{ deg/s/ft/s}$$

$$\delta_{rms} = 0.44 \text{ deg/ft/s}$$

$$\dot{\beta}_{rms} = 14.26 \text{ deg/s/ft/s}$$

$$\beta_{rms} = 0.4 \text{ deg/ft/s}$$

The variation of the control activity with Q_D for various values of g is shown in Fig. 4. The block diagram for the control system associated with control law 1 is shown in Fig. 5.

At this stage it may be observed that the R's presented in Eq.(2) represent transfer functions of second order systems. Since actuators often have the form of third order systems, it was decided to increase the order of the R's to yield three poles, so that normal actuators may be compensated through the newly derived control law. This point will be made clear in the following section.

Control Law II:

This control law was derived by using the synthesis technique[4] in the presence of a filter 300/(S+300) which multiplies the transfer functions shown in Eq.(1). The above value of 300 was determined following a parametric study in conjunction with the synthesis technique mentioned earlier. The values obtained for the R's appearing in Eq.(1) are given by

$$R_{T.E.} = \frac{4S^2}{S^2 + 2 \times 0.43 \times 57.4 \times S + (57.4)^2}$$

$$R_{L.E.} = \frac{2.07S^2}{S^2 + 2 \times 0.5 \times 41.5 \times S + (41.5)^2} \tag{3}$$

with $C_{22} = -1.86$ and $g = 0$.

The closed loop root locus plot (with $g = 0$) is shown in Fig. 6. As can be seen, there is no flutter up to $Q_D = 200$ psf. The maximum control activity (for $g = 0$) is given at $Q_D = 143$ psf by the following values:

$\dot{\delta}_{rms} = 21.38$ deg/s/ft/s

$\delta_{rms} = 0.51$ deg/ft/s

$\dot{\beta}_{rms} = 19.35$ deg/s/ft/s

$\beta_{rms} = 0.52$ deg/ft/s .

The variation of the control activity with Q_D for various values of g is shown in Fig. 7. Since $C_{22} \neq 0$ in this case, (cancellation of C_{22}

leads to flutter at $Q_D = 145$ psf), this implies that acceleration signals have to be integrated. Integrations of the form $1/(S+\varepsilon)$ and $1/(S+\varepsilon)^2$ had been tested in the region of $0.1 < \varepsilon < 1$ and no visible effects could be detected on the root locus plots.

The block diagram for the above control law is presented in Fig. 8. The transfer functions representing third order systems can clearly be seen in Fig. 8. Furthermore, a third order actuator can readily be compensated. This can be illustrated for the T.L. control surface having an actuator transfer function T(S) of the form

$$T(S) = \frac{\omega_n^2 d}{(S^2 + 2 * \zeta * \omega_n \times S + \omega_n^2)(S + d)} \tag{4}$$

The following compensation procedure (see Fig. 9)

$$\frac{300}{(S + 300)(S^2 + 2 \times 0.43 \times 57.4 \cdot S + (57.4)^2)} =$$

$$= \frac{300 * (S^2 + 2 * \zeta * \omega_n * S + \omega_n^2)(S + d)}{(S + 300)(S^2 + 2 \times 0.43 \times 57.4 * S + (57.4)^2) * \omega_n^2 d} * T(S)$$

can be seen to yield the same effective control law.

Summary of Analysis:

Two control laws were derived. Control Law I, suitable for second order actuators and Control Law II suitable for third order actuators.

CONTROL SYSTEM MECHANIZATION FOR WIND TUNNEL TESTING

Control law II was chosen for the mechanization performed by Northrop. Fig. 9 represents the block diagram of the L.E.-T.E. control system. The control surface actuator transfer functions are denoted by $G_{S,L.E.}$ and $G_{S,T.E.}$ and are defined by the following expressions:

$$G_{S,L.E.} = \frac{\left(\frac{S+24}{24}\right)\left(\frac{S+260}{260}\right)}{\left(\frac{S+28}{28}\right)\left(\frac{S+94}{94}\right)\left(\frac{S^2+204S+28,900}{28,900}\right)\left(\frac{S^2+616S+193,600}{193,600}\right)} \tag{5}$$

$$G_{S,T.E.} = \frac{\frac{S+260}{260}}{\left(\frac{S+124}{124}\right)\left(\frac{S^2+138S+19,044}{19,044}\right)\left(\frac{S^2+440S+98,596}{98,596}\right)}$$

THESE EXPRESSIONS WERE SUPPLIED TO THE PRESENT AUTHORS LONG AFTER CONTROL LAWS I AND II WERE DETERMINED AND PRESENTED AT NASA.

As can be seen, the above actuator transfer functions include some built in filters which were introduced by Northrop. As a result, the effective expressions for the transfer functions in the mechanized system are given by

$$T(S)_{L.E.,EFF.} = \frac{\left(\frac{S+24}{24}\right)\left(\frac{S+260}{260}\right)}{\left(\frac{S+28}{28}\right)\left(\frac{S^2+204S+28,900}{28,900}\right)\left(\frac{S^2+616S+193,600}{193,600}\right)} \; T(S)_{L.E.}$$

$$T(S)_{T.E.,EFF.} = \frac{\left(\frac{S+260}{260}\right)}{\left(\frac{S^2+440S+98,596}{98,596}\right)} * T(S)_{T.E.} \tag{6}$$

where $T(S)_{L.E.}$, $T(S)_{T.E.}$ denote the desired transfer functions.

As can be seen, the effective control law had been varied by a considerable factor representing an additional transfer function. <u>As a result, the mechanized control law represents a different control law than the original control law II.</u> Furthermore, the integration in Fig. 10 was performed by $1/(S+5)$ (instead of $1/(S+\varepsilon)$, with $0.1 \leq \varepsilon \leq 1$) without checking its possible effects. It is also tacitly assumed that proper account had been taken of the accelerometers and actuators' sensitivities (does not appear in the block diagram in Fig. 9). It is further assumed that the changes between the assumed accelerometer locations and the actual locations are too small to have any significant effects on the gains of control law II.

At this stage, the authors of this paper decided to rederive the control law, in the presence of $G_{S,L.E.}$, $G_{S,T.E.}$ and some additional filters used by Northrop (denoted by $H(S)$). The results of this latter analysis are presented in Appendix 1, and are based on an updated dynamic model and a refined calculation of the aerodynamic forces. This latter model was supplied by Northrop, through NASA. It arrived too late to be included in the derivation of control laws I and II.

Unfortunately, the results appearing in Appendix 1 arrived Northrop at to late a stage to be incorporated into the tunnel model. Consequently, the tunnel tests were performed using the $T(S)_{L.E.,EFF}$ and $T(S)_{T.E.,EFF}$ (see Eq.(6)), which are different from $T(S)_{L.E.}$ and $T(S)_{T.E.}$ of control law II (based on an older mathematical model).

WIND TUNNEL TEST RESULTS

The wind tunnel test results as reported to the authors of this paper, reveal the following picture:

"Because of high frequency problems associated with the control law, and a lack of knowledge concerning this law, testing could not be continued above a dynamic pressure of 70 psf. This was a condition below passive flutter (q_F = 75 psf). Attachments 1, 2, and 3 are included to assist in describing the problems encountered in the tunnel. The first attachment presents zero airspeed transfer functions for the control law using either the leading or trailing edge surface as input. As can be seen, the gains are quite high across the frequency range. This is particularly true for the T.E. surface. Attachment 2 presents peak hold data taken during the test, while attachment 3 provides model response data at the various test points.

Initial tests indicated significant wing response near 30 HZ. Response data for test point 419 with the expanded time scale illustrates the problem which is particularly noticeable in the wing bending response. For test point 414, the control law was turned off while a Northrop leading edge law was activated. This also shows the significant frequency content of the command signals.

Since there was no one available at the test who could offer guidance in modifying the control law, ... , 30 HZ notch filters were incorporated into the control law. With this change, test point 475 still shows some high frequency content and significant L.E. commands. As a result, the global gain was reduced 25%. While increasing dynamic pressure from 65 to 70 psf, a divergent oscillation was encountered and the control law was deactivated. The frequency of the divergent oscillation was about 14 HZ. Further modifications to the control law were not attempted. All high frequency modifications affect the performance of the overall control law and without guidance it was not practical to compensate for these changes in the flutter frequency range."

Part of the attachment 3, relating to test point 419, is presented herein as Fig. 10.

ANALYSIS OF WIND-TUNNEL TEST RESULTS

It was found impossible even to attempt any correlation between analysis and test results, since the control laws used in each case were widely different. The changes introduced in control law II (see Eq.(6)) include high frequency transfer functions which, as noted in the previous section, "affect the performance of the overall control law." Consequently, it was decided to analyze the control law, as mechanized by Northrop, and compare the analytical results with those obtained during the wind-tunnel tests.

The new analysis reported herein, is based on the updated mathematical model and the refined aerodynamic coefficients. Since the wind tunnel problems reported above relate to high frequency regions, no attempts are made to investigate the possible effects of the $1/(s+5)$ integration. The effective control law tested in the wind tunnel is given by the following expressions

$$\begin{Bmatrix} \beta \\ \delta \end{Bmatrix} = \frac{300}{S+300} \begin{bmatrix} Q_{L.E.} & 0 \\ 0 & Q_{T.E.} \end{bmatrix} \left(\begin{bmatrix} 0 & 0 \\ 0 & -1.86 \end{bmatrix} + \begin{bmatrix} R_{L.E.} & 0 \\ 0 & R_{T.E.} \end{bmatrix} \times \right.$$

$$\left. \times \begin{bmatrix} -4 & 4 \\ 4 & 2.8 \end{bmatrix} \right) \begin{Bmatrix} \dfrac{h_1 - h_r}{b} \\ \alpha_1 - \alpha_r \end{Bmatrix} \tag{7}$$

where $Q_{L.E.}$ and $Q_{T.E.}$ are the transfer functions transforming the original control law II into the mechanized control law II, and where $R_{L.E.}$ and $R_{T.E}$ are defined in Eq.(3). Using Eq.(6) the following relations can be written

$$Q_{L.E.}(S) = \frac{\left(\dfrac{S+24}{24}\right)\left(\dfrac{S+260}{260}\right)}{\left(\dfrac{S+28}{28}\right)\left(\dfrac{S^2+204S+28{,}900}{28{,}900}\right)\left(\dfrac{S^2+616S+193{,}600}{193{,}600}\right)}$$

$$Q_{T.E.}(S) = \frac{\left(\dfrac{S+260}{260}\right)}{\left(\dfrac{S^2+440S+98{,}596}{98{,}596}\right)} \tag{8}$$

The control law defined in Eqs.(3), (7), (8), will be refered to as the Northrop modified control law II.

The root locus plot for the closed loop system is shown in Fig. 11 (with $g = 0$). Similarly, for comparison purposes, the closed loop root locus plot for the original control law II, but with the updated dynamical model and aerodynamics, is shown in Fig. 12. As can be seen, the changes in the mathematical model degrade the root locus plot for the original control law II (Fig. 12). For $g = 0$ flutter occurs at $Q_{DF} = 128$ psf, whereas for $g = 0.015$, flutter occurs at $Q_{DF} = 152$ psf. In addition, there is a lower frequency flutter branch yielding $Q_{DF} = 143$ psf ($g = 0$) with $\omega_F = 16$ rad/s, and a high frequency negative damping mode at around $\omega = 270$ rad/s. This latter high frequency mode becomes stable for values of $g \geq 0.015$. It can be concluded that the updating of the mathematical model, especially the changes introduced in the control surface aerodynamic coefficients, degrades the closed loop performance of control law II (see for comparison Fig. 6) to the extent which warrants its modification.

The root locus plot for the Northrop modified control law II (Fig. 11) shows flutter at $Q_{DF} = 68$ psf ($g = 0$) or $Q_{DF} = 82$ psf with $g = 0.015$. The flutter frequency lies around 110-115 rad/s. In addition, some high frequency modes show low damping when compared to the $g = 0.015$ line shown in Fig. 11. Hence, there is no wonder that the wind tunnel tests could not proceed beyond $Q_D = 70$ psf. Furthermore, at $Q_D = 60$ psf (relating to TP 419, see also Fig. 10) low damping modes can be observed at $\omega = 160$ rad/s and around $\omega = 260$ rad/s, thus explaining the high frequency content of the responses of the system and of the control signals.

An example of PSD representation for control surface deflections, using the Northrop modified control law II, is shown in Figs. 13, 14 (with values of g as defined by ground resonance tests (GRT)). Fig. 13 shows the PSD representation for β_{out} and δ_{out} (at Q_D = 60 psf) and Fig. 14 shows a similar representation for β_{in} and δ_{in} (also at Q_D = 60 psf). These latter figures were computed for comparison purposes with the test recordings, shown in Fig. 10.

Three main points emerge from the above comparison: First -- both Figs. 10, 13, show correlation with respect to the low frequency content (around 15-17 HZ) of the δ_{out} signal, and with respect to the lack of any significant high frequency signal. Second -- both Figs. 10, 14 show that β_{in} has the largest high frequency content (around 40-50 HZ). Third -- β_{out} in both Figs. 10, 14 show lower amplitudes in the high frequency content of the signal. The superposition of two signals with frequencies of order 15 and 40 HZ can be seen in both figures.

The analytical simulation of the wind tunnel test results relating to the 34 HZ notch filter was found impossible since no data regarding the notch filter was supplied to the authors of this work.

The control surface activity, with values of g as determined by GRT of the model, at various values of Q_D, are shown in Fig. 15 for the Northrop modified control law II. The control activities can be seen to be much larger than those relating to the original control law II (by a factor of about 3) and presented in Fig.7.

CONCLUDING REMARKS

The control law, as mechanized by Northrop and tested in the wind tunnel, bears no analytical resemblance to the original control law II. The main deviation lies in the form of the effective control law used, which does not compensate for the actuator transfer functions (part of them could have easily been compensated). A second, smaller deviation, originates from the fact that control law II was derived using the older mathematical model (the updated model was sent too late to be included in the original analysis). The control surface aerodynamic derivatives in the updated model were computed by Northrop using a more rational box allocation over the control surfaces than in the older model (both computations used the Doublet Lattice method).

The analytical simulation of the flutter suppression performance of the YF-17 model (using control law II, as mechanized by Northrop) shows good correlation with the wind tunnel tests both with respect to flutter dynamic pressure and to the response characteristics of the model.

REFERENCES

1. Nissim, E., and Lottati, I., "Active External Store Flutter Suppression In the Modified YF-17 Flutter Model," Report sent to NASA, April 1979.

2. Nissim, E., "Recent Advances in the Aerodynamic Energy Concept for Flutter Suppression and Gust Alleviation Using Active Controls," NASA TN-D 8519, 1977.

3. Nissim, E., and Lottati, I., "Active External Store Flutter Suppression in the YF-17 Flutter Model," J. Guidance and Control, Sept.-Oct. 1979.

4. Nissim, E., and Abel, I., "Development and Application of an Optimization Procedure for Flutter Suppression Using the Aerodynamic Energy Concept," NASA TP-1137, 1978.

APPENDIX 1: OPTIMIZATION OF A CONTROL LAW IN THE PRESENCE OF TRANSFER FUNCTIONS REPRESENTING ACTUATORS AND FILTERS.

The control law for the YF-17 flutter model has been recomputed using the following data:

(a) The new mode shapes and dynamic data and the new aerodynamic coefficients.

(b) The new sensor locations (at W.S. 51.45 instead of W.S. 44.85 previously used).

(c) Incorporation of the following filters for both the L.E. and T.E. control surfaces, following a specific request.

$$H(S) = \frac{S^2 + 21S + (213)^2}{S^2 + 299S + (213)^2} \cdot \frac{S^2 + (552.6)^2}{S^2 + 552S + (552.6)^2} \cdot \frac{(264)^2}{S^2 + 264S + (264)^2}$$

(d) Incorporation of the following actuator transfer functions taken from Northrop's papers attached to the above mentioned letter:

$$G_{S,T.E.} = \frac{S + 260}{260} \cdot \frac{124}{S + 124} \cdot \frac{(138)^2}{S^2 + 138S + (138)^2} \cdot \frac{(314)^2}{S^2 + 440S + (314)^2}$$

$$G_{S,L.E.} = \frac{S + 24}{24} \cdot \frac{S + 260}{260} \cdot \frac{28}{S + 28} \cdot \frac{94}{S + 94} \cdot \frac{(170)^2}{S^2 + 204S + (170)^2} \cdot \frac{(440)^2}{S^2 + 616S + (440)^2}$$

The results presented earlier[1] employ an older set of dynamic data and were computed using the doublet lattice box distribution used by Northrop at an earlier stage of the work. None of the filters H(S) and G(S) were then used, although G(S) could have partially been accounted for by a simple transfer function compensation.

No attempt was made to rederive the previous control laws, using the new information included in the above paragraphs (a) and (b). Instead, the recomputation includes all the new elements mentioned in the above paragraphs (a) through (d).

Before presenting the new results it should be stressed that the constraints imposed by having to use the filters denoted by H(S) and the form of G(S) which appear to include compensation filters, do not seem to be justified. These filters represent an integral part of the control law developed by Northrop and they were required for stabilization of their resulting closed loop system. It is difficult to see the need for their introduction herein since if it is assumed that the mathematical representation is satisfactory, why is it not possible to rely on the control laws previously derived, which stabilize the closed loop system and have to resort to the statement that "based on previous testing experience, Northrop has found it necessary to insert filters in all the feedback signals to prevent system instability?" If, on the other hand, the mathematical model is not satisfactory, then there is no value to the present results and there is very little trust one can put in them.

As already mentioned, the above constraints were adopted in the new computations (some of these constraints were eventually compensated by the introduction of appropriate transfer functions in the control laws).

It was found possible to stabilize the system by using different control laws which yielded reasonably high flutter margins. The chosen control law gives the smallest flutter margin but shows the best behaviour at lower values of dynamic pressure and at lower values of structural damping (g). The results include a root locus computer run which includes the values of g defined during GRT of the model. To cut down labour, the results are brought to the form used by Northrop (degrees per g) and their sign convention is used (in this Appendix only).

Finally, before presenting the results, attention should be drawn to the fact that the control law requires that a free flying model (that is, having plunge and pitch degrees of freedom) should be fitted with reference accelerometers located along the center line of the fuselage. or near it. In the present results, the location used for these accelerometers is denoted.

RESULTS - YF 17

Sensor Location, Units and Sign Convention:

Four accelerometers are used, a_1, a_2, a_{r1}, a_{r2}. The accelereometers a_1, a_2 are located at W.S. 51.45, F.S. 145.18 (25% C) and F.S. 158.00 (76%C) respectively. The accelerometers a_{r1} and a_{r2} are located along the fuselage centerline, at F.S. 131.85 and F.S. 165.5 respectively. The accelerations are positive downwards and the units are assumed to be given in "g" units. The deflection of the control surfaces is given in degrees with positive rotations obtained by deflecting the T.E. control downwards $(\delta_{T.E.})$ and the L.E. control upwards $(\beta_{L.E.})$

Suggested Control Law:

The suggested control law involves the activation of a combined L.E.-T.E. system. The block diagram for the activation of the L.E.-T.E. control is shown in Fig. A.1 and the expressions for the different transfer functions are given in Table 1.

Flutter Resuts:

Figure A.2 shows a root locus plot using the above control laws with zero structural damping. Fig. A.3 shows a similar root locus plot using the values of structural damping as measured by Northrop. The parameter of variation in the root locus plots is the dynamic pressure Q. The spacing between adjacent points along each branch represents a change in Q of 10 psf. The plots were obtained by varying Q between 0 and 200 psf.

It can be seen that the flutter dynamic pressure is around 158 psf when structural damping is present and 147 psf with zero structural damping. Figs. A.4-A.7 show the variations of the activities of both L.E. and T.E. control surfaces (due to unit RMS gust input with dynamic pressure Q). It can be seen that both the deflections and the rates are relatively small. Structural damping (Northrop's measurement) was assumed to be present in deriving Figs. A.4-A.7.

TABLE 1. EXPRESSIONS FOR THE VARIOUS TRANSFER FUNCTIONS USED IN ACTIVATING THE SUGGESTED L.E.-T.E. SYSTEM

$$H(S) = \frac{S^2 + 21S + (213)^2}{S^2 + 299S + (213)^2} \cdot \frac{S^2 + (552.6)^2}{S^2 + 552S + (552.6)^2} \cdot \frac{(264)^2}{S^2 + 264S + (264)^2}$$

$$G_{S,T.E.}(S) = \frac{S + 260}{260} \cdot \frac{124}{S + 124} \cdot \frac{(138)^2}{S^2 + 138S + (138)^2} \cdot \frac{(314)^2}{S^2 + 440S + (314)^2}$$

$$G_{S,L.E.}(S) = \frac{S + 260}{260} \cdot \frac{94}{S + 94} \cdot \frac{S + 24}{24} \cdot \frac{28}{S + 28} \cdot \frac{(170)^2}{S^2 + 204S + (170)^2} \cdot \frac{(440)^2}{S^2 + 616S + (440)^2}$$

$$T_{T.E.}(S) = R(S) \cdot \frac{S + 124}{124} \cdot \frac{S^2 + 138S + (138)^2}{(138)^2} \cdot K_{T.E.}(S)$$

$$R(S) = \frac{S^2 + 264S + (264)^2}{(264)^2} \cdot \frac{260}{S + 260} \cdot \frac{S + 60}{60} \cdot \frac{225}{S + 225} \cdot \frac{(347.9)^2}{S^2 + 492S + (347.9)^2}$$

$$T_{L.E.}(S) = R(S) \cdot \frac{S + 94}{94} \cdot \frac{S + 28}{28} \cdot \frac{24}{S + 24} \cdot \frac{S^2 + 204S + (170)^2}{(170)^2} \cdot K_{L.E.}(S)$$

$$K_{T.E.}(S) = 3.09 \cdot \frac{[S^2 + 43.3S + (94.3)^2]}{[S^2 + 21.6S + (45)^2][S^2 + 88.3S + (152.3)^2]}$$

$$K_{L.E.}(S) = 1.874 \quad \frac{[S^2 + 291.1S + (168.6)^2]}{[S^2 + 39.8S + (41.5)^2][S^2 + 400S + (200)^2]}$$

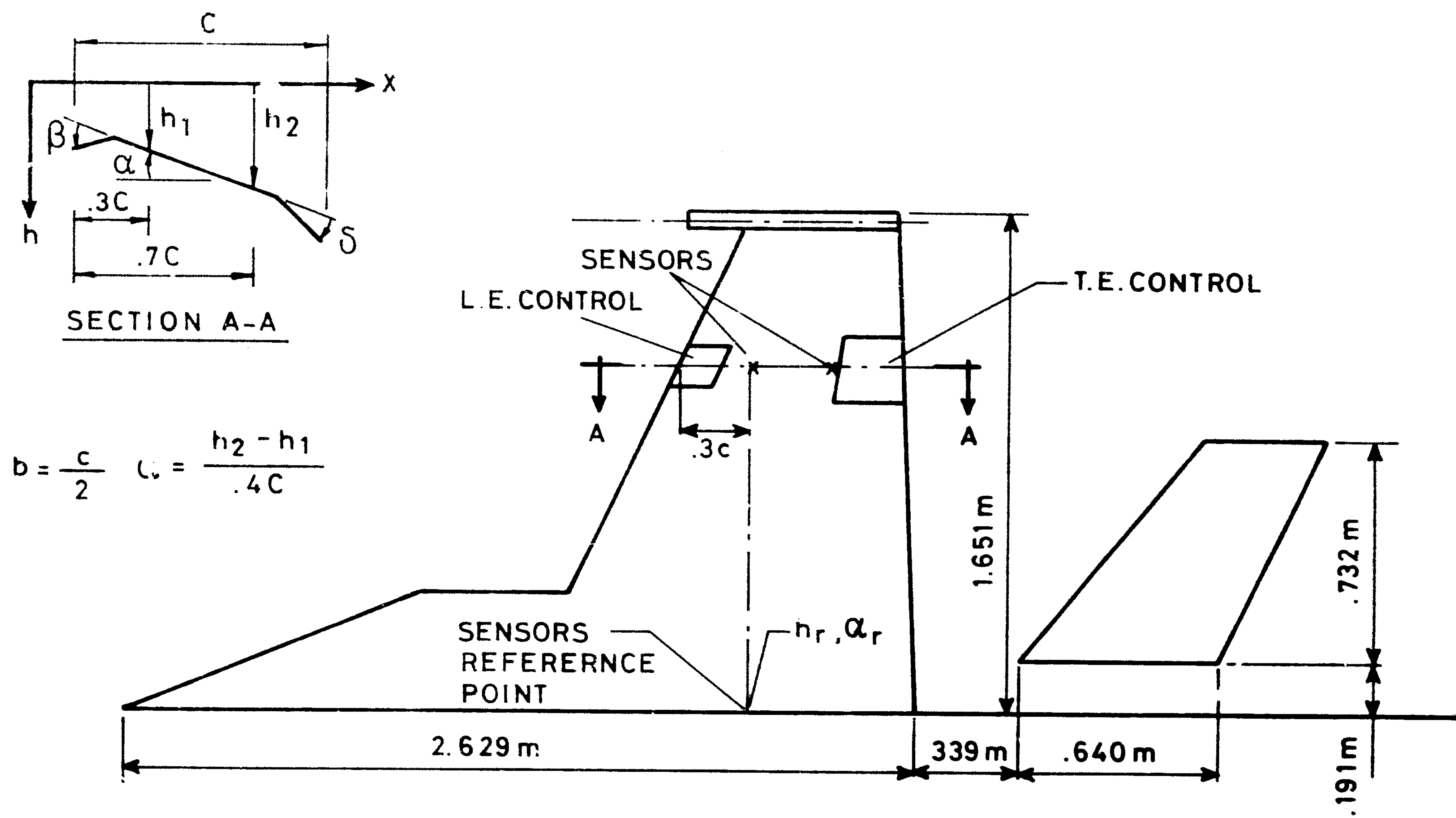

Figure 1: Plan view of YF-17 flutter model and geometrical description of the active control system

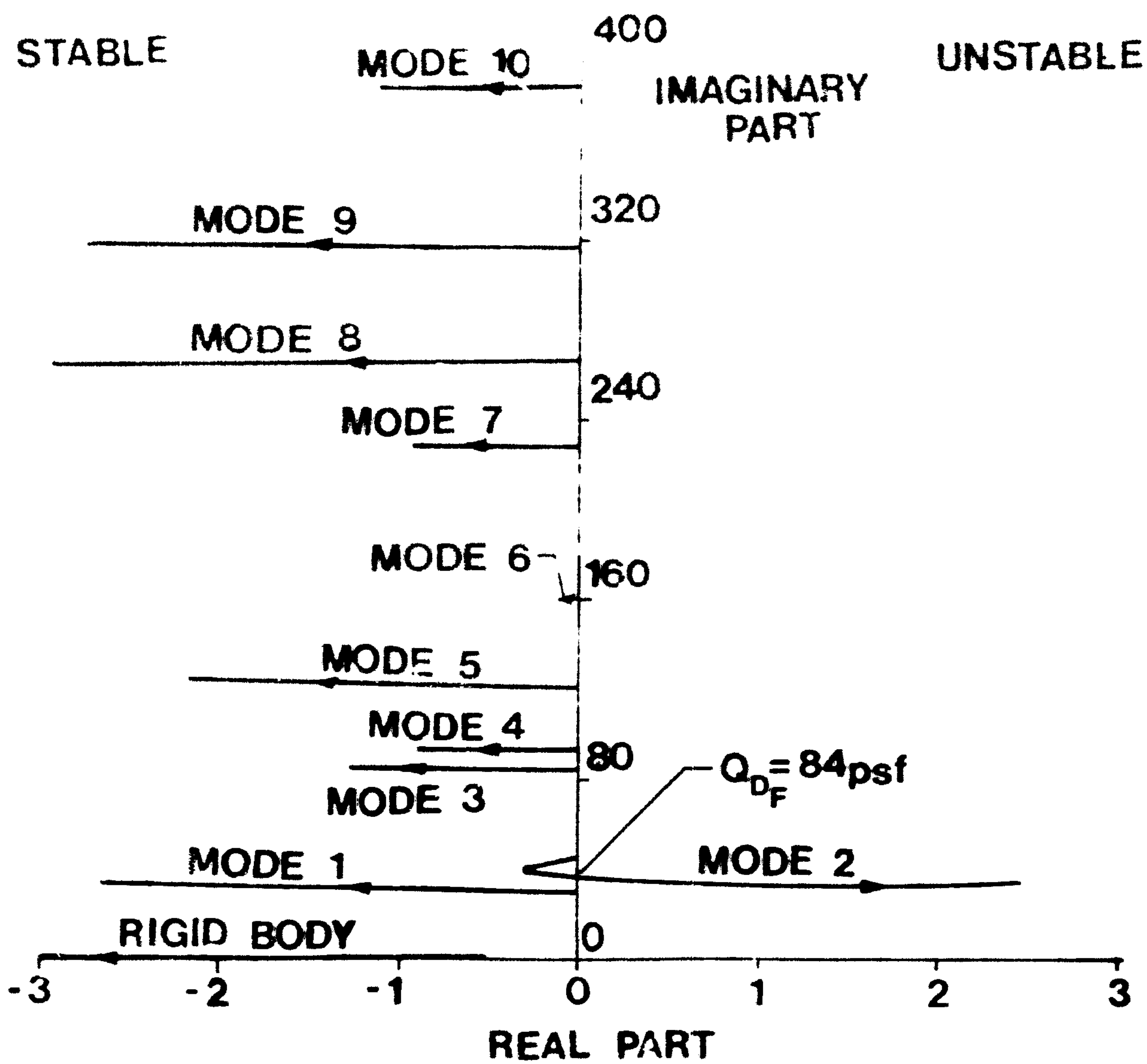

Figure 2: Open loop root locus plot (M = 0.8)

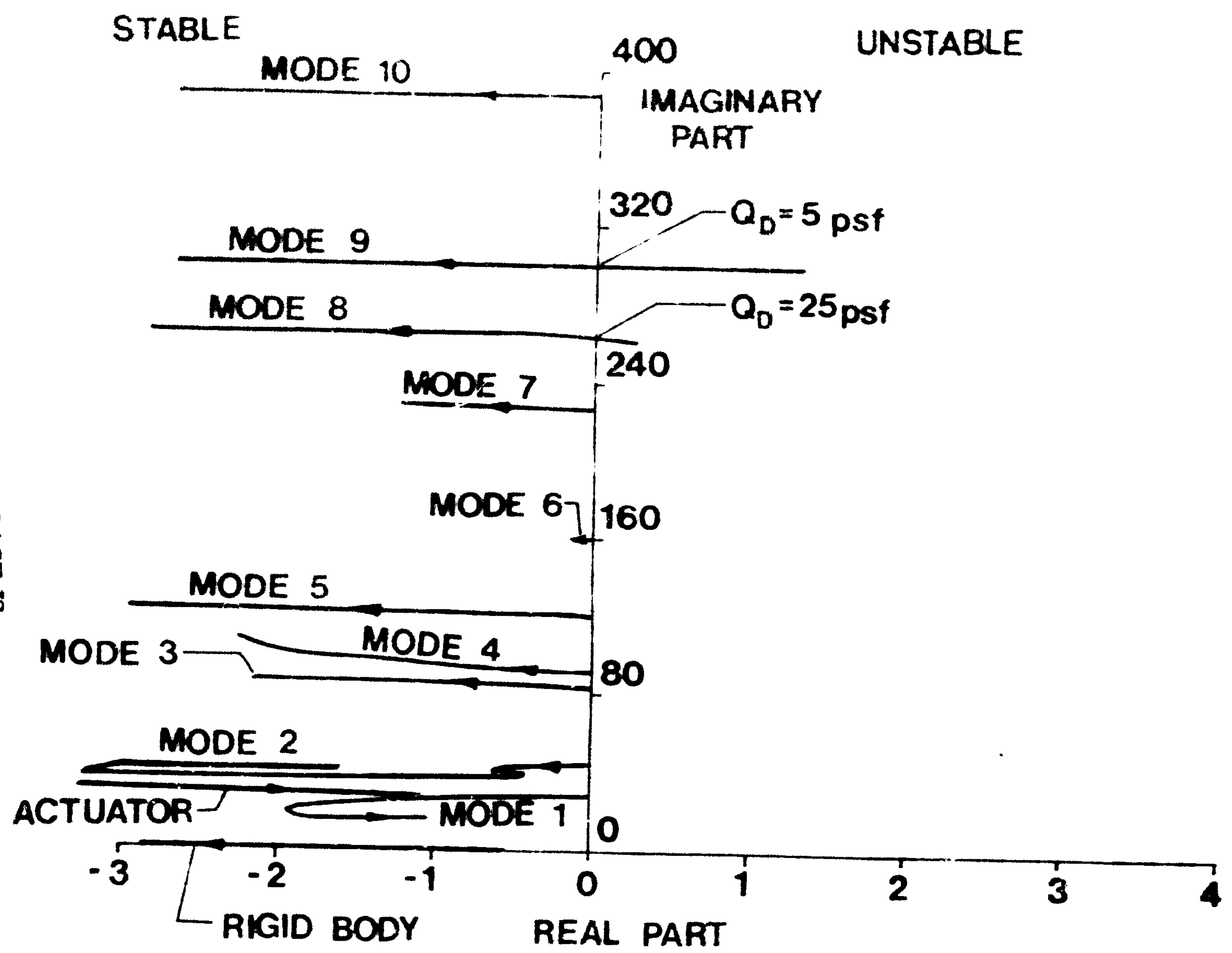

Figure 3: Closed loop root locus plot using control law I with unbalanced control surfaces (M = 0.8)

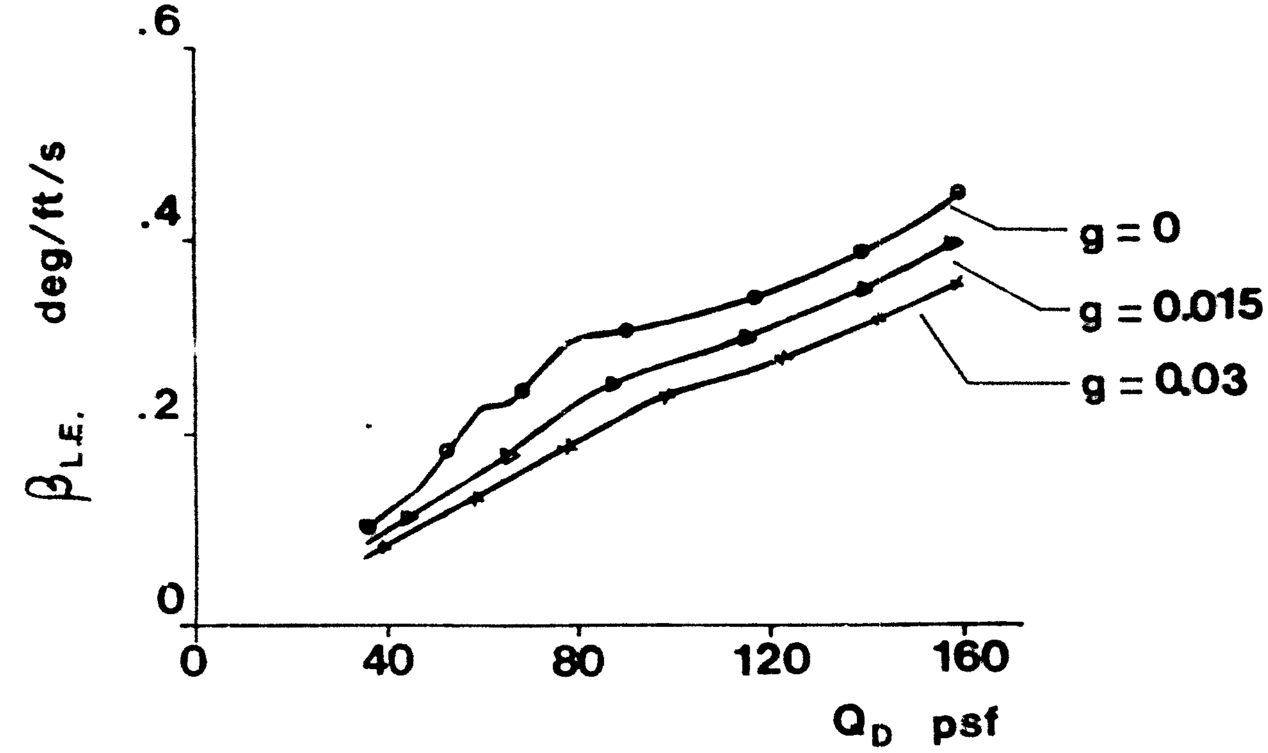

Figure 4a: L.E. control deflection

Figure 4: Variation with Q_D of control surface activity, using control law I with unbalanced control surfaces (M = 0.8)

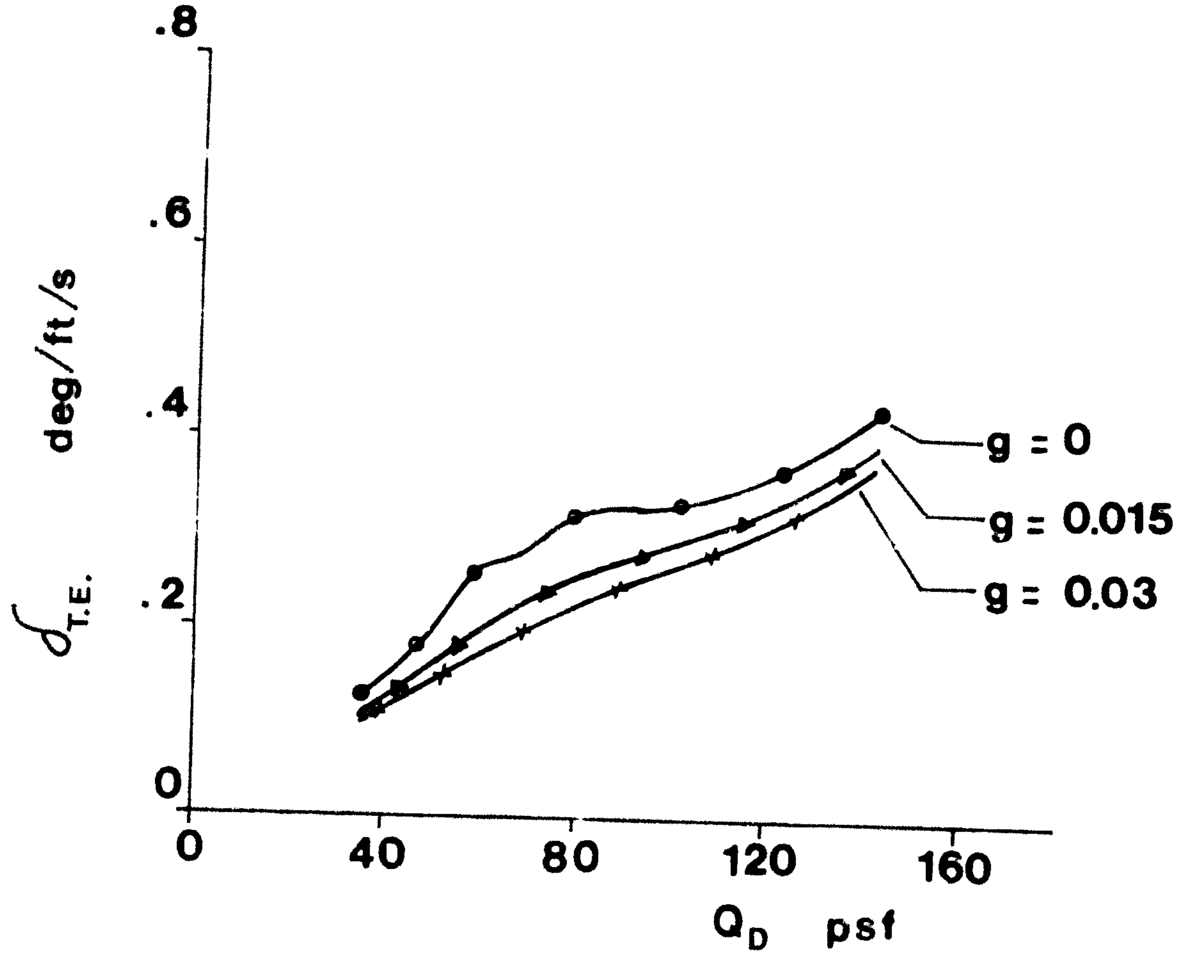

Figure 4b: T.E. control deflection

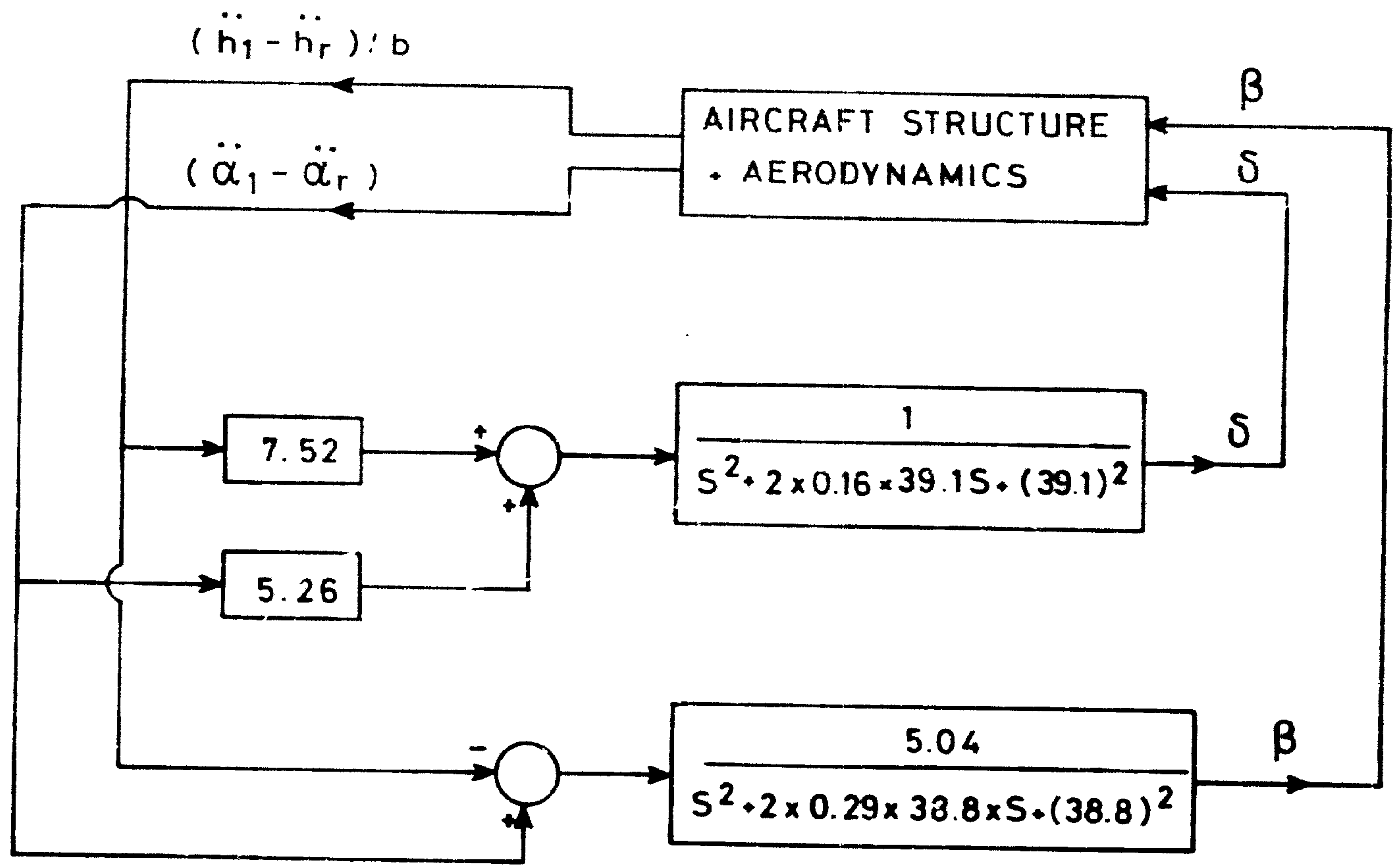

Figure 5: **Block diagram representation** of control law I

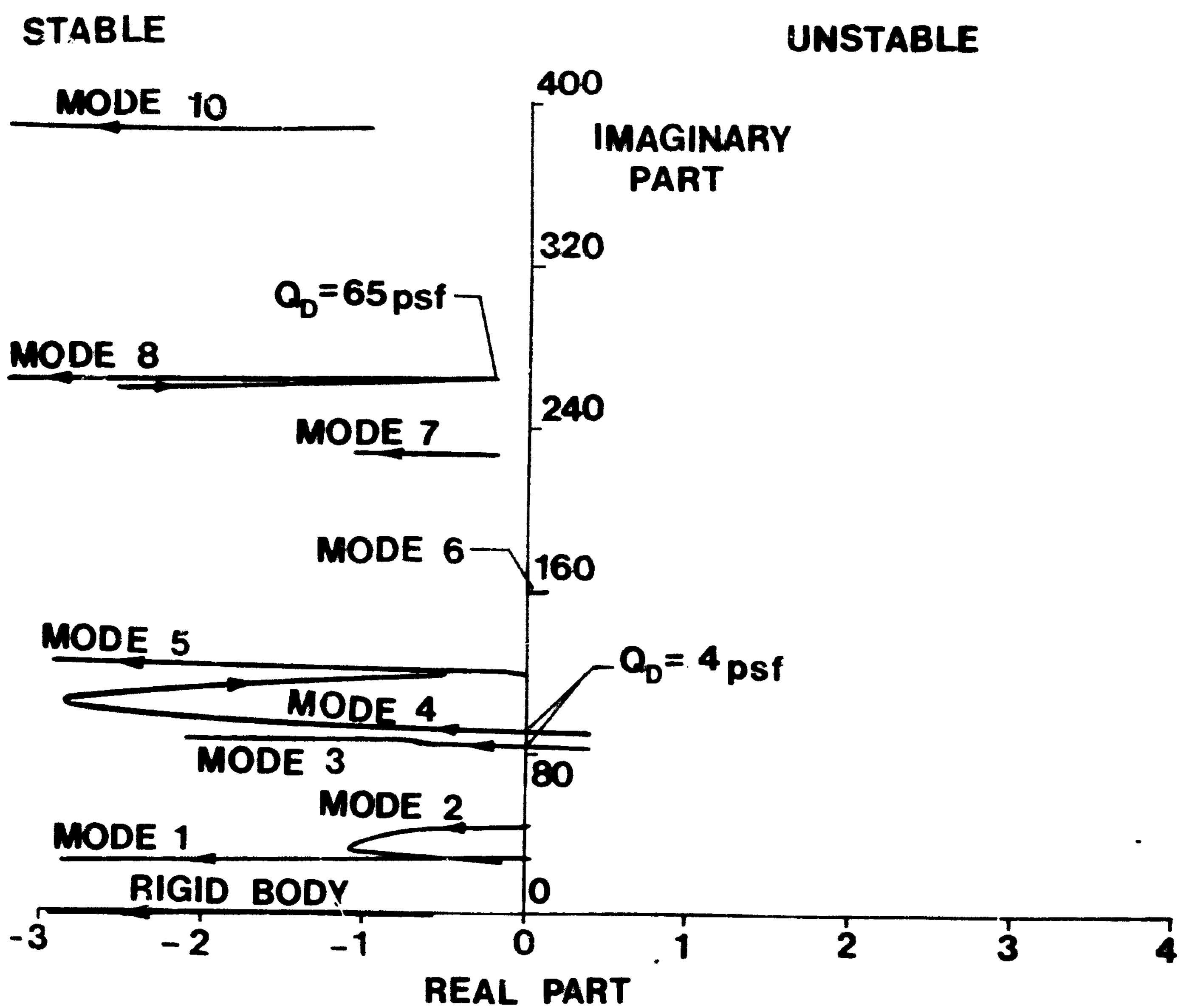

Figure 6: Closed loop root locus plot using control law II with unbalanced control surfaces (M = 0.8)

C-2

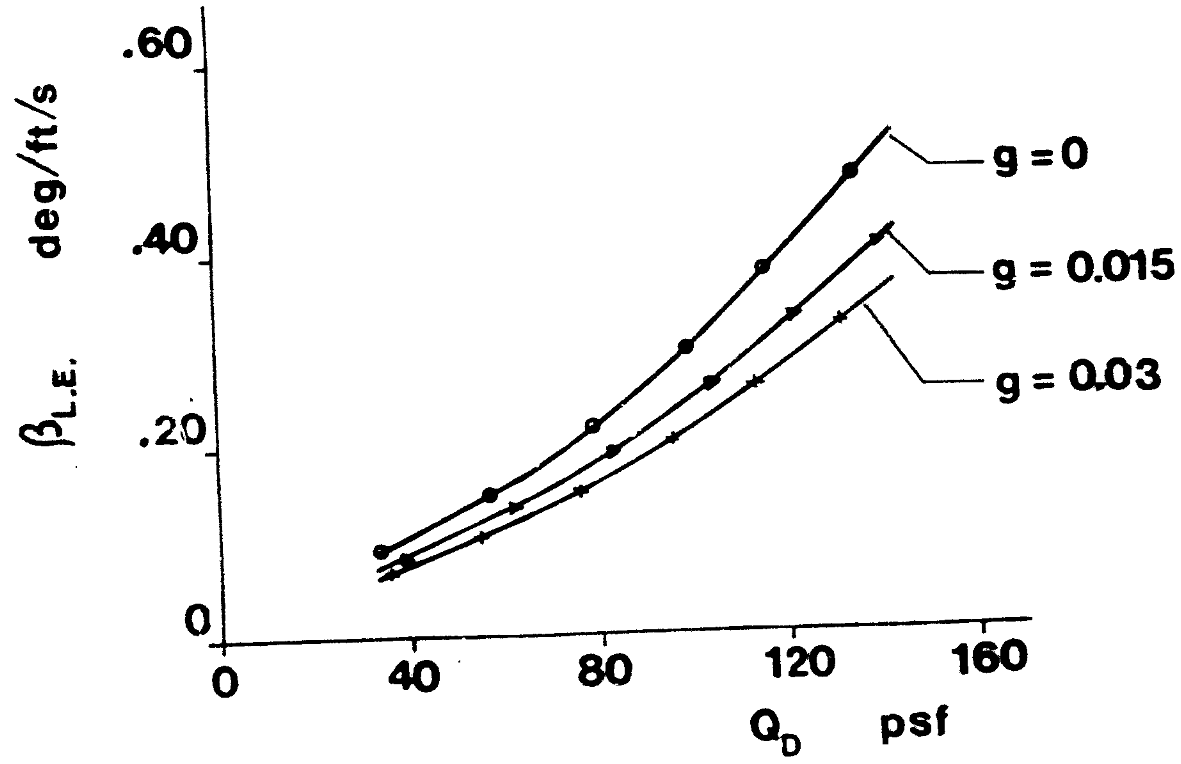

Figure 7a: L.E. control deflection

Figure 7: Variation with Q_D of control surface activity, using control law II with unbalanced control surfaces (M = 0.8).

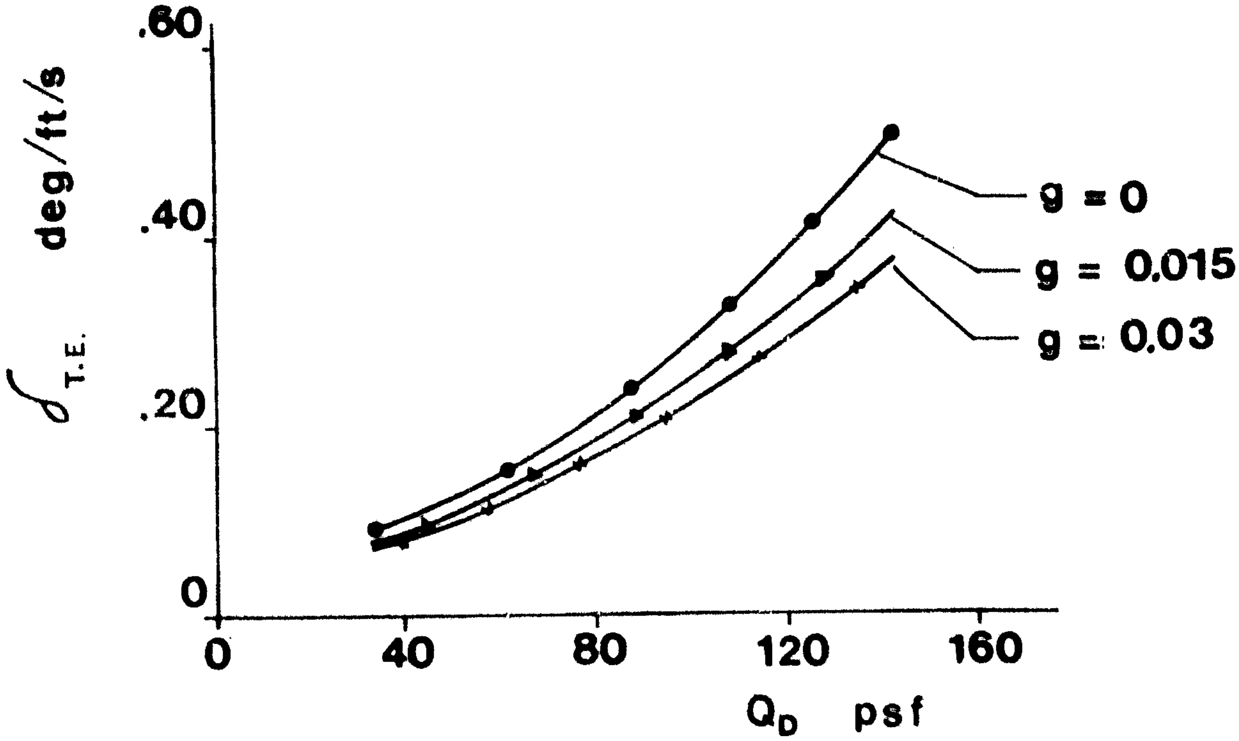

Figure 7b: T.E. control deflection

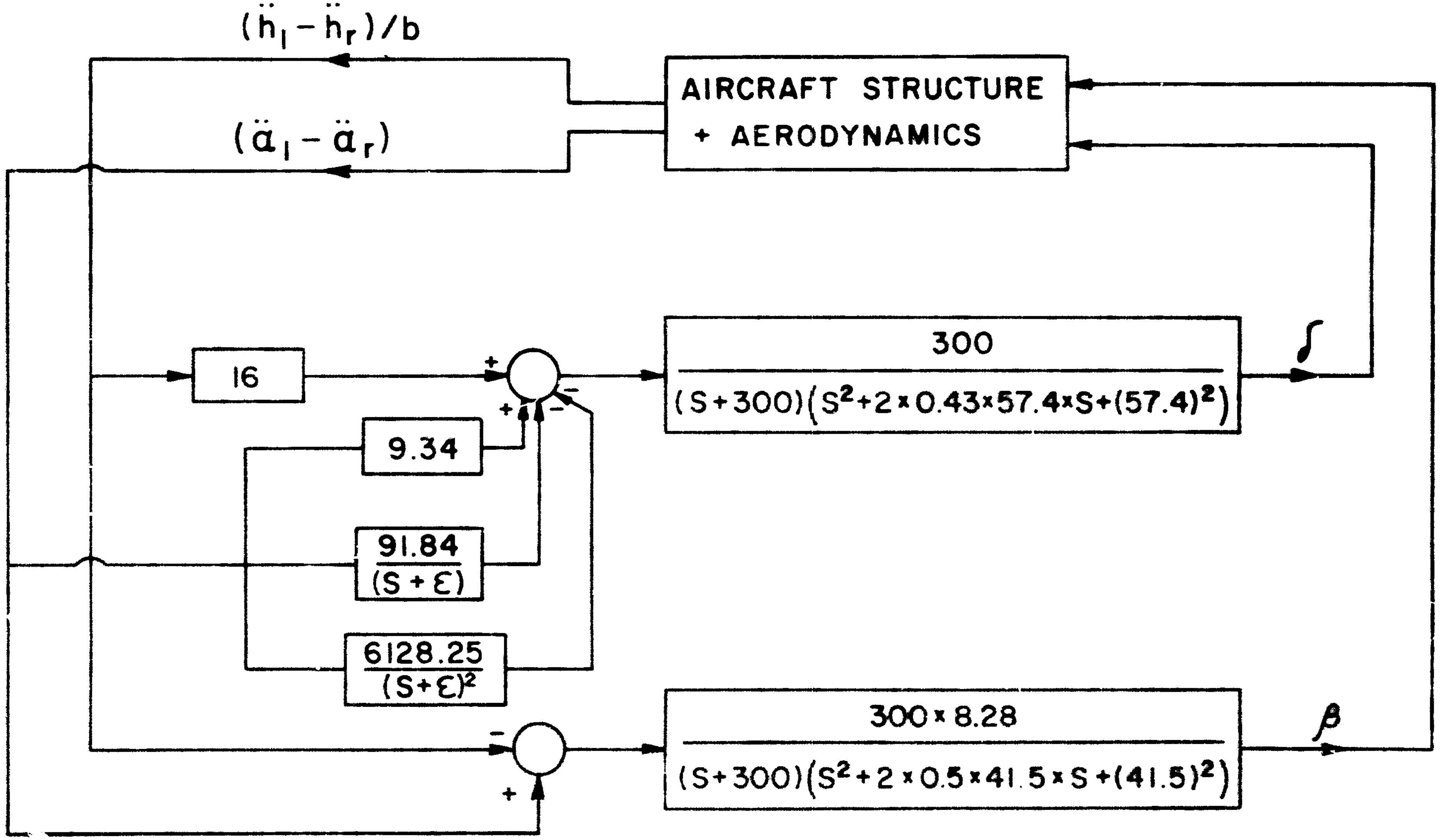

Figure 8: Block Diagram Representation of Control Law II

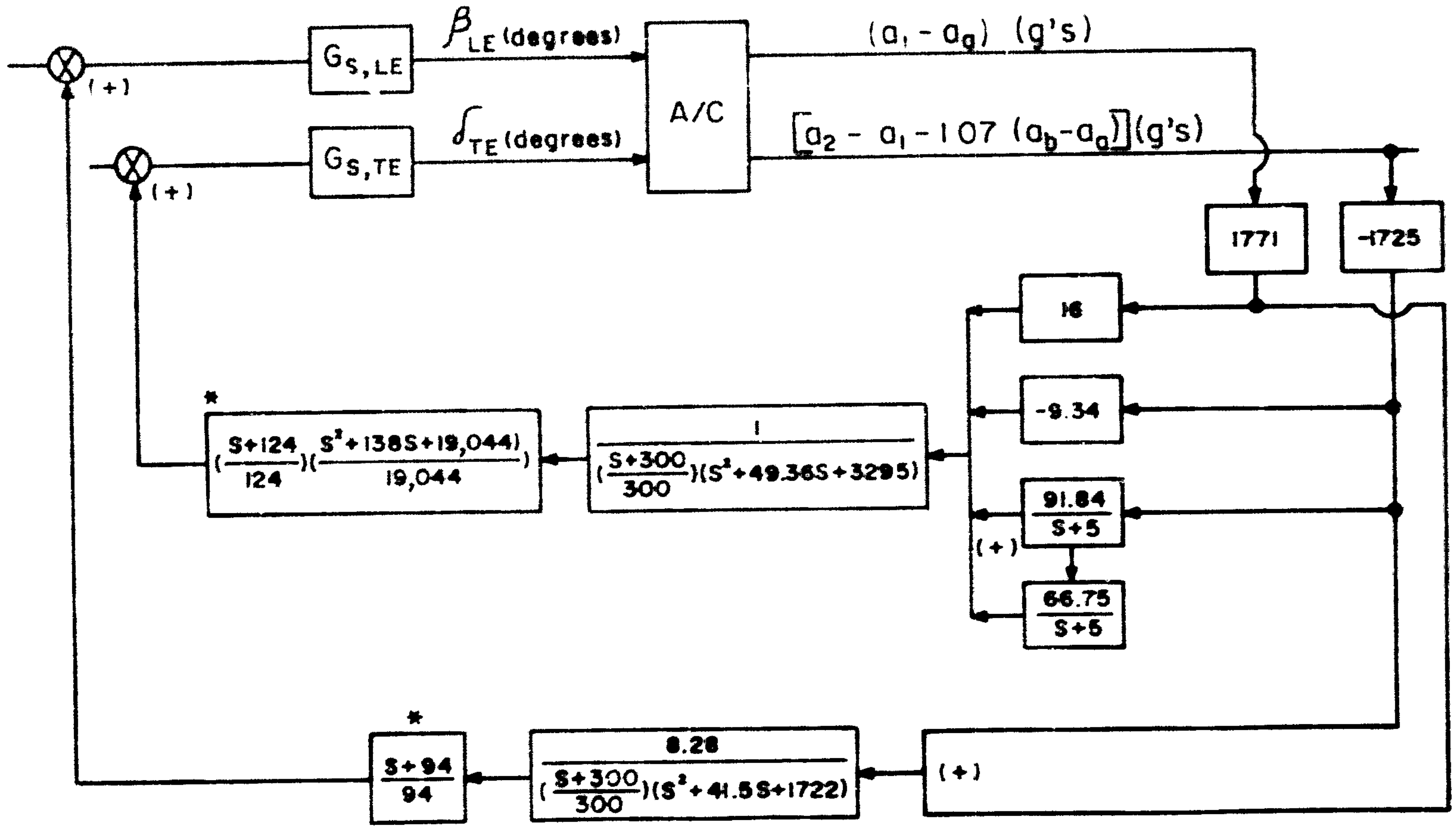

Figure 9: Block Diagram Representation of the Northrop Mechanization of Control Law II

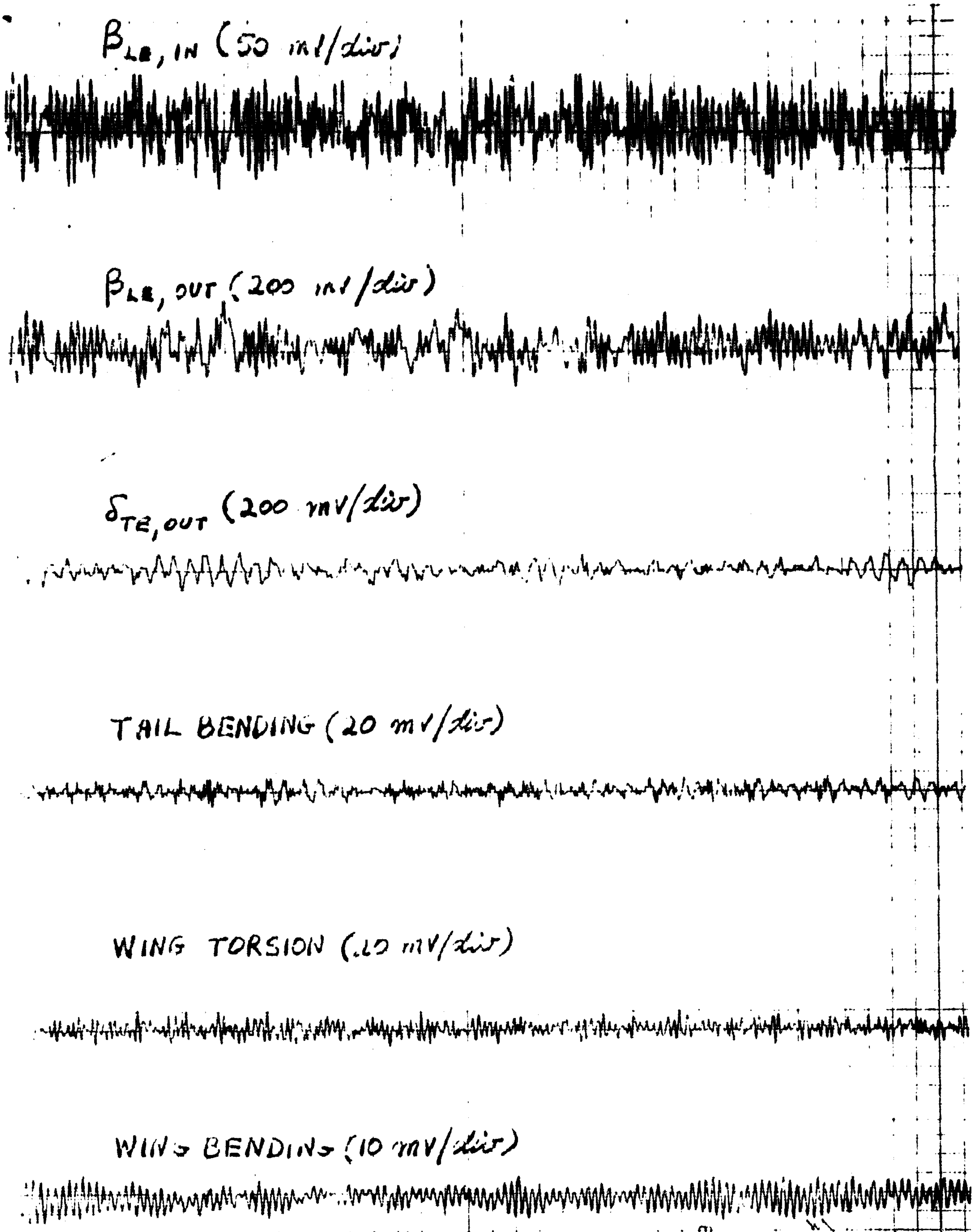

Figure 10: Wind Tunnel Signal Responses of the Model at M = 0.8 and Q_D = 60.6 psp (TP 419)

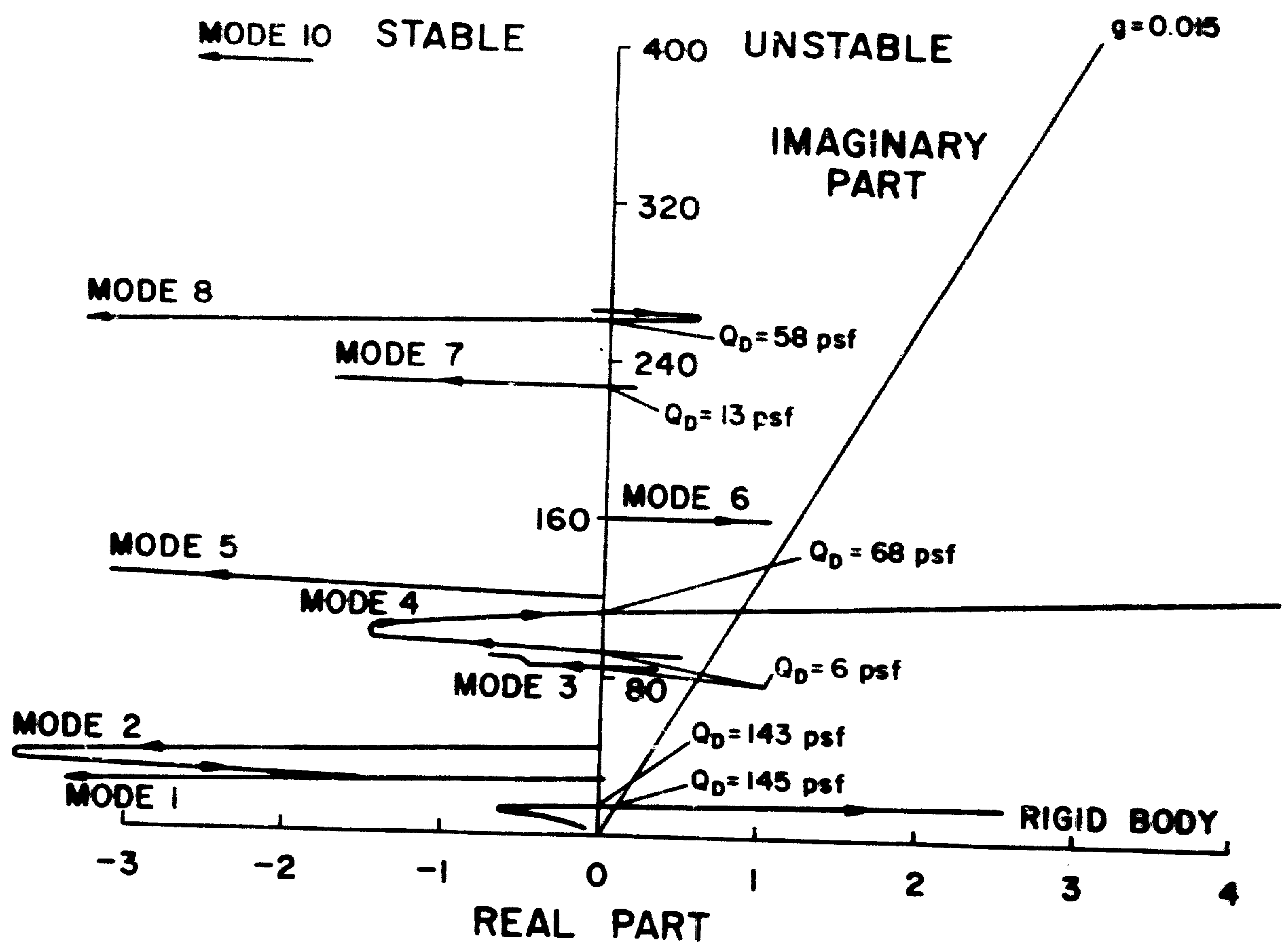

Figure 11: Closed Loop Root Locus Plot Using the Northrop Mechanized Control Law II (with g = 0, M = 0.8)

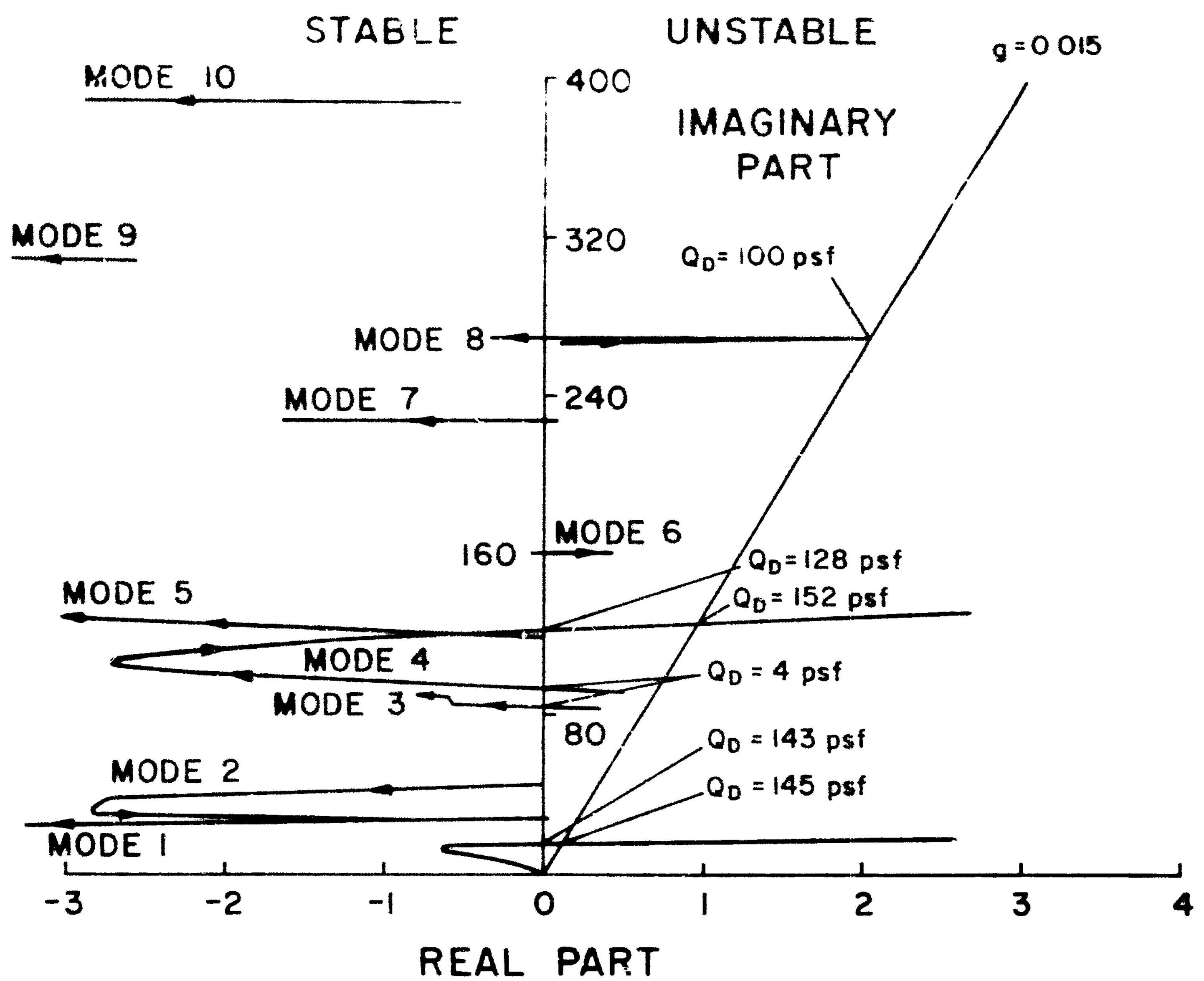

Figure 12: Closed Loop Root Locus Plot Using the Original Control Law II in Conjunction with the New Dynamic Model (g = 0, M = 0.8)

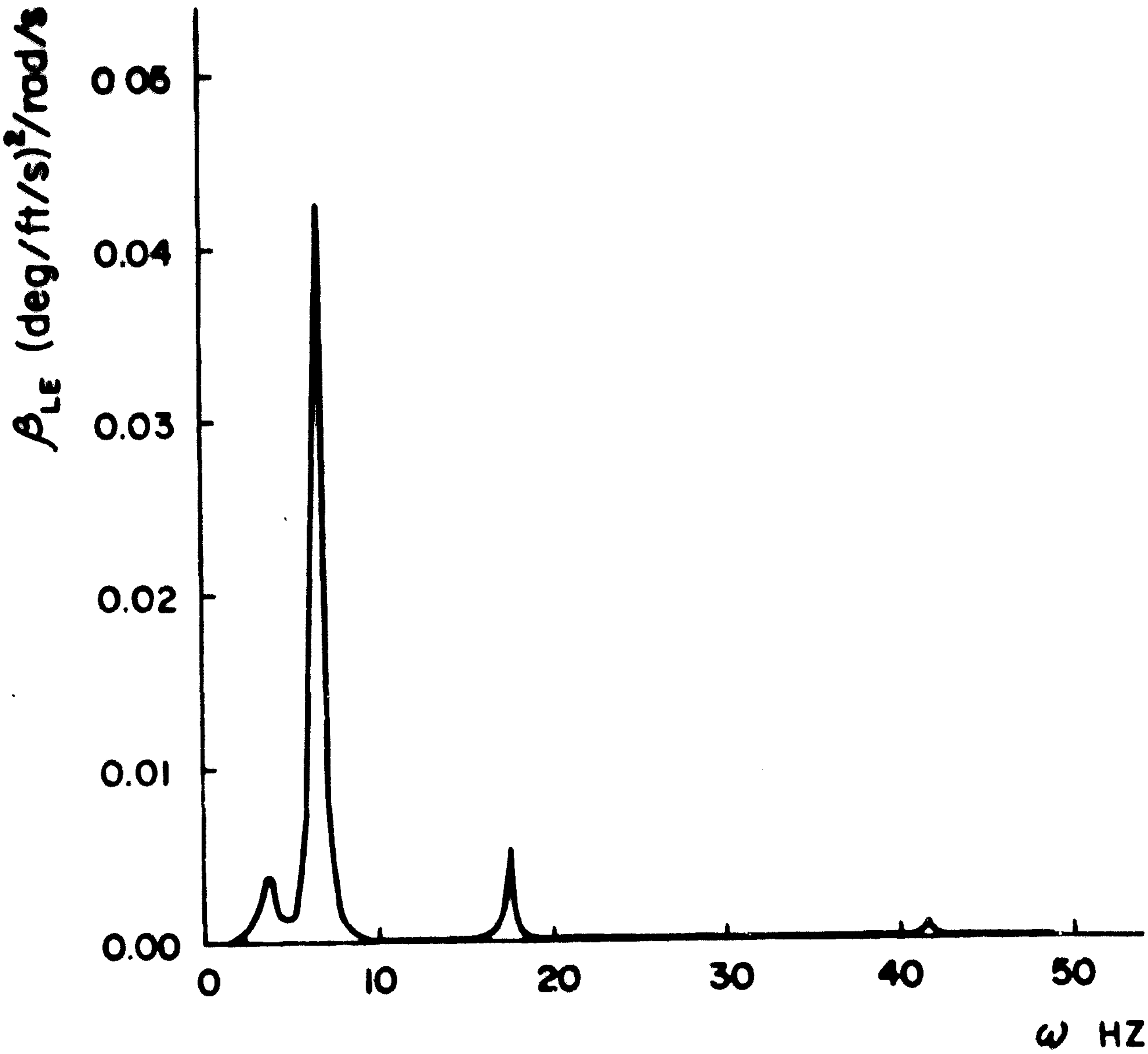

Figure 13a: PSD of Control Surface Response β_{LE} out

Figure 13· PSD of Control Surface Responses $\beta_{LE\,OUT}$, $\delta_{TE\,OUT}$ at $M = 0.8$, $Q_D = 60$ psf, Using Northrop Mechanization of Control Law II (using GRT values of g)

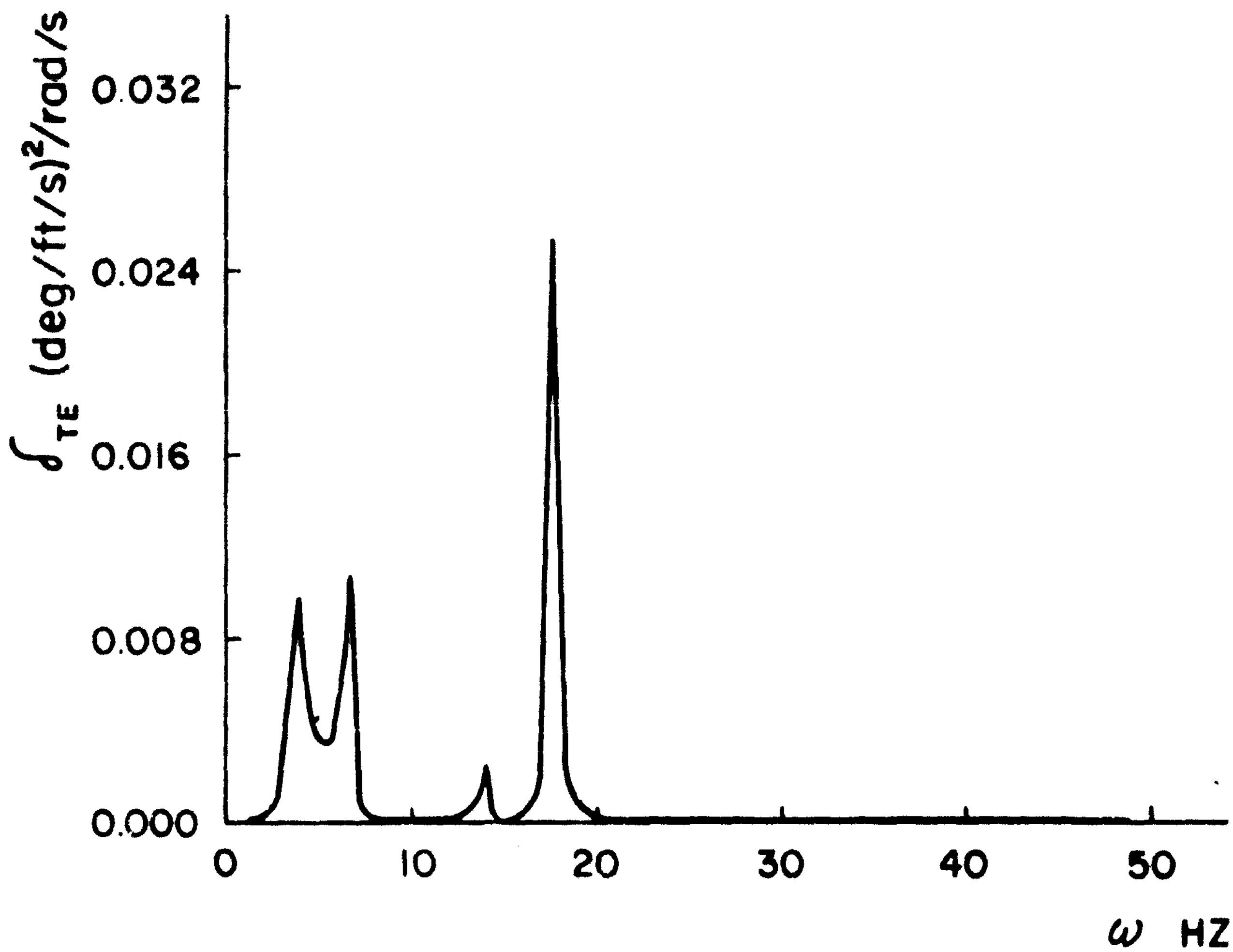

Figure 13b: PSD of Control Surface Response $\beta_{TE\ out}$

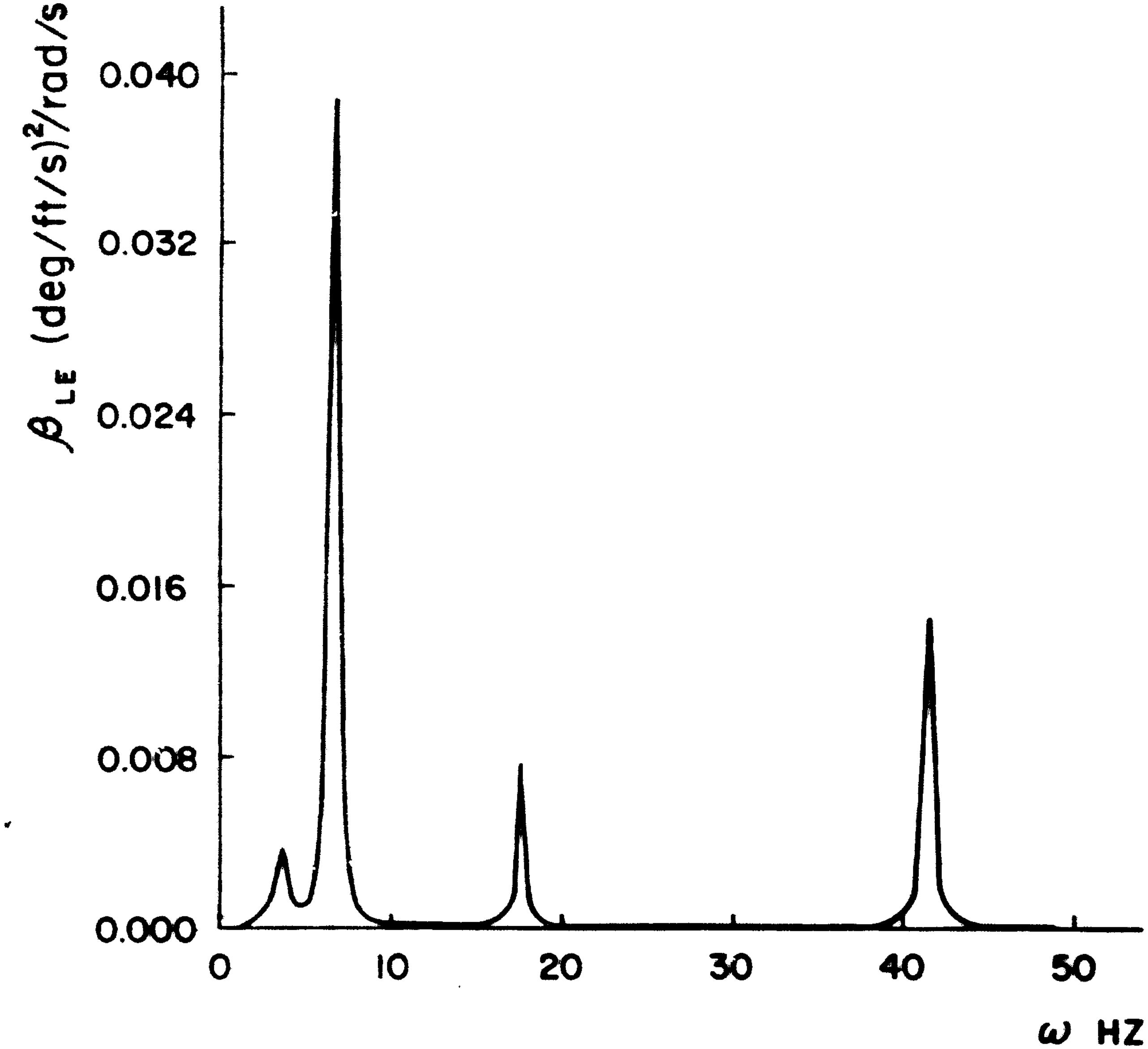

Figure 14a: PSD of Control Surface Response β_{LE} in

Figure 14: PSD of Control Surface Responses $\beta_{LE\,w}$, $\delta_{TE\,w}$ at M = 0.8, Q_D = 60 psf, Using Northrop Mechanization of Control Law II (using GRT values of g)

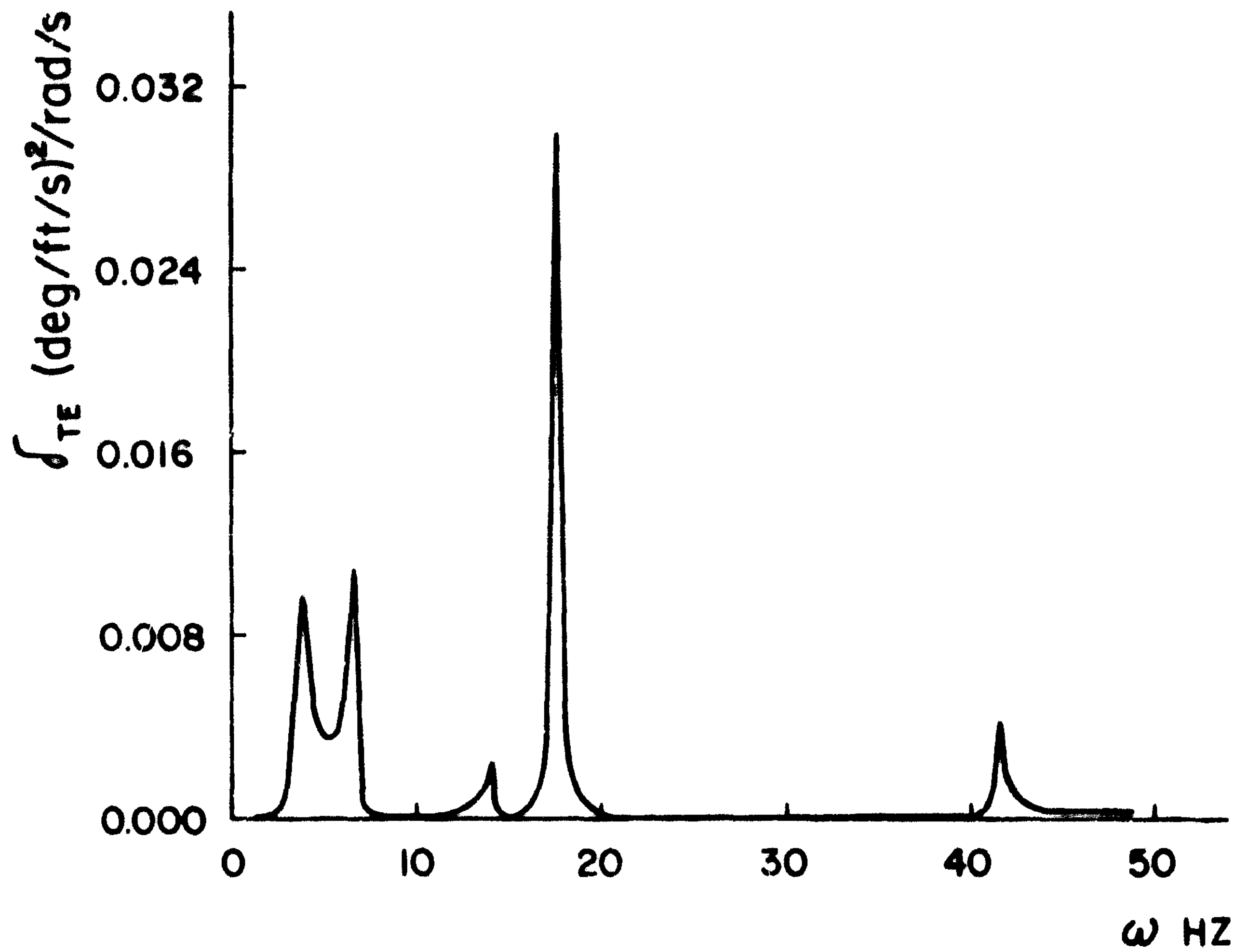

Figure 14b: PSD of Control Surface Response β_{TE} in

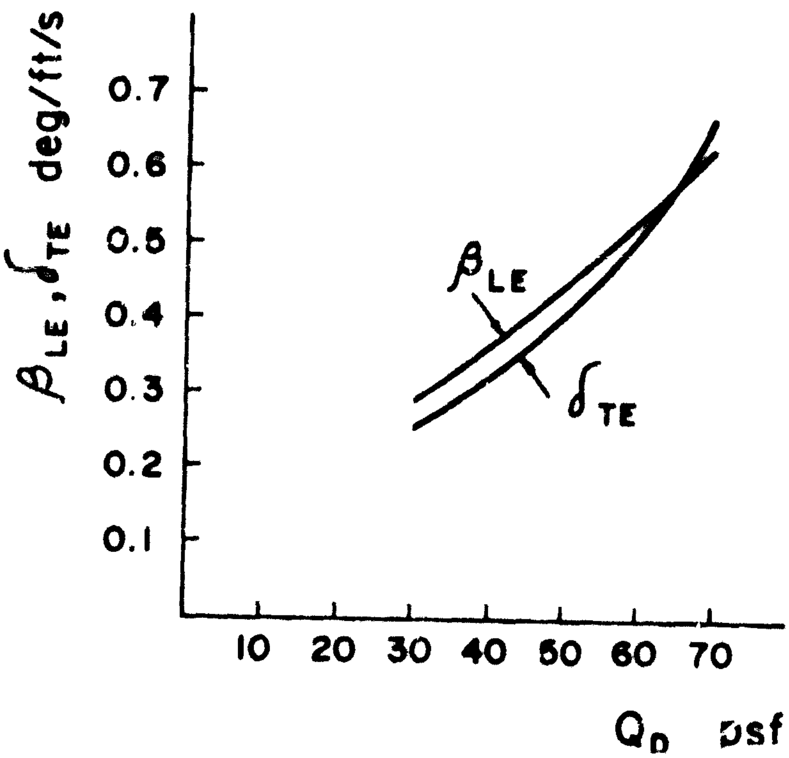

Figure 15: Variation with Q_D of rms Contol Surface Deflections due to Unit rms Gust Input, Using Northrop Mechanization of Control Law II (with GRT values of g, M = 0.8)

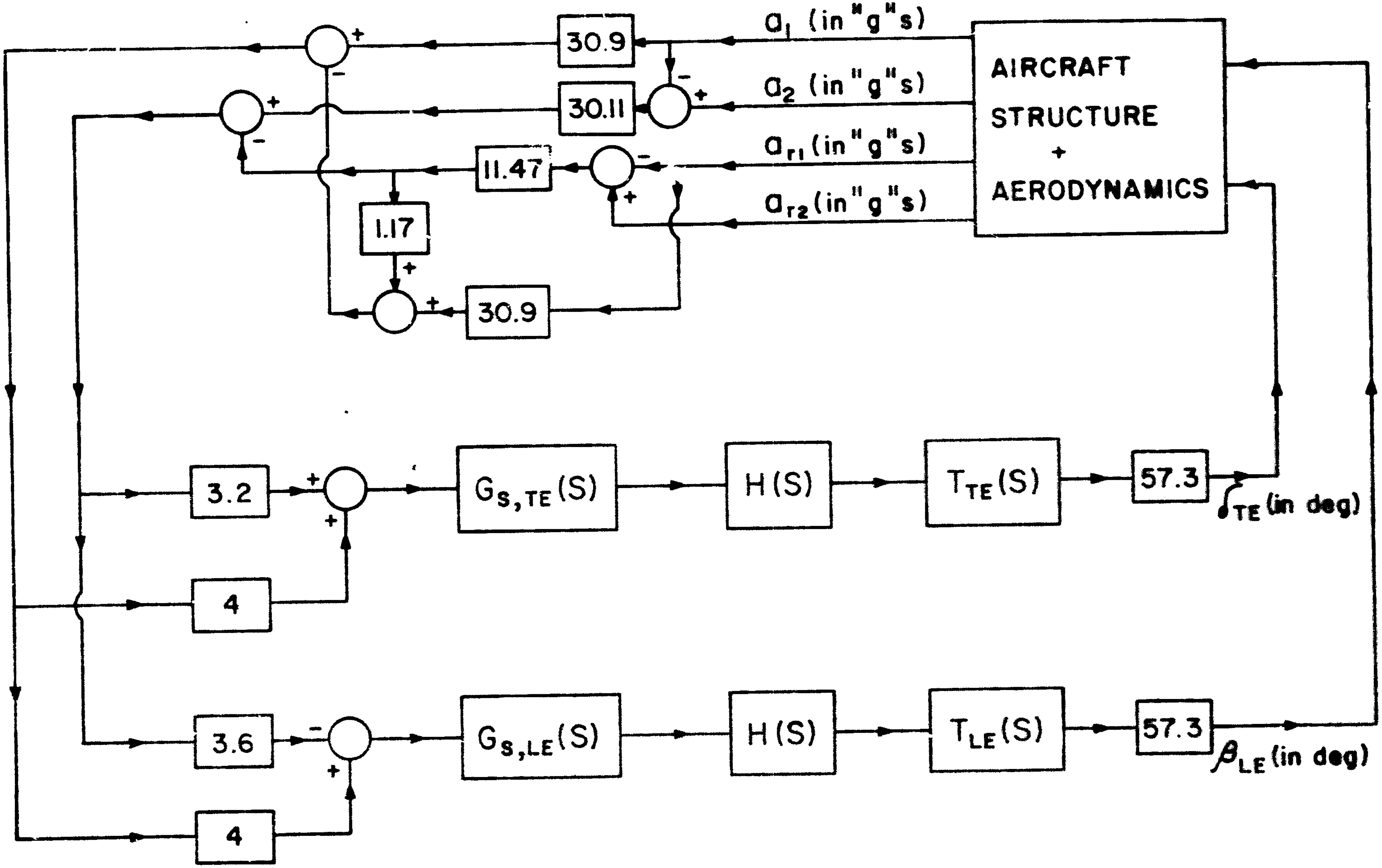

Figure A1: Block Diagram Representation of the Suggested L.E.-T.E. Control System

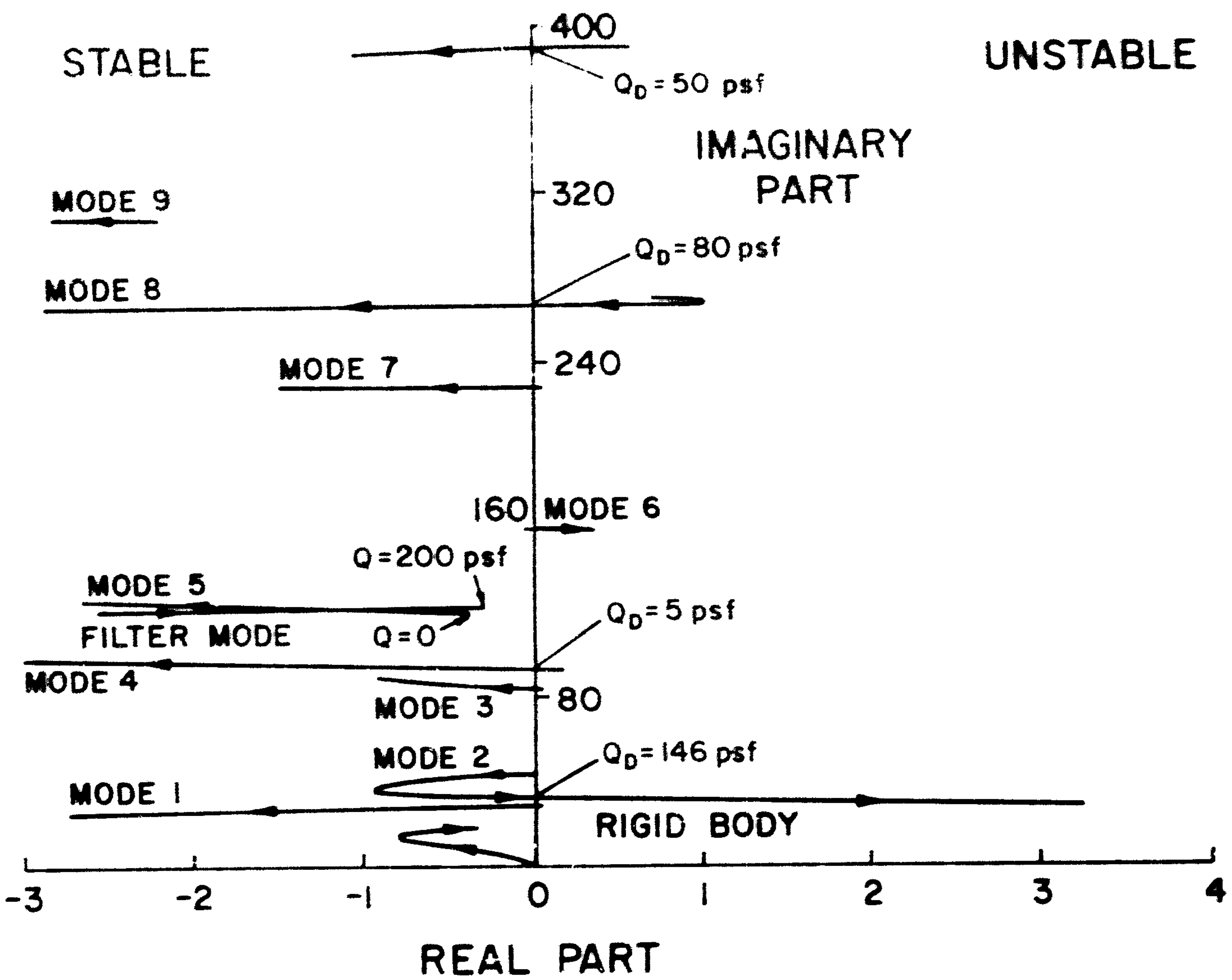

Figure A2: Root Locus Plot-Closed Loop System (g = 0, M = 0.8)

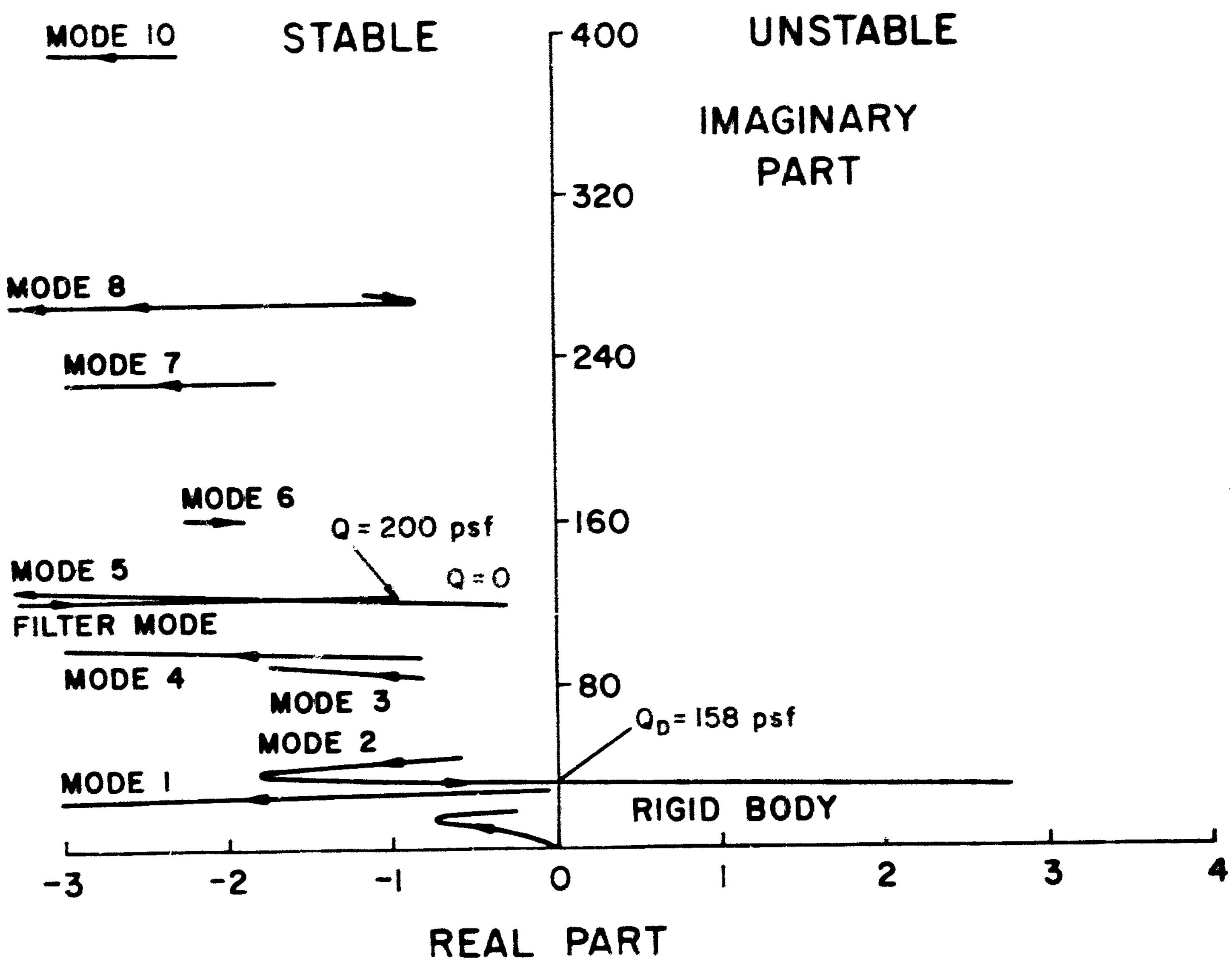

Figure A3: Root Locus Plot-Closed Loop System with Structural Damping (as measured in GRT)

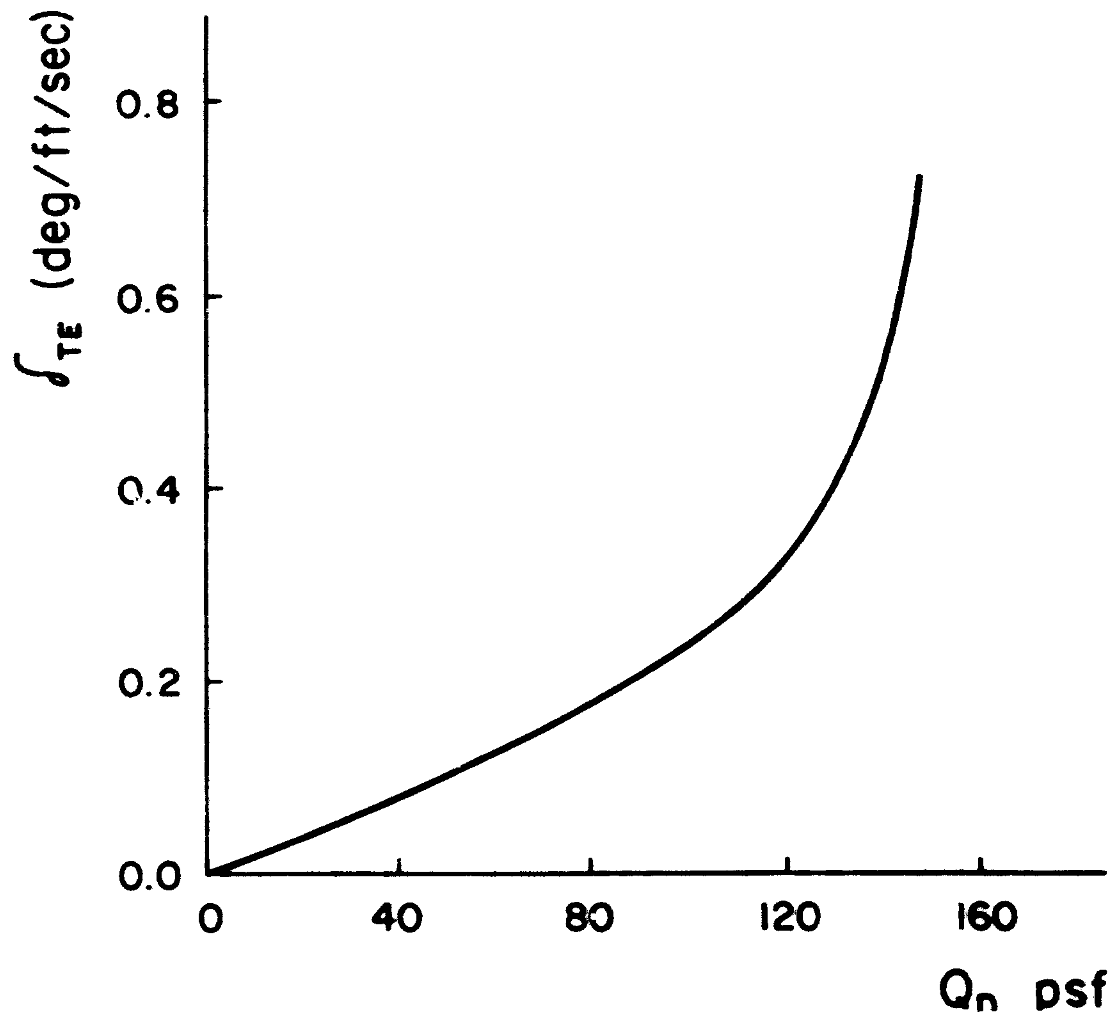

Figure A4: Variation with Q_D of rms T.E. Control Rotation due to Unit rms Gust Input (g = 0)

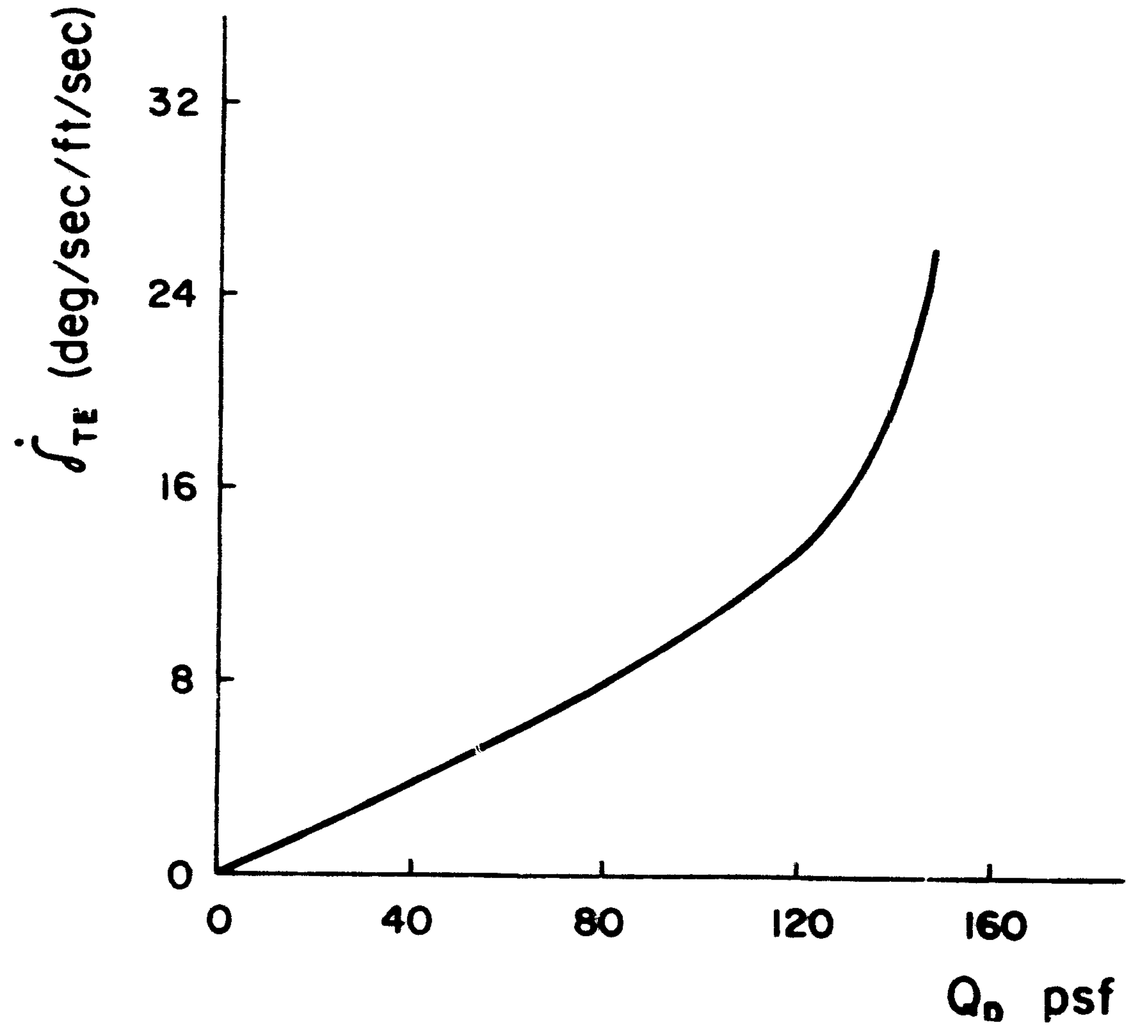

Figure A5: Variation with Q_D of rms T.E. Control Rate due to Unit rms Gust Input ($g = 0$)

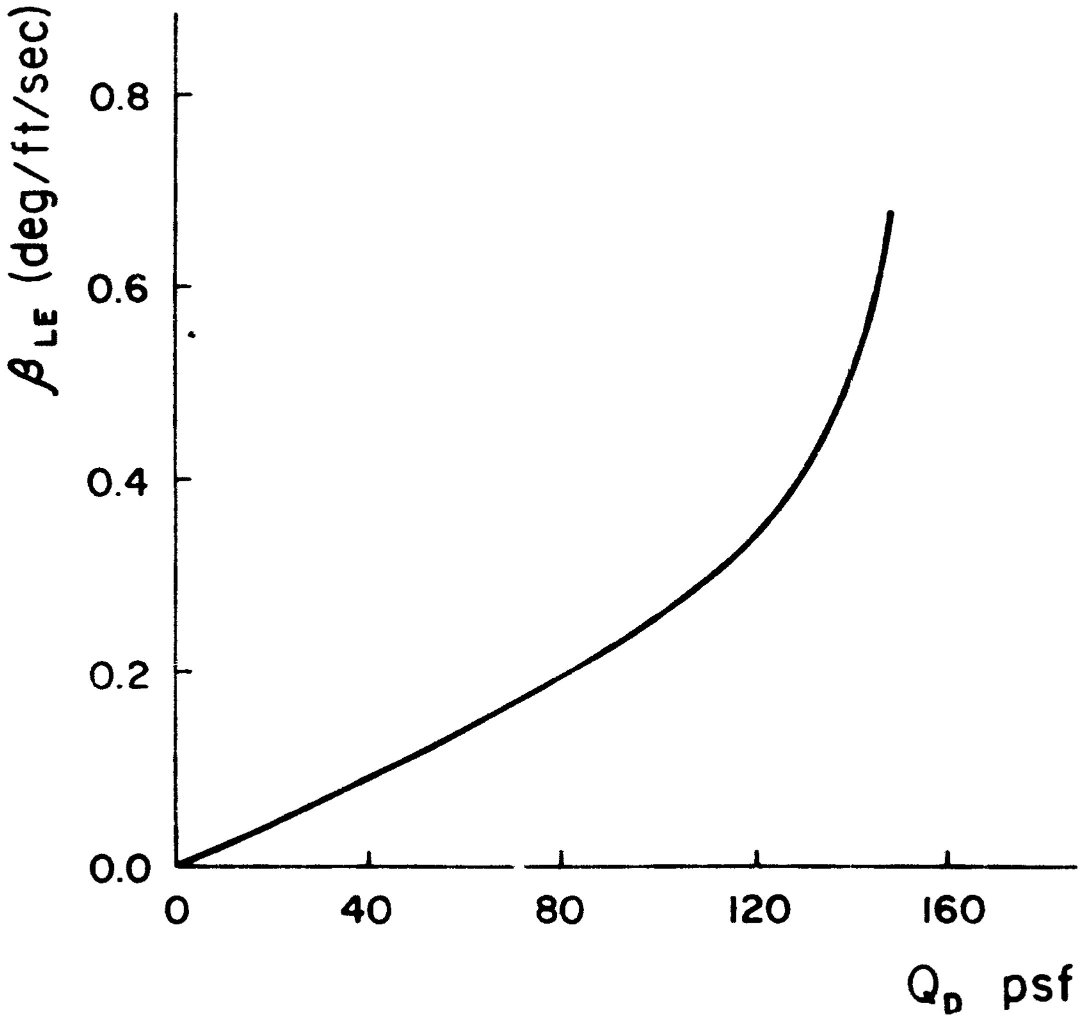

Figure A6: Variation with Q_D of rms L.E. Control Rotation Due to Unit rms Gust Input ($g = 0$)

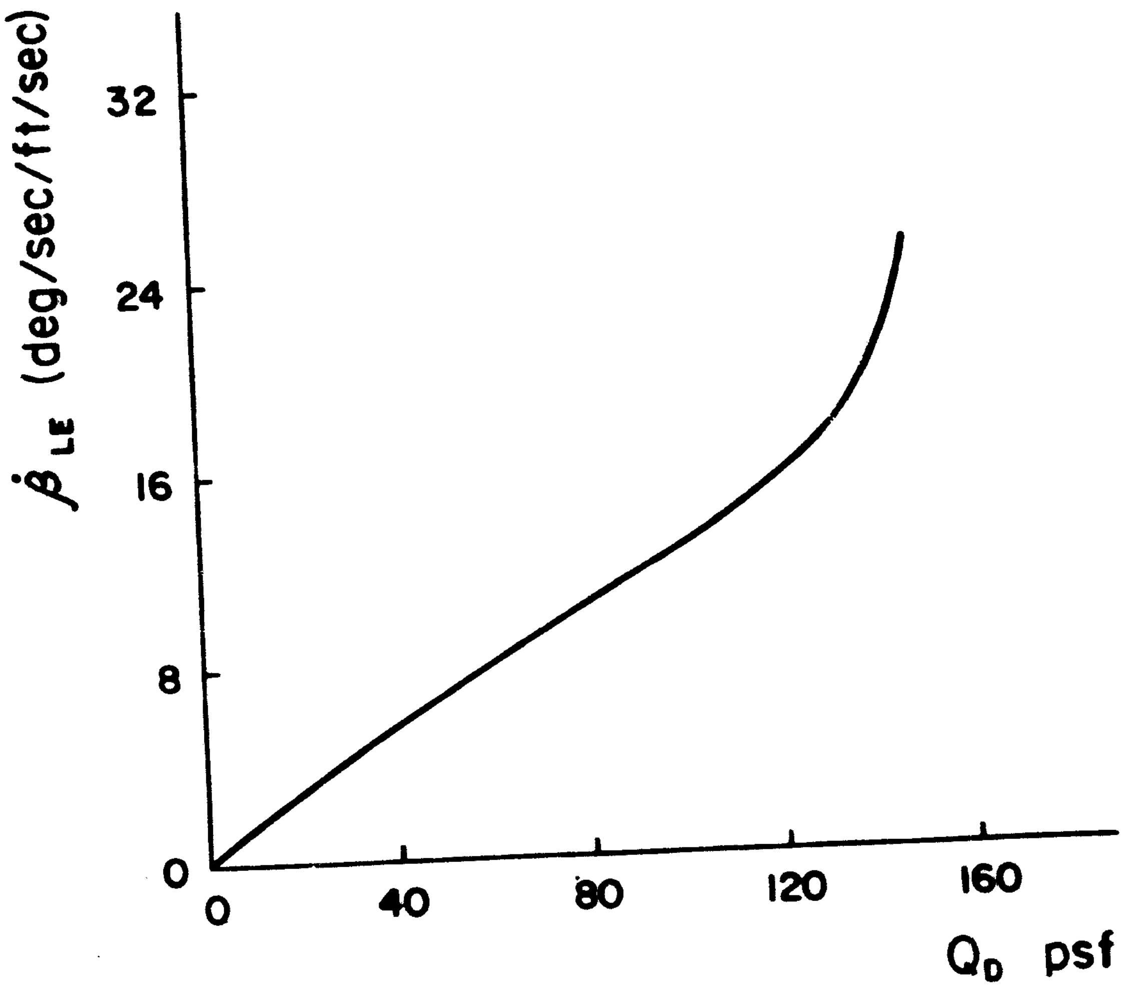

Figure A7: Variation with Q_D of rms L.E. Control Rate Due to Unit rms Gust Input (g = 0)

FLUTTER AND CONTINUOUS GUST COMPUTATIONS

WITH MULTI-ACTIVE CONTROLS

CONTENTS

1. THE EQUATIONS OF MOTION FOR FLUTTER ANALYSIS WITH MULTI-ACTIVE CONTROLS

A simplified method of formulation of the equations of motion for flutter analysis with any number of active control systems is presented in this work. The suggested method combines computational economy and programming simplicity with generality of formulation. It enables the treatment of multi-active control systems with no limitations on the form of the activated control laws. By way of introduction, two current methods of analysis will first be described and their limitations will be discussed. Following the presentation of these current methods, the new proposed method will be presented and its special features will be described.

The Equations of Motion

Let the n_s equations

$$\left([M]s^2 + \frac{1}{2}\rho V^2 [A] + [K]\right)\overline{q} = 0 \qquad (1)$$

represent the equations of motion of n_s structural modes (including rigid body modes) with n_c activated controls where [M] represents the mass matrix; [A], the complex aerodynamic matrix; [K], the stiffness matrix; ρ, the density of the surrounding fluid; V, the velocity of the fluid; and $\overline{q}$, the response vector. All the matrices in equation (1) are of size $n_s \times (n_s + n_c)$, that is, n_s structural modes + n_c active controls. The response vector $\overline{q}$ can be expressed in terms of n_s structural responses and n_c control deflections, that is,

$$\overline{q} = \begin{Bmatrix} q_s \\ q_c \end{Bmatrix} \qquad (2)$$

Equation (1) can therefore be written as

$$([M_s \quad M_c]s^2 + \tfrac{1}{2}\rho V^2[A_s \quad A_c] + [K_s \quad K_c]) \begin{Bmatrix} q_s \\ q_c \end{Bmatrix} = 0 \tag{3}$$

where subscript s denotes a structural quantity and c, a control quantity. Assume now a control law of the form

$$q_c = [T] \quad q_s \tag{4}$$

where [T] is a $n_c \times n_s$ matrix representing the transfer functions of the control law. Substitution of equation (4) into equation (3) yields

$$([M_s] + [M_c][T])s^2 + \frac{\rho V^2}{2}([A_s] + [A_c][T]) + [K_s] + [K_c][T]) \quad q_s = 0 \tag{5}$$

Typically, the elements of the aerodynamics matrices A_s and A_c are available as functions of the reduced frequency k and the Mach number M whereas the transfer function matrix [T] is a function of the Laplace variable s, normally expressed in terms of rational polynomials in s.

FLUTTER ANALYSIS BASED ON THE COMMON DENOMINATOR METHOD (CDM)

This method of analysis is described in ref. 1. It is based on the representation of the matrix [T] by

$$[T] = \frac{1}{Q(s)} [T_N] \tag{6}$$

where Q(s) is a scalar polynomial representing the common denominator of all the T_{ij} terms and where $[T_N]$ is a matrix involving the resulting numerators (as a function of s).

The variation with s of the aerodynamic matrix $[A_s \quad A_c]$ can be approximated by the following Pade representation

$$[A] = [A_0] + [A_1](\tfrac{b}{V})s + [A_2](\tfrac{b}{V})^2 s^2 + \sum_{j=1}^{r} \frac{[A_{(2+j)}]\, s}{s + \frac{V}{b}\beta_j} \tag{7}$$

where all the matrix coefficients and the a_j values are real and constants and where r normally varies between $1 \le r \le 4$. Substitution of equations (6) and (7) into equation (5) yields a rational matrix equation in s. The common denominator of the equation of motion is given by the scalar D(s) defined by

$$D(s) = Q(s) \prod_{j=1}^{r} [s + \frac{V}{b} a_j] \tag{8}$$

To solve the above rational equation of motion, it is multiplied by D(s) where D(s) is assumed to be of order $s^{(p-2)}$. Hence equation (5) which is of order s^2 turns to be of order s^p and assumes the form of a matrix polynomial expression

$$([F_o] + [F_1]s + [F_2]s^2 + \ldots\ldots + [F_p]s^p) \; q_s = 0 \tag{9}$$

where the matrix coefficients $[F_j]$ are functions of M, V, and dynamic pressure $q_D (= \frac{1}{2}\rho V^2)$. Equation (9) can be reduced to the following canonical form for eigenvalue solution

$$s \; X = [U] \; X \tag{10}$$

where [U] is of size $(p \times n_s) \times (p \times n_s)$ defined by

$$[U] = \begin{bmatrix} [-F_p^{-1}F_{p-1}] & [-F_p^{-1}F_{p-2}] & \cdots & [-F_p^{-1}F_1] & [-F_p^{-1}F_o] \\ [I] & 0 & \cdots & 0 & 0 \\ 0 & [I] & \cdots & 0 & 0 \\ \vdots & \vdots & & \vdots & \vdots \\ 0 & 0 & \cdots & [I] & 0 \end{bmatrix} \tag{11}$$

and X is given by

$$X = \begin{Bmatrix} s^{(p-1)} & q_s \\ s^{(p-2)} & q_s \\ \vdots & \vdots \\ s & q_s \\ s^o & q_s \end{Bmatrix} \tag{12}$$

It can thus be seen that the original n_s structural equations of motion end up with $(p \times n_s)$ equations which need to be solved for their eigenvalues.

The main disadvantage of this method lies in the very rapid expansion with control law transfer function of the order of the eigenvalue problem. For illustration purposes, consider a 10 degree of freedom flutter problem (n_s=10) with aerodynamics approximated using 4 lag terms (r=4) and with two active control surfaces driven by control laws having four poles each. Hence Q(S) will be of order S^8 and D(S) of order S^{12} (see eq. (8)). The value of p will therefore be equal to p=14. It can therefore be seen that the original 10 degree of freedom flutter problem turns into an eigenvalue problem of order (14 x 10), that is, of order 140.

FLUTTER ANALYSIS BASED ON OPTIMAL CONTROL FORM OF TRANSFER FUNCTIONS (OCF) (Ref.2)

Consider equation (3), substitute equation (7) and multiply by the common denominator of the lag terms to obtain a matrix polynomial equation of the form

$$([F_{o_s}\ F_{o_c}] + [F_{1_s}\ F_{1_c}]s + [F_{2_s}\ F_{2_c}]s^2 + \ldots + [F_{(r+2)_s}\ F_{(r+2)_c}]s^{(r+2)})\begin{Bmatrix} q_s \\ q_c \end{Bmatrix} = 0 \quad (13)$$

where r represents the number of lag terms in equation (7) and where the matrix coefficients $[F_j]$ are functions of M, V and q_D. As in the previous case treated above, equation (13) can be brought to the form

$$s\ X_s = [\bar{A}_s]\ X_s + [\bar{B}_c]\ X_c \quad (14)$$

where

$$X_s = \begin{Bmatrix} s^{(r+1)} & q_s \\ s^r & q_s \\ & \vdots & \\ s & q_s \\ s^0 & q_s \end{Bmatrix} \tag{15}$$

$$X_c = \begin{Bmatrix} s^{(r+2)} & q_c \\ s^{(r+1)} & q_c \\ & \vdots & \\ s & q_c \\ s^0 & q_c \end{Bmatrix} \tag{16}$$

$$[\bar{A}_s] = \begin{bmatrix} [G_s \bar{F}_{(r+1)_s}] & [G_s \bar{F}_{r_s}] & \cdots & [G_s \bar{F}_{1_s}] & [B_s \bar{F}_{0_s}] \\ [I] & 0 & \cdots & 0 & 0 \\ 0 & [I] & \cdots & 0 & 0 \\ \vdots & \vdots & & & \\ 0 & 0 & \cdots & [I] & 0 \end{bmatrix} \tag{17}$$

where

$$[G_s] = [\bar{F}_{(r+2)_s}]^{-1} \tag{18}$$

and where

$$[\bar{B}_c] = \begin{bmatrix} [G_s \bar{F}_{(r+2)_c}] & [G_s \bar{F}_{(r+1)_c}] & \cdots & [G_s \bar{F}_{1_c}] & [G_s \bar{F}_{0_c}] \\ 0 & 0 & \cdots & 0 & 0 \\ \vdots & \vdots & & \vdots & \vdots \\ 0 & 0 & \cdots & 0 & 0 \end{bmatrix} \tag{19}$$

To include the effects of actuator dynamics using optimal control form of transfer functions, the actuator model is described in state-space form. For simplicity of illustration, consider the case of a single actuator that is, when q_c is a scalar rational polynomial quantity. Assume the following form for the actuator transfer function

$$\frac{q_c(s)}{q_{c,I}(s)} = \frac{b_o}{s^n + a_{n-1}s^{n-1} + \ldots a_o} \tag{20}$$

where $q_{c,I}(s)$ represents the input signal to the actuator.

Equation (12) can be brought to the form

$$(s^n + a_{n-1}s^{n-1} + \ldots a_o)q_c = b_o q_{c,I} \tag{21}$$

which, in turn, can be represented by

$$s \; X_{a,c} = [A_{a,c}] \; X_{a,c} + [B_{a,c}] \; u_{a,c} \tag{22}$$

where

$$X_{a,c} = \begin{Bmatrix} s^{n-1} & q_c \\ s^{n-2} & q_c \\ \vdots & \\ s & q_c \\ s^o & q_c \end{Bmatrix} \tag{23}$$

$$u_{a,c} = q_{c,I} \tag{24}$$

$$[A_{a,c}] = \begin{bmatrix} -a_{n-1} & -a_{n-2} & \cdots\cdots & -a_1 & -a_o \\ 1 & 0 & \cdots\cdots & 0 & 0 \\ 0 & 1 & & 0 & 0 \\ \vdots & \vdots & & \vdots & \vdots \\ 0 & 0 & \cdots\cdots & 1 & 0 \end{bmatrix} \tag{25}$$

$$[B_{a,c}] = \begin{Bmatrix} b_o \\ 0 \\ \vdots \\ 0 \end{Bmatrix} \tag{26}$$

For a number of control surfaces, an equation similar to equation (22) is obtained.

Denote by $\overline{X}_c$ the longest of the vectors X_c and $X_{a,c}$ and modify either $[A_{a,c}]$ or $[B_c]$ accordingly (denoted by adding an additional bar to these matrices. In so doing, it is possible to merge equations (14) and (22) into a single equation of the form

$$s\begin{Bmatrix} X_s \\ \overline{X}_c \end{Bmatrix} = \begin{bmatrix} \overline{A}_s & \overline{\overline{B}}_c \\ 0 & \overline{A}_{a,c} \end{bmatrix} \begin{Bmatrix} X_s \\ \overline{X}_c \end{Bmatrix} + \begin{bmatrix} 0 \\ \overline{B}_{a,c} \end{bmatrix} u_{a,c} \tag{27}$$

The matrix A_s is of order $[n_s x(r+2)]x[n_s x(r+2)]$;whereas $[\overline{A}_{a,c}]$ is of order $n_{a,c} \times n_{a,c}$ where

$$n_{a,c} = \max \left[\sum_{i=1}^{n_c} n_i \;;\quad (r+3) \times n_c\right] \tag{28}$$

where n_i denotes the value of n for the ith control.

Optimal control analysis yields control laws of the following form

$$u_{a,c} = [E] \begin{Bmatrix} X_s \\ \overline{X}_c \end{Bmatrix} \tag{29}$$

where [E] is a matrix of constants. Substitution of equation (29) into eq. (27) yields the following eigenvalue equation which forms the basic equation for flutter analysis

$$s\begin{Bmatrix} X_s \\ \overline{X}_c \end{Bmatrix} = \left(\begin{bmatrix} \overline{A}_s & \overline{\overline{B}}_c \\ 0 & \overline{A}_{a,c} \end{bmatrix} + \begin{bmatrix} 0 \\ \overline{B}_{a,c} \end{bmatrix} [E] \right) \begin{Bmatrix} X_s \\ \overline{X}_c \end{Bmatrix} \tag{30}$$

The order of this eigenvalue equation is therefore $[n_s x(r+2)+n_{a,c}]x[n_s x(r+2)+n_{a,c}]$.

For comparison purposes, consider the example treated earlier, that is, the case where

$n_s = 10$, $n_c = 2$, $r = 4$, $n = 4$ (for each control)

Hence, the order of the eigernvalue equation (30) will be, in this case,

$10 \times (4+2) + 7 \times 2 = 74$

which is almost half the order obtained by using the CDM method (= 140).

The main disadvantage of this method involves the limitation brought about by the use of a control law defined by equation (29). In this latter equation, the control law transfer function is linear with X_s

and is therefore limited to derivatives of q_s not exceeding the order of $(r+1)$ whereas a general transfer function may employ any order of q_s derivatives provided it is smaller than the order of its denominator.

In the following section, a different method is presented which is very similar to the method just described but which avoids the use of the limiting forms of control laws, such as the one described by equation (29).

THE PROPOSED METHOD

Consider equations (3) and (4) and represent the matrix [T] in equation (4) by

$$[T] = [\frac{1}{Q(s)}]\ [P(s)] \tag{31}$$

where $[\frac{1}{Q(s)}]$ is a diagonal matrix consisting of the common denominators of each of the rows of matrix [T] and where [P(s)] represents the remaining numerator polynomial (in s) of matrix [T]. Substituting equation (31) into equation (4) and combining it with equation (3) we obtain

$$\left[\begin{array}{cc} [[M_s & M_c]s^2 + q_o[A_s \quad A_c] + [K_s \quad K_c]] \\ \hline [-[\frac{1}{Q(s)}]\ [P(s)] & I\ ] \end{array}\right] \begin{Bmatrix} q_s \\ q_c \end{Bmatrix} = 0 \tag{32}$$

or, after some rearrangement

$$\left[\begin{array}{cc} [M_s & M_c]s^2 + q_o[A_s \quad A_c] + [K_s \quad K_c] \\ \hline [-P(s) & Q(s)] \end{array}\right] \begin{Bmatrix} q_s \\ q_c \end{Bmatrix} = 0 \tag{33}$$

Substitute equation (7) into equation (33) and multiply the structural equations by the common denominator of the lag terms to obtain after some rearrangements

$$\left[\begin{array}{cc} E(s) & G(s) \\ \hline -P(s) & Q(s) \end{array}\right] \begin{Bmatrix} q_s \\ q_c \end{Bmatrix} = 0 \tag{34}$$

where E(s) and G(s) are matrix polynomials of order $s^{(r+2)}$.

Define the following matrices

$$R(s) = \begin{bmatrix} E(s) \\ -\,- \\ P(s) \end{bmatrix} \tag{35}$$

$$D(s) = \begin{bmatrix} G(s) \\ -\,- \\ Q(s) \end{bmatrix} \tag{36}$$

where R(s) and D(s) can be written in the following matrix polynomial form.

$$R(s) = R_0 + R_1 s + R_2 s^2 + \ldots R_m s^m \tag{37}$$

$$D(s) = D_0 + D_1 s + D_2 s^2 + \ldots D_n s^n \tag{38}$$

The value of m is (r+2) unless the order of the numerators P(s) is larger than (r+2). In this latter case, m assumes the maximum value of the power (in s) of the numerators. Similarly, the value of n is equal to the largest value of the powers of Q(s) (which represents the denominators of the control laws transfer functions), provided it is larger than (r+2). Otherwise, m will assume the value of (r+2).

It should be stated at this stage that the representation of D(s) by equation (38) is convenient for mathematical representation and for programming, but is somewhat wasteful regarding the final order of the eigenvalue problem. However, these changes in the order of the eigenvalue problem are generally small, and do not, therefore, warrant a different, more cumbersome formulation. It should also be observed that the highest powers in s of both E(s) and G(s) are of order (r+2) and that the highest powers in s of P(s) are either equal or smaller than the highest powers in s of Q(s) (since P(s) appears in the numerator of the transfer functions whereas Q(s) appears in the denominator). Hence it can be stated that

$$m \leq n \tag{39}$$

substituting equations (35) - (38) into equation (34) and rearranging yields the following equation

$$[[R_m \quad D_n]s\ [R_{m-1} \quad D_{n-1}][R_{m-2} \quad D_{n-2}] \ . \ . \ . \ [R_o \quad D_{n-m}]\ [D_{n-m-1}] \ . \ . \ .$$
$$. \ . \ . \ [D_o]] \begin{Bmatrix} Z \\ Y \end{Bmatrix} = 0 \qquad (40)$$

where

$$Y = \begin{Bmatrix} s^{m-1} & q_s \\ s^{n-1} & q_c \\ s^{m-2} & q_s \\ s^{n-2} & q_c \\ & \vdots \\ s^{o} & q_s \\ s^{n-m} & q_c \\ s^{n-m-1} & q_c \\ & \vdots \\ s^{o} & q_c \end{Bmatrix} \ ; \ Z = \begin{Bmatrix} s^{m-1} & q_s \\ s^{n-1} & q_c \end{Bmatrix} \qquad (41)$$

For the case where n=m, all the terms appearing in equations (40), (41) which involve powers or indices smaller than (n-m), should be omitted from the equations.

Premultiplying equation (4) by $[R_m \quad D_n]^{-1}$ and defining

$$[\bar{R}_j \quad \bar{D}_i] = -[R_m \quad D_n]^{-1}\ [R_j \quad D_i] \qquad (42)$$

we obtain the following equation

$$[[I]s\ [\bar{R}_{m-1} \quad \bar{D}_{n-1}][\bar{R}_{m-2} \quad \bar{D}_{n-2}]\cdots[\bar{R}_o \quad \bar{D}_{n-m}][\bar{D}_{n-m-1}]\cdots[\bar{D}_o]] \begin{Bmatrix} Z \\ Y \end{Bmatrix} = 0 \qquad (43)$$

Finally, equation (43) can be written in the form

$$s\ Y = \begin{bmatrix} [\bar{R}_{m-1} \quad \bar{D}_{n-1}] & [\bar{R}_{m-2} \quad \bar{D}_{n-2}] & \cdots & [\bar{R}_1 \quad \bar{D}_{n-m-1}] & [\bar{R}_0 \quad \bar{D}_{n-m}] & [\bar{D}_{n-m-1}] & \cdots & [\bar{D}_1] & [\bar{D}_o] \\ [I] & 0 & \cdots & 0 & 0 & 0 & \cdots & 0 & 0 \\ 0 & [I] & \cdots & 0 & 0 & 0 & \cdots & 0 & 0 \\ \vdots & \vdots & \cdots & \vdots & \vdots & \vdots & & \vdots & \vdots \\ 0 & 0 & \cdots & [I] & 0 & 0 & \cdots & 0 & 0 \\ 0 & 0 & \cdots & 0 & [0 \quad I^*] & 0 & \cdots & 0 & 0 \\ \vdots & \vdots & & \vdots & \vdots & \vdots & & \vdots & \vdots \\ 0 & 0 & & 0 & 0 & 0 & \cdots & [I^*] & 0 \end{bmatrix} Y \qquad (44)$$

or $$s\,Y = [U]\,Y \tag{45}$$

where $[I]$ is a unit matrix of order (n_s+n_c) and $[I^*]$ is a unit matrix of order n_c. Equation (44) represents therefore an eigenvalue problem of order $(m \times n_s + n \times n_c)$.

For illustration purposes, consider the example treated earlier in this work, that is

$n_s = 10$, $n_c = 2$, $r = 4$

with control surfaces transfer function with 4 poles each. In this case

$m = 6$; $n = 6$

Hence, the order of the eigenvalue equation will be

$6 \times 10 + 6 \times 2 = 72$

This is about the same order as the OCF method ($=$ 74) and is of considerably smaller order than the CDM method ($=$ 140). Hence, the method proposed herein, enjoys the compactness of the OCF method while maintaining the utmost generality in the form of the control law used for activation. It should be mentioned at this stage that care must be exercised while setting up equation (40) so as to ensure that the matrix $[R_m \quad D_n]$ is non-singular (since it needs to be inverted). This point is important while programming equation (40).

2. THE EQUATIONS OF MOTION FOR GUST RESPONSE OPTIMIZATION ANALYSIS WITH MULTI-ACTIVE CONTROLS

The n_s equations of motion represented by eq. (1) now assume the following form

$$([M]s^2 + \frac{1}{2}\rho V^2[A] + [K])\ \bar{q} = F_G \tag{46}$$

where F_G represents the gust force acting on the system due to a sinusoidal gust velocity of unit amplitude at a specified Mach number and a specified dynamic pressure. Following identical steps represented by eqs (2-4), the following equivalent form of eq. (5) is obtained

$$[([M_s] + [M_c]\ [T])s^2 + \frac{\rho V^2}{2}([A_s] + [A_c][T]) + ([K_s] + [K_c][T])]\ q_s = F_G \tag{47}$$

Eq. (47) yields

$$q_s = [B]\ F_G \tag{48}$$

where

$$[B] = [([M_s]+[M_c][T])s^2 + \frac{\rho V^2}{2}([A_s]+[A_c][T])+([K_s]+[K_c][T])]^{-1} \tag{49}$$

Using eqs. (4), (48), the control response can be computed

$$q_c = [T][B]\ F_G \tag{50}$$

The control rates can similarly be represented by

$$\dot{q}_c = s[T][B]\ F_G \tag{51}$$

The i^{th} root-mean-square (rms) control deflection or the i^{th} rms control surface rate per unit rms gust input is then computed using the following relations for the i^{th} control surface

$$(q_{c_i})_{rms} = (\int_{\omega_1}^{\omega_2} q_{c_i}^2\ \phi(\omega)d\omega)^{1/2} \tag{52}$$

or

$$(\dot{q}_{c_i})_{rms} = \left(\int_{\omega_1}^{\omega_2} \dot{q}_{c_i}^2 \, \phi(\omega) d\omega\right)^{1/2} \quad (53)$$

where $\phi(\omega)$ represents the Von-Karman gust spectrum.

The gust optimization program seeks to minimize a target function consisting of weighted rms responses or weighted rms response rates of the control surfaces by varying the various specified control gains available in matrix [T]. For the optimization results to yield sensible values it is absolutely necessary that the initial values of [T] (for the specified flight dynamic pressure and the specified Mach number) be such as to yield a stable system. Under this condition, stability is maintained during the optimization process while the control surface rms responses are reduced.

Further details regarding the gust optimization method for flutter suppression are presented in ref. 1.

REFERENCES

1. Nissim, E., Abel, I.: Development and Application of an Optimization Procedure for Flutter Suppression Using the Aerodynamic Energy Concept. NASA TP 1137, Feb. 1978.
2. Newsom, J.R.: A Method for Obtaining Practical Flutter-Suppression Control Laws Using Results of Optimal Control Theory. NASA TP 1471, Aug. 1979.
3. Nissim, E.: Recent Advances in Aerodynamic Energy Concept for Flutter Suppression and Gust Alleviation Using Active Controls. NASA TN D-8519, Sept. 1977.

3. APPENDIX A

OPERATION INSTRUCTIONS FOR THE FLUTTER PROGRAM

The program computes the eigenvalues of the flutter equations of motion with active controls. The dimensions assigned to the different arrays permit the simultaneous activation of up to 6 controls (of leading-edge (L.E.), and/or trailing edge (T.E.) types) with resulting augmented eigenvalue problem of up to 100 values (the basic unaugmented system is limited to 15 modes, including rigid body modes). The input data is organized on file 5, with the aerodynamic data (defined by array AERO(I,J,K)) located on file 2. The printed output is located on file 6. The control law transfer function matrix is computed in subroutine CONTRL. The program includes two versions for CONTRL based on the concept of aerodynamic energy. It is imperative to extract one of these two versions of CONTRL before running the program. For other types of control laws, subroutine CONTRL needs to be reprogrammed. To ease this task, details relating to subroutine CONTRL are given in Appendix C.

The output of the program consists of the input data together with the system's eigenvalues over a selected range of dynamic pressures. The package includes all the subroutines used by the program except for the plotting subroutines (which are installation oriented) and the eigenvalue routines (IMSL routines). To ease the substitution of these eigenvalue routines by other ones (should the IMSL library be unavailable) a full description of the COMMON parameters of these routines is given in Appendix D. A root-locus plot (with dynamic pressure as variable) may form a part of the output when desired.

The program is written in FORTRAN and was developed on an IBM 370/168 computer. Double precision is used throughout the program due to the shorter IBM word length relative to the CDC computers. For CDC installations, it is recommended to convert the program to a single precision version. An example of an input and an output is included herein.

INPUT OF DATA

In the following, the data required for the operation of the flutter program is described. For sake of clarity and brevity READ statements are reproduced here together with the specified FORMAT and with the full explanation of the various parameters.

READ (FORMAT (15A4)), (HDR(I), I=1,15)

HDR — an alphanumeric header for the job (up to 60 characters, including spaces).

READ (5, CASE)

where 5 designates the input file and CASE is a namelist defind by NAMELIST/CASE/NM, NC, NAER, B, NG, NL

where

NM — Integer specifying the number of modes (≤ 15)

NC — Integer specifying the number of controls (≤ 6)

NAER - 1 — Input aerodynamics will be introduced by means of PADE interpolation coefficients

- 0 — Input aerodynamics will be introduced by means of aerodynamic coefficients at different values of reduced frequency k.

B — Array of values of lag terms to be used during the PADE interpolation (≤ 4)

NG = 1 If gust aerodynamic coefficients are included in the aerodynamic data.

= 0 If gust aerodynamic coefficients are not included in the aerodynamic data.

NL Integer specifying the number of lag terms to be used during the PADE interpolation (≤ 4)

The aerodynamic data is then introduced as follows:

```
    If NAER = 1 then
    DO 1 I  = 1, NM
    DO 1 J  = 1, (NM+NC)
READ (FORMAT (6X, 7E10.4)), A0(I,J), A1(I,J), A2(I,J), A3(I,J), A4(I,J),
A5(I,J), A6(I,J)
    1 CONTINUE
```

where the aerodynamic matrix A (see eq. (1)) is assumed to be expressed by

$$[A] = [A0] + [A1](ik) + [A2](ik)^2 + \sum_{L=1}^{NL} \frac{[AL]\ (ik)}{ik + B(L)}$$

and k denotes the reduced frequency. The aerodynamic matrix [A] should be arranged so that control coefficients are located in the last columns with the gust coefficients at the very last column.

```
    If NAER = 0 then
READ (5, FT)
    DO 1 K = 1, NK
    DO 1 J = 1, (NM + NC + NG)
    DO 1 I = 1, NM
READ (2, FORMAT (2E15.5))  AERO (I,J,K)
    1 CONTINUE
```

where FT is a namelist defined by

NAMELIST/FT/NK, AK, MAXNK, NPRINT, NPUNCH, IRIGID, JRIGID

and where 2 designates the file in which the aerodynamic data is located. The various parameters are defined as follows:

NK Number of reduced frequencies k used for the interpolation of the aerodynamic coefficients.

AK Array ($\leq$ 20) containing the values of k corresponding to the aerodynamic coefficients. The first value of k must be zero. The order of the frequency values must correspond to the order of the aero coefficients AERO (I,J,K) - see below.

MAXNK Maximum value of NK (= 20 in present program).

NPRINT - 0 No printed output from the Pade interpolation routine (named subroutine FIT).

- 1 Printed output is available.

NPUNCH - 0 No punched output from subroutine FIT.

IRIGID,JRIGID

Interpolation coefficients for the aerodynamic coefficients (PADE representation) of the first IRIGID rows and first JRIDIG columns are determined using the first few values of reduced frequency k (assumed to be the lowest) without resorting to a least squares procedure. In this case the rigid body modes must be located so as to be the first modes. This is done in order to increase the accuracy of the aerodynamic coefficients at low k values where steady state stiffness and damping terms are zero (the least square routine may render them negative).

AERO(I,J,K) Array containing the values of the aerodynamic matrix A (see eq. (1)) - that is, the $(I,J)^{th}$ coefficient at the K^{th} reduced frequency. The order at which the different K values are arranged must correspond to the AK values The first k value must correspond to k=0. For order of columns in [A] see remark for case NAER≠0.

The program proceeds to the construction of the equations of motion (in subroutine FLUTCA) in first order form, as explained in the theoretical section of this work. The data required for this purpose is the following:

READ (5, FLUT)

where FLUT is a namelist defined by

NAMELIST /FLUT/MASS, OMEGAN, QBEGIN, QEND, NQ, VEL, BTRAN, CTRAN, CREF, ZW, ZREF, IPLOT, CLF, CTR, NCACT.

and the parameters are as follows:

MASS MASS matrix ($\leq$ (15 x 15)

OMEGAN Array containing the values of the natural frequencies (in HZ). Stiffness is computed from MASS and OMEGAN and is therefore correct for diagonal mass matrices only. For nondiagonal mass matrices the stiffness computation in cards 331-333 (in FLUTCA) must be replaced by an appropriate READ statement.

QBEGIN, QEND, NQ

The flutter eignevalue equations are solved for (NQ + 1) values of dynamic pressure Q, starting with the value of Q=QBEGIN and ending with the value of Q=QEND.

VEL Flight velocity.

BTRAN	Array of semichord lengths of wing (and/or tail) sections where the different controls are located (at mid-span of control sections). - (≤ 6)
CTRAN	Array of distances between the two transducers at each control surface mid-section (used to compute the angle of deformation) - (≤ 6).
CREF	Reference semi-chord length (normally wing root semi-chord length) - should be consistent with the reference length used in computing te reduced frequency k (in aero program).
ZW	Matrix where ZW (I,J) indicates the displacement (positive down) of the I^{th} transducer due to the J^{th} mode. For each section, two transducers are allowed. The fore transducer should be placed (in the data) ahead of the aft transducer. The present subroutines CONTRL assume the fore transducer to be located at 30 chord from leading edge (L.E.) and these sets of transducers should be arranged in the same order as the controls - ($\leq$ (12 x 15)). For other types of subroutines CONTRL see Appendix C.
ZREF	Values like Zw of reference transducers are used to detect the rigid body motion of the aircraft. They are used in this program to determine the elastic deformation of the wing. If not needed, use zero values for ZREF - ($\leq$ (2 x 15)).
IPLOT - 1	A root locus plot will be made.
- 0	No plotted output.

CLR Array of X distances (positive aft) between the fore reference transducer and the fore control transducer - (≤ 6).

CTR - Distance between the two transducers at the reference section.

NCACT - Number of active controls starting from control No. 1. No intermediate controls can be assumed to be inactive (control gains can, in this case, be made equal to zero).

Remark: The transducer data as indicated above is tailored fit to the control laws employed using the aerodynamic energy concept. The form of control law assumed is as follows:

$$q_c = \begin{Bmatrix} \delta_1 \\ \delta_2 \\ \vdots \\ \delta_{NC} \end{Bmatrix} = \underbrace{\begin{bmatrix} \frac{1}{Q_1(s)} & & \\ & \frac{1}{Q_2(s)} & \\ & & \frac{1}{Q_{NC}(s)} \end{bmatrix}}_{[\frac{1}{Q(s)}]} \underbrace{\begin{bmatrix} \bar{P}_{1,1}(s) & \cdots & \bar{P}_{1,NA}(s) \\ \vdots & & \vdots \\ \bar{P}_{NC,1}(s) & & \bar{P}_{NC,NA}(s) \end{bmatrix}}_{[\bar{P}(s)]} \begin{Bmatrix} h_1 \\ h_2 \\ \vdots \\ h_{NA} \end{Bmatrix}$$

where the vector $[h_1, h_2 \ldots h_{NA}]^T$ denotes relative displacements and/or relative rotations. The aerodynamic energy control law assume that δ_1 is driven by h_1 and h_2, that δ_2 is driven by h_3 and h_4 and so forth, so that NA = 2*NC. The matrices $[\frac{1}{Q(s)}]$ and $[\bar{P}(s)]$ are computed in subroutine CONTRL (see Appendix C). The above form, however, is very general and can be readily used for other types of control laws which are driven by any number of either relative or absolute (or both) displacements (and/or rotations) at any chordwise location. The cards 473-482 in FLUTCA process the transformations matrix [H] (or order NA*NM) connecting the vector $\lfloor h_1, h_2 \ldots h_{NA} \rfloor^T$ with the generalized coordinates

$$\begin{Bmatrix} h_1 \\ h_2 \\ \vdots \\ h_{NA} \end{Bmatrix} = [H] \quad q_s \qquad (A.2)$$

. and computes the product P(s) (see eq. (31)) denoted by PH in the program), that is

$$[P(s)] = [\bar{P}(s)][H] \quad \text{(A3)}$$

where [P(s)] is of order (NC * NM).

In summary, subroutine CNTRL provides the matrices $[\frac{1}{Q(s)}]$ and $[\bar{P}(s)]$ whereas the matrix (P(s)] is computed in cards 473-482 (in FLUTCA).

If and only if the parameter IPLOT = 1 the program then reads the namelist PLOTPA

READ (5, PLOTPA)

defined by

NAMELIST /PLOTPA/XZ, YZ, XSCALE, YSCALE, XL, YL, ISYM, IENTRY

where

XZ	Left hand limit of real part of root locus.
YZ = 0	
XSCALE	Abscissa scale (value per inch).
YSCALE	Ordinate scale (value per inch).
XL	Length of abscissa in inches.
YL	Length of ordinate in inches.
ISYM	Integer defining symbol during root locus plot (=3 is recommended).
IENTRY = 1	

The program then reads the namelist MXSIZE

READ (5, MXSIZE)

defined by

NAMELIST/MXSIZE/MAXC, MAXNM, MAXK, MAXT

where

MAXC	Maximum number of controls (6 in this program).
MAXNM	Maximum number of modes (15 in this program).

MAXK Maximum number of polynomial terms per element in the transfer function numerator and denominator matrices (= 10 herein).

MAXT Maximum order of final matrix [U] (where d Y /dt = [U] Y- - - assigned the value 100 in this program.

If, and only if, NCACT ≠ 0 the program reads the namelist CONC

READ (5, CONC)

defined by

NAMELIST/CONC/WR,NTE, X

where

WR Reference frequency (rad/sec) used only for the D.T.T.F. control law (aerodynamic energy) - the value chosen is normally around the value of the flutter frequency.

NTE Integer array (following the order of the controls) which identifies between L.E. and T.E. controls.

= 1, T.E. control

= 0, L.E. control.

Note that whenever a control is not active, put NTE = 0 when using aerodynamic energy versions for CONTRL.

X Array of gains. There are 6 gains per control surface for the L.D.T.T.F. and 1 gain per control surface for the D.T.T.F. ($\le$ 36). The values of X(I) for the L.D.T.T.F. should be used considering the following basic form for the Ith control surface transfer function

$$F_I = \frac{X(1+6*(I-1))*s^2}{s^2 + 2*X(2+6*(I-1))*X(3+6*(I-1))*s + (X(2+6*(I-1))^2} + \frac{X(4+6*(I-1))*s^2}{s^2 + 2*X(5+6*(I-1))*X(6+6*(I-1))*s + (X(5+6*(I-1))^2}$$

For L.E. control

$$\delta_I = F_I \lfloor -4 \quad 4 \rfloor \begin{Bmatrix} (h/b) & 0.3C \\ \alpha & \end{Bmatrix}$$

For T.E. control

$$\delta_I = F_I \lfloor 4 \quad 2.8 \rfloor \begin{Bmatrix} (h/b) & 0.3C \\ \alpha & \end{Bmatrix} - 1.8\alpha$$

For further details see Ref. 3.

4. APPENDIX B

OPERATION INSTRUCTIONS FOR THE GUST OPTIMIZATION/GUST SENSITIVITY PROGRAM

The gust package permits the computation of the spectral responses of an aircraft due to a continuous gust environment. The effects of active controls (up to 6 controls) on the gust response can be accounted for. Furthermore, the basic gust program is coupled, in the present package, with an optimization routine which enables the determination of the various control gains which minimize the control responses to gust. Sensitivity studies (with plotted output) around the given or optimal control gains can also be made.

The input data is organized on file 5, with aerodynamic data (defined by array AERO (I,J,K)) located on file 2. Most of the printed output is located on file 6 with some additional output (arising from the optimization stage) located on file 4. File 13 is used by the package for labelling of plots and needs to be declared by the programmer.

The control law transfer function is computed in subroutined CONTRL. The program includes two versions for CONTRL based on the concept of aerodynamic energy. It is imperative to extract one of these two versions of CONTRL before running the program. For other types of control laws, subroutine control needs to be reprogrammed. To ease this task, details relating to subroutine CONTRL are given in Appendix C.

The output of the program consists of the input data together with the optimal control gains and the power spectral density (PSD) plots of the control responses, when used in its gust optimization version. When used as a control gain sensitivity program, the output is supplemented by sensitivity plots showing the variation of the rms control responses with the various control law gains. The package includes all the subroutines used by the program except for the plotting subroutines (which are installation oriented).

The program is written in FORTRAN and was developed on an IBM 370/168 computer. Double precision is used throughout the program due to the shorter IBM word length relative to the CDC computers. For CDC installations, it is recommended to convert the program to a single precision version. Input/output examples are included herein.

When using the program in its gust optimization version it is advisable to extract subroutines GUSPLT and PLT from the package. The input data for the gust optimization version will first be presented. The changes required in the data and in the program when running the program in its gust sensitivity version will then be presented.

INPUT OF DATA - GUST OPTIMIZATION VERSION

In the following, the data required for the operation of the gust optimization program is described. Here again READ statements will be reproduced together with the specified FORMAT and with the full explanation of the various parameters

READ (FORMAT (15A4)), (HDR(I), I=1,15)

HDR An alphanumeric header for the job (up to 60 characters, including spaces).

READ (5, CASE)

where 5 designates the input file and CASE is a namelist defined by

NAMELIST/CASE/NM, NC, NAER, B NG, NL

where

NM Integer specifying the number of modes ($\leq$15).

NC Integer specifying the number of controls ($\leq$6).

NAER - 1 Input aerodynamics will be introduced by means of PADE interpolation coefficients.

- 0 Input aerodynamics will be introduced by means of aerodynamic coefficients at different values of reduced frequency k.

B Array of values of lag terms to be used during the PADE interpolation (≤ 4).

NG - 1 If gust aerodynamic coefficient are included in the aerodynamic data.

- 0 If gust aerodynamic coefficients are not included in the aerodynamic data.

NL Integer specifying the number of lag terms to be used during the PADE interpolation (≤ 4).

The aerodynamic data is then introduced as follows:

If NAER $\neq$ 0 then

```
DO 1 I = 1, NM
DO 1 J = 1, (NM + NC + NG)
READ (FORMAT(6X,7E10.4)), A0(I,J), A1(I,J), A2(I,J), A3(I,J), A4(I,J),
A5(I,J), A6(I,J)
1 CONTINUE
```

Where the aerodynamic matrix A is assumed to be expressed by

$$A = A0 + A1(ik) + A2(ik)^2 + \sum_{L=1}^{NL} \frac{AL(ik)}{ik+B(L)}$$

and k denotes the reduced frequency. The aerodynamic matrix [A] should be arranged so that control coefficients are located in the last columns with the gust coefficients at the very last column.

The program proceeds to read the namelist GST defined by

NAMELIST/GST/RMASS, OMEGAN, VEL, BTRAN, CTEAN, CREF, ZW, ZREF, Q, CLR, CTR, WR, NTE, NCACT

where

RMASS Mass matrix ($\leq$ 15 x 15)

OMEGAN Array containing the values of the natural frequencies (in HZ). Stiffness is computed from RMASS and OMEGAN and is therefore correct for diagonal mass matrices only. For non-diagonal mass matrices the stiffness computation in card 437 (in subroutine SOLGST) should be replaced by an appropriate READ statement. It is important to note that 1.5 structural damping is assumed in the program. Modify card 438 if other values are desired.

VEL Flight velocity.

BTRAN Array of semichord lengths of wing (and/or tail) sections where the different controls are located (at mid-span of control sections) - ($\leq$6).

CTRAN Array of distances between the two transducers at each control surface mid-section (used to compute the angle of deformation - ($\leq$6)).

CREF Reference semichord length (normally wing root semichord length) - should be consistent with the reference length used in computing the reduced frequency k (in aero program).

ZW Matrix where ZW (I,J) indicates the displacement (positive down) of the I^{th} transducer due to the J^{th} mode. For each section, two transducers are allowed - the fore transducer should be placed (in the data) ahead of the aft transducer. The present subroutines CONTRL assume the fore transducer to be located at 30 chord from leading- edge (L.E.) and these sets of transducers should be arranged in the same order as the controls - ($\leq$(12 x 15)). For other types of subroutines CONTRL see Appendix C.

ZREF	Values like ZW of reference transducers used to detect the rigid body motion of the aircraft. Used in this program to determine the elastic deformation of the wing. If not needed, use zero values for ZREF - ($\leq$ (2 x 15)).
Q	Flight dynamic pressure
CLR	Array of X distances (positive aft) between the fore reference transducer and the fore control transducer - ($\leq$6).
CTR	Distance between the two transducers at the reference section.
WR	Reference frequency (rad/sec), used only for the D.T.T.F. control laws (aerodynamic energy) - the value chosen is normally around the value of the flutter frequency.
NTE	Integer array following the order of the controls which identifies between L.E. and T.E. controls.
= 1	T.E. control
= 0	L.E. control
NCACT	Number of active controls

Note that whenever a control is not active, put NTE = 0 when using aerodynamic energy versions for CONTRL.

<u>Remark</u>: The transducer data as indicated above is tailored fit to the control laws employed using the aerodynamic energy concept. The form of control law asumed is as follows:

$$q_c = \begin{Bmatrix} \delta_1 \\ \delta_2 \\ \vdots \\ \delta_{NC} \end{Bmatrix} = \underbrace{\begin{bmatrix} \frac{1}{Q_1(s)} & & & \\ & \frac{1}{Q_2(s)} & & \\ & & \ddots & \\ & & & \frac{1}{Q_{NC}(s)} \end{bmatrix}}_{\left[\frac{1}{Q(s)} \right]} \underbrace{\begin{bmatrix} \bar{P}_{1,1}(s) & \cdots & \bar{P}_{1,NA}(s) \\ \vdots & & \vdots \\ \bar{P}_{NC,1}(s) & & \bar{P}_{NC,NA}(s) \end{bmatrix}}_{[\bar{P}(s)]} \begin{matrix} h_1 \\ h_2 \\ \vdots \\ h_{NA} \end{matrix} \qquad (B1)$$

where the vector $\lfloor h_1, h_2 \ldots h_{NA} \rfloor^T$ denotes relative displacements and/or relative rotations. The aerodynamic energy control laws assume that δ_1 is driven by h_1 and h_2, that δ_2 is driven by h_3 and h_4 and so forth so that NA = 2*NC. The matrices $[\frac{1}{Q(s)}]$ and $[\bar{P}(s)]$ are computed in subroutine CONTRL (See Appendix C). The above form, however, is very general and can be readily used for other types of control laws which are driven by any number of either relative or absolute (or both) dsplacements (and/or rotations) at any chordwise locations. The cards 282-288 in the main program process the transformation matrix [H] (of order NA x NM) connecting the vector $\lfloor h_1 \ h_2 \ldots h_{NA} \rfloor^T$ with the generalized coordinates

$$\begin{Bmatrix} h_1 \\ h_2 \\ \vdots \\ h_{NA} \end{Bmatrix} = [H] \ q_s \qquad \text{(B2)}$$

so that the matrix [P(s)] in eq. 31 can be computed by

$$[P(s)] = [\bar{P}(s)][H] \qquad \text{(B3)}$$

In summary, subroutine CONTRL provides the matrices $[\frac{1}{Q(s)}]$ and $[\bar{P}(s)]$ whereas the matrix [H] is computed in cards 282-288 (in MAIN).

If NAER = 0 then

```
READ (5,FT)
    DO 1  K = 1, NK
    DO 1  J = 1, (NM + NC + NG)
    DO 1  I = 1, NM
READ (2, FORMAT(2E15.5))   AERO (I,J,K)
    1 CONTINUE
```

where FT is a namelist defined by

NAMELIST/FT/NK, AK, MAXNK, NPRINT, NPUNCH, IRIGID, JRIGID

and where 2 designates the file in which the aerodynamic data is located. The various parameters are defined as follows:

NK — Number of reduced frequencies k used for the interpolation of the aerodynamic coefficients.

AK — Array (≤ 20) containing the values of k corresponding to the aerodynamic coefficients. The first value of k must be zero. The order of the frequency value must correspond to the order of the aerodynamic coefficients. AERO (I,J,K) - see below.

MAXNK — Maximum value of NK (= 20 in present program).

NPRINT - 0 No printed output from the PADE interpolation routine (called FIT).

- 1 Printed output is available.

NPUNCH - 0 No punched output from subroutine FIT.

- 1 Interpolation coefficients are punched.

IRIGID, JRIGID

Interpolation coefficients for the aerodynamic coefficients (PADE representation) for the first IRIGID rows and first JRIGID are determined using the first few values of reduced frequency k (assumed to be the lowest) without resorting to a least squares procedure. In this case the rigid body modes must be located so as to be the first modes. This is done in order to increase the accuracy of the aero-coefficients at low k values where steady state stiffness and damping terms are zero (the least square routine may render them negative).

AERO(I,J,K) Array containing the values of the aerodynamic matrix A (see eq. (1)) - that is, the $(I,J)^{th}$ coefficient at the K^{th} reduced frequency. The order at which the different K values are arranged must correspond to the AK values. The first k value must correspond to k=0. For order of columns in [A] see the remark above for case NAER≠0.

READ (FORMAT (4E10.0)), ETA1, PHI

ETA1 Accuracy of computer relative to 1 (on I.B.M. double precision = 5.E-13). Absolute accuracy = X*ETA1 (value unimportant for gust sensitivity-version).

PHI Relative size of "suction zone" within which the optimized parameter is "sucked" to the constraint in order to avoid false convergence. Absolute size of zone = X1(I)*PHI or X2(I)*PHI depending on whether near lower or upper constraints (value unimportant for gust sensitivity version).

READ (FORMAT (5I5), NV, NPR, NDR

NV Number of independent control gains in the control laws ($\leq$ 36).

NPR = 0

NDR - 0 Optimization is based on the minimization of the RMS responses of controls.

- 1 Optimization is based on the minimization of the RMS response rates of controls.

READ (FORMAT (5I5), NONACT

NONACT Number of non-active optimization parameters (that is, number of control gains kept fixed during optimization).

READ (FORMAT (5I5), (NA(I), I = 1, NONACT)

NA — Integer Array containing the location of the non-active parameters in the X array (see below). If NONACT = 0, a blank card should be placed here.

READ (FORMAT (4E10.0), WL, WT

WL, WT — Two weights for emphasizing the contributions of any of the control responses in the target function expression (defined as FUNCTN in subroutine SOLGST, cards 461 and 467). More details regarding the target function FUNCTN will be given below at the end of the data description.

```
    DO 200 I = 1, NV
READ (FORMAT (4E10.0)), X1(I), X(I), X2(I), EPS(I)
    200 CONTINUE
```

X1(I) — Value of the lowest bound of the I^{th} control parameter (during optimization).

X(I) — Initial value of the I^{th} control parameter (at the onset of the optimization process). There are 6 gains per control surface for the L.D.T.T.F. and 1 gain per control surface for the D.T.T.F. ($\leq$ 36). The values of X(I) for the L.D.T.T.F. should be used considering the following basic form for the I^{th} control surface transfer function

$$F_I = \frac{X(1+6*(I-1))*s^2}{s^2 + 2*X(2+6*(I-1))*X(3+6*(I-1))*s + (X(2+6*(I-1))^2} + \frac{X(4+6*(I-1))*s^2}{s^2 + 2*X(5+6*(I-1))*X(6+6*(I-1))*s + (X(5+6*(I-1))^2}$$

For L.E. control

$$\delta_I = F_I \ \text{L-4} \quad 4\text{J} \begin{Bmatrix} (h/b) & 0.3C \\ \alpha & \end{Bmatrix}$$

For T.E. control

$$\delta_1 = F_I L \; 4 \quad 2.8 \left\{ \frac{(h/b)}{\alpha} \; 0.3C \right\} - 1.8\alpha$$

For further details see Ref. 3.

X2(I) Value of the upper bound of the I^{th} control parameter (during optimization).

EPS(I) The desired absolute accuracy of the optimal final X(I) value.

READ (FORMAT (4E10.0)), FMIN, ETA

FMIN Parameter containing an approximate value to the minimum of the target function FUNCTN (see remark at the end of this section). If unknown, use FMIN = 0.

ETA Parameter containing an estimate of the relative accuracy of the rms response computations. Used to determine the type of difference approximation to the gradient (value unimportant for the gust sensitivity version).

READ (FORMAT (5I5)), ITMAX, IW

ITMAX An input/output integer. On input, ITMAX contains the maximum allowable number of optimization iterations. On output, ITMAX contains the number of iterations used (value unimportant for the gust sensitivity version).

IW An integer code for printing during computation (value unimportant for the gust sensitivity version).

- 0 No printing.
- 1 Print gradient vector, direction of each linear minimization and function value before and after each linear minimization.
- 2 In addition to the above, print function values calculated during the course of linear minimizations.

- 3 In addition to the above, print function values calculated in evaluating the gradients.

READ (FORMAT (I10, 2E10.0)), NF FBEGIN, FEND

NF Number of frequency intervals used in computing the spectral response (Total number of frequencies used = NFT = NF+1, should be $\leq$ 100).

FBEGIN Lower value of frequency (in HZ) in computing the spectral response.

FEND Upper value of frequency (in HZ) in computing the spectral response.

READ (FORMAT (4E10.0)), LENGTH

LENGTH Gust scale length. Used to determine the Von Karman gust spectrum.

READ (FORMAT (4E10.0)), EM

EM Flight Mach number.

Remark: The definition of the target function FUNCTN (in subroutine SOLGST, card 461 for function based on rms control deflections and card 467 for function based on rms rates of control deflections) is left open to the user. It can be defined for example as a weighted sum of the rms responses, that is

$$\text{FUNCTN} = \sum_{i=1}^{NC} W_i \, (q_{c_i})_{rms}$$

or

$$\text{FUNCTN} = \sum_{i=1}^{NC} W_i \, (\dot{q}_{c_i})_{rms}$$

where W_i represents the i^{th} weight.

In some cases it may be of interest to keep the various rms control responses equal and a penalty function may be introduced into the target function. Note the following equivalence relations between the notations used in eqs. (52), (53) and those used in the program:

$$(q_{c_i})_{rms} \equiv \text{DRMS (I)}$$

$$(\dot{q}_{c_i})_{rms} \equiv \text{DRRMS(I)}$$

Important: Do not forget to check whether the definition of FUNCTN in the program (cards 461, 467) is applicable.

INPUT OF DATA - GUST SENSITIVITY VERSION

As already mentioned earlier, the gust sensitivity version of this program yields plots showing the sensitivity of the rms responses of the controls with respect to variations of the various X(I) gain parameters. To accomplish this, the following moifications should be made to the program:

1) Replace cards 299-309 by the following

   IFINAL = 1 *

   CALL GUSPLT (XX, X1ACT, X2ACT, EPSACT, QQ, EM)

2) Delete cards 320-321.

3) Delete cards 472-526.

4) Delete one of the two subroutines CONTRL present in the package or replace both of them by a new one.

One should make sure that both subroutines (GUSPLT and PLT) are included in the source program.

The data required is identical to the one outlined in the above gust optimization version except for the following change in the meaning of the following data:

DO 200 I = 1, NV

```
READ (FORMAT (4E10.0)), X1(I), X(I), X2(I), EPS(I)
    200 CONTINUE
```

X1(I) Value of the lowest bound of the Ith control parameter (during sensitivity variations of this parameter).

X(I) Initial value of the Ith control parameter (at the onset of the sensitivity variation).

X2(I) Value of the upper bound of the Ith control parameter (during sensitivity variations of this parameter).

EPS(I) The step size used in moving from X(I) to both X1(I) and X2(I).

Furthermore, some of the data needed for the gust optimization version is still read but the values are irrelevant for the gust-sensitivity version since they are not used. These parameters had been indicated while explaining their meaning in the gust optimization version of the program.

5. APPENDIX C

SUBROUTINE CONTRL

DETAILS ON THE COMMON PARAMETERS

Subroutine CONTRL computes the control laws used for either the flutter package or the gust package (including gust optimization program, or control response sensitivity to control law parameter variation program). The subroutines included in the above packages relate to aerodynamic energy control laws of the D.T.T.F and of the L.D.T.T.F. Whenever other types of control laws are required, subroutine CONTRL has to be reprogrammed (the same subroutine CONTRL can be used for both packages mentioned above). In the following, some explanations regarding the COMMON prameters employed by subroutine CONTRL, will be given in order to facilitate the reprogramming of subroutine CONTRL whenever deemed necessary. The subroutine is defined by

SUBROUTINE CONTRL (NP, P, ND, QD, NC, WR, NTE, X)

where

NP Two-dimensional integer output array. NP(I,J) contains the number of polynomial terms (as function of s, starting from s°) in the numerator control law element (I,J) of matrix $[\overline{P}(s)]$ (see eqs. (31), (B3) above) - $(I \leq 6)$.

P Three-dimensional output array representing the numerator control law matrix $[\overline{P}(s)]$. P(I,J,K) represents the coefficient of $s^{(k-1)}$ in the numerator polynomial located at position (I,J) in $[\overline{P}(s)]$.

ND One-dimensional integer output array. ND(I) represents the number cf polynomial terms (as function of s, starting from s°) in the denominator of the I^{th} element in the diagonal matrix $[\frac{1}{Q(s)}]$ which forms a part of the control law transfer function matrix [T.]

QD Two-dimensional output array representing the denominator control law diagonal matrix $[\frac{1}{Q(s)}]$. QD(I,K) represents the coefficient of $s^{(k-1)}$ in the denominator of the I^{th} element in the diagonal matrix $[\frac{1}{Q(s)}]$.

NC Number of controls.

WR An input parameter. Used in present program for the aerodynamic energy control law of the D.T.T.F. to represent reference frequency (rad/sec). The value chosen is normally around the value of the flutter frequency.

NTE One dimensional input array used to distinguish between L.E. and T.E. control surfaces.

= 1, T.E. control.

= 0, L.E. control.

X One-dimensional input array of control gains used for computing both $[\overline{P}(s)]$ and $[\frac{1}{Q(s)}]$.

Note that matrix [P(s)] (see eq. (31)) is not computed in subroutine CONTRL ($[P(s)] = [\overline{P}(s)] * [H]$ where [H] is the modal matrix connecting the deflection at the different sensor locations with the generalized coordinates of the system, (see also eq. (B3)).

APPENDIX D

EIGENVALUE SUBROUTINES

DETAILS ON THE COMMON PARAMETERS

The subroutines described in the following pages belong to the IMSL library. They can easily be used in installations enjoying access to the IMSL library. Their replacement by other routines, if necessary, involves little effort and can be easily accomplished using the information included herein.

```
C       SUBROUTINE EBALAF (A,N,IA,D,K,L)                                    EBAL0010
C                                                                           EBAL0020
C-EBALAF--------D--------LIBRARY 1------------------------------------------EBAL0030
C                                                                           EBAL0040
C   FUNCTION            - BALANCE A REAL MATRIX A.                          EBAL0050
C   USAGE               - CALL EBALAF(A,N,IA,D,K,L)                         EBAL0060
C   PARAMETERS   A      - THE N X N MATRIX GIVING THE ELEMENTS OF THE       EBAL0070
C                           MATRIX TO BE BALANCED. THE INPUT A IS           EBAL0080
C                           REPLACED BY THE BALANCED MATRIX.                EBAL0090
C                N      - THE ORDER OF THE MATRIX A AND THE LENGTH OF D     EBAL0100
C                IA     - ROW DIMENSION OF A IN CALLING PROGRAM             EBAL0110
C                D      - THE OUTPUT ARRAY OF LENGTH N WHICH CONTAINS       EBAL0120
C                           INFORMATION DETERMINING THE PERMUTATIONS        EBAL0130
C                           USED AND THE SCALING FACTORS                    EBAL0140
C                K      - K AND L ARE TWO OUTPUT INTEGERS SUCH THAT         EBAL0150
C                           A(I,J) = 0. IF                                  EBAL0160
C                           (1) I IS GREATER THAN J AND                     EBAL0170
C                           (2) J = 1,....,K-1 OR                           EBAL0180
C                               I = L+1,....,N                              EBAL0190
C                L      - SEE ABOVE. IF L .EQ. 0 THE ORIGINAL MATRIX A      EBAL0200
C                           IS IN HESSENBERG FORM.                          EBAL0210
C   PRECISION           - SINGLE/DOUBLE                                     EBAL0220
C   LANGUAGE            - FORTRAN                                           EBAL0230
C---------------------------------------------------------------------------EBAL0240
```

```
C       SUBROUTINE EHESSF (A,K,L,N,IA,D)                                    EHES0010
C                                                                           EHES0020
C-EHESSF--------D--------LIBRARY 1------------------------------------------EHES0030
C                                                                           EHES0040
C   FUNCTION            - REDUCE A NONSYMMETRIC MATRIX TO UPPER             EHES0050
C                           HESSENBERG FORM BY ORTHOGONAL                   EHES0060
C                           TRANSFORMATIONS                                 EHES0070
C   USAGE               - CALL EHESSF (A,K,L,N,IA,D)                        EHES0080
C   PARAMETERS   A      - N BY N NONSYMMETRIC MATRIX TO BE REDUCED TO       EHES0090
C                           UPPER HESSENBURG FORM. (INPUT)                  EHES0100
C                         ON OUTPUT, A CONTAINS THE UPPER HESSENBERG        EHES0110
C                           MATRIX.                                         EHES0120
C                K      - THE ROUTINE REDUCES ONLY THE SUB-MATRIX OF        EHES0130
C                           ORDER L-K+1, WHERE K IS GREATER THAN OR         EHES0140
C                           EQUAL TO 1 AND LESS THAN OR EQUAL TO L. K       EHES0150
C                           IS THE ROW AND COLUMN INDEX OF THE STARTING     EHES0160
C                           ELEMENT. (INPUT)                                EHES0170
C                L      - THE ROW AND COLUMN INDEX OF THE LAST ELEMENT.     EHES0180
C                           L IS LESS THAN OR EQUAL TO N. (INPUT)           EHES0190
C                N      - ORDER OF A  AND THE LENGTH OF D.(INPUT)           EHES0200
C                IA     - ROW DIMENSION OF A IN CALLING PROGRAM.(INPUT)     EHES0210
C                D      - OUTPUT VECTOR OF LENGTH N CONTAINING THE          EHES0220
C                           DETAILS OF THE TRANSFORMATION                   EHES0230
C   PRECISION           - SINGLE/DOUBLE                                     EHES0240
C   LANGUAGE            - FORTRAN                                           EHES0250
C---------------------------------------------------------------------------EHES0260
```

```
C       SUBROUTINE EQRH3F (H,N,IH,K,L,WR,WI,Z,IZ,IER)                       EQRN0010
C                                                                           EQRN0020
```

ORIGINAL PAGE IS
OF POOR QUALITY

```
C-EQRH3F---------D--------LIBRARY 1------------------------------------EQRN0030
C                                                                       EQRN0040
C   FUNCTION            - FIND THE EIGENVALUES AND (OPTIONALLY) EIGEN-  EQRN0050
C                           VECTORS OF A REAL UPPER HESSENBERG MATRIX.  EQRN0060
C   USAGE               - CALL EQRH3F(H,N,IH,K,L,WR,WI,Z,IZ,IER)        EQRN0070
C   PARAMETERS   H      - ON INPUT, H CONTAINS THE UPPER HESSENBERG     EQRN0080
C                           MATRIX. THE REMAINING TRIANGLE UNDER H MAY  EQRN0090
C                           CONTAIN INFORMATION FROM THE HESSENBERG     EQRN0100
C                           REDUCTION PROGRAM EHESSF. ON OUTPUT H IS    EQRN0110
C                           DESTROYED.                                  EQRN0120
C                N      - N IS THE ORDER OF THE H MATRIX.               EQRN0130
C                IH     - IH IS THE ROW DIMENSION OF H IN THE           EQRN0140
C                           CALLING PROGRAM.                            EQRN0150
C                K      - K AND L ARE PRODUCED BY THE BALANCING         EQRN0160
C                L          ROUTINE EBALAF. IF EBALAF HAS NOT BEEN USED,EQRN0170
C                           SET K=1, L=N.                               EQRN0180
C                WR     - ON OUTPUT, THE VECTORS WR AND WI OF LENGTH N  EQRN0190
C                WI         CONTAIN THE REAL AND IMAGINARY PARTS OF THE EQRN0200
C                           EIGENVALUES, RESPECTIVELY.                  EQRN0210
C                           THE EIGENVALUES ARE UNORDERED               EQRN0220
C                           EXCEPT THAT COMPLEX CONJUGATE PAIRS OF      EQRN0230
C                           VALUES APPEAR CONSECUTIVELY WITH THE EIGEN- EQRN0240
C                           VALUE HAVING THE POSITIVE IMAGINARY PART    EQRN0250
C                           FIRST. IF AN ERROR EXIT IS MADE, THE        EQRN0260
C                           EIGENVALUES SHOULD BE CORRECT FOR INDICES   EQRN0270
C                           J+1,....,N WHERE J=IER-128.                 EQRN0280
C                Z      - ON INPUT, Z CONTAINS THE IDENTITY MATRIX      EQRN0290
C                           OF ORDER N IF THE EIGENVECTORS OF THE UPPER EQRN0300
C                           HESSENBERG MATRIX ARE DESIRED.              EQRN0310
C                           IF THE EIGENVECTORS OF A REAL GENERAL MATRIXEQRN0320
C                           ARE DESIRED, THEN ON INPUT, Z CONTAINS THE  EQRN0330
C                           TRANSFORMATION MATRIX PRODUCED IN EHESSF    EQRN0340
C                           WHICH REDUCED THE GENERAL MATRIX TO         EQRN0350
C                           HESSENBERG FORM. THIS MATRIX CAN BE         EQRN0360
C                           OBTAINED BY SETTING Z TO THE N BY N IDENTITYEQRN0370
C                           MATRIX AND CALLING EHBCKF BEFORE CALLING    EQRN0380
C                           EQRH3F.                                     EQRN0390
C                         ON OUTPUT THE N BY N MATRIX Z CONTAINS THE    EQRN0400
C                           REAL AND IMAGINARY PARTS OF THE EIGEN-      EQRN0410
C                           VECTORS. THE I-TH COLUMN OF Z IS A REAL     EQRN0420
C                           EIGENVECTOR IF THE I-TH EIGENVALUE IS REAL. EQRN0430
C                           IF THE I-TH EIGENVALUE IS COMPLEX WITH      EQRN0440
C                           POSITIVE IMAGINARY PART, THE I-TH AND       EQRN0450
C                           (I+1)-TH COLUMNS OF Z CONTAIN THE REAL      EQRN0460
C                           AND IMAGINARY PARTS OF ITS EIGENVECTOR.     EQRN0470
C                           IF THE I-TH EIGENVALUE IS COMPLEX WITH NEGA-EQRN0480
C                           TIVE IMAGINARY PART, THE (I-1)-TH COLUMN OF EQRN0490
C                           Z CONTAINS THE REAL PART OF ITS EIGENVECTOR EQRN0500
C                           AND THE I-TH COLUMN OF Z CONTAINS MINUS THE EQRN0510
C                           IMAGINARY PART OF ITS EIGENVECTOR.          EQRN0520
C                           THE EIGENVECTORS ARE UNNORMALIZED. IF AN    EQRN0530
C                           ERROR EXIT IS MADE, NONE OF THE EIGENVECTORSEQRN0540
C                           HAVE BEEN FOUND.                            EQRN0550
C                IZ     - IZ IS THE ROW DIMENSION OF Z IN THE           EQRN0560
C                           CALLING PROGRAM. IF IZ IS LESS THAN N, THE  EQRN0570
C                           EIGENVECTORS ARE NOT COMPUTED. IN THIS      EQRN0580
C                           CASE Z IS NOT USED.                         EQRN0590
C                IER    - ERROR PARAMETER                               EQRN0600
C                         TERMINAL ERROR                                EQRN0610
C                           IER = 128 + J, INDICATES THAT EQRH3F FAILED EQRN0620
C                           TO CONVERGE ON EIGENVALUE J. EIGENVALUES    EQRN0630
```

```
C                            J+1,J+2,....,N HAVE BEEN COMPUTED CORRECTLY. EQRN0640
C                            EIGENVALUES 1,....,J ARE SET TO ZERO. IF IZ  EQRN0650
C                            IS GREATER THAN OR EQUAL TO N, EIGENVECTORS EQRN0660
C                            ARE SET TO ZERO.                              EQRN0670
C   PRECISION           - SINGLE/DOUBLE                                   EQRN0680
C   REQD. IMSL ROUTINES - UERTST                                          EQRN0690
C   LANGUAGE            - FORTRAN                                         EQRN0700
C-----------------------------------------------------------------------EQRN0710
```

APPENDIX E

SOURCE LISTING AND INPUT/OUTPUT EXAMPLE FOR FLUTTER PROGRAM

The first part of the Appendix consists of the source listing of the program and is followed by an input/output example. The example chosen relates to the DAST configuration at M=0.9 with one active T.E. control surface based on the L.D.T.T.F. The output of the computer run includes a root-locus plot together with all the data rquired by the program. The aerodynamic coefficients AERO (I,J,K) used by the program are listed for convenience (this aerodynamic data is retrieved by the program from file 2).

It is recommended to use the plotting symbol '+' in the root locus plot. The symbol used in the present example is a result of some transient difficulties encountered using a new plotter.

```
      IMPLICIT  REAL*8(A-H,O-Z)
CCCCCCCCCCCCCCCCCCCCCCCCCCCCCCCCCCCCCCCCCCCCCCCCCCCCCCCCCCCCCCCCCCCCCCC
C                                                                      C
C     FLUTTER SUPRESSION  PACKAGE(WITH OR WITHOUT ACTIVE CONTROLS)     C
C     USING ROOT LOCUS TECHNIQUES. THE FOLLOWING INPUT DATA IS REQUIREDC
C                                                                      C
C     HDR - HEADER (FORMAT 15A4)                                       C
C                                                                      C
C     NAMELIST/CASE -                                                  C
C     NM - NUMBER OF MODES(15 MAX)                                     C
C                                                                      C
C     NC - NUMBER OF  CONTROLS(6 MAX)                                  C
C                                                                      C
C     NAER - 1 INPUT AERO IN TERMS OF INTERPOLATION COEFFICIENTS OF K  C
C          - 0 INPUT AERO FOR DIFFERENT VALUES OF K - INTRPOLATION     C
C     COEFFICIENTS TO BE COMPUTED IN SUBROUTINE FIT.                   C
C                                                                      C
C     B - ARRAY OF LAG TERMS USED DURING INTERPOLATION(4 MAX)          C
C                                                                      C
C     NG - 1 IF GUST AERO IS SUPPLIED                                  C
C        - 0 IF GUST AERO IS NOT SUPPLIED.                             C
C                                                                      C
C     NL - NUMBER OF LAG TERMS TO BE USED DURING INTERPOLATION.        C
C                                                                      C
C     IF  NAER=1  THEN AERO COEFFICIENTS ARE READ(FORMAT 6X,7E10.4)    C
C     IF  NAER=0  NEXT INPUTS ARE READ IN SUBROUTINE FIT.              C
C     SUBSEQUENT INPUTS ARE READ IN SUBROUTINE FLUTCA.                 C
C                                                                      C
CCCCCCCCCCCCCCCCCCCCCCCCCCCCCCCCCCCCCCCCCCCCCCCCCCCCCCCCCCCCCCCCCCCCCCC
      EXTERNAL  DREAL,DAIMAG
      COMMON/AERF/A0(15,22),A1(15,22),A2(15,22),A3(15,22),A4(15,22),
     *A5(15,22),A6(15,22)
      COMMON/ICASE/B(4),NM,NC,NG,NL
      DIMENSION HDR(15)
      NAMELIST/CASE/NM,NC,NAER,B,NG,NL
      READ 100,(HDR(I),I=1,15)
      PRINT 101,(HDR(I),I=1,15)
      READ(5,CASE)
      WRITE(6,CASE)
      NMNC=NM+NC
      IF(NAER.EQ.0) CALL FIT
      IF(NAER.EQ.0)  GO TO 10
      DO 1 II=1,NM
      DO 1 JJ=1,NMNC
      READ 200,A0(II,JJ),A1(II,JJ),A2(II,JJ),A3(II,JJ),A4(II,JJ),
```

```
     *AS(II,JJ),AS(II,JJ)
    1 CONTINUE
   10 CONTINUE
      CALL  FLUTCA
      STOP
  100 FORMAT(15A4)
  101 FORMAT(1H ,15A4)
  200 FORMAT(6X,7E10.4)
      END
      SUBROUTINE  CONTRL(NP,P,ND,QD,NC,WR,NTE,X)
CCCCCCCCCCCCCCCCCCCCCCCCCCCCCCCCCCCCCCCCCCCCCCCCCCCCCCCCCCCCCCCCCCCCCCCC
C                                                                       C
C     L.D.T.T.F. CONTROL LAW FOR ANY NUMBER OF CONTROL SURFACES. CAN    C
C     BE USED FOR BOTH FLUTTER AND GUST PROGRAMS. THE BASIC GAINS       C
C     USED HEREIN ARE APPROPRIATE FOR 20 PERCENT L.E. AND  20 PERCENT   C
C     T.E. CONTROL SYSTEMS WITH THE FORE SENSOR LOCATED AT THE 30       C
C     PERCENT CHORD LOCATION - DIMENSIONS ARE LIMITED TO 6 CONTROLS.    C
C                                                                       C
CCCCCCCCCCCCCCCCCCCCCCCCCCCCCCCCCCCCCCCCCCCCCCCCCCCCCCCCCCCCCCCCCCCCCCCCCC
      IMPLICIT  REAL*8(A-H,O-Z)
      DIMENSION NP(6,1),P(6,12,1),QD(10,1),E(2,2),NTE(6),X(36),CN(3),
     *CD1(3),CD2(3),TEMP1(5),TEMP2(5),ND(6)
      E(1,1)=-4.D0
      E(1,2)=4.D0
      E(2,1)=4.D0
      E(2,2)=2.8D0
      C21=-1.86D0
      NC2=2*NC
      DO  1  I=1,NC
      DO  1  J=1,NC2
      NP(I,J)=1
      DO  1  K=1,10
      P(I,J,K)=0.D0
    1 CONTINUE
      DO  2 I=1,NC
C
C   CASE OF   T.E.   CONTROL
C
      EH=E(2,1)
      EA=E(2,2)
      IF(NTE(I).EQ.1)   GO  TO   3
C
C   CASE  OF  L.E.  CONTROL
C
      EH=E(1,1)
      EA=E(1,2)
    3 CONTINUE
C
C     DETERMINATION OF  THE DENOMINATOR POLYNOMIAL  FOR EACH CONTROL SURF.
C
      CN(1)=0.D0
      CN(2)=0.D0
      CD1(1)=X(6*I-4)**2
      CD1(2)=2.D0*X(6*I-4)*X(6*I-3)
      CD1(3)=1.D0
      CD2(1)=X(6*I-1)**2
      CD2(2)=2.D0*X(6*I-1)*X(6*I)
      CD2(3)=1.D0
      CALL   PROPOL(CD1,3,CD2,3,QD(1,I),ND(I))
```

```
C
C     DETERMINATION OF THE NUMERATOR POLYNOMIAL FOR EACH CONTROL SURFACE
C
      CN(3)=X(6*I-5)
      CALL  PROPOL(CD2,3,CN,3,TEMP1,N)
      CN(3)=X(6*I-2)
      CALL  PROPOL(CD1,3,CN,3,TEMP2,N)
      DO  4  K=1,N
      P(I,2*I-1,K)=EH*(TEMP1(K)+TEMP2(K))
      P(I,2*I,K)=EA*(TEMP1(K)+TEMP2(K))+C21*NTE(I)*QD(K,I)
    4 CONTINUE
      NP(I,2*I-1)=N
      NP(I,2*I)=N
    2 CONTINUE
      RETURN
      END
      SUBROUTINE  CONTRL(NP,P,ND,QD,NC,WR,NTE,X)
CCCCCCCCCCCCCCCCCCCCCCCCCCCCCCCCCCCCCCCCCCCCCCCCCCCCCCCCCCCCCCCCCCCCCCCC
C                                                                      C
C     D.T.T.F. CONTROL LAW FOR ANY NUMBER OF CONTROL SURFACES. CAN     C
C     BE USED FOR BOTH FLUTTER AND GUST PROGRAMS. THE BASIC GAINS      C
C     USED HEREIN ARE APPROPRIATE FOR 20 PERCENT L.E. AND  20 PERCENT  C
C     T.E. CONTROL SYSTEMS WITH THE FORE SENSOR LOCATED AT THE 30      C
C     PERCENT CHORD LOCATION - DIMENSIONS ARE LIMITED TO 6 CONTROLS.   C
C                                                                      C
CCCCCCCCCCCCCCCCCCCCCCCCCCCCCCCCCCCCCCCCCCCCCCCCCCCCCCCCCCCCCCCCCCCCCCCC
      IMPLICIT  REAL*8(A-H,O-Z)
      DIMENSION NP(6,1),P(6,12,1),QD(13,1),E(2,2),NTE(6),X(36),ND(6)
      E(1,1)=-4.D0
      E(1,2)=4.D0
      E(2,1)=4.D0
      E(2,2)=3.2D0
      C21=-1.86D0
      A=10000.D0
      NC2=2*NC
      DO  1  I=1,NC
      DO  1  J=1,NC2
      NP(I,J)=1
      DO  1  K=1,2
      P(I,J,K)=0.D0
    1 CONTINUE
      DO  2  I=1,NC
      P(I,2*I-1,1)=0.D0
      P(I,2*I,1)=A*C21*NTE(I)
C
C    CASE OF  T.E.  CONTROL
C
      EH=E(2,1)
      EA=E(2,2)
      IF(NTE(I).EQ.1)  GO  TO  3
C
C    CASE  OF  L.E.  CONTROL
C
      EH=E(1,1)
      EA=E(1,2)
    3 CONTINUE
C
C     DETERMINATION OF THE NUMERATOR POLYNOMIAL FOR EACH CONTROL SURFACE
C
```

```
      P(I,2*I-1,2)=A*LH*X(I)/WH
      P(I,2*I,2)=A*LA*X(I)/WH
C
C     DETERMINATION OF THE DENOMINATOR POLYNOMIAL FOR EACH CONTROL SURF.
C
      QD(1,I)=A
      QD(2,I) 1.D0
      NP(I,2*I-1)=2
      NP(I,2*I)=2
      ND(I)=2
    2 CONTINUE
      RETURN
      END
      SUBROUTINE  FLUTCA
      IMPLICIT  REAL*8(A-H,O-Z)
CCCCCCCCCCCCCCCCCCCCCCCCCCCCCCCCCCCCCCCCCCCCCCCCCCCCCCCCCCCCCCCCCCCCCCCC
C
C     THE EQUATIONS OF MOTION ARE BROUGHT IN THIS SUBROUTINE TO A
C     CONVENIENT FIRST ORDER FORM DY/DT=GY AND SOLVED FOR A GIVEN
C     VELOCITY AND MACH NUMBER AS A FUNCTION OF THE DYNAMIC PRESSURE Q
C     (WHICH IS VARIED WITHIN A PRESCRIBED RANGE).  UP TO SIX ACTIVE
C     CONTROLS CAN BE USED IN THIS SUBROUTINE. RESULTS ARE SUITABLE
C     FOR ROOT LOCUS PLOTS.
C
C     NAMELIST/FLUT
C     MASS - MASS MATRIX (15 X 15 MAX)
C
C     OMEGAN - NATURAL FREQUENCIES ARRAY(IN HZ) - (15 MAX)  -  NOTE-
C     STIFFNESS IS COMPUTED FROM MASS AND OMEGAN AND IS THEREFORE
C     CORRECT FOR DIAGONAL MASS MATRIX ONLY.
C
C     QBEGIN - INITIAL VALUE OF DYNAMIC PRESSURE Q.
C
C     QEND - FINAL VALUE OF DYNAMIC PRESSURE Q.
C
C     NQ - NUMBER OF EQUAL INTERVALS DIVIDING THE Q RANGE (NUMBER OF
C     VALUES OF Q=NQ+1).
C
C     VEL - FLIGHT VELOCITY
C
C     BTRAN - ARRAY OF SEMICHORD LENGTHS OF WING(OR TAIL) SECTIONS
C     WHERE THE DIFFERENT CONTROLS ARE LOCATED(AT MID CONTROL SPAN
C     SECTIONS) - (6 MAX)
C
C     CTRAN - ARRAY OF DISTANCES BETWEEN THE TWO TRANSDUCERS AT EACH
C     CONTROL SURFACE MID SECTION(USED TO COMPUTE THE ANGLE OF
C     DEFORMATION) - (6 MAX).
C
C     CREF - REFERENCE SEMI CHORD LENGTH (NORMALLY WING ROOT SEMI
C     CHORD) - SHOULD BE CONSISTENT WITH THE REFERENCE LENGTH USED IN
C     COMPUTING THE REDUCED FREQUENCY K.
C
C     ZW - MATRIX WHERE ZW(I,J) INDICATES THE DISPLACEMENT(POSITIVE
C     DOWN) OF THE I-TH TRANSDUCER DUE TO THE J-TH MODE. FOR EACH
C     SECTION THERE ARE TWO TRANSDUCERS -- THE FORE TRANSDUCER SHOULD
C     BE LOCATED AHEAD OF THE AFT TRANSDUCER(AT 30 PERCENT CHORD FROM
C     L.E.). THESE SETS OF TRANSDUCERS SHOULD BE ARRANGED IN THE SAME
C     ORDER AS THE CONTROLS - (12 X 15 MAX).
C
```

```
C       ZREF - VALUES LIKE ZW OF REFERENCE TRANSDUCERS USED TO DETECT
C       THE RIGID BODY MOTION OF THE AIRCRAFT - (2 X 15 MAX).
C
C       IPLOT - 1--- ROOT LOCUS PLOT WILL BE MADE
C             - 0 ---NO PLOT WILL BE MADE
C
C       CLR - ARRAY OF X DISTANCES (POSITIVE AFT) BETWEEN THE FORE
C       REFERENCE TRANSDUCER AND THE FORE CONTROL TRANSDUCER - (6MAX)
C
C       CTR - DISTANCE BETWEEN THE TWO TRANSDUCERS AT THE REFERENCE
C       SECTION.
C
C       NCACT - NUMBER OF ACTIVE CONTROLS FOLLOWING THE ORDER OF THE
C       CONTROLS.
C
C       NAMELIST/PLOTPA
C       XZ - LEFT HAND LIMIT OF REAL PART OF ROOT LOCUS
C
C       YZ=0.
C
C       XSCALE - ABSCISSA SCALE(VALUE PER INCH)
C
C       YSCALE - ORDINATE SCALE(VALUE PER INCH)
C
C       XL - LENGTH OF ABSCISSA IN INCHES
C
C       YL - LENGTH OF ORDINATE IN INCHES
C
C       ISYM - INTEGER DEFINING SYMBOL DURING ROOT LOCUS PLOT(=3 IS
C       RECOMMENDE).
C
C       IENTRY - 1
C
C       NAMELIST/MXSIZE
C       MAXC - MAXIMUM NUMBER OF CONTROLS(=6 IN THIS PROGRAM)
C
C       MAXNM - MAXIMUM NUMBER OF MODES(=15 IN THIS PROGRAM)
C
C       MAXK- MAXIMUM NUMBER OF POLYNOMIAL TERMS PER ELEMENT IN THE
C       TRANSFER FUNCTION NUMERATOR AND DENOMINATOR MATRICES(=10 HEREIN)
C
C       MAXT - MAXIMUM ORDER OF FINAL MATRIX A(WHERE DY/DT=UY --  =100
C       IN THIS PROGRAM)
C
C       NAMELIST/CONC
C       NOTE THAT IT IS NECESSARY TO DELETE ONE OF THE TWO SUBROUTINES
C       NAMED CONTRL ACCORDING TO THE DESIRED CONTROL LAW.
C
C       WR - REFERENCE FREQUENCY(RAD/SEC),USED ONLY FOR THE D.T.T.F.
C       CONTROL LAWS --VALUE CHOSEN IS NORMALLY AROUND THE FLUTTER
C       FREQUENCY VALUE.
C
C       NTE - INTEGER ARRAY FOLLOWING THE ORDER OF THE CONTROLS AND
C       IDENTIFYING BETWEEN L.E. AND T.E. CONTROLS.
C             =1, T.E. CONTROL
C             =0, L.E. CONTROL
C       IT IS IMPORTANT TO NOTE  THAT WHENEVER A CONTROL IS NOT ACTIVE
C       PUT NTE=0
C
```

```
C     X - ARRAY OF GAINS.THERE ARE 6 GAINS PER CONTROL SURFACE FOR
C     THE L.D.T.T.F. AND 1 GAIN PER CONTROL SURFACE FOR THE D.T.T.F.
C     (=36 MAX)
C     X(1)*S**2/(S**2+2*X(2)*X(3)*S+X(2)**2) +
C                     X(4)*S**2/(S**2+2*X(5)*X(6)*S+X(5)**2)
C
CCCCCCCCCCCCCCCCCCCCCCCCCCCCCCCCCCCCCCCCCCCCCCCCCCCCCCCCCCCCCCCCCCCCCCCC
      REAL*4   XZ,YZ,XSCALE,YSCALE,XL,YL,BUF(100)
      COMMON/AERF/A0(15,22),A1(15,22),A2(15,22),A3(15,22),A4(15,22),
     *A5(15,22),A6(15,22)
      COMMON/ICASE/B(4),NM,NC,NQ,NL
      DIMENSION OMEGAN(15),H(12,15),A0C(15,6),A1C(15,6),A2C(15,6),
     *A3C(15,6),A4C(15,6),A5C(15,6),A6C(15,6),ZW(12,15),ZREF(2,15),
     *BTRAN(6),CTRAN(6),ACL(15,6,4),AL(15,15,4),FCT(5,5),D(3),
     *D1(15),CM(15,15,7),CA(15,15,7),CAC(15,6,7),NP(6,12),NPIMX(6),
     *ND(6),QD(10,6),RM(21,15,10),DM(21,6,10),P(6,12,10),PH(6,15,10),
     *C(5),RDMN(21,21),ER(189),EI(189),PV(189),CLR(6),NPC(6),
     *NTE(6),X(36),
     *T(100,100)
      REAL*8   MASS(15,15),KBAR(15,15)
      NAMELIST/FLUT/MASS,OMEGAN,QBEGIN,QEND,NQ,VEL,BTRAN,CTRAN,CREF,ZW,
     *ZREF,IPLOT,CLR,CTR,NCACT
      NAMELIST/PLOTPA/XZ,YZ,XSCALE,YSCALE,XL,YL,ISYM,IENTRY
      NAMELIST/MXSIZE/MAXC,MAXNM,MAXK,MAXT
      NAMELIST/CONC/WR,NTE,X
      READ(5,FLUT)
      WRITE(6,FLUT)
C
C
C
      PRINT   500
      DQ=(QEND-QBEGIN)/NQ
      NQT=NQ+1
      PI=3.14159265400
      CALL   PLOTS(BUF,100,6,10.0)
      CALL   PLOT(1.,1.,-3)
      IF(IPLOT.EQ.1)  READ(5,PLOTPA)
      IF(IPLOT.EQ.1)  WRITE(6,PLOTPA)
      READ(5,MXSIZE)
      WRITE(6,MXSIZE)
      IF(NCACT.NE.0)   READ(5,CONC)
      IF(NCACT.NE.0)   WRITE(6,CONC)
      NC=NCACT
      MAX=MAXC+MAXNM
C
C     COMPUTATION OF  THE STIFFNESS MATRIX  KBAR
C
      DO   1   I=1,NM
      OMEGAN(I)=2.D0*PI*OMEGAN(I)
      DO   1   J=1,NM
      KBAR(I,J)=MASS(I,J)*OMEGAN(I)**2
    1 CONTINUE
C
C     FORMATION OF   THE   VARIOUS AERO MATRICES
C
      VEL1=CREF/VEL
      VEL2=VEL1*VEL1
      IF(NC.EQ.0)   GO   TO   60
      DO   2   I=1,NM
```

```
      DO  2  J=1,NC
      A0C(I,J)=A0(I,NM+J)
      A1C(I,J)=A1(I,NM+J)
      A2C(I,J)=A2(I,NM+J)
      ACL(I,J,1)=A3(I,NM+J)
      IF(NL.LT.2)  GO  TO  2
      ACL(I,J,2)=A4(I,NM+J)
      IF(NL.LT.3)  GO  TO  2
      ACL(I,J,3)=A5(I,NM+J)
      IF(NL.LT.4)  GO  TO  2
      ACL(I,J,4)=A6(I,NM+J)
    2 CONTINUE
   60 CONTINUE
      DO  3  I=1,NM
      DO  3  J=1,NM
      AL(I,J,1)=A3(I,J)
      IF(NL.LT.2)  GO  TO  3
      AL(I,J,2)=A4(I,J)
      IF(NL.LT.3)  GO  TO  3
      AL(I,J,3)=A5(I,J)
      IF(NL.LT.4)  GO  TO  3
      AL(I,J,4)=A6(I,J)
    3 CONTINUE
      DO  4  I=1,NL
      B(I)=B(I)/VEL1
    4 CONTINUE
C
C     REDUCTION OF THE EQUATIONS OF MOTION TO A COMMON DENOMINATOR -
C     IN THE FOLLOWING TWO STAGES:-
C     (I) THE  NM  STRUCTURAL EQUATIONS WITHOUT THE CONTROL CONTRIBUTION
C
      CALL  FACTR(FCT,H,NL,LP,LF)
      LSMX=LF+2
      DO  6  K=1,LF
      C(K)=FCT(K,LF)
    6 CONTINUE
      DO  5  I=1,NM
      DO  5  J=1,NM
      D(1)=KBAR(I,J)
      D(2)=0.D0
      D(3)=MASS(I,J)
      CALL  PROPOL(C,LF,D,3,D1,LS)
      DO  7  K=1,LS
      CM(I,J,K)=D1(K)
    7 CONTINUE
      D(1)=A0(I,J)
      D(2)=A1(I,J)*VEL1
      D(3)=A2(I,J)*VEL2
      CALL  PROPOL(C,LF,D,3,D1,LS)
      DO  8  K=1,LS
      CA(I,J,K)=D1(K)
    8 CONTINUE
      DO  9  K=1,NL
      D(1)=0.D0
      D(2)=AL(I,J,K)
      CALL  PROPOL(FCT(1,K),LP,D,2,D1,LS)
      DO  10  KK=1,LS
      CA(I,J,KK)=CA(I,J,KK)+D1(KK)
   10 CONTINUE
```

```
    3 CONTINUE
    5 CONTINUE
      NRR=LSMX
      NRD=LSMX
      NMT=NM+NC
      NM1=NM+1
      NC2=2*NC
      MAXC2=2*MAXC
      IF(NC.EQ.0)  GO  TO  48
C
C     (2) ADDITIONS TO THE NM STRUCTURAL EQUATIONS DUE TO THE NC
C     CONTROL SURFACES
C
      DO  11  I=1,NM
      DO  11  J=1,NC
      D(1)=A0C(I,J)
      D(2)=A1C(I,J)*VEL1
      D(3)=A2C(I,J)*VEL2
      CALL  PROPOL(C,LF,D,3,D1,LS)
      DO  12  K=1,LS
      CAC(I,J,K)=D1(K)
   12 CONTINUE
      DO  13  K=1,NL
      D(1)=0.D0
      D(2)=ACL(I,J,K)
      CALL  PROPOL(FCT(1,K),LP,D,2,D1,LS)
      DO  14  KK=1,LS
      CAC(I,J,KK)=CAC(I,J,KK)+D1(KK)
   14 CONTINUE
   13 CONTINUE
   11 CONTINUE
      DO  33  I=1,NC
      DO  33  J=1,NC2
      DO  33  K=1,MAXK
      P(I,J,K)=0.D0
   33 CONTINUE
C
C     FORMATION OF THE NC CONTROL SURFACE EQUATIONS THROUGH THE USE
C     OF THE CONTROL LAW
C
      CALL  CONTRL(NP,P,ND,QD,NC,WR,NTE,X)
C
C
C
C
C
C
C
C
      NCMX=0
      NPMX=0
      DO  45  I=1,NC
      NPIMX(I)=NP(I,1)
      IF(ND(I).GT.NCMX)  NCMX=ND(I)
      DO  45  J=1,NC2
      IF(NP(I,J).GT.NPIMX(I))  NPIMX(I)=NP(I,J)
      IF(NP(I,J).GT.NPMX)  NPMX=NP(I,J)
   45 CONTINUE
      IF(NPMX.GT.LSMX)  NRR=NPMX
```

```
      IF(NCMX.GT.LSMX)   NRD=NCMX
   48 CONTINUE
      DO  46   I=1,NMT
      DO  46   J=1,NM
      DO  46   K=1,MAXK
      RM(I,J,K)=0.D0
   46 CONTINUE
      IF(NC.EQ.0)   GO   TO   51
      DO  47   I=1,NMT
      DO  47   J=1,NC
      DO  47   K=1,MAXK
      DM(I,J,K)=0.D0
   47 CONTINUE
      INC=0
      DO  31   I=1,NC2,2
      INC=INC+1
      DO  31   J=1,NM
      H(I,J)=(ZW(I,J)+(CLR(INC)/CTR-1.D0)*ZREF(1,J)-CLR(INC)/CTR*
     *ZREF(2,J))/DTRAN(INC)
      H(I+1,J)=(ZW(I+1,J)-ZW(I,J))/CTRAN(INC)-(ZREF(2,J)-ZREF(1,J))/CTR
   31 CONTINUE
      DO  30   K=1,NPMX
      CALL   MXPROD(P(1,1,K),H,PH(1,1,K),NC,NC2,NM,MAXC,MAXC2,MAXC)
   30 CONTINUE
      DO  17   I=1,NC
      NN=ND(I)
      NPC(I)=NRD-ND(I)
      DO  17   K=1,NN
      DM(NM+I,I,NRD-K+1)=Q)(NN-K+1,I)
   17 CONTINUE
      DO  18   I=1,NC
      NN=NPIMX(I)
      NR=NPC(I)+NPIMX(I)
      NPIMX(I)=NR
      DO  18   J=1,NM
      DO  18   K=1,NN
      RM(NM+I,J,NR-K+1)=-PH(I,J,NN-K+1)
   18 CONTINUE
      NNPMX=0
      DO  52   I=1,NC
      IF(NPIMX(I).GT.NNPMX)   NNPMX=NPIMX(I)
   52 CONTINUE
      IF(NNPMX.GT.NRR)   NRR=NNPMX
   51 CONTINUE
      NRRM1=NRR-1
      NRDM1=NRD-1
      NT=NRRM1*NMT+(NRD-NRR)*NC
      NTS=NMT*(NRR-2)
      NTSS=NRD-NRR
      NTS1=NMT*NRRM1
      NTSC=(NRD-NRR)*NC
      PRINT   901,NRR,NRD,NMT
C
C     FORMATION OF THE EXPANDED FIRST ORDER DIFFERENTIAL EQUATIONS
C     OF MOTION (SUITABLE FOR EIGENVALUE SOLUTION OF THE  T  MATRIX) -
C     REPEATED IN A LOOP FOR THE VARIOUS VALUES OF DYNAMIC PRESSURE Q
C
      DO  1000 ICASE=1,NQT
      DO  32   I=1,NT
```

```
      DO  32  J=1,NT
      T(I,J)=0.D0
   32 CONTINUE
      Q=QBEGIN+(ICASE-1)*DQ
C
      PRINT 100,Q
      DO  15  I=1,NM
      DO  15  J=1,NM
      DO  15  K=1,LSMX
      RM(I,J,NRR-K+1)=CM(I,J,LSMX-K+1)+Q*CA(I,J,LSMX-K+1)
   15 CONTINUE
      IF(NC.EQ.0)  GO  TO  49
      DO  16  I=1,NM
      DO  16  J=1,NC
      DO  16  K=1,LSMX
      DM(I,J,NRR-K+1)=Q*CAC(I,J,LSMX-K+1)
   16 CONTINUE
   49 CONTINUE
      DO  19  I=1,NMT
      DO  20  J=1,NM
      RDMN(I,J)=-RM(I,J,NRR)
   20 CONTINUE
      IF(NC.EQ.0)  GO  TO  19
      DO  21  J=1,NC
      RDMN(I,J+NM)=-DM(I,J,NRD)
   21 CONTINUE
   19 CONTINUE
      CALL  MXINVR(NMT,0,MAX,RDMN)
      DO  22  K=1,NRRM1
      NJ=NMT*(K-1)+1
      KK=NRR-K
      CALL  MXPROD(RDMN,RM(1,1,KK),T(1,NJ),NMT,NMT,NM,MAX,MAX,MAXT)
   22 CONTINUE
      IF(NC.EQ.0)  GO  TO  50
      DO  23  K=1,NRDM1
      KK=NRD-K
      IF(K.LE.NRRM1)  NJ=NMT*K-NC+1
      IF(K.GT.NRRM1)  NJ=NMT*NRRM1+NC*(K-NRRM1-1)+1
      CALL  MXPROD(RDMN,DM(1,1,KK),T(1,NJ),NMT,NMT,NC,MAX,MAX,MAXT)
   23 CONTINUE
   50 CONTINUE
      DO  24  I=1,NTS
      T(NMT+I,I)=1.D0
   24 CONTINUE
      IF(NTSS.EQ.0)  GO  TO  26
      DO  25  I=1,NTSC
      T(NTS1+I,NTS1-NC+I)=1.D0
   25 CONTINUE
   26 CONTINUE
C
C     EIGENVALUE  SOLUTION  OF  THE  FINAL  T  MATRIX
C
      CALL  EBALAF(T,NT,MAXT,PV,INK,INL)
      CALL  EHESSF(T,INK,INL,NT,MAXT,PV)
      CALL  EQRH3F(T,NT,MAXT,INK,INL,FR,EI,ZZ,0,IERR)
      PRINT  600,IERR
      DO  82  I=1,NT
      PRINT  200,FR(I),EI(I)
   82 CONTINUE
```

```
      IF(IPLOT.EQ.1)  CALL  PLTDAT(NT,ER,EI,XZ,YZ,XSCALE,YSCALE,XL,YL,
     +ISYM,IENTRY)
 1000 CONTINUE
      CALL  PLOT(0.,0.,999)
  100 FORMAT(//10X' DYNAMIC PRESSURE =',F10.3,/)
  200 FORMAT(10X,E15.4,' +I ',E15.4)
  500 FORMAT(//10X' ROOT LOCUS - CLOSED LOOP -REAL ACTUATORS '//)
  600 FORMAT(10X' IERR = 'I4)
  900 FORMAT(7E13.6)
  901 FORMAT(5I5)
  902 FORMAT(9E13.5)
  903 FORMAT(4X,E14.6)
      RETURN
      END
      SUBROUTINE  FACTR(FCT,B,NL,LP,LF)
CCCCCCCCCCCCCCCCCCCCCCCCCCCCCCCCCCCCCCCCCCCCCCCCCCCCCCCCCCCCCCCCCCCCCCCC
C                                                                      C
C     THIS SUBROUTINE COMPUTES THE VARIOUS FACTORS WHICH ARE NECESSARY C
C     SO AS TO BRING THE AERO PADE APPROXIMANTS TO A COMMON DENOMINATORC
C     FCT(I,J) IS THE FACTOR WHICH MULTIPLIES THE J-TH LAG AERO TERM - C
C     IN TERMS OF POLYNOMIAL FCT(1,J)+FCT(2,J)*S+FCT(3,J)*S**2+....... C
C                                                                      C
CCCCCCCCCCCCCCCCCCCCCCCCCCCCCCCCCCCCCCCCCCCCCCCCCCCCCCCCCCCCCCCCCCCCCCCC
      REAL*8  FCT(5,5),B(4)
      IF(NL.NE.1)  GO  TO  1
      LP=1
      LF=2
      FCT(1,1)=1.D0
      FCT(1,2)=B(1)
      FCT(2,2)=1.D0
      RETURN
    1 IF(NL.NE.2)  GO  TO  2
      LP=2
      LF=3
      FCT(1,1)=B(2)
      FCT(2,1)=1.D0
      FCT(1,2)=B(1)
      FCT(2,2)=1.D0
      FCT(1,3)=B(1)*B(2)
      FCT(2,3)=B(1)+B(2)
      FCT(3,3)=1.D0
      RETURN
    2 IF(NL.NE.3)  GO  TO  3
      LP=3
      LF=4
      FCT(1,1)=B(2)*B(3)
      FCT(2,1)=B(2)+B(3)
      FCT(3,1)=1.D0
      FCT(1,2)=B(1)*B(3)
      FCT(2,2)=B(1)+B(3)
      FCT(3,2)=1.D0
      FCT(1,3)=B(1)*B(2)
      FCT(2,3)=B(1)+B(2)
      FCT(3,3)=1.D0
      FCT(1,4)=B(1)*B(2)*B(3)
      FCT(2,4)=B(1)*B(2)+B(1)*B(3)+B(2)*B(3)
      FCT(3,4)=B(1)+B(2)+B(3)
      FCT(4,4)=1.D0
      RETURN
```

```
    3 IF(NL.NE.4)  GO  TO  4
      LP=4
      LF=5
      FCT(1,1)=B(2)*B(3)*B(4)
      FCT(2,1)=B(2)*B(3)+B(2)*B(4)+B(3)*B(4)
      FCT(3,1)=B(2)+B(3)+B(4)
      FCT(4,1)=1.D0
      FCT(1,2)=B(1)*B(3)*B(4)
      FCT(2,2)=B(1)*B(3)+B(1)*B(4)+B(3)*B(4)
      FCT(3,2)=B(1)+B(3)+B(4)
      FCT(4,2)=1.D0
      FCT(1,3)=B(1)*B(2)*B(4)
      FCT(2,3)=B(1)*B(2)+B(1)*B(4)+B(2)*B(4)
      FCT(3,3)=B(1)+B(2)+B(4)
      FCT(4,3)=1.D0
      FCT(1,4)=B(1)*B(2)*B(3)
      FCT(2,4)=B(1)*B(2)+B(1)*B(3)+B(2)*B(3)
      FCT(3,4)=B(1)+B(2)+B(3)
      FCT(4,4)=1.D0
      FCT(1,5)=B(1)*B(2)*B(3)*B(4)
      FCT(2,5)=B(1)*B(2)*B(3)+B(1)*B(2)*B(4)+B(1)*B(3)*B(4)+B(2)*B(3)*
     *B(4)
      FCT(3,5)=B(1)*B(2)+B(1)*B(3)+B(1)*B(4)+B(2)*B(3)+B(2)*B(4)+B(3)*
     *B(4)
      FCT(4,5)=B(1)+B(2)+B(3)+B(4)
      FCT(5,5)=1.D0
      RETURN
    4 PRINT 100
  100 FORMAT(5X' NUMBER OF AERODYNAMIC LAG TERMS EXCEEDS THE MAXIMUM OF
     *FOUR  TERMS ',/)
      STOP
      END
      SUBROUTINE  FIT
      IMPLICIT  REAL*8(A-H,O-Z)
CCCCCCCCCCCCCCCCCCCCCCCCCCCCCCCCCCCCCCCCCCCCCCCCCCCCCCCCCCCCCCCCCCCCCCCC
C                                                                      C
C     FITS THE  AERO COEFFICIENTS IN TERMS OF PADE APPROXIMANTS USING  C
C     LEAST SQUARE TECHNIQUE.                                          C
C                                                                      C
C     NAMELIST/FIT                                                     C
C     NK - NUMBER OF REDUCED FREQUENCIES K USED FOR INTERPOLATION      C
C                                                                      C
C     AK - ARRAY CONTAINING THE K VALUES(20 MAX) - (FIRST REDUCED K    C
C     MUST BE EQUAL TO ZERO)                                           C
C                                                                      C
C     MAXNK - MAX VALUE OF NK(MAX NK=20 IN PRESENT PROGRAM)            C
C                                                                      C
C     NPRINT - 0 NO PRINTED OUTPUT FROM SUBROUTINE FIT.                C
C            - 1 PRINTED OUTPUT IS AVAILABLE(FOR DEBUGGING PURPOSES)   C
C                                                                      C
C     NPUNCH - 0 NO PUNCHED OUTPUT FROM SUBROUTINE FIT                 C
C            - 1 PUNCHED OUTPUT(INTERPOLATION COEFFICIENTS).           C
C                                                                      C
C     IRIGID,JRIGID - CURVE FITTING(WITH NO LEAST SQUARES TECHNIQUE)   C
C     OF THE FIRST IRIGID ROWS AND JRIGID COLUMNS OF AERO MATRIX -     C
C     ASSUMED TO CONTAIN RIGID BODY AERO - TO IMPROVE RESULTS.         C
C                                                                      C
C     READ(2,   )  AERO(I,J,K)   FORMAT(2E15.5)                        C
C                                                                      C
```

```
CCCCCCCCCCCCCCCCCCCCCCCCCCCCCCCCCCCCCCCCCCCCCCCCCCCCCCCCCCCCCCCCCCCCCCCC
      COMMON/AERF/A0(15,22),A1(15,22),A2(15,22),A3(15,22),A4(15,22),
     *A5(15,22),A6(15,22)
      COMMON/ICASE/B(4),NM,NC,NG,NL
      COMPLEX*16  AERO(15,22,20),CCEF
      DIMENSION  AK(20),AK2(20),X(40,6),XT(6,40),Y(40),XTX(6,6),
     *XTY(6),S(6),CLR(4,20),CLI(4,20)
      NAMELIST/FT/NK,AK,MAXNK,NPRINT,NPUNCH,IRIGID,JRIGID
      READ(5,FT)
      WRITE(6,FT)
      MAXNK2=2*MAXNK
      NMNC=NM+NC+NG
      DO  1  K=1,NK
      AK2(K)=AK(K)*AK(K)
      DO  1  J=1,NMNC
      DO  1  I=1,NM
      READ(2,201)  AERO(I,J,K)
    1 CONTINUE
      DO  5  I=1,NL
      B2=B(I)*B(I)
      DO  5  K=1,NK
      CLR(I,K)=AK2(K)/(B2+AK2(K))
      CLI(I,K)=B(I)*AK(K)/(B2+AK2(K))
    5 CONTINUE
      IF(AK(1).NE.0.D0)  PRINT  100
      IF(AK(1).NE.0.D0)  STOP
C
C     DETERMINATION OF THE INTRPOLATION LEAST SQUARE MATRIX  XTX AND
C     THE KNOWN AERO VECTOR  XTY
C
      DO  2  I=1,NM
      DO  2  J=1,NMNC
      IF(I.GT.IRIGID.OR.J.GT.JRIGID) GO  TO  7
      NKT=NK
      NK=(3+NL)/2+1
    7 CONTINUE
      DO  3  K=2,NK
      X(2*K-3,1)=0.D0
      X(2*K-2,1)=AK(K)
      X(2*K-3,2)=-AK2(K)
      X(2*K-2,2)=0.D0
      Y(2*K-3)=DREAL(AERO(I,J,K)-AERO(I,J,1))
      Y(2*K-2)=DAIMAG(AERO(I,J,K))
      DO  3  L=1,NL
      X(2*K-3,2+L)=CLR(L,K)
      X(2*K-2,2+L)=CLI(L,K)
    3 CONTINUE
      NROWS=2*(NK-1)
      NCOLS=2+NL
      IF(NROWS.LT.NCOLS)  PRINT  110
      IF(NROWS.LT.NCOLS)  STOP
      DO  4  IR=1,NROWS
      DO  4  JR=1,NCOLS
      XT(JR,IR)=X(IR,JR)
    4 CONTINUE
      CALL  MXPROD(XT,X,XTX,NCOLS,NROWS,NCOLS,6,MAXNK2,6)
      CALL  MXPROD(XT,Y,XTY,NCOLS,NROWS,1,6,MAXNK2,6)
C
C     SOLUTION FOR THE UNKNOWN INTERPOLATION COEFFICIENTS
```

```
C
      CALL  MXINVR(NCOLS,0,6,XTX)
      CALL  MXPROD(XTX,XTY,S,NCOLS,NCOLS,1,6,6,6)
      A0(I,J)=AERO(I,J,1)
      A1(I,J)=S(1)
      A2(I,J)=S(2)
      A3(I,J)=S(3)
      IF(NL.LT.2)  GO  TO  10
      A4(I,J)=S(4)
      IF(NL.LT.3)  GO  TO  10
      A5(I,J)=S(5)
      IF(NL.LT.4)  GO  TO  10
      A6(I,J)=S(6)
   10 CONTINUE
      IF(I.LE.IRIGID.AND.J.LE.JRIGID)  NK=NKT
C
C     PRINTED AND/OR PUNCHED OUTPUTS
C
      IF(NPRINT.NE.1.AND.NPUNCH.NE.1)  GO  TO  2
      IF(NPUNCH.NE.1)  GO  TO  9
      PUNCH  600,I,J,A0(I,J),(S(JJ),JJ=1,NCOLS)
    9 CONTINUE
      IF(NPRINT.NE.1)  GO  TO  2
      PRINT  700,I,J
      PRINT  200,A0(I,J),(S(JJ),JJ=1,NCOLS)
      DO  8  IK=1,NK
      COEF=DCMPLX(0.D0,0.D0)
      DO  6  II=1,NL
      COEF=COEF+S(2+II)*DCMPLX(CLR(II,IK),CLI(II,IK))
    6 CONTINUE
      COEF=COEF+AERO(I,J,1)+S(1)*DCMPLX(0.D0,AK(IK))-S(2)*AK2(IK)
      QUOTR=DREAL(AERO(I,J,IK))
      QUOTI=DAIMAG(AERO(I,J,IK))
      IF(QUOTR.EQ.0.D0)  QUOTR=1.D-20
      IF(QUOTI.EQ.0.D0)  QUOTI=1.D-20
      ERR=DREAL(AERO(I,J,IK)-COEF)*100.D0/QUOTR
      ERI=DAIMAG(AERO(I,J,IK)-COEF)*100.D0/QUOTI
      PRINT  210,I,J,IK,AK(IK),AERO(I,J,IK),COEF,ERR,ERI
    8 CONTINUE
    2 CONTINUE
  200 FORMAT(10X' COEFF = '8E12.4)
  210 FORMAT(2X,3I5,4X,7E12.4)
  600 FORMAT(2X,2I2,2X,7E10.4)
  700 FORMAT(20X'  AERO( DEF MODE = ',I2,' PRES MODE = 'I2, ')'/)
      RETURN
  100 FORMAT('  FIRST  REDUCED  FREQUENCY  MUST  BE  EQUAL  TO  ZERO'/)
  110 FORMAT('  THERE  ARE  LESS  EQUATIONS  THAN  UNKNOWNS',/)
  201 FORMAT(2E15.5)
      END
      SUBROUTINE PLTDAT(N,ELR,ELI,XZ,YZ,XSCALE,YSCALE,XL,YL,ISYM,IENTRY
     +)
      REAL*8  ELR(1),ELI(1)
CCCCCCCCCCCCCCCCCCCCCCCCCCCCCCCCCCCCCCCCCCCCCCCCCCCCCCCCCCCCCCCCCCCCCCCC
C
C         ROOT LOCUS PLOT - FOR FLUTTER PROGRAM
C
C         NUM = 4*NUMBER OF MODES
C
C         XZ = LEFT HAND LIMIT OF REAL PART
```

```
C                                                                      C00000813
C        YZ = 0.                                                       C00000814
C                                                                      C00000815
C        XSCALE = ABSCISSA SCALE                                       C00000816
C                                                                      C00000817
C        YSCALE = ORDINATE SCALE                                       C00000818
C                                                                      C00000819
C        XL = LENGTH OF PLOT IN INCHES OF PAPER                        C00000820
C                                                                      C00000821
C        YL = HEIGHT OF PLOT IN INCHES OF PAPER                        C00000822
C                                                                      C00000823
CCCCCCCCCCCCCCCCCCCCCCCCCCCCCCCCCCCCCCCCCCCCCCCCCCCCCCCCCCCCCCCCCCCCCCC00000824
      DIMENSION ER(150),EI(150),EX(150),EY(150)                         00000825
      M=0                                                               00000826
      DO 1 I=1,N                                                        00000827
      ER(I)=ELR(I)                                                      00000828
      EI(I)=ELI(I)                                                      00000829
      RGHTLM=XZ+XSCALE*XL                                               00000830
      UPLMT=YZ+YL*YSCALE                                                00000831
      IF(ER(I).LT.XZ) GO TO 1                                           00000832
      IF(EI(I).LT.0.) GO TO 1                                           00000833
      IF(ER(I).GT.RGHTLM) GO TO 1                                       00000834
      IF(EI(I).GT.UPLMT) GO TO 1                                        00000835
      IF(ABS(ER(I)).LT.0.50.AND.ABS(EI(I)).LT.0.50)   GO  TO  1         00000836
      M=M+1                                                             00000837
      EX(M)=ER(I)                                                       00000838
      EY(M)=EI(I)                                                       00000839
    1 CONTINUE                                                          00000840
      EX(M+1)=XZ                                                        00000841
      EY(M+1)=YZ                                                        00000842
      EX(M+2)=XSCALE                                                    00000843
      EY(M+2)=YSCALE                                                    00000844
      GO TO (2,3),IENTRY                                                00000845
    2 CONTINUE                                                          00000846
      YAXISO=ABS(XZ/XSCALE)                                             00000847
      CALL  AXIS(0.,0.,'REAL PART',-9,XL,0.,XZ,XSCALE)                  00000848
      CALL  AXIS(YAXISO,0.,'FREQ',-4,YL,90.,YZ,YSCALE)                  00000849
      IENTRY=2                                                          00000850
    3 CONTINUE                                                          00000851
      CALL PLOT(0.,0.,3)                                                00000852
      CALL  LINE(EX,EY,M,1,-1,ISYM)                                     00000853
      RETURN                                                            00000854
      END                                                               00000855
      FUNCTION DREAL(Z)                                                 00000856
C     THIS SUBROUTINE CAN BE USED WITH EITHER THE SLOW OR FAST,IBM,     00000857
C     DOUBLE PRECISION , COMPRESSIBLE AERODYNAMIC COEFFICIENTS PROGRAM .00000858
      IMPLICIT REAL*8(D)                                                00000859
      REAL*8 Z(2)                                                       00000860
      DREAL=Z(1)                                                        00000861
      RETURN                                                            00000862
      ENTRY DAIMAG(Z)                                                   00000863
      DAIMAG=Z(2)                                                       00000864
         RETURN                                                         00000865
         END                                                            00000866
      SUBROUTINE PRDPOL(A,N,B,M,C,L)                                    00000867
      IMPLICIT  REAL*8(A-H,O-Z)                                         00000868
CCCCCCCCCCCCCCCCCCCCCCCCCCCCCCCCCCCCCCCCCCCCCCCCCCCCCCCCCCCCCCCCCCCCCC 00000869
C                                                                      C00000870
C     A ROUTINE FOR MULTIPLYING POLYNOMIALS  C=A*B  WHERE A,B,C  ARE   C00000871
```

```
C     POLYNOMIALS OF THE FORM
C     A=A(1)+A(2)*X+A(3)*X**2+A(4)*X**3+..........A(N)*X**(N-1)
C     B=B(1)+B(2)*X+B(3)*X**2+B(4)*X**3+...........B(M)*X**(M-1)
C     C=C(1)+C(2)*X+C(3)*X**2+C(4)*X**3+.......C(N+M-1)*X**(N+M-2)
C     AND WHERE         L=N+M-1
C
CCCCCCCCCCCCCCCCCCCCCCCCCCCCCCCCCCCCCCCCCCCCCCCCCCCCCCCCCCCCCCCCCCCCCCCC
      DIMENSION C(1),A(1),B(1)
      NM=N+M-1
      DO 1 I=1,NM
    1 C(I)=0.D0
      DO 2 I=1,N
      DO 2 J=1,M
    2 C(I+J-1)=A(I)*B(J)+C(I+J-1)
      L=NM
      RETURN
      END
C          SUBROUTINE MXINVR  _  DOUBLE PRECISION
      SUBROUTINE  MXINVR(N,M,MAX,A)
C
C          REAL MATRIX INVERSION WITH SOLUTION OF LINEAR EQUATIONS
C
C          CAVM = DABS(A(MAX)),   CAVA = DABS(A(I,J))
C          CADM = DABS(DETERM),   CAPV = DABS(PIVOT)
C
      IMPLICIT REAL*8(A-H,O-Z)
      DIMENSION  A(MAX,1),B(150,1),IPIV(150),INDX(150,2)
      IF(M.NE.0)  GO  TO  1
      DO   2   I=1,N
    2 B(I,1)=0.D0
      GO   TO   10
    1 PRINT   1000
 1000 FORMAT('  NO SOLUTION  OF   LINEAR   EQUATIONS   IS   ALLOWED FOR   IN
     + THIS VERSION OF MXINVR')
      STOP
   10 CONTINUE
C
C          CONSTANTS, INITIALIZATION
C
      C0=0.D0
      C1=1.D0
      DET = C1
      CADM=1.0D0
      DO 20 J=1,N
   20 IPIV(J) = 0
      DO 500 I=1,N
C
C          SEARCH FOR PIVOT ELEMENT
C
      CAVM=0.0D0
      DO 105 J=1,N
      IF (IPIV(J) .EQ. 1) GO TO 105
      DO 100 K=1,N
      IF (IPIV(K) - 1) 50,100,750
   50 CONTINUE
      CAVA=DABS(A(J,K))
      IF (CAVM .GE. CAVA) GO TO 100
      IROW = J
      ICOL = K
```

```
      CAVM = CAVA
  100 CONTINUE
  105 CONTINUE
      IF(CAVM.EQ.0.0D0) GO TO 720
      IPIV(ICOL) = IPIV(ICOL) + 1
C
C        INTERCHANGE ROWS TO PUT PIVOT ELEMENT ON DIAGONAL
C
      IF (IROW .EQ. ICOL) GO TO 230
      DET = -DET
      DO 200 L=1,N
      SWAP = A(IROW,L)
      A(IROW,L) = A(ICOL,L)
      A(ICOL,L) = SWAP
  200 CONTINUE
      IF (M .LE. 0) GO TO 230
      DO 220 L=1,M
      SWAP = B(IROW,L)
      B(IROW,L) = B(ICOL,L)
      B(ICOL,L) = SWAP
  220 CONTINUE
  230 CONTINUE
      INDX(I,1) = IROW
      INDX(I,2) = ICOL
      PIV = A(ICOL,ICOL)
      CAPV=DABS(PIV)
      IF(CAPV.EQ.0.0D0) GO TO 720
C
C        DIVIDE PIVOT ROW BY PIVOT ELEMENT
C
      A(ICOL,ICOL) = C1
      PIVR=1.D0/PIV
      DO 350 L=1,N
  350 A(ICOL,L) = A(ICOL,L)*PIVR
      IF (M .LE. 0) GO TO 380
      DO 370 L=1,M
  370 B(ICOL,L) = B(ICOL,L)*PIVR
C
C        REDUCE NON-PIVOT ROWS
C
  380 CONTINUE
      DO 500 L1=1,N
      IF (L1 .EQ. ICOL) GO TO 500
      SWAP = A(L1,ICOL)
      A(L1,ICOL) = C0
      DO 400 L=1,N
  400 A(L1,L) = A(L1,L) - A(ICOL,L)*SWAP
      IF (M .LE. 0) GO TO 500
      DO 450 L=1,M
  450 B(L1,L) = B(L1,L) - B(ICOL,L)*SWAP
  500 CONTINUE
C
C        INTERCHANGE COLUMNS
C
      DO 700 I=1,N
      L = N+1-I
      IF (INDX(L,1) .EQ. INDX(L,2))GO TO 700
      IROW = INDX(L,1)
      ICOL = INDX(L,2)
```

```
      DO 690 K=1,N
      SWAP = A(K,IROW)
      A(K,IROW) = A(K,ICOL)
      A(K,ICOL) = SWAP
  690 CONTINUE
  700 CONTINUE
      GO TO 750
  720 DET = 0.0
      ISCALE = 0
  750 RETURN
      END
      SUBROUTINE  MXPROD(A,B,C,NIA,NIB,NJB,MAXA,MAXB,MAXC)
      REAL*8 A,B,C,D
      DIMENSION  A(MAXA,1),B(MAXB,1),C(MAXC,1),D(150)
      DO   100 I=1,NIA
      DO   200  J=1,NJB
      D(J)=0.D0
      DO   200  KK=1,NIB
      D(J)=D(J)+A(I,KK)*B(KK,J)
  200 CONTINUE
      DO   300  J=1,NJB
  300 C(I,J)=D(J)
  100 CONTINUE
      RETURN
      END
      SUBROUTINE   MXADD(A,B,C,NIA,NJ,MAXA,MAXB,MAXC)
      REAL*8   A,B,C
      DIMENSION  A(MAXA,1),B(MAXB,1),C(MAXC,1)
      DO   100 I=1,NIA
      DO   100 J=1,NJ
  100 C(I,J)=A(I,J)+B(I,J)
      RETURN
      END
      SUBROUTINE   MXSUB(A,B,C,NIA,NJ,MAXA,MAXB,MAXC)
      REAL*8   A,B,C
      DIMENSION  A(MAXA,1),B(MAXB,1),C(MAXC,1)
      DO   100 I=1,NIA
      DO   100 J=1,NJ
  100 C(I,J)=A(I,J)-B(I,J)
      RETURN
      END
      SUBROUTINE   MXSCAL(A,B,C,NIB,NJB,MAXA,MAXB,MAXC)
      REAL*8   A,B,C
      DIMENSION  B(MAXB,1),C(MAXC,1)
      DO   100 I=1,NIB
      DO   100 J=1,NJB
  100 C(I,J)=A*B(I,J)
      RETURN
      END
END OF JOB.  CONDITION CODE WAS     0
```

```
 DAST CONFIGURATION AT M=0.9, DATA FOR FLUTTER CALCULATIONS
&CASE
NM=            9,NC=           2,NAER=          0,B= 0.1000000000000000D 00,
 0.2000000000000000       , 0.3000000000000000      , 0.4000000000000000      ,NG=
          1,NL=            4
&END
&FI
NK=          10,AK= 0.0                        , 0.4999999999999999D-01,
 0.1000000000000000D 00, 0.2000000000000000      , 0.3000000000000000      ,
 0.4000000000000000      , 0.5000000000000000      , 0.6000000000000000      ,
 0.7000000000000000      , 0.8000000000000000      , 0.0                     ,
 0.0                     , 0.0                     , 0.0                     ,
 0.0                     , 0.0                     , 0.0                     ,
 0.0                     , 0.0                     , 0.0                     ,MAXNK=
         20,NPRINT=          0,NPUNCH=          0,IRIGID=          2,JRIGID=
          1
&END
&FLUT
MASS=  3.619500000000000     , 0.0                     , 0.0                     ,
 0.0                     , 0.0                     , 0.0                     ,
 0.0                     , 0.0                     , 0.0                     ,
 0.0                     , 0.0                     , 0.0                     ,
 0.0                     , 0.0                     , 0.0                     ,
 0.0                     ,  13595.00000000000      , 0.0                     ,
 0.0                     , 0.0                     , 0.0                     ,
 0.0                     , 0.0                     , 0.0                     ,
 0.0                     , 0.0                     , 0.0                     ,
 0.0                     , 0.0                     , 0.0                     ,
 0.0                     , 0.0                     , 0.2361000000000000D-01,
 0.0                     , 0.0                     , 0.0                     ,
 0.0                     , 0.0                     , 0.0                     ,
 0.0                     , 0.0                     , 0.0                     ,
 0.0                     , 0.0                     , 0.0                     ,
 0.0                     , 0.0                     , 0.0                     ,
 0.3339999999999999D-01, 0.0                     , 0.0                     ,
 0.0                     , 0.0                     , 0.0                     ,
 0.0                     , 0.0                     , 0.0                     ,
 0.0                     , 0.0                     , 0.0                     ,
 0.0                     , 0.0                     , 0.0                     ,
 0.0                     , 0.5462999999999999D-01, 0.0                     ,
 0.0                     , 0.0                     , 0.0                     ,
 0.0                     , 0.0                     , 0.0                     ,
 0.0                     , 0.0                     , 0.0                     ,
 0.0                     , 0.0                     , 0.0                     ,
 0.0                     , 0.0                     , 0.5079999999999999D-02,
 0.0                     , 0.0                     , 0.0                     ,
 0.0                     , 0.0                     , 0.0                     ,
 0.0                     , 0.0                     , 0.0                     ,
 0.0                     , 0.0                     , 0.0                     ,
 0.0                     , 0.0                     , 0.0                     ,
 0.1205000000000000D-01, 0.0                     , 0.0                     ,
 0.0                     , 0.0                     , 0.0                     ,
 0.0                     , 0.0                     , 0.0                     ,
 0.0                     , 0.0                     , 0.0                     ,
 0.0                     , 0.0                     , 0.0                     ,
 0.0                     , 0.1631000000000000D-01, 0.0                     ,
 0.0                     , 0.0                     , 0.0                     ,
 0.0                     , 0.0                     , 0.0                     ,
 0.0                     , 0.0                     , 0.0                     ,
 0.0                     , 0.0                     , 0.0                     ,
 0.0                     , 0.0                     , 0.1552000000000000D-01,
```

```
 0.0                 , 0.0                   , 0.0                     ,
 0.0                 , 0.0                   , 0.0                     ,
 0.0                 , 0.0                   , 0.0                     ,
 0.0                 , 0.0                   , 0.0                     ,
 0.0                 , 0.0                   , 0.0                     ,
 0.0                 , 0.0                   , 0.0                     ,
 0.0                 , 0.0                   , 0.0                     ,
 0.0                 , 0.0                   , 0.0                     ,
 0.0                 , 0.0                   , 0.0                     ,
 0.0                 , 0.0                   , 0.0                     ,
 0.0                 , 0.0                   , 0.0                     ,
 0.0                 , 0.0                   , 0.0                     ,
 0.0                 , 0.0                   , 0.0                     ,
 0.0                 , 0.0                   , 0.0                     ,
 0.0                 , 0.0                   , 0.0                     ,
 0.0                 , 0.0                   , 0.0                     ,
 0.0                 , 0.0                   , 0.0                     ,
 0.0                 , 0.0                   , 0.0                     ,
 0.0                 , 0.0                   , 0.0                     ,
 0.0                 , 0.0                   , 0.0                     ,
 0.0                 , 0.0                   , 0.0                     ,
 0.0                 , 0.0                   , 0.0                     ,
 0.0                 , 0.0                   , 0.0                     ,
 0.0                 , 0.0                   , 0.0                     ,
 0.0                 , 0.0                   , 0.0                     ,
 0.0                 , 0.0                   , 0.0                     ,
 0.0                 , 0.0                   , 0.0                     ,
 0.0                 , 0.0                   , 0.0                     ,
 0.0                 , 0.0                   , 0.0                     ,
 0.0                 , 0.0                   , 0.0                     ,
 0.0                 , 0.0                   , 0.0                     ,
 0.0                 , 0.0                   , 0.0                     ,
OMEGAN= 0.0                  , 0.0                    , 9.9410000000000000    ,
  31.557000000000000 ,  34.951000000000000   ,  50.254000000000000     ,
  84.308000000000000 ,  119.51000000000000   ,  127.98000000000000     ,
 0.0                 , 0.0                   , 0.0                     ,
 0.0                 , 0.0                   , 0.0                     ,
GBEGIN= 0.0                  ,GEND=  2.0000000000000000     ,NG=          4,
VEL=  11496.000000000000      ,FTRAN=  8.1970000000000000     ,
  8.1970000000000000 , 0.0                   , 0.0                     ,
 0.0                 , 0.0                   ,CTRAN=  6.5570000000000000   ,
  6.5570000000000000 , 0.0                   , 0.0                     ,
 0.0                 , 0.0                   ,CREF=  13.543000000000000    ,
ZW=  1.0000000000000000      ,  1.0000000000000000     ,  1.0000000000000000     ,
  1.0000000000000000 , 0.0                   , 0.0                     ,
 0.0                 , 0.0                   , 0.0                     ,
 0.0                 , 0.0                   , 0.0                     ,
  39.720000000000000 ,  46.230000000000000   ,  39.720000000000000     ,
  46.230000000000000 , 0.0                   , 0.0                     ,
 0.0                 , 0.0                   , 0.0                     ,
 0.0                 , 0.0                   , 0.0                     ,
 0.64000000000000000 , 0.74000000000000000   , 0.64000000000000000     ,
 0.74000000000000000 , 0.0                   , 0.0                     ,
 0.0                 , 0.0                   , 0.0                     ,
 0.0                 , 0.0                   , 0.0                     ,
-[illegible]         , 0.21000000000000000   ,-0.46000000000000000     ,
 [illegible]         , 0.0                   , 0.0                     ,
 0.0                 , 0.0                   , 0.0                     ,
 0.0                 , 0.0                   , 0.0                     ,
-0.51000000000000000 , 0.28000000000000000   ,-0.51000000000000000     ,
 0.28000000000000000 , 0.0                   , 0.0                     ,
```

```
 0.0                     , 0.0                   , 0.0                     ,
 0.0                     , 0.0                   , 0.0                     ,
-0.360000000000000     ,-0.449999999999999D-01,-0.360000000000000      ,
-0.449999999999999D-01, 0.0                   , 0.0                     ,
 0.0                     , 0.0                   , 0.0                     ,
 0.0                     , 0.0                   , 0.0                     ,
 0.360000000000000     , 0.100000000000000D 00, 0.360000000000000      ,
 0.100000000000000D 00, 0.0                   , 0.0                     ,
 0.0                     , 0.0                   , 0.0                     ,
 0.0                     , 0.0                   , 0.0                     ,
 0.200000000000000D-01, 0.260000000000000     , 0.200000000000000D-01,
 0.260000000000000     , 0.0                   , 0.0                     ,
 0.0                     , 0.0                   , 0.0                     ,
 0.0                     , 0.0                   , 0.0                     ,
-0.999999999999999D-02,-0.220000000000000     ,-0.999999999999999D-02,
-0.220000000000000     , 0.0                   , 0.0                     ,
 0.0                     , 0.0                   , 0.0                     ,
 0.0                     , 0.0                   , 0.0                     ,
 0.0                     , 0.0                   , 0.0                     ,
 0.0                     , 0.0                   , 0.0                     ,
 0.0                     , 0.0                   , 0.0                     ,
 0.0                     , 0.0                   , 0.0                     ,
 0.0                     , 0.0                   , 0.0                     ,
 0.0                     , 0.0                   , 0.0                     ,
 0.0                     , 0.0                   , 0.0                     ,
 0.0                     , 0.0                   , 0.0                     ,
 0.0                     , 0.0                   , 0.0                     ,
 0.0                     , 0.0                   , 0.0                     ,
 0.0                     , 0.0                   , 0.0                     ,
 0.0                     , 0.0                   , 0.0                     ,
 0.0                     , 0.0                   , 0.0                     ,
 0.0                     , 0.0                   , 0.0                     ,
 0.0                     , 0.0                   , 0.0                     ,
 0.0                     , 0.0                   , 0.0                     ,
 0.0                     , 0.0                   , 0.0                     ,
 0.0                     , 0.0                   , 0.0                     ,
 0.0                     , 0.0                   , 0.0                     ,
 0.0                     , 0.0                   , 0.0                     ,
 0.0                     , 0.0                   , 0.0                     ,
 0.0                     , 0.0                   , 0.0                     ,
 0.0                     , 0.0                   , 0.0                     ,
 0.0                     , 0.0                   , 0.0                     ,ZREF=
  1.00000000000000000  ,  1.00000000000000000 , -38.2000000000000000  ,
-1.23000000000000000  , 0.0                   , 0.0                     ,
 0.0                     , 0.0                   , 0.0                     ,
 0.0                     , 0.0                   , 0.0                     ,
 0.0                     , 0.0                   , 0.0                     ,
 0.0                     , 0.0                   , 0.0                     ,
 0.0                     , 0.0                   , 0.0                     ,
 0.0                     , 0.0                   , 0.0                     ,
 0.0                     , 0.0                   , 0.0                     ,
 0.0                     , 0.0                   , 0.0                     ,IPLCT=
         1,CLR=   77.9200000000000      ,  77.9200000000000      ,
 0.0                     , 0.0                   , 0.0                     ,
 0.0                     ,CTR=   36.9700000000000     ,NCACT=           1
&END
```

ROOT LOCUS - CLOSED LOOP -REAL ACTUATORS

```
&PLOTPA
XZ= -100.00000      ,YZ= 0.0            ,XSCALE=   20.000000     ,YSCALE=
  200.00000     ,XL=  7.0000000     ,YL=  5.0000000       ,ISYM=              3,IENTRY=
          1
&END
&MXSIZE
MAXL=              6,MAXNM=           15,MAXK=           10,MAXT=          100
&END
&CONC
WR=  100.000000000000      ,NTE=           1,            0,            0,            0,
         0,          0,X=   3.630000000000000      ,  50.0000000000000     ,
 0.750000000000000      , 0.0                        , 0.0                         ,
 0.0                    , 0.0                        , 0.0                         ,
 0.0                    , 0.0                        , 0.0                         ,
 0.0                    , 0.0                        , 0.0                         ,
 0.0                    , 0.0                        , 0.0                         ,
 0.0                    , 0.0                        , 0.0                         ,
 0.0                    , 0.0                        , 0.0                         ,
 0.0                    , 0.0                        , 0.0                         ,
 0.0                    , 0.0                        , 0.0                         ,
 0.0                    , 0.0                        , 0.0                         ,
 0.0                    , 0.0                        , 0.0                         ,
 0.0
&END
   7       7     10


            DYNAMIC PRESSURE =        0.0

            IERR =       0
                 0.0          +I        0.0
                 0.0          +I        0.0
                 0.0          +I        0.0
                 0.0          +I        0.0
                 0.0          +I        0.0
                 0.0          +I        0.0
                 0.0          +I        0.0
                 0.0          +I        0.0
              -0.6821D-12  +I        0.3041D 03
              -0.6821D-12  +I       -0.3041D 03
              -0.1876D-11  +I        0.7528D 03
              -0.1876D-11  +I       -0.7528D 03
              -0.1346D-11  +I        0.5297D 03
              -0.1346D-11  +I       -0.5297D 03
              -0.1595D-11  +I        0.3158D 03
              -0.1595D-11  +I       -0.3158D 03
              -0.1410D-11  +I        0.1983D 03
              -0.1410D-11  +I       -0.1983D 03
              -0.1524D-11  +I        0.2196D 03
              -0.1524D-11  +I       -0.2196D 03
              -0.3750D 02  +I        0.3307D 02
              -0.3750D 02  +I       -0.3307D 02
              -0.1069D-11  +I        0.6246D 02
              -0.1069D-11  +I       -0.6246D 02
              -0.3395D 03  +I        0.9583D-10
              -0.3395D 03  +I       -0.9583D-10
              -0.3395D 03  +I        0.0
              -0.3395D 03  +I        0.2203D-11
              -0.3395D 03  +I       -0.2203D-11
              -0.3395D 03  +I        0.0
              -0.3395D 03  +I        0.1579D-11
```

-0.3395D	03	+I	-0.1579D-11
-0.3395D	03	+I	0.0
-0.2547D	03	+I	0.1027D-09
-0.2547D	03	+I	-0.1027D-09
-0.2547D	03	+I	0.0
-0.2547D	03	+I	0.0
-0.2547D	03	+I	0.0
-0.2547D	03	+I	0.3147D-11
-0.2547D	03	+I	-0.3147D-11
-0.2547D	03	+I	0.0
-0.2547D	03	+I	0.0
-0.1698D	03	+I	0.2565D-10
-0.1698D	03	+I	-0.2565D-10
-0.1698D	03	+I	0.0
-0.1698D	03	+I	0.0
-0.1698D	03	+I	0.3391D-11
-0.1698D	03	+I	-0.3391D-11
-0.1698D	03	+I	0.0
-0.1698D	03	+I	0.0
-0.1598D	03	+I	0.0
-0.8489D	02	+I	0.1226D-12
-0.8489D	02	+I	-0.1226D-12
-0.8489D	02	+I	0.9958D-12
-0.8489D	02	+I	-0.9958D-12
-0.8489D	02	+I	0.1287D-11
-0.8489D	02	+I	-0.1289D-11
-0.8489D	02	+I	0.7529D-12
-0.8489D	02	+I	-0.7529D-12
-0.8489D	02	+I	0.0

DYNAMIC PRESSURE = 0.500

ITER = 0

0.0		+I	0.0
-0.9693D	01	+I	0.8343D 03
-0.9693D	01	+I	-0.8343D 03
-0.9212D	00	+I	0.7533D 03
-0.9212D	00	+I	-0.7533D 03
-0.3559D	01	+I	0.5284D 03
-0.3559D	01	+I	-0.5284D 03
-0.1395D	01	+I	0.3167D 03
-0.1395D	01	+I	-0.3167D 03
-0.7154D	00	+I	0.2180D 03
-0.7154D	00	+I	-0.2180D 03
-0.1881D	01	+I	0.1944D 03
-0.1881D	01	+I	-0.1944D 03
-0.2151D	02	+I	0.9338D 02
-0.2151D	02	+I	-0.9338D 02
-0.2964D	03	+I	0.2964D 02
-0.2964D	03	+I	-0.2964D 02
-0.1452D	02	+I	0.3011D 02
-0.1452D	02	+I	-0.3011D 02
-0.3352D	03	+I	0.9670D 00
-0.3352D	03	+I	-0.9670D 00
-0.3418D	03	+I	0.1465D 01
-0.3418D	03	+I	-0.1465D 01
-0.3399D	03	+I	0.0
-0.3394D	03	+I	0.0
-0.3397D	03	+I	0.0
-0.1577D	00	+I	0.2943D 01

-0.1577D 00	+I	-0.2948D 01
0.1259D 00	+I	0.0
0.2854D-01	+I	0.1169D 00
0.2854D-01	+I	-0.1169D 00
-0.9183D-01	+I	0.5921D-01
-0.9183D-01	+I	-0.5921D-01
-0.3395D 03	+I	0.0
-0.2605D 03	+I	0.6517D 01
-0.2605D 03	+I	-0.6517D 01
-0.2518D 03	+I	0.0
-0.2539D 03	+I	0.0
-0.2550D 03	+I	0.0
-0.2542D 03	+I	0.0
-0.2546D 03	+I	0.0
-0.2547D 03	+I	0.0
-0.1633D 03	+I	0.0
-0.1653D 03	+I	0.1348D 01
-0.1658D 03	+I	-0.1348D 01
-0.1710D 03	+I	0.0
-0.1701D 03	+I	0.0
-0.1694D 03	+I	0.0
-0.1699D 03	+I	0.0
-0.1698D 03	+I	0.0
-0.1698D 03	+I	0.0
-0.8674D 02	+I	0.0
-0.8621D 02	+I	0.0
-0.8463D 02	+I	0.0
-0.8495D 02	+I	0.7274D-01
-0.8495D 02	+I	-0.7274D-01
-0.8495D 02	+I	0.0
-0.8489D 02	+I	0.0
-0.8438D 02	+I	0.0
-0.8488D 02	+I	0.0

DYNAMIC PRESSURE - 1.000

IERR = 0

0.0	+I	0.0
-0.1935D 02	+I	0.8040D 03
-0.1933D 02	+I	-0.8040D 03
-0.1657D 01	+I	0.7558D 03
-0.1657D 01	+I	-0.7558D 03
-0.7156D 01	+I	0.5271D 03
-0.7156D 01	+I	-0.5271D 03
-0.2723D 01	+I	0.3177D 03
-0.2723D 01	+I	-0.3177D 03
-0.1135D 01	+I	0.2167D 03
-0.1135D 01	+I	-0.2167D 03
-0.4865D 01	+I	0.1902D 03
-0.4865D 01	+I	-0.1902D 03
-0.2411D 02	+I	0.1190D 03
-0.2411D 02	+I	-0.1190D 03
-0.2949D 03	+I	0.5809D 02
-0.2949D 03	+I	-0.5809D 02
-0.3440D 03	+I	0.2725D 01
-0.3440D 03	+I	-0.2725D 01
-0.3305D 03	+I	0.2388D 01
-0.3305D 03	+I	-0.2388D 01
-0.3402D 03	+I	0.0
-0.3393D 03	+I	0.0

-0.3398D 03	+1	0.0
-0.3396D 03	+1	0.0
-0.2663D 03	+1	0.1280D 02
-0.2663D 03	+1	-0.1280D 02
-0.1039D 02	+1	0.2526D 02
-0.1039D 02	+1	-0.2526D 02
-0.3080D 00	+1	0.4143D 01
-0.3080D 00	+1	-0.4143D 01
0.2301D 00	+1	0.1754D 00
0.2301D 00	+1	-0.1754D 00
-0.9776D-01	+1	0.2596D 00
-0.9776D-01	+1	-0.2596D 00
-0.2675D 00	+1	0.0
-0.2489D 03	+1	0.0
-0.2554D 03	+1	0.0
-0.2531D 03	+1	0.0
-0.2538D 03	+1	0.0
-0.2546D 03	+1	0.0
-0.2547D 03	+1	0.0
-0.1572D 03	+1	0.0
-0.1630D 03	+1	0.24[illegible]D 01
-0.1630D 03	+1	-0.24[illegible]D 01
-0.1723D 03	+1	0.0
-0.1705D 03	+1	0.0
-0.1691D 03	+1	0.0
0.1701D 03	+1	0.0
-0.1699D 03	+1	0.0
-0.1698D 03	+1	0.0
-0.8703D 02	+1	0.16[illegible]D 01
-0.8703D 02	+1	-0.16[illegible]D 01
-0.8433D 02	+1	0.0
-0.8502D 02	+1	0.14[illegible]D 00
-0.8502D 02	+1	-0.14[illegible]D 00
-0.8501D 02	+1	0.0
-0.8489D 02	+1	0.0
-0.8488D 02	+1	0.0
-0.8488D 02	+1	0.0

DYNAMIC PRESSURE = 1.500

IERR = 0

0.0	+1	0.0
-0.2889D 02	+1	0.8049D 03
-0.2389D 02	+1	-0.8049D 03
-0.[illegible]325D 01	+1	0.7[illegible]D 03
-0.2825D 01	+1	-0.7[illegible]D 03
-0.1079D 02	+1	0.5258D 03
-0.1079D 02	+1	-0.5258D 03
-0.3991D 01	+1	0.3188D 03
-0.3991D 01	+1	-0.3188D 03
-0.1530D 01	+1	0.2158D 03
-0.1530D 01	+1	-0.2158D 03
-0.9779D 01	+1	0.1859D 03
-0.9779D 01	+1	-0.1859D 03
-0.2267D 02	+1	0.1383D 03
-0.2267D 02	+1	-0.1383D 03
-0.2929D 03	+1	0.7582D 02
-0.2929D 03	+1	-0.7582D 02
-0.3461D 03	+1	0.3813D 01
-0.3461D 03	+1	-0.3813D 01

```
-0.3256D 03 +1      0.4693D 01
-0.3256D 03 +1     -0.4693D 01
-0.3406D 03 +1      0.0
-0.3392D 03 +1      0.0
-0.3399D 03 +1      0.0
-0.3395D 03 +1      0.0
-0.2720D 03 +1      0.1961D 02
-0.2720D 03 +1     -0.1961D 02
-0.8758D 01 +1      0.2238D 02
-0.8758D 01 +1     -0.2238D 02
-0.4509D 00 +1      0.5045D 01
-0.4509D 00 +1     -0.5045D 01
-0.2436D 00 +1      0.1303D 00
-0.2436D 00 +1     -0.1303D 00
 0.9564D-01 +1      0.2786D 00
 0.9564D-01 +1     -0.2786D 00
 0.2892D 03 +1      0.0
-0.2458D 03 +1      0.0
-0.2525D 03 +1      0.0
-0.2557D 03 +1      0.0
-0.2534D 03 +1      0.0
-0.2546D 03 +1      0.0
-0.2547D 03 +1      0.0
-0.1514D 03 +1      0.0
-0.1608D 03 +1      0.3[illegible]1D 01
-0.1608D 03 +1     -0.3[illegible]1D 01
-0.1733D 03 +1      0.0
-0.1768D 03 +1      0.0
-0.1688D 03 +1      0.0
-0.1702D 03 +1      0.0
-0.1699D 03 +1      0.0
-0.1698D 03 +1      0.0
-0.8727D 02 +1      0.2741D 01
-0.8727D 02 +1     -0.2741D 01
-0.8413D 02 +1      0.0
-0.8509D 02 +1      0.2312D 00
-0.8509D 02 +1     -0.2312D 00
-0.8507D 02 +1      0.0
-0.8489D 02 +1      0.0
-0.8480D 02 +1      0.0
-0.8480D 02 +1      0.0


DYNAMIC PRESSURE        2.000

ITER =       0
   0.0          +1      0.0
-0.3833D 02 +1      0.1[illegible]D 03
-0.3833D 02 +1     -0.1[illegible]D 03
-0.3329D 01 +1      0.7346D 03
-0.3329D 01 +1     -0.7346D 03
-0.1447D 02 +1      0.3244D 03
-0.1447D 02 +1     -0.3244D 03
-0.3204D 01 +1      0.3147D 03
-0.3204D 01 +1     -0.3147D 03
-0.1337D 01 +1      0.2150D 03
-0.1337D 01 +1     -0.2150D 03
-0.1928D 02 +1      0.1339D 03
-0.1928D 02 +1     -0.1339D 03
-0.1606D 02 +1      0.1515D 03
-0.1606D 02 +1     -0.1515D 03
```

-0.29060D 03	+1	0.39[illegible]0D 02
-0.29060D 03	+1	-0.89[illegible]0D 02
-0.34810D 03	+1	0.47570D 01
-0.34810D 03	+1	-0.47570D 01
-0.32120D 03	+1	0.81790D 01
-0.32120D 03	+1	-0.81790D 01
-0.34090D 03	+1	0.0
-0.33910D 03	+1	0.0
-0.34010D 03	+1	0.0
-0.33950D 03	+1	0.0
-0.27710D 03	+1	0.27320D 02
-0.27710D 03	+1	-0.27320D 02
-0.79920D 01	+1	0.21380D 02
-0.79920D 01	+1	-0.21380D 02
-0.[illegible]58[illegible] 00	+1	0.57410D 01
-0.58580D 00	+1	-0.57410D 01
-0.21090D 00	+1	0.0
-0.65560D-01	+1	0.1[illegible]780 00
-0.65560D-01	+1	-0.1[illegible]780 00
0.16490D 00	+1	0.12650D 00
0.16490D 00	+1	-0.12650D 00
-0.[illegible] 01	+1	0.0
[illegible]	+1	0.0
[illegible]	+1	0.0
[illegible]	+1	0.0
[illegible]	+1	0.0
-0.[illegible]470	+1	0.0
-0.14[illegible]	+1	0.0
-0.1[illegible]	+1	0.[illegible] 01
-0.15[illegible]	+1	-0.[illegible] 01
-0.17[illegible]	+1	0.0
-0.1711[illegible]	+1	0.0
-0.16[illegible]	+1	0.0
-0.17640	+1	0.0
-0.1700[illegible]	+1	0.0
-0.16[illegible]	+1	0.0
-0.[illegible]870	+1	0.[illegible]170 01
-0.[illegible]7[illegible]	+1	-0.[illegible]170 01
-0.13[illegible]	+1	0.0
-0.[illegible]170 0[illegible]	+1	0.[illegible]1730 00
-0.[illegible]170	+1	-0.[illegible]1730 00
-0.[illegible]120	+1	0.0
-0.14930 0[illegible]	+1	0.0
-0.[illegible]30[illegible]	+1	0.0
-0.[illegible]4[illegible]7[illegible]	+1	0.0

0.	0.	00000001
0.	0.	00000002
0.	0.	00000003
0.	0.	00000004
0.	0.	00000005
0.	0.	00000006
0.	0.	00000007
0.	0.	00000008
0.	0.	00000009
1.25673E+04	0.	00000010
2.40172E+05	0.	00000011
2.22548E+03	0.	00000012
-3.29855E+03	0.	00000013
-2.67916E+03	0.	00000014
3.16667E+02	0.	00000015
-1.75990E+03	0.	00000016
-6.04537E+02	0.	00000017
-2.85253E+03	0.	00000018
6.11493E+01	0.	00000019
1.71304E+03	0.	00000020
1.27689E+01	0.	00000021
-2.12503E+01	0.	00000022
-1.82420E+01	0.	00000023
1.04465E-01	0.	00000024
-2.96416E+00	0.	00000025
1.82873E+00	0.	00000026
-1.01416E+01	0.	00000027
3.38162E+02	0.	00000028
1.01850E+04	0.	00000029
1.18412E+02	0.	00000030
-1.18650E+02	0.	00000031
-1.04061E+02	0.	00000032
-5.83382E+00	0.	00000033
4.16126E+00	0.	00000034
-8.16986E+00	0.	00000035
-5.01833E+01	0.	00000036
3.77306E+02	0.	00000037
1.15655E+04	0.	00000038
1.33068E+02	0.	00000039
-1.30853E+02	0.	00000040
-1.14719E+01	0.	00000041
-6.09245E+00	0.	00000042
3.41597E+00	0.	00000043
-9.07521E+00	0.	00000044
-5.85824E+01	0.	00000045
2.79968E+02	0.	00000046
6.09712E+03	0.	00000047
7.44970E+01	0.	00000048
-9.11365E+01	0.	00000049
-7.55899E+01	0.	00000050
9.86292E+00	0.	00000051
-1.81633E+01	0.	00000052
-1.38655E+01	0.	00000053
-2.27128E+01	0.	00000054
4.81521E+02	0.	00000055
6.18082E+03	0.	00000056
6.24811E+01	0.	00000057
-1.61281E+02	0.	00000058
-1.25764E+02	0.	00000059
4.75291E+01	0.	00000060
-9.18169E+01	0.	00000061

-3.27440E+01	0.	00000062
-7.24327E+00	0.	00000063
-1.19392E+02	0.	00000064
2.75914E+03	0.	00000065
1.03221E+00	0.	00000066
2.37031E+01	0.	00000067
1.50023E+01	0.	00000068
-1.26968E+01	0.	00000069
4.24687E+01	0.	00000070
2.70750E+01	0.	00000071
-6.73426E+01	0.	00000072
5.03199E+01	0.	00000073
-4.71463E+03	0.	00000074
-1.47155E+01	0.	00000075
-3.44207E+00	0.	00000076
-4.29138E-02	0.	00000077
2.54182E+00	0.	00000078
-3.30968E+01	0.	00000079
-1.77131E+01	0.	00000080
8.03334E+01	0.	00000081
2.63719E+02	0.	00000082
1.23292E+04	0.	00000083
1.62183E+02	0.	00000084
1.98475E+01	0.	00000085
3.35788E+01	0.	00000086
-6.37048E+00	0.	00000087
4.24908E+01	0.	00000088
4.08835E+01	0.	00000089
-7.09232E+01	0.	00000090
-3.07403E+01	0.	00000091
-6.31179E+02	0.	00000092
-5.43123E+00	0.	00000093
4.60744E+01	0.	00000094
4.77191E+01	0.	00000095
1.50689E+01	0.	00000096
1.71941E+01	0.	00000097
2.20651E+00	0.	00000098
2.83767E+00	0.	00000099
1.23673E+04	0.	00000100
2.40172E+03	0.	00000101
3.22548E+03	0.	00000102
-3.29855E+03	0.	00000103
-2.67916E+03	0.	00000104
3.16667E+02	0.	00000105
-1.75990E+03	0.	00000106
-6.64537E+02	0.	00000107
-2.85253E+03	0.	00000108
2.31633E+00	4.52369E+01	00000109
-1.25961E+02	9.23531E+02	00000110
9.00244E-01	7.86518E+00	00000111
-1.42943E+00	-1.16712E+01	00000112
-1.28145E+00	-9.45433E+00	00000113
-2.49837E-01	1.23382E+00	00000114
-6.06737E-01	-6.24322E+00	00000115
3.59557E-01	-2.30999E+00	00000116
2.80370E+00	-1.14212E+01	00000117
1.23952E+04	1.03640E+03	00000118
2.56327E+03	1.30600E+05	00000119
2.14645E+03	-1.51710E+01	00000120
-3.19305E+03	9.28345E+01	00000121
-2.58729E+03	1.19067E+02	00000122

3.28419E+02	1.48411E+02	00000123
-1.70935E+03	1.29760E+02	00000124
-6.39081E+02	-3.20751E+02	00000125
-3.19405E+03	-2.59102E+03	00000126
5.96511E+01	1.57746E+00	00000127
1.73026E+03	1.31803E+02	00000128
1.84191E+01	1.92677E+00	00000129
-2.07907E+01	-8.11569E-01	00000130
-1.78681E+01	-7.34590E-01	00000131
9.29222E-02	-1.49001E-01	00000132
-2.08643E+00	1.20913E+00	00000133
-1.85970E+00	1.80783E-01	00000134
-1.06316E+01	2.28776E-01	00000135
3.23878E+02	-3.95297E+01	00000136
1.00583E+04	-1.02718E+03	00000137
1.15790E+02	-4.83335E+00	00000138
-1.14404E+02	1.44415E+01	00000139
-1.00520E+02	1.28005E+01	00000140
-5.89249E+00	6.38277E-01	00000141
6.80372E+00	9.41191E+00	00000142
-7.82512E+00	2.54835E+00	00000143
-4.93579E+01	1.56419E+01	00000144
3.01682E+02	-4.06398E+01	00000145
1.14274E+04	-1.05487E+03	00000146
1.30203E+02	-4.74748E+00	00000147
-1.26218E+02	1.56400E+01	00000148
-1.10860E+02	1.34397E+01	00000149
-6.16130E+00	8.41300E-01	00000150
1.12910E+01	9.67590E+00	00000151
-8.22445E+00	2.76051E+00	00000152
-5.76997E+01	1.02845E+01	00000153
2.70842E+02	-1.96112E+01	00000154
6.16696E+03	1.77200E+01	00000155
7.24710E+01	-3.33181E+00	00000156
-8.80177E+01	8.18925E+00	00000157
-7.29052E+01	7.71530E+00	00000158
9.90640E+00	2.51027E+00	00000159
-1.2375[illegible]E+01	5.98200E+00	00000160
-1.3966[illegible]E+01	-2.52048E-01	00000161
-2.50619E+01	-9.31637E-01	00000162
4.60312E+02	-4.52730E+01	00000163
6.40614E+03	2.56740E+02	00000164
7.60738E+01	-6.42421E+00	00000165
-1.55078E+02	1.60304E+01	00000166
-1.20969E+02	1.45145E+01	00000167
4.79158E+01	5.35900E+00	00000168
-8.26294E+01	1.06538E+01	00000169
-3.34207E+01	-1.09230E+00	00000170
-1.42645E+01	-6.01433E+00	00000171
-1.19000E+02	-9.84367E-01	00000172
2.36427E+03	-1.81601E+03	00000173
2.02069E+00	3.77365E+00	00000174
2.24573E+01	-3.77467E+00	00000175
1.39083E+01	-3.72486E+00	00000176
-1.30582E+01	-2.63045E+00	00000177
4.19773E+01	-2.76094E+00	00000178
2.79418E+01	5.93810E+00	00000179
-5.97217E+01	2.88841E+01	00000180
5.19132E+01	-1.13332E+01	00000181
-4.30017E+03	-1.352[illegible]E+01	00000182
-1.52447E+01	-2.8430[illegible]E+00	00000183

-2.91444E+00	3.07179E+00	00000184
5.00407E-01	2.61394E+00	00000185
2.86470E+00	8.24081E-01	00000186
-3.80495E+01	4.75360E+00	00000187
-1.85099E+01	-2.61294E+00	00000188
7.36528E+01	1.79646E+00	00000189
2.52092E+02	-2.48718E+01	00000190
1.21141E+04	-1.07584E+03	00000191
1.60183E+02	-4.95333E+00	00000192
2.31821E+01	8.72722E+00	00000193
3.63341E+01	7.91076E+00	00000194
-6.63754E+00	1.81225E-01	00000195
4.43055E+01	7.05926E-01	00000196
4.14575E+01	2.16331E+00	00000197
-7.44546E+01	1.32136E+01	00000198
-2.95678E+01	2.01963E+00	00000199
-6.19310E+02	5.31873E+01	00000200
-5.25675E+00	-7.58298E-01	00000201
4.57925E+01	-2.46240E-01	00000202
4.74923E+01	-6.70406E-02	00000203
1.50681E+01	3.90476E-01	00000204
1.09403E+01	-1.57303E+00	00000205
2.15994E+00	-9.03108E-01	00000206
2.07693E+00	-1.48244E+00	00000207
1.18861E+04	-2.25293E+03	00000208
2.25466E+05	-7.95256E+04	00000209
2.09688E+03	-4.70153E+02	00000210
-3.10397E+03	6.75868E+02	00000211
-2.51656E+03	5.71803E+02	00000212
3.11534E+02	-1.10103E+01	00000213
-1.05682E+03	3.04053E+02	00000214
-5.76094E+02	1.19710E+02	00000215
-2.67259E+03	1.01805E+03	00000216
5.79512E+00	8.73500E+01	00000217
-4.32599E+02	2.02546E+03	00000218
2.63813E+00	1.45082E+01	00000219
-4.32109E+00	-2.16540E+01	00000220
-3.93257E+00	-1.74291E+01	00000221
-9.41428E-01	2.58301E+00	00000222
-2.51762E+00	-1.17177E+01	00000223
1.29636E+00	-5.02239E+00	00000224
9.30443E+00	-2.09535E+01	00000225
1.22519E+01	2.41072E+03	00000226
2.95525E+03	2.85193E+05	00000227
1.99761E+03	8.14159E+01	00000228
-3.01739E+03	2.39554E+01	00000229
-2.43133E+03	9.34920E+01	00000230
3.56725E+02	2.85380E+02	00000231
-1.64735E+03	1.78318E+02	00000232
-7.26957E+02	-6.09298E+02	00000233
-4.01744E+03	-4.31229E+03	00000234
5.71945E+01	5.06987E+00	00000235
1.74664E+03	2.23556E+02	00000236
1.78512E+01	4.31999E+00	00000237
-2.01409E+01	-2.31010E+00	00000238
-1.73617E+01	-2.03939E+00	00000239
3.73224E-02	-3.23930E-01	00000240
-2.28082E+00	2.01648E+00	00000241
-1.89195E+00	4.37826E-01	00000242
-1.12601E+01	1.38527E+00	00000243
2.98214E+02	-6.00580E+01	00000244

9.49789E+03	-2.03084E+03	00000245
1.11682E+02	-8.94149E+00	00000246
-1.07429E+02	2.30671E+01	00000247
-9.47336E+01	2.07647E+01	00000248
-6.16213E+00	1.34692E+00	00000249
1.12563E+01	1.52336E+01	00000250
-6.40676E+00	4.92810E+00	00000251
-4.20268E+01	3.27176E+01	00000252
3.33808E+02	-6.04134E+01	00000253
1.00110E+04	-2.08202E+03	00000254
1.25754E+02	-5.42190E+00	00000255
-1.18674E+02	2.37222E+01	00000256
-1.04621E+02	2.15629E+01	00000257
-6.55139E+00	1.72591E+00	00000258
1.60658E+01	1.54079E+01	00000259
-7.13999E+00	5.33415E+00	00000260
-4.90634E+01	3.41023E+01	00000261
2.54892E+02	-2.68330E+01	00000262
6.21700E+03	-1.09362E+02	00000263
6.90317E+01	-3.79888E+00	00000264
-8.27118E+01	1.20326E+01	00000265
-6.84949E+01	1.17668E+01	00000266
9.92404E+00	4.90630E+00	00000267
-1.34160E+01	9.45995E+00	00000268
-1.40063E+01	-2.52630E-01	00000269
-2.80854E+01	2.18411E+00	00000270
4.38094E+02	-7.11109E+01	00000271
7.05675E+03	3.70631E+01	00000272
7.15989E+01	-1.15684E+01	00000273
-1.45355E+02	2.45086E+01	00000274
-1.120[illegible]2E+02	2.24541E+01	00000275
4.89146E+01	9.02602E+00	00000276
-8.26862E+01	2.79993E+01	00000277
-3.49060E+01	-2.31733E+00	00000278
-2.82740E+01	-8.61122E-01	00000279
-1.18865E+02	-3.75741E+00	00000280
1.31517E+03	-2.82634E+03	00000281
4.47423E+00	6.13100E+00	00000282
1.95315E+01	-5.61629E+00	00000283
1.11750E+01	-5.76985E+00	00000284
-1.39733E+01	-4.91157E+00	00000285
4.10162E+01	-4.09573E+00	00000286
3.02361E+01	1.09884E+01	00000287
-3.94579E+01	4.92277E+01	00000288
5.56121E+01	-2.38279E+01	00000289
-3.34413E+03	-3.49600E+02	00000290
-1.67565E+01	-4.98060E+00	00000291
-1.38517E+00	5.33413E+00	00000292
2.04909E+00	4.44597E+00	00000293
3.73590E+00	1.35622E+00	00000294
-3.78430E+01	5.36289E+00	00000295
-2.07517E+01	-4.46561E+00	00000296
5.46190E+01	9.92505E+00	00000297
2.34657E+02	-3.22211E+01	00000298
1.13192E+04	-1.90397E+03	00000299
1.57540E+02	-7.06757E+00	00000300
2.77543E+01	1.26517E+01	00000301
4.60912E+01	1.19016E+01	00000302
-7.41458E+00	7.46512E-01	00000303
4.61106E+01	-1.65779E+00	00000304
4.32485E+01	3.51109E+00	00000305

-6.31378E+01	2.58464E+01	00000306
-2.69356E+01	2.76534E+00	00000307
-5.08025E+02	1.24332E+02	00000308
-4.98247E+00	-1.78040E+00	00000309
4.52874E+01	-1.12203E-01	00000310
4.71032E+01	1.86087E-01	00000311
1.50829E+01	8.17164E-01	00000312
1.63389E+01	-2.86396E+00	00000313
1.97525E+00	-1.86219E+00	00000314
1.89335E+00	-3.25767E+02	00000315
1.95671E+04	-3.70435E+03	00000316
[illegible]75E+03	-1.45515E+03	00000317
[illegible]30E+03	-7.64877E+02	00000318
[illegible]505E+03	1.11900E+03	00000319
-2.22153E+03	9.47943E+02	00000320
2.988[illegible]5E+02	-1.57282E+01	00000321
-1.47321E+03	4.80422E+02	00000322
-4.98859E+02	2.12431E+02	00000323
-2.09374E+03	1.89161E+03	00000324
1.12987E+01	1.70263E+02	00000325
-9.27682E+02	3.06463E+03	00000326
5.74918E+00	2.51343E+01	00000327
-1.07483E+01	-3.86077E+01	00000328
-1.00037E+01	-3.06577E+01	00000329
-3.02499E+00	6.18151E+00	00000330
-7.09452E+00	-2.12505E+01	00000331
3.48125E+00	-1.23140E+01	00000332
1.91220E+01	-7.53522E+01	00000333
1.26689E+04	4.93490E+03	00000334
4.05682E+05	4.75494E+05	00000335
1.77341E+03	4.43542E+02	00000336
-2.60827E+03	-2.80837E+02	00000337
-2.23695E+03	-1.02681E+02	00000338
4.33862E+02	4.91107E+02	00000339
-1.59366E+03	2.47703E+02	00000340
-9.72484E+02	-1.01312E+03	00000341
-6.19689E+03	-7.69447E+03	00000342
5.30344E+01	1.47975E+01	00000343
1.66084E+03	3.82075E+02	00000344
1.69635E+01	9.62140E+00	00000345
-1.95821E+01	-6.09267E+00	00000346
-1.70708E+01	-5.31636E+00	00000347
-3.27876E-01	-6.55697E-01	00000348
-1.90895E+00	3.05730E+00	00000349
-1.70536E+00	9.57542E-01	00000350
-1.05370E+01	4.40366E+00	00000351
2.57816E+02	-6.58529E+01	00000352
7.61861E+03	-2.65782E+03	00000353
1.06335E+02	-3.52615E+00	00000354
-9.72916E+01	3.22266E+01	00000355
-8.62896E+01	3.01966E+01	00000356
-6.93875E+00	3.38397E+00	00000357
1.74247E+01	2.16804E+01	00000358
-2.28251E+00	6.34211E+00	00000359
-1.35312E+01	4.06505E+01	00000360
2.90743E+02	-6.20264E+01	00000361
6.77861E+03	-2.60632E+03	00000362
1.20302E+02	-1.85617E+00	00000363
-1.07688E+02	3.24525E+01	00000364
-9.56936E+01	3.09302E+01	00000365
-7.65001E+00	4.81101E+00	00000366

C - 3

2.24113E+01	2.13335E+01	00000367
-2.81396E+00	6.73807E+00	00000368
-1.90664E+01	4.72613E+01	00000369
2.29623E+02	-2.21698E+01	00000370
5.99266E+03	-3.09840E+02	00000371
6.41981E+01	-6.26657E-01	00000372
-7.48260E+01	1.39814E+01	00000373
-6.18900E+01	1.48993E+01	00000374
9.86229E+00	9.66591E+00	00000375
-9.29216E+00	1.28067E+01	00000376
-1.33686E+01	-3.87683E-01	00000377
-2.78210E+01	1.15342E+01	00000378
3.81507E+02	-8.66387E+01	00000379
7.30822E+03	-1.06142E+03	00000380
6.05182E+01	-6.38738E+00	00000381
-1.28320E+02	2.74569E+01	00000382
-9.75942E+01	2.63553E+01	00000383
5.01239E+01	1.73319E+01	00000384
-7.16015E+01	4.36249E+01	00000385
-3.58463E+01	-5.91957E-01	00000386
-3.86657E+01	3.59913E+01	00000387
-1.21447E+02	-2.39549E+00	00000388
-1.40752E+03	-3.02667E+03	00000389
8.67326E+00	7.22380E+00	00000390
1.45906E+01	-5.58772E+00	00000391
6.41473E+00	-5.99690E+00	00000392
-1.63026E+01	-7.47354E+00	00000393
3.88892E+01	-7.71559E+00	00000394
3.59215E+01	1.06661E+01	00000395
1.10832E+01	5.01692E+01	00000396
6.52737E+01	-5.97653E+01	00000397
-5.16377E+02	-3.05674E+03	00000398
-1.98322E+01	-6.79203E+00	00000399
1.72466E+00	7.57063E+00	00000400
5.30128E+00	5.65407E+00	00000401
6.08533E+00	6.34766E-01	00000402
-3.70011E+01	1.04255E+01	00000403
-2.67995E+01	-3.59862E+00	00000404
3.26110E+00	6.34234E+01	00000405
2.20917E+02	-3.41041E+01	00000406
1.00455E+04	-1.86713E+03	00000407
1.54363E+02	-9.74959E+00	00000408
3.26977E+01	1.77921E+01	00000409
4.47122E+01	1.78363E+01	00000410
-6.16526E+00	3.68561E+00	00000411
4.48796E+01	-6.03370E+00	00000412
4.50271E+01	2.31609E+00	00000413
-4.40635E+01	2.36126E+01	00000414
-2.15428E+01	-2.19905E+00	00000415
-2.01161E+02	6.21563E+01	00000416
-4.79933E+00	-4.[illegible]156E+00	00000417
4.47203E+01	1.13263E+00	00000418
4.67844E+01	1.42571E+00	00000419
1.53799E+01	1.54894E+00	00000420
1.51630E+01	-4.38225E+00	00000421
7.86285E-01	-3.27364E+00	00000422
-4.00277E+00	-3.32970E+00	00000423
7.74854E+03	-4.80009E+03	00000424
6.67447E+04	-2.04798E+05	00000425
1.38096E+03	-1.14264E+03	00000426
-2.02407E+03	1.55535E+03	00000427

-1.61114E+03	1.33102E+03	00000428
2.70578E+02	1.09113E+01	00000429
-1.14150E+03	5.78497E+02	00000430
-2.87119E+02	2.50851E+02	00000431
-3.59510E+02	2.53825E+03	00000432
2.49329E+01	2.52759E+02	00000433
-5.27920E+01	8.68915E+03	00000434
7.14037E+00	3.38054E+01	00000435
-1.69238E+01	-5.17097E+01	00000436
-1.57979E+01	-4.01709E+01	00000437
-5.11734E+00	1.06747E+01	00000438
-1.38969E+01	-2.96802E+01	00000439
3.39545E+00	-2.12924E+01	00000440
1.26831E+00	-1.35434E+02	00000441
1.30329E+04	6.52065E+03	00000442
4.77136E+05	5.60240E+05	00000443
1.60325E+03	8.70991E+02	00000444
-2.69905E+03	-6.23102E+03	00000445
-2.13999E+03	-3.60321E+02	00000446
4.69349E+02	6.29211E+02	00000447
-1.58441E+03	3.75061E+02	00000448
-1.16150E+03	-1.19680E+03	00000449
-7.60818E+03	-8.58027E+03	00000450
4.94429E+01	2.47347E+01	00000451
1.49915E+03	5.62180E+02	00000452
1.62145E+01	1.50048E+01	00000453
-1.97907E+01	-9.81371E+00	00000454
-1.75279E+01	-3.49724E+00	00000455
-8.78226E-01	-6.76329E-01	00000456
-1.93831E+00	4.19068E+00	00000457
-1.44316E+00	1.42005E+00	00000458
-8.32375E+00	7.32068E+00	00000459
2.33127E+02	-6.00699E+01	00000460
6.34816E+03	-2.28982E+03	00000461
1.03786E+02	2.52208E-01	00000462
-9.00805E+01	3.92007E+01	00000463
-6.04515E+01	3.78620E+01	00000464
-6.47439E+00	6.31035E+00	00000465
2.22203E+01	2.72335E+01	00000466
2.85621E-01	5.86763E+00	00000467
7.37786E+00	4.43183E+01	00000468
2.64513E+02	-5.24039E+01	00000469
7.45318E+03	-2.10637E+03	00000470
1.17209E+02	3.07702E+00	00000471
-1.00823E+02	3.90001E+01	00000472
-8.95292E+01	3.85309E+01	00000473
-7.50568E+00	8.42595E+00	00000474
2.71771E+01	2.64423E+01	00000475
2.72052E-01	6.17902E+00	00000476
2.40256E+00	4.37725E+01	00000477
2.11274E+02	-1.11203E+01	00000478
5.50583E+03	-5.77926E+02	00000479
6.16695E+01	4.06073E+00	00000480
-7.01977E+01	1.[illegible]7585E+01	00000481
-5.80660E+01	1.55735E+01	00000482
9.01364E+00	1.44849E+01	00000483
-7.60228E+00	1.54436E+01	00000484
-1.24347E+01	-4.47188E-01	00000485
-2.20956E+01	2.13333E+01	00000486
3.39841E+02	-7.67368E+01	00000487
6.20496E+03	-2.34568E+03	00000488

6.50457E+01	-9.70539E-01	00000489
-1.19980E+02	2.43792E+01	00000490
-9.06524E+01	2.52806E+01	00000491
5.08659E+01	2.53309E+01	00000492
-6.47714E+01	5.64200E+01	00000493
-3.40981E+01	6.12174E-01	00000494
-2.20976E+01	6.94993E+01	00000495
-1.16983E+02	1.25248E+00	00000496
-2.75205E+03	-1.65778E+03	00000497
1.11713E+01	6.34729E+00	00000498
1.19732E+01	-2.90964E+00	00000499
3.99973E+00	-3.72710E+00	00000500
-1.73529E+01	-8.79882E+00	00000501
3.78884E+01	-9.75580E+00	00000502
3.83032E+01	1.75121E+01	00000503
3.71759E+01	2.30569E+01	00000504
6.45439E+01	-9.37724E+01	00000505
1.03794E+03	-7.47721E+03	00000506
-2.16700E+01	-6.76157E+00	00000507
3.27823E+00	7.59384E+00	00000508
6.84458E+00	4.63248E+00	00000509
7.25719E+00	-1.42678E+00	00000510
-3.65048E+01	1.46434E+01	00000511
-2.98031E+01	1.12948E+00	00000512
-2.55435E+01	1.47602E+02	00000513
2.04878E+02	-3.48439E+01	00000514
9.21066E+03	-1.83091E+03	00000515
1.51063E+02	-1.21109E+01	00000516
3.88661E+01	2.17581E+01	00000517
5.03166E+01	2.24476E+01	00000518
-7.94123E+00	6.12378E+00	00000519
4.38256E+01	-1.00577E+01	00000520
4.52423E+01	2.14365E+00	00000521
-3.14498E+01	1.99315E+01	00000522
-2.21555E+01	-6.63069E+00	00000523
-1.63647E+02	-2.86905E+02	00000524
-5.09016E+00	-6.71707E+00	00000525
4.49864E+01	1.98620E+00	00000526
4.70921E+01	2.24930E+00	00000527
1.53861E+01	2.04095E+00	00000528
1.42629E+01	-6.14701E+00	00000529
1.32339E-01	-3.89491E+00	00000530
-4.62990E+00	9.44808E-01	00000531
5.47667E+03	-4.60029E+03	00000532
-2.87870E+04	-1.90248E+03	00000533
9.42828E+02	-1.29512E+03	00000534
-1.41542E+03	1.68236E+03	00000535
-1.08786E+03	1.45342E+03	00000536
2.82637E+02	5.56191E+01	00000537
-9.16147E+02	5.46279E+02	00000538
-1.36231E+02	1.60463E+02	00000539
1.00689E+03	2.03267E+03	00000540
4.94165E+01	3.20654E+02	00000541
2.47890E+03	1.11269E+04	00000542
6.73864E+00	4.19369E+01	00000543
-2.30357E+01	-6.32670E+01	00000544
-2.14025E+01	-4.86368E+01	00000545
-6.85627E+00	1.47231E+01	00000546
-2.29376E+01	-3.56317E+01	00000547
3.53932E-01	-2.81574E+01	00000548
-4.93921E+01	-1.73461E+02	00000549

1.24920E+04	7.65925E+03	00000550
4.44320E+05	6.00314E+05	00000551
1.47828E+03	1.31786E+03	00000552
-2.61383E+03	-9.39308E+02	00000553
-2.09478E+03	-6.03106E+02	00000554
4.21993E+02	7.33344E+02	00000555
-1.49830E+03	5.34053E+02	00000556
-1.13728E+03	-1.27845E+03	00000557
-7.06800E+03	-8.64785E+03	00000558
4.50823E+01	3.53364E+01	00000559
1.23595E+03	8.00316E+02	00000560
1.53171E+01	2.02720E+01	00000561
-2.02188E+01	-1.33380E+01	00000562
-1.82632E+01	-1.14419E+01	00000563
-1.65047E+00	-9.67528E-01	00000564
-2.15269E+00	5.23729E+00	00000565
-1.00886E+00	1.75013E+00	00000566
-4.54338E+00	9.00311E+00	00000567
2.19785E+02	-4.82210E+01	00000568
5.60815E+03	-1.51808E+03	00000569
1.02448E+02	4.35381E+03	00000570
-8.56215E+01	4.47944E+01	00000571
-7.56405E+01	4.42984E+01	00000572
-5.28190E+00	9.39761E+00	00000573
2.57535E+01	3.17261E+01	00000574
1.68731E+00	4.59945E+00	00000575
1.95402E+01	3.52524E+01	00000576
2.49684E+02	-3.57950E+01	00000577
6.67068E+03	-1.22314E+03	00000578
1.15564E+02	8.37789E+00	00000579
-9.53302E+01	4.40511E+01	00000580
-8.44318E+01	4.47925E+01	00000581
-6.76002E+00	1.19981E+01	00000582
3.04661E+01	3.04749E+01	00000583
1.88727E+00	4.85328E+00	00000584
1.47827E+01	3.41087E+01	00000585
1.96650E+02	3.68834E+00	00000586
4.91771E+03	-5.93035E+02	00000587
6.05068E+01	8.89522E+00	00000588
-6.71997E+01	1.17069E+01	00000589
-5.56789E+01	1.63297E+01	00000590
8.09428E+00	1.94968E+01	00000591
-5.72057E+00	1.78754E+01	00000592
-1.09426E+01	-9.45210E-01	00000593
-1.15428E+01	2.80873E+01	00000594
3.09727E+02	-5.79146E+01	00000595
4.62222E+03	-3.49115E+03	00000596
5.35050E+01	6.06064E+00	00000597
-1.16018E+02	2.21770E+01	00000598
-8.73644E+01	2.52271E+01	00000599
5.18666E+01	3.38228E+01	00000600
-5.86227E+01	6.88324E+01	00000601
-3.11917E+01	[illegible].48027E-01	00000602
6.31598E+00	8.93951E+01	00000603
-1.07396E+02	4.31050E+00	00000604
-2.75569E+03	-1.78068E+01	00000605
1.18358E+01	5.30661E+00	00000606
1.12793E+01	-9.50701E-01	00000607
3.55891E+00	-2.04094E+00	00000608
-1.72754E+01	-1.01889E+01	00000609
3.70646E+01	-1.23654E+01	00000610

3.76450E+01	1.85937E+01	00000611
3.83026E+01	-1.45726E+01	00000612
5.90415E+01	-1.33677E+02	00000613
1.33850E+03	-1.16801E+04	00000614
-2.19870E+01	-6.64717E+00	00000615
3.11691E+00	7.80153E+00	00000616
6.62169E+00	3.90499E+00	00000617
7.30742E+00	-3.13100E+00	00000618
-3.65744E+01	1.90210E+01	00000619
-2.98626E+01	5.66148E+00	00000620
-3.14581E+01	2.32205E+02	00000621
1.96409E+02	-3.11251E+01	00000622
8.74001E+03	-1.45470E+03	00000623
1.47446E+02	-1.26058E+01	00000624
4.32719E+01	2.31058E+01	00000625
5.40341E+01	2.46208E+01	00000626
-7.31756E+00	8.82183E+00	00000627
4.02668E+01	-1.24019E+01	00000628
4.43570E+01	1.92028E+00	00000629
-2.54527E+01	1.23716E+01	00000630
-2.12908E+01	-1.10389E+01	00000631
-1.78910E+02	-5.14362E+02	00000632
-5.49650E+00	-8.79628E+00	00000633
4.48153E+01	2.63264E+00	00000634
4.70131E+01	2.90000E+00	00000635
1.54050E+01	2.54247E+00	00000636
1.27534E+01	-6.99289E+00	00000637
-6.65240E-01	-4.57674E+00	00000638
-3.92118E+00	3.83376E+00	00000639
5.88647E+03	-3.84950E+03	00000640
-8.16433E+04	-1.44363E+05	00000641
5.55431E+02	-1.32749E+03	00000642
-9.30799E+02	1.64855E+03	00000643
-6.59460E+02	1.43639E+03	00000644
3.29700E+02	8.75259E+01	00000645
-7.88893E+02	4.81788E+02	00000646
-7.60711E+01	2.35492E+01	00000647
1.63526E+03	1.08329E+03	00000648
7.12727E+01	5.61403E+02	00000649
5.29374E+03	1.09930E+04	00000650
4.78537E+00	5.01773E+01	00000651
-2.84951E+01	-7.25041E+01	00000652
-2.60410E+01	-5.56464E+01	00000653
-9.27171E+00	1.75242E+01	00000654
-3.30724E+01	-3.79011E+01	00000655
-2.94009E+00	-3.01489E+01	00000656
-1.07147E+02	-1.63232E+02	00000657
1.10247E+04	9.12995E+03	00000658
3.12806E+05	6.73420E+05	00000659
1.37069E+03	1.76690E+03	00000660
-2.52088E+03	-1.26521E+03	00000661
-2.00998E+03	-8.42439E+02	00000662
3.00061E+02	8.70841E+02	00000663
-1.34138E+03	6.60384E+02	00000664
-9.21987E+02	-1.41820E+03	00000665
-4.69612E+03	-9.33920E+03	00000666
4.01677E+01	4.08415E+01	00000667
9.15965E+02	1.12806E+03	00000668
1.41606E+01	2.55965E+01	00000669
-2.08676E+01	-1.67317E+01	00000670
-1.92655E+01	-1.42127E+01	00000671

-2.65157E+00	-8.73761E-01	00000672
-2.66537E+00	6.40329E+00	00000673
-5.48767E-01	1.92366E+03	00000674
9.93850E-03	9.12744E+00	00000675
2.15177E+02	-3.62469E+01	00000676
5.32122E+03	-6.91934E+02	00000677
1.02537E+02	6.85463E+00	00000678
-8.22176E+01	5.01196E+01	00000679
-7.20477E+01	5.04003E+01	00000680
-3.31719E+00	1.25636E+01	00000681
2.91587E+01	3.64797E+01	00000682
2.19176E+00	3.52[illegible]E+00	00000683
2.52038E+01	2.55238E+01	00000684
2.43205E+02	-2.11770E+01	00000685
6.31521E+03	-3.21896E+02	00000686
1.15393E+02	1.41321E+01	00000687
-9.15994E+01	4.36032E+01	00000688
-8.00651 +01	5.02954E+01	00000689
-5.37376E+00	1.52784E+01	00000690
3.35511E+01	3.49193E+01	00000691
2.68526E+00	3.33560E+00	00000692
2.11760E+01	2.43591E+01	00000693
1.64315E+02	2.01334E+01	00000694
4.13593E+03	-3.97012E+02	00000695
6.02966E+01	1.36[illegible]E+01	00000696
-6.51777E+01	1.39[illegible]E+01	00000697
-5.41332E+01	1.73545E+01	00000698
7.00878E+00	2.47217E+01	00000699
-4.60677E+00	2.06932E+01	00000700
-9.07064E+00	-1.72453E+00	00000701
2.40577E+00	5.10[illegible]E+01	00000702
2.66[illegible]E+0[illegible]	-3.51156E+01	00000703
[illegible].93735E+03	-5.34796E+02	00000704
5.34144E+01	1.20386E+01	00000705
-1.13543E+02	2.08642E+01	00000706
-8.51277E+01	2.60416E+01	00000707
5.35586E+01	4.25010E+01	00000708
-5.25867E+01	8.07327E+01	00000709
-2.80227E+01	-1.29716E+00	00000710
3.794[illegible]E+01	9.6[illegible]E+01	00000711
-9.24731E+01	5.00[illegible]E+00	00000712
-1.75786E+03	1.29[illegible]E+03	00000713
1.17532E+01	4.9[illegible]511E+00	00000714
1.00950E+01	2.10694E-01	00000715
3.55277E+00	-1.2[illegible]E+00	00000716
-1.60630E+01	-1.20139E+01	00000717
3.563[illegible]E+01	-1.[illegible]E+01	00000718
3.43220E+01	2.[illegible]E+01	00000719
2.06084E+01	-4.32031E+01	00000720
5.09783E+01	-1.63633E+02	00000721
8.86962E+02	-1.57746E+04	00000722
-2.15727E+01	-6.99771E+00	00000723
2.31139E+00	6.78636E+00	00000724
5.73916E+00	4.05477E+00	00000725
7.08559E+00	-4.14320E+00	00000726
-3.63180E+01	2.36621E+01	00000727
-2.815[illegible]E+01	9.10812E+00	00000728
-2.32632E+01	3.37257E+02	00000729
1.91904E+02	-2.66154E+01	00000730
8.53061E+03	-1.04713E+03	00000731
1.45551E+0[illegible]	-1.27934E+01	00000732

4.65464E+01	2.52190E+01	00000733
5.81626E+01	2.73705E+01	00000734
-6.07128E+00	1.09360E+01	00000735
3.83563E+01	-1.37552E+01	00000736
4.37105E+01	2.59377E+00	00000737
-2.29333E+01	3.26407E+00	00000738
-2.19204E+01	-1.50807E+01	00000739
-2.56324E+02	-6.08515E+02	00000740
-5.47396E+00	-1.11108E+01	00000741
4.47239E+01	3.97093E+00	00000742
4.70091E+01	4.19689E+00	00000743
1.56773E+01	3.57132E+00	00000744
1.23672E+01	-7.64471E+00	00000745
-1.15845E+00	-4.94334E+00	00000746
-1.70657E+00	4.14490E+00	00000747
2.84337E+03	-2.97918E+03	00000748
-9.76083E+04	-9.51713E+04	00000749
2.22907E+02	-1.27748E+03	00000750
-5.54013E+02	1.33412E+03	00000751
-3.18129E+02	1.33913E+03	00000752
3.96007E+02	8.71751E+01	00000753
-7.20367E+02	4.29750E+02	00000754
-8.98971E+01	-1.02552E+02	00000755
1.64299E+03	1.04233E+02	00000756
6.91322E+01	3.76374E+02	00000757
6.27297E+03	3.36947E+03	00000758
1.59962E+03	5.89591E+01	00000759
-3.22297E+01	-7.98271E+01	00000760
-3.10837E+01	-6.13170E+01	00000761
-1.37777E+01	1.31299E+01	00000762
-4.20831E+01	-3.03277E+01	00000763
-2.13953E+00	-2.74095E+01	00000764
-1.32062E+02	-1.02964E+02	00000765
9.14611E+03	1.13636E+04	00000766
1.34324E+03	8.24352E+03	00000767
1.27225E+03	2.21332E+03	00000768
-2.43098E+03	-1.61413E+03	00000769
-2.06124E+03	-1.07897E+03	00000770
1.45440E+02	1.06811E+03	00000771
-1.14378E+03	7.26847E+02	00000772
-6.15056E+02	-1.76382E+03	00000773
-1.45902E+03	-1.14751E+04	00000774
3.53327E+01	5.92843E+01	00000775
3.79978E+02	1.55244E+03	00000776
1.27931E+01	3.39624E+01	00000777
-2.16173E+01	-1.79394E+01	00000778
-2.64113E+01	-1.67211E+01	00000779
-3.54937E+00	-6.27125E-01	00000780
-3.04747E+00	7.57723E+00	00000781
-6.39760E-02	1.92901E+00	00000782
4.57106E+00	7.51486E+00	00000783
2.16206E+01	-2.62201E+01	00000784
5.33967E+01	7.94516E+01	00000785
1.03758E+02	1.29645E+01	00000786
-7.93357E+01	5.55276E+01	00000787
-6.87151E+01	5.64563E+01	00000788
-9.52717E-01	1.47661E+01	00000789
3.20761E+01	4.06394E+01	00000790
2.34078E+00	2.50192E+00	00000791
2.64872E+01	1.64351E+01	00000792
2.41773E+02	-7.37105E+00	00000793

6.21984E+03	5.27503E+02	00000794
1.16391E+02	1.96076E+01	00000795
-8.83783E+01	5.36421E+01	00000796
-7.72250E+01	5.68729E+01	00000797
-3.74886E+00	1.81664E+01	00000798
3.66966E+01	3.87801E+01	00000799
3.28792E+00	2.03734E+00	00000800
2.40388E+01	1.53337E+01	00000801
1.72832E+02	3.83353E+01	00000802
3.24445E+03	6.48166E+01	00000803
6.06947E+01	1.81979E+01	00000804
-6.33192E+01	1.03319E+01	00000805
-5.27694E+01	1.86374E+01	00000806
5.88169E+00	3.01457E+01	00000807
-3.40426E+00	2.33491E+01	00000808
-6.78225E+00	-3.08525E+00	00000809
1.89901E+01	2.90370E+01	00000810
2.72131E+02	-6.84770E+00	00000811
1.25283E+03	-2.50077E+03	00000812
5.42511E+01	1.74799E+01	00000813
-1.11810E+02	2.00742E+01	00000814
-8.33424E+01	2.73092E+01	00000815
5.59939E+01	5.11449E+01	00000816
-4.59316E+01	9.19959E+01	00000817
-2.48665E+01	-4.17217E+00	00000818
7.08910E+01	8.94599E+01	00000819
-7.22622E+01	6.13985E-01	00000820
-1.44406E+01	1.96735E+03	00000821
1.14195E+01	5.05927E+00	00000822
1.01478E+01	1.03001E+00	00000823
3.33285E+00	-8.92102E-01	00000824
-1.57692E+01	-1.43029E+01	00000825
3.33343E+01	-1.79386E+01	00000826
2.92917E+01	2.36033E+01	00000827
-1.05121E+01	-5.96513E+01	00000828
4.08765E+01	-1.87773E+02	00000829
-8.60791E+00	-1.38955E+04	00000830
-2.08687E+01	-7.80096E+00	00000831
1.71653E+00	1.02566E+01	00000832
5.03977E+00	4.83827E+00	00000833
6.93156E+00	-4.50429E+00	00000834
-3.53061E+01	2.84728E+01	00000835
-2.53368E+01	1.09469E+01	00000836
-6.65941E+00	3.67888E+02	00000837
1.88339E+02	-2.44130E+01	00000838
8.46946E+03	-8.06081E+02	00000839
1.43300E+02	-1.34162E+01	00000840
5.04218E+01	2.63566E+01	00000841
6.22293E+0[illegible]	2.90781E+01	00000842
-5.02066E+00	1.28751E+01	00000843
3.54353E+01	-1.54108E+01	00000844
4.29722E+01	3.01705E+00	00000845
-2.38175E+01	-2.64297E+00	00000846
-2.25291E+01	-1.92042E+01	00000847
-2.63632E+02	-8.24124E+02	00000848
-6.05594E+00	-1.38919E+01	00000849
4.54449E+01	4.99439E+00	00000850
4.77535E+01	5.16193E+00	00000851
1.57751E+01	4.16357E+00	00000852
1.14578E+01	-9.11115E+00	00000853
-1.52262E+00	-5.58310E+00	00000854

-1.98130E+00	4.29659E+03	00000855
2.16764E+03	-2.18495E+03	00000856
-8.96786E+04	-5.69539E+04	00000857
-5.68063E+01	-1.16572E+03	00000858
-2.66006E+02	1.37493E+03	00000859
-5.36926E+01	1.19049E+03	00000860
4.62034E+02	5.16023E+01	00000861
-6.84720E+02	3.93477E+02	00000862
-1.49571E+02	-1.94405E+02	00000863
1.27377E+03	-4.34640E+02	00000864
2.65374E+01	3.85307E+02	00000865
3.78621E+03	4.91968E+03	00000866
-2.60421E+00	6.82179E+01	00000867
-3.33329E+01	-8.62398E+01	00000868
-3.42982E+01	-6.62091E+01	00000869
-2.13527E+01	2.14955E+01	00000870
-4.81766E+01	-3.23782E+01	00000871
6.00963E+00	-2.34901E+01	00000872
-9.55942E+01	-3.13758E+01	00000873
7.46353E+03	1.44085E+04	00000874
-3.14651E+04	1.05130E+06	00000875
1.17307E+03	2.65561E+02	00000876
-2.36665E+03	-1.99003E+03	00000877
-2.07256E+03	-1.31836E+03	00000878
2.76229E+00	1.32128E+03	00000879
-9.62166E+02	7.13103E+02	00000880
-3.40041E+02	-2.13545E+03	00000881
1.53879E+03	-1.50425E+04	00000882
2.98192E+01	7.27603E+01	00000883
2.51675E+02	2.07267E+03	00000884
1.11481E+01	3.64187E+01	00000885
-2.24313E+01	-2.29932E+01	00000886
-2.16569E+01	-1.90747E+01	00000887
-4.61412E+00	-1.91592E-01	00000888
-3.70812E+00	8.78884E+00	00000889
3.45378E-01	1.75410E+00	00000890
8.68489E+00	4.25561E+00	00000891
2.21198E+02	-1.75331E+01	00000892
5.58869E+03	8.27170E+02	00000893
1.05735E+02	1.67713E+01	00000894
-7.70228E+01	6.07517E+01	00000895
-6.37267E+01	6.22190E+01	00000896
1.82374E+00	1.66113E+01	00000897
3.61657E+01	4.34978E+01	00000898
2.02619E+00	1.54228E+00	00000899
2.45635E+01	7.34201E+00	00000900
2.43776E+02	5.62448E+00	00000901
6.30091E+03	1.38824E+03	00000902
1.18154E+02	2.47802E+01	00000903
-8.57429E+01	5.62485E+01	00000904
-7.41630E+01	6.21451E+01	00000905
-1.85291E+00	2.06622E+01	00000906
3.97499E+01	4.24212E+01	00000907
3.56337E+00	1.81674E+00	00000908
2.46443E+01	5.74142E+00	00000909
1.62394E+02	5.96903E+01	00000910
2.33842E+03	9.23224E+02	00000911
6.14946E+01	2.25164E+01	00000912
-6.15920E+01	9.66595E+00	00000913
-5.14862E+01	1.99303E+01	00000914
4.64663E+00	3.58692E+01	00000915

-2.15981E+00	2.57583E+01	00000916
-4.34476E+03	-6.28006E+00	00000917
3.62929E+01	1.94811E+01	00000918
2.82049E+02	2.20658E+01	00000919
-1.12957E+02	-8.36011E+02	00000920
8.57925E+01	2.21578E+01	00000921
-1.10300E+02	1.94396E+01	00000922
-6.15072E+01	2.88967E+01	00000923
5.91415E+01	5.96337E+01	00000924
-3.88837E+01	1.01603E+02	00000925
-2.21150E+01	-8.67327E+00	00000926
9.87013E+01	6.66310E+01	00000927
-4.92985E+01	-1.22934E+01	00000928
2.11144E+03	1.67536E+03	00000929
1.10437E+01	5.48678E+00	00000930
8.95430E+00	2.09145E+00	00000931
2.74944E+00	-5.66825E-01	00000932
-1.48209E+01	-1.73300E+01	00000933
3.04171E+01	-1.96262E+01	00000934
2.31292E+01	2.36615E+01	00000935
-4.80596E+01	-5.61206E+01	00000936
3.09196E+01	-2.32841E+02	00000937
-1.00159E+03	-2.10156E+04	00000938
-2.01657E+01	-9.19458E+00	00000939
1.51311E+00	1.15578E+01	00000940
4.75539E+00	5.70192E+00	00000941
7.05304E+00	-4.23759E+00	00000942
-3.38165E+01	3.21476E+01	00000943
-2.20804E+01	1.06624E+01	00000944
1.15753E+01	4.09676E+02	00000945
1.86396E+02	-2.14063E+01	00000946
6.48035E+03	-3.77659E+02	00000947
1.41153E+02	-1.32991E+01	00000948
5.31921E+01	2.69638E+01	00000949
6.52804E+01	3.31773E+01	00000950
-3.60213E+00	1.45747E+01	00000951
3.28140E+01	-1.56678E+01	00000952
4.19743E+01	4.08355E+00	00000953
-2.57249E+01	-8.04415E+00	00000954
-2.37241E+01	-2.27920E+01	00000955
-3.13622E+02	-9.68238E+02	00000956
-7.02074E+03	-1.61391E+01	00000957
4.57445E+01	5.53931E+00	00000958
4.80819E+01	5.70366E+00	00000959
1.59399E+01	3.01385E+00	00000960
1.01086E+01	-9.65586E+00	00000961
-2.19704E+03	-6.14929E+03	00000962
-1.48603E+00	5.23575E+00	00000963
1.71398E+03	-1.54257E+03	00000964
-6.97636E+04	-3.36950E+04	00000965
-2.78779E+02	-1.00903E+03	00000966
-5.17016E+01	1.19543E+03	00000967
1.42122E+02	1.01660E+03	00000968
5.12561E+02	-1.53472E+01	00000969
-6.56990E+02	3.89107E+02	00000970
-2.29194E+02	-2.43581E+02	00000971
7.51703E+02	-7.14859E+02	00000972
-5.66290E+01	4.14107E+02	00000973
-2.25403E+03	3.19999E+03	00000974
-7.47950E+00	7.34787E+01	00000975
-3.18526E+01	-9.35356E+01	00000976

-3.62830E+01	-7.11350E+01	00000977
-3.17170E+01	2.60122E+01	00000978
-5.08481E+01	-2.83938E+01	00000979
2.18484E+01	-2.38960E+01	00000980
6.24488E+00	1.22039E+01	00000981
6.41832E+03	1.78189E+04	00000982
-1.42089E+05	1.32027E+06	00000983
1.07267E+03	3.09810E+03	00000984
-2.36121E+03	-2.3868[illegible]E+03	00000985
-2.11473E+03	-1.84657E+03	00000986
-1.00138E+02	1.59924E+03	00000987
-8.30476E+02	6.52882E+02	00000988
-1.77032E+02	-2.63516E+03	00000989
3.81019E+03	-1.93942E+04	00000990
2.80499E+01	8.72697E+01	00000991
-2.50411E+01	2.08895E+03	00000992
9.29977E+00	4.20544E+01	00000993
-2.33783E+01	-2.59320E+01	00000994
-2.30490E+01	-2.12197E+01	00000995
-5.69409E+00	4.12713E-01	00000996
-4.47178E+00	1.00708E+01	00000997
6.39500E-01	1.43898E+00	00000998
1.15867E+01	-5.32000E-01	00000999
2.30223E+02	-1.09132E+01	00001000
6.12325E+03	1.49794E+03	00001001
1.06543E+02	2.00957E+01	00001002
-7.50809E+01	6.61178E+01	00001003
-6.29067E+01	6.79815E+01	00001004
4.93868E+03	1.79771E+01	00001005
3.97595E+01	4.77571E+01	00001006
1.31722E+00	6.73442E-01	00001007
1.82347E+01	-9.48339E-01	00001008
2.49542E+02	1.75780E+01	00001009
6.03837E+03	2.24403E+03	00001010
1.23803E+02	2.95143E+01	00001011
-4.34959E+01	6.29804E+01	00001012
-7.13094E+01	6.77509E+01	00001013
2.71242E-01	2.31275E+01	00001014
4.28612E+01	4.54971E+01	00001015
3.56747E+00	7.13537E-01	00001016
2.14137E+01	-4.26316E+00	00001017
1.55028E+02	8.40915E+01	00001018
1.65499E+03	2.22665E+03	00001019
6.27254E+01	2.66159E+01	00001020
-6.00181E+01	6.90062E+00	00001021
-5.02618E+01	2.12498E+01	00001022
3.49099E+03	4.19081E+01	00001023
-1.02504E+03	2.76340E+01	00001024
-2.16754E+00	-3.40906E+00	00001025
4.98704E+01	1.45284E+00	00001026
2.61409E+02	5.72501E+01	00001027
-6.84371E+02	1.54264E+03	00001028
5.77011E+01	2.61836E+01	00001029
-1.09322E+02	1.85628E+01	00001030
-7.98114E+01	3.32230E+01	00001031
6.32069E+01	6.79281E+01	00001032
-3.22530E+01	1.05574E+02	00001033
-2.09300E+01	-1.47023E+01	00001034
1.12273E+02	2.97452E+01	00001035
-2.86223E+01	-3.54752E+01	00001036
4.06049E+03	2.77081E+02	00001037

1.07140E+01	6.09931E+00	00001038
7.71789E+00	3.79296E+00	00001039
2.03813E+00	6.36008E-02	00001040
-1.41438E+01	-2.10022E+01	00001041
2.75607E+01	-2.00908E+01	00001042
1.69746E+01	3.66240E+01	00001043
-8.38763E+01	-3.61648E+01	00001044
2.84592E+01	-2.07773E+02	00001045
-1.61238E+03	-2.20427E+04	00001046
-1.96404E+01	-1.07164E+01	00001047
1.32101E+00	1.22148E+01	00001048
4.64246E+00	6.22493E+00	00001049
7.70893E+00	-3.35037E+00	00001050
-3.24687E+01	3.46512E+01	00001051
-1.93707E+01	8.07820E+00	00001052
2.23922E+01	4.31113E+02	00001053
1.85510E+02	-2.02268E+01	00001054
8.57380E+03	-4.73721E+02	00001055
1.39592E+02	-1.33536E+01	00001056
5.59955E+01	2.77771E+01	00001057
6.83936E+01	3.13805E+01	00001058
-2.27501E+00	1.5[illegible]153E+01	00001059
3.06310E+01	-1.61281E+01	00001060
4.13191E+01	5.22013E+00	00001061
-2.89414E+01	-1.12322E+01	00001062
-2.43029E+01	-2.65653E+01	00001063
-3.40688E+02	-1.14733E+02	00001064
-7.64015E+00	-1.83478E+01	00001065
4.59763E+01	6.61605E+00	00001066
4.63761E+01	6.74741E+00	00001067
1.63193E+01	5.76305E+00	00001068
9.53234E+00	-1.00603E+01	00001069
-2.79620E+00	-6.41149E+00	00001070
-1.20358E+00	5.81335E+00	00001071
1.36774E+03	-1.06077E+03	00001072
-4.77622E+04	-2.45082E+04	00001073
-4.43572E+02	-8.22451E+02	00001074
1.02206E+02	1.01037E+03	00001075
2.77593E+02	8.31702E+02	00001076
5.36164E+02	-1.03832E+02	00001077
-6.[illegible]336[illegible]E+02	4.05776E+02	00001078
-3.08694E+02	-2.53067E+02	00001079
2.59638E+02	-6.89741E+02	00001080
-2.55123E+02	6.08068E+02	00001081
-1.66258E+04	1.19735E+04	00001082
-1.76933E+01	1.01650E+02	00001083
-2.69096E+01	-1.15196E+02	00001084
-3.90776E+01	-6.34149E+01	00001085
-5.35836E+01	4.67158E+01	00001086
-5.22489E+01	-2.77599E+01	00001087
5.74614E+01	-5.03717E+01	00001088
2.56337E+02	-1.19137E+02	00001089
6.23428E+03	2.37257E+04	00001090
-1.89076E+05	1.79172E+05	00001091
8.56829E+02	3.96753E+03	00001092
-2.43766E+03	-3.01937E+03	00001093
-2.26374E+03	-1.92222E+03	00001094
-1.99373E+02	2.09453E+03	00001095
-7.54515E+02	5.60409E+02	00001096
-1.89843E+02	-3.45944E+03	00001097
4.19151E+03	-2.69436E+04	00001098

1.84343E+01	1.17080E+02	00001099
-2.86373E+02	4.06301E+03	00001100
5.18937E+00	5.37550E+01	00001101
-2.86426E+01	-3.13113E+01	00001102
-2.60610E+01	-2.48867E+01	00001103
-7.73432E+00	2.07903E+00	00001104
-6.49725E+00	1.28860E+01	00001105
5.20881E-01	2.67770E-01	00001106
1.09080E+01	-1.23532E+01	00001107
2.56546E+02	-8.43692E+00	00001108
7.86796E+03	2.08565E+03	00001109
1.15420E+02	2.47322E+01	00001110
-7.17068E+01	7.68645E+01	00001111
-5.73271E+01	7.68807E+01	00001112
1.18940E+01	1.90150E+01	00001113
4.62669E+01	5.30018E+01	00001114
-1.47932E+00	1.32352E-01	00001115
-5.28630E+00	-6.00822E+00	00001116
2.70843E+02	3.36951E+01	00001117
6.10349E+03	3.48045E+03	00001118
1.27519E+02	3.76368E+01	00001119
-7.90588E+01	7.23215E+01	00001120
-6.57778E+01	7.63665E+01	00001121
5.18932E+00	2.60769E+01	00001122
4.81799E+01	5.04511E+01	00001123
2.05941E+00	-1.00225E+00	00001124
2.07027E+00	-1.77172E+01	00001125
1.58486E+02	1.39208E+02	00001126
1.95863E+03	5.53655E+03	00001127
6.61663E+01	3.39237E+01	00001128
-5.78472E+01	7.12360E+00	00001129
-4.81540E+01	3.38093E+01	00001130
2.25420E+00	5.45509E+01	00001131
-3.82344E-01	3.05294E+01	00001132
-9.66598E-01	-1.45312E+01	00001133
4.71651E+01	-4.03933E+01	00001134
2.98964E+02	1.19609E+02	00001135
1.88876E+03	6.20787E+03	00001136
6.24928E+01	3.20760E+01	00001137
-1.09667E+02	1.76367E+01	00001138
-7.71508E+01	3.30568E+01	00001139
7.46420E+01	[illegible].21528E+01	00001140
-2.20921E+01	1.22263E+02	00001141
-2.60510E+01	-2.68709E+01	00001142
7.17316E+01	-4.62990E+01	00001143
-1.73957E+01	-1.01897E+02	00001144
5.17571E+03	-4.79501E+03	00001145
9.94430E+00	7.74530E+00	00001146
7.02236E+00	6.62547E+00	00001147
1.28223E+00	2.09377E+00	00001148
-1.53717E+01	-2.96863E+01	00001149
2.45056E+01	-1.84372E+01	00001150
9.86414E+00	5.75267E+01	00001151
-1.00474E+02	4.76505E+01	00001152
4.80533E+01	-1.97356E+02	00001153
3.66598E+02	-2.18361E+04	00001154
-1.87057E+01	-1.40512E+01	00001155
-8.96219E-01	1.20673E+01	00001156
3.77048E+00	6.41620E+00	00001157
1.19368E+01	-5.21426E-01	00001158
-3.24479E+01	3.09731E+01	00001159

-2.00008E+01	-2.25666E+00	00001160
-1.86737E+01	4.32298E+02	00001161
1.82608E+02	-1.99507E+01	00001162
8.64828E+03	-5.14285E+02	00001163
1.38880E+02	-1.33976E+01	00001164
6.06991E+01	2.79440E+01	00001165
7.36369E+01	3.21006E+01	00001166
3.19871E-01	1.80969E+01	00001167
2.61332E+01	-1.56302E+01	00001168
4.00368E+01	8.14781E+00	00001169
-3.38388E+01	-1.30573E+01	00001170
-2.79373E+01	-3.50102E+01	00001171
-4.98251E+02	-1.52734E+03	00001172
-9.81429E+00	-2.34547E+01	00001173
4.75298E+01	8.05251E+00	00001174
4.99817E+01	8.06053E+00	00001175
1.70262E+01	7.12968E+00	00001176
7.69977E+00	-1.15040E+01	00001177
-3.52989E+00	-7.24064E+00	00001178
-5.88069E-02	7.64321E+00	00001179
7.48160E+02	-4.42960E+02	00001180
-2.03112E+04	-2.97030E+04	00001181
-6.00046E+02	-4.15001E+02	00001182
2.70604E+02	[illegible].56510E+02	00001183
3.99539E+02	4.74330E+02	00001184
4.84452E+02	-2.95986E+02	00001185
-5.04720E+02	4.62664E+02	00001186
-4.17184E+02	-1.97196E+02	00001187
-[illegible]1747E+02	-1.30477E+02	00001188
-3.05720E+02	[illegible].12347E+02	00001189
-1.72893E+04	3.09173E+04	00001190
-2.65591E+01	1.26613E+02	00001191
-3.12770E+01	-1.41346E+02	00001192
-4.21193E+01	-4.64539E+01	00001193
-6.30706E+01	7.67104E+01	00001194
-6.35634E+01	-3.27340E+01	00001195
6.33002E+01	-9.92909E+01	00001196
2.50643E+02	-4.33332E+02	00001197
6.23081E+03	2.67869E+04	00001198
-2.12671E+05	2.02222E+06	00001199
6.11471E+02	4.82533E+03	00001200
-2.52065E 03	-3.43649E+03	00001201
-2.41202E+03	-2.14081E+03	00001202
-3.22063E+02	2.42234E+03	00001203
-7.51502E+02	6.69375E+02	00001204
-2.04734E+02	-3.76318E+03	00001205
4.31971E+03	-3.01045E+04	00001206
1.58468E+01	1.45538E+02	00001207
-2.00792E+01	5.17675E+03	00001208
6.47378E-01	6.86020E+01	00001209
-2.79809E+01	-3.56562E+01	00001210
-2.92346E+01	-2.74164E+01	00001211
-9.45754E+00	3.99995E+00	00001212
-9.02087E+00	1.63840E+01	00001213
-3.93202E-01	3.20010E-01	00001214
1.12076E+00	-1.85636E+01	00001215
2.81794E+02	-2.26443E+01	00001216
9.43245E+03	1.32033E+03	00001217
1.22956E+02	2.68565E+01	00001218
-6.82065E+01	8.76471E+01	00001219
-5.15736E+01	8.66626E+01	00001220

1.86373E+01	1.78198E+01	00001221
5.24260E+01	5.70418E+01	00001222
-4.02383E+00	2.09149E+00	00001223
-2.46032E+01	1.08140E+01	00001224
2.96017E+02	3.36403E+01	00001225
9.90462E+03	3.42888E+03	00001226
1.35406E+02	4.20034E+01	00001227
-7.60599E+01	8.18951E+01	00001228
-6.02264E+01	8.34016E+01	00001229
1.02980E+01	2.82093E+01	00001230
5.26692E+01	5.46007E+01	00001231
-1.71136E-01	-5.50508E-01	00001232
-2.22615E+01	-1.03129E+01	00001233
1.86947E+02	1.76122E+02	00001234
4.74623E+03	7.43157E+03	00001235
7.05536E+01	3.96505E+01	00001236
-5.69052E+01	6.59174E+00	00001237
-4.03626E+01	2.69702E+01	00001238
2.71709E+00	6.60967E+01	00001239
-2.16529E+00	1.43282E+01	00001240
-4.73222E+00	-[illegible].22443E+01	00001241
-3.64105E-01	-7.37867E+01	00001242
3.65128E+02	1.31333E+02	00001243
7.51164E+03	[illegible].09670E+03	00001244
6.60278E+01	3.47436E+01	00001245
-1.1105[illegible]E+02	1.96827E+01	00001246
-7.45593E+01	3.65349E+01	00001247
8.82009E+01	9.06573E+01	00001248
-1.56744E+01	1.34060E+02	00001249
-3.78102E+01	-1.03400E+01	00001250
-2.57523E+01	-4.71003E+01	00001251
-5.74317E+01	-1.46031E+02	00001252
1.14043E+0[illegible]	-[illegible].26060E+03	00001253
9.17763E+00	1.03373E+01	00001254
9.69182E+00	1.21733E+01	00001255
1.96533E+00	3.65576E+00	00001256
-2.10252E+01	-3.64241E+01	00001257
2.64061E+01	-1.77482E+01	00001258
1.29237E+01	7.61741E+01	00001259
-2.21786E+01	1.30783E+02	00001260
1.23231E+02	-2.06191E+02	00001261
7.62523E+03	-2.20521E+04	00001262
-1.79931E+01	-1.60723E+01	00001263
-6.47167E+00	1.27437E+01	00001264
1.43601E+00	6.72206E+00	00001265
2.05865E+01	3.65213E-01	00001266
-3.73196E+01	3.96998E+01	00001267
-3.11759E+01	-1.37180E+01	00001268
-1.51682E+02	4.35624E+02	00001269
1.77757E+02	-2.05699E+01	00001270
8.50639E+03	-6.55158E+02	00001271
1.32259E+02	-1.31393E+01	00001272
6.44806E+01	2.76411E+01	00001273
7.78190E+01	3.21977E+01	00001274
2.57787E+00	1.97331E+01	00001275
2.26249E+01	-1.44928E+01	00001276
3.95950E+01	1.13589E+01	00001277
-3.49444E+01	-1.27658E+01	00001278
-3.26124E+01	-4.21447E+01	00001279
-7.19839E+02	-1.83430E+02	00001280
-1.25208E+01	-2.79250E+01	00001281

4.88483E+01	9.36452E+00	00001282
5.13241E+01	9.27680E+00	00001283
1.79840E+01	8.49698E+00	00001284
6.22028E+00	-1.23726E+01	00001285
-4.30558E+00	-7.91618E+00	00001286
1.75811E+00	8.62567E+00	00001287
1.64325E+02	-2.03412E+00	00001288
-1.86327E+04	-3.24478E+04	00001289
-3.53518E+02	-4.82927E+01	00001290
3.05780E+02	3.33150E+02	00001291
3.70684E+02	1.79619E+02	00001292
3.20044E+02	-4.31183E+02	00001293
-3.24646E+02	4.84637E+02	00001294
-4.47050E+02	-1.14784E+02	00001295
-1.47831E+01	3.46279E+02	00001296

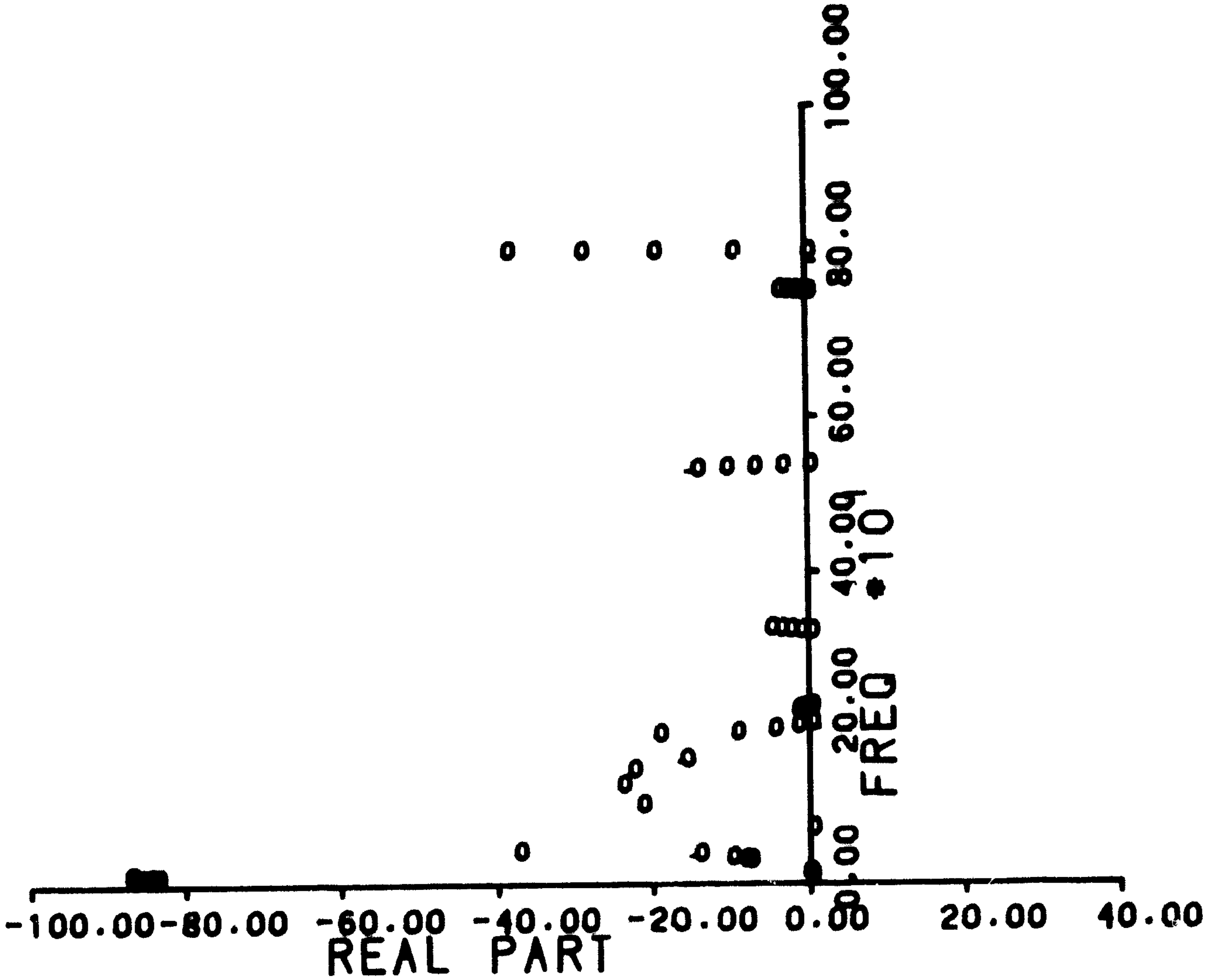
-100.00
-80.00
-60.00
-40.00
-20.00
0.00
20.00
40.00
REAL PART
0.00
20.00
40.00
60.00
80.00
100.00
FREQ *10

APPENDIX F

SOURCE LISTING AND INPUT/OUTPUT EXAMPLE FOR GUST OPTIMIZATION PROGRAM

The first part of the Appendix consists of the source listing of the program which is used for both gust optimization and gust sensitivity purposes. The operating instructions indicate which subroutines and which cards need be deleted or replaced.

The example chosen relates to the same DAST configuration (M=0.9) chosen for the flutter example with one active T.E. control surface, (using L.D.T.T.F.). Therefore, the aerodynamic data AERO (I,J,K) which resides on file 2) is not listed again in this Appendix. All the data required by the program appears in the output. The two PSD plots for the control surface deflection and for the control surface rate of deflection are supplemented by a tabulation of these plots. These appear in four tables as follows:

The first table shows XF(I)(=ω rad/sec), DEFLN(I)(=$\delta_{i,PSD}$) and PSD(I) (= the Von Karman gust spectrum).

The second table is similar to the first but shows DEFNR(I)(= $\delta_{i,PSD}$).

The third table shows DEFLN2(I)(=$\delta^2_{i,PSD}$)

The fourth table similarly shows DEFLNR2(I)(= $\delta^2_{i,PSD}$).

Note that all the control defections are given in degrees per unit gust velocity.

The last table summarizes the optimization iterations and is very important in studying the progress of the minimization process. The notation used is as follows:

PRECEDING PAGE BLANK NOT FILMED

ITERNS Iteration number.

FOPT. Value of the target function FUNCTN during the present iteration.

GMAX The absolute value of the maximum gradient component during the present iteration.

IGMAX The active control law variable number to which GMAX relates.

DELMAX The maximum absolute value of the optimum direction component during the present iteration.

IDMAX The active control law variable number to which DELMAX relates.

E(LOWEST) The step size to the minimum along the optimum direction.

The output also includes the initial values of the gradients G(I) (with respect to the control variables) and the final values of the gradients G(I) (after completing the minimization process) together with the optimum values for the control variables X(I) and the minimum value of the target function FUNCTN.

Note also that when a control variable resides on a constraint and its gradient leads to the violation of that constraint, the gradient is artificially changed to assume zero value.

Note that the plotted output shows labels which appear to be displaced. These displacements reflect transient difficulties encountered while using a new plotter and they do not originate from the programs used.

```
      IMPLICIT REAL*8(A-H,O-Z)
CCCCCCCCCCCCCCCCCCCCCCCCCCCCCCCCCCCCCCCCCCCCCCCCCCCCCCCCCCCCCCCCCCCCCCCC
C                                                                      C
C     GUST RESPONSE PACKAGE WHICH PERMITS THE COMPUTATION OF THE        C
C     SPECTRAL RESPONSE OF AIRCRAFT DUE TO CONTINUOUS GUST ENVIRONMENT.C
C     THE EFFECTS OF ACTIVE CONTROLS ON THE RESPONSE CAN BE ACCOUNTED  C
C     FOR. FURTHERMORE,THE BASIC GUST PROGRAM IS COUPLED IN THE        C
C     PRESENT PACKAGE WITH AN OPTIMIZATION ROUTINE WHICH ENABLES THE   C
C     DETERMINATION OF THE VARIOUS CONTROL GAINS SO AS TO MINIMIZE THE C
C     AIRCRAFT RESPONSE TO GUST.  SENSITIVITY STUDIES AROUND THE       C
C     GIVEN (OR OPTIMAL ) CONTROL GAINS CAN ALSO BE MADE. THE          C
C     FOLLOWING DATA IS REQUIRED:---                                   C
C                                                                      C
C     HDR - HEADER (FORMAT 15A4)                                       C
C                                                                      C
C     NAMELIST/CASE -                                                  C
C     NM - NUMBER OF MODES(15 MAX)                                     C
C                                                                      C
C     NC  - NUMBER OF  CONTROLS(6 MAX)                                 C
C                                                                      C
C     NAER - 1 INPUT AERO IN TERMS OF INTERPOLATION COEFFICIENTS OF K  C
C          - 0 INPUT AERO FOR DIFFERENT VALUES OF K - INTRPOLATION     C
C     COEFFICIENTS TO BE COMPUTED IN SUBROUTINE FIT.                   C
C                                                                      C
C     B - ARRAY OF LAG TERMS USED DURING INTERPOLATION(4 MAX)          C
C                                                                      C
C     NG - 1 IF GUST AERO IS SUPPLIED                                  C
C        - 0 IF GUST AERO IS NOT SUPPLIED.                             C
C                                                                      C
C     NL - NUMBER OF LAG TERMS TO BE USED DURING INTERPOLATION.        C
C                                                                      C
C     IF  NAER=1  THEN AERO COEFFICIENTS ARE READ(FORMAT 6X,7E10.4)    C
C                                                                      C
```

```
C     NAMELIST/GST
C     RMASS - MASS MATRIX(15*15 MAX)
C
C     OMEGAN - NATURAL FREQUENCIES ARRAY(IN HZ) - (15 MAX)  -  NOTE-
C     STIFFNESS IS COMPUTED FROM MASS AND OMEGAN AND IS THEREFORE
C     CORRECT FOR DIAGONAL MASS MATRIX ONLY.
C
C     VEL - FLIGHT VELOCITY
C
C     UTRAN - ARRAY OF SEMICHORD LENGTHS OF WING(OR TAIL) SECTIONS
C     WHERE THE DIFFERENT CONTROLS ARE LOCATED(AT MID CONTROL SPAN
C     SECTIONS) - (6 MAX)
C
C     CTRAN - ARRAY OF DISTANCES BETWEEN THE TWO TRANSDUCERS AT EACH
C     CONTROL SURFACE MID SECTION(USED TO COMPUTE THE ANGLE OF
C     DEFORMATION) - (6 MAX).
C
C     CREF - REFERENCE SEMI CHORD LENGTH (NORMALLY WING ROOT SEMI
C     CHORD) - SHOULD BE CONSISTENT WITH THE REFERENCE LENGTH USED IN
C     COMPUTING THE REDUCED FREQUENCY K.
C
C     ZW - MATRIX WHERE ZW(I,J) INDICATES THE DISPLACEMENT(POSITIVE
C     DOWN) OF THE I-TH TRANSDUCER DUE TO THE J-TH MODE. FOR EACH
C     SECTION THERE ARE TWO TRANSDUCERS -- THE FORE TRANSDUCER SHOULD
C     BE LOCATED AHEAD OF THE AFT TRANSDUCER(AT 30 PERCENT CHORD FROM
C     L.E.). THESE SETS OF TRANSDUCERS SHOULD BE ARRANGED IN THE SAME
C     ORDER AS THE CONTROLS - (12 X 15 MAX).
C
C     ZREF - VALUES LIKE ZW OF REFERENCE TRANSDUCERS USED TO DETECT
C     THE RIGID BODY MOTION OF THE AIRCRAFT - (2 X 15 MAX).
C
C     Q - FLIGHT DYNAMIC PRESSURE
C
C     CLR - ARRAY OF X DISTANCES (POSITIVE AFT) BETWEEN THE FORE
C     REFERENCE TRANSDUCER AND THE FORE CONTROL TRANSDUCER - (6MAX)
C
C     CTR - DISTANCE BETWEEN THE TWO TRANSDUCERS AT THE REFERENCE
C     SECTION.
C
C     WR - REFERENCE FREQUENCY(RAD/SEC)-USED ONLY FOR THE D.T.T.F.
C     CONTROL LAWS --VALUE CHOSEN IS NORMALLY AROUND THE FLUTTER
C     FREQUENCY VALUE.
C
C     NTE - INTEGER ARRAY FOLLOWING THE ORDER OF THE CONTROLS AND
C     IDENTIFYING BETWEEN L.E. AND T.E. CONTROLS.
C            =1, T.E. CONTROL
C            =0, L.E. CONTROL
C     IT IS IMPORTANT TO NOTE  THAT WHENEVER A CONTROL IS NOT ACTIVE
C     PUT NTE=0
C
C     NCACT - NUMBER OF ACTIVE CONTROLS
C
C
C     IF  NAER=0  NEXT INPUTS ARE READ IN SUBROUTINE FIT.
C
C     ETA1,PHI - ETA1 - ACCURACY OF COMPUTER RELATIVE TO 1 (ON I.B.M.
C                  DOUBLE PRECISION=5.E-13). ABSOLUTE ACCURACY=X*ETA1.
C               - PHI - RELATIVE SIZE OF 'SUCTION ZONE' WITHIN WHICH
C                  THE OPTIMIZED PARAMETER IS SUCKED TO THE COSTRAINT
```

```
C              IN ORDER TO AVOID FALSE CONVERGENCE. ABSOLUTE SIZE
C              OF ZONE=X1(I)*PHI OR X2(I)*PHI DEPENDING WHETHER NEAR
C              LOWER OR UPPER CONSTRAINTS(FORMAT 4E10.0)
C
C     NV,NPR,NOR - NV - AN INPUT INTEGER(36 MAX) CONTAINING THE
C                  NUMBER OF INDEPENDENT CONTROL GAINS IN THE SYSTEM
C                - NPR - 0
C                - NOR - 0 OPTIMIZATION BASED ON MINIMIZATION OF RMS
C                          RESPONSE OF CONTROLS.
C                      - 1 OPTIMIZATION BASED ON MINIMIZATION OF RMS
C                          RESPONSE RATES OF CONTROLS.(FORMAT 5I5)
C
C     NONACT - NUMBER OF NON ACTIVE OPTIMIZATION PARAMETERS(FORMAT 5I5)
C
C     NA - INTEGER INPUT ARRAY CONTAINING THE LOCATION OF THE NON
C     ACTIVE PARAMETERS IN THE X ARRAY(SEE BELOW) - (FORMAT 5I5).
C     IF  NONACT=0, A BLANK CARD SHOULD BE PLACED HERE.
C
C     WL,WT - TWO WEIGHTS FOR EMPASIZING THE RMS CONTROL RESPONSE
C     (OR RATE) OF ANY DESIRED SPECIFIC CONTROL SURFACE. THIS IS USED
C     IN CONJUNCTION WITH THE DEFINITION OF THE TARGET FUNCTION
C     'FUNCTN' . (FORMAT 4E10.0).
C
C     X1(I),X(I),X2(I),EPS(I) - THERE ARE NV SUCH CARDS(FORMAT 4E10.0)
C           X1(I) - DENOTES THE LOWEST BOUND OF THE I - TH CONTROL
C                   GAIN PARAMETER.
C           X(I) - DENOTES THE INITIAL VALUE OF THE I - TH CONTROL
C                   GAIN PARAMETER.
C           X2(I) - DENOTES THE UPPER BOUND OF THE I - TH CONTROL
C                   GAIN PARAMETER.
C           EPS(I) - THE DESIRED ABSOLUTE ACCURACY OF THE OPTIMAL
C                    FINAL X(I) VALUE(IN CASE MINIMIZATION IS MADE).IN
C     CASE OF CONTROL GAIN SENSITIVITY STUDY EPS(I) DENOTES THE
C     INCREMENTAL VARIATION OF X(I) WITHIN THE REGION X1(I)--X2(I).
C     MAX. NUMBER OF INCREMENTS=34. MAX. SIZE OF ARRAYS=36.
C
C     FMIN,ETA - FMIN - INPUT PARAMETER CONTAINING AN APPROXIMATION
C                       TO THE MINIMUM RMS RESPONSE VALUE. IF UNKNOWN
C                       USE FMIN=0.
C                ETA - INPUT PARAMETER CONTAINING AN ESTIMATE OF THE
C                      RELATIVE ACCURACY OF THE RMS RESPONSE EVALUAT-
C                      IONS WHICH ARE USED TO DETERMINE THE TYPE OF
C                      DIFFERENCE APPROXIMATION TO THE GRADIENT.
C                      (FORMAT 4E10.0).
C
C     ITMAX,IW - ITMAX - AN INPUT/OUTPUT INTEGER. ON INPUT, ITMAX
C                        CONTAINS THE MAXIMUM ALLOWABLE NUMBER OF
C                        OPTIMIZATION ITERATIONS. ON OUTPUT, ITMAX
C                        CONTAINS THE NUMBER OF ITERATIONS USED.
C                IW - AN INPUT INTEGER CODE FOR PRINTING DURING
C                     COMPUTATION.
C                   - 0 NO PRINTING
C                   - 1 PRINT GRADIENT VECTOR,DIRECTION OF EACH LINEAR
C                     MINIMIZATION,AND FUNCTION VALUE BEFORE AND AFTER
C                     EACH LINEAR MINIMIZATION.
C                   - 2 IN ADDITION TO THE ABOVE,PRINT FUNCTION VALUES
C                     CALCULATED DURING THE COURSE OF LINEAR MINIMIZAT.
C                   - 3 IN ADDITION TO THE ABOVE,PRINT FUNCTION VALUES
C                     CALCULATED IN EVALUATING THE GRADIENT(FORMAT 5I5)
```

```
C
C     NF,FBEGIN,FEND - NUMBER OF FREQUENCY INTERVALS USED IN COMPUTING
C                      THE SPECTRAL RESPONSE,LOWER VALUE OF FREQUENCY
C                      (IN HZ),RESPECTIVELY(FORMAT I10,2E10.0). TOTAL
C                      NUMBER OF FREQUENCIES USED NFT=NF+1
C
C     LENGTH - GUST SCALE LENGTH. USED TO DETERMINE THE VON
C              KARMAN GUST SPECTRUM(FORMAT 4E10.0)
C
C     EM - FLIGHT MACH NUMBER (FORMAT 4E10.0).
C
C     NOTE THAT THE MAIN PROGRAM WRITES AND READS FROM A TEMPORARY
C     FILE 13.(SHOULD BE DEFINED AS NEW,PASS). FILE4 IS USED TO OUTPUT
C     OPTIMIZATION RESULTS AND SHOULD BE DEFINED AS EQUAL TO OUTPUT.
C
C     NOTE ALSO THAT PLOTS SHOWING THE SENSITIVITY OF ANY CONTROL
C     LAW WITH RESPECT TO THE VARIOUS X(I) PARAMETERS CAN BE MADE
C     USING THIS PACKAGE. TO ACCOMPLISH THIS, THE CALL TO SUBROUTINE
C     SDFP SHOULD BE REPLACED WITH A CALL TO SUBROUTINE GUSPLT. WHEN
C     SENSITIVITY PLOTS ARE NOT REQUIRED IT IS POSSIBLE TO DELETE THE
C     SUBROUTINES GUSPLT AND PLT(WHICH IS CALLED BY GUSPLT). THE
C     SENSITIVITY RANGE IS FOUND BETWEEN X1(I) AND X2(I) IN STEPS OF
C     EPS(I),STARTING WITH X(I).
C
C     NOTE ALSO THAT TWO GENERALIZED CONTROL LAWS ARE INCLUDED IN
C     THIS PACKAGE:-THE L.D.T.T.F. AND THE D.T.T.F. CONTROL LAWS.
C     MAKE SURE TO DELETE THE SUPERFLUOUS CONTROL LAW.
C
CCCCCCCCCCCCCCCCCCCCCCCCCCCCCCCCCCCCCCCCCCCCCCCCCCCCCCCCCCCCCCCCCCCCCCCC
      REAL*4  XR,Y
      EXTERNAL SOLGST,DREAL,DAIMAG
      COMMON/COSTFN/X(36),PSD(101),CREF,XF(103),Q,VEL,H(12,15),
     *RMASS(15,15),OMEGAN(15),WL,WT,XR(103),Y(103),WR,DRMS(6),DRRMS(6)
      COMMON/COSTFN/NFT,NVACT,IFINAL,NDR,NA(36),NV,LABELX(15,6),NMNC,
     *NCACT,NTE(6)
      COMMON/AERF/A0(15,22),A1(15,22),A2(15,22),A3(15,22),A4(15,22)
     +,A5(15,22),A6(15,22)
      COMMON/ICASE/B(4),NM,NC,NG,NL
      DIMENSION  HDR(15),ZW(12,15),ZREF(2,15),EPS(36),XX(36),EPSACT(36),
     *DRV(36),DRVACT(36),X1(36),X1ACT(36),X2(36),X2ACT(36),BTRAN(6),
     *CTRAN(6),CLR(6)
      REAL*8 LENGTH
      NAMELIST/GST/RMASS,OMEGAN,VEL,BTRAN,CTRAN,CREF,ZW,ZREF,Q,CLR,CTF
     *,WR,NTE,NCACT
      NAMELIST/CASE/NM,NC,NAER,B,NG,NL
C
C     INPUT/OUTPUT OF DATA
C
      READ 133,(HDR(I),I=1,15)
      PRINT 131,(HDR(I),I=1,15)
      READ(5,CASE)
      WRITE(6,CASE)
      NMNC=NM+NC+NG
      IF(NAER.EQ.0) GO TO 10
      DO 1 II=1,NM
      DO 1 JJ=1,NMNC
      READ 132,A0(II,JJ),A1(II,JJ),A2(II,JJ),A3(II,JJ),A4(II,JJ)
     +,A5(II,JJ),A6(II,JJ)
    1 CONTINUE
```

```
   10 CONTINUE
      READ(5,GST)
      WRITE(6,GST)
      IF(NAER.EQ.0)  CALL  FIT
      NNNC=NM+NC+NG
  108 FORMAT(' NF=',I3,' FBEGIN=',E13.6,' FEND=',E13.6,/)
      NC2=2*NC
      READ 100,ETA1,PHI
      IUI=6
C
C
      PI=3.14159265400
      READ 103,NV,NPR,NDR
      READ 103,NONACT
      READ 103,(NA(I),I=1,NONACT)
      NVACT=NV-NONACT
      READ 100,WL,WT
      WRITE(IUI,115)
      WRITE(IUI,108)
      DO 200 I=1,NV
      READ 100,X1(I),X(I),X2(I),EPS(I)
  200 WRITE(IUI,102) X1(I),X(I),X2(I),EPS(I)
      DO 205 I=1,NV
      DRV(I)=0.0001D0
  205 CONTINUE
      READ 100,FMIN,ETA
      READ 103,ITMAX,IW
      READ 123,NF,FBEGIN,FEND
      READ 100,LENGTH
      PRINT 131,LENGTH
      DF=(FEND-FBEGIN)/NF
      PRINT 105,NF,FBEGIN,FEND
      NFT=NF+1
      READ 100,EM
      PRINT  135,EM
C
C
C     ENCODING THE PLOT LABELS
C
      DO  206  I=1,NC
      REWIND  13
      WRITE(13,133)  EM,Q,I
      REWIND  13
  206 READ(13,140)  (LABELX(J,I),J=1,9)
C
C     COMPUTATION OF THE VON KARMAN GUST PSD.
C
      DO 220 I=1,NFT
      XF(I)=(FBEGIN+DF*(I-1))*2.D0*PI
      XR(I)=XF(I)/(2.D0*PI)
      F=XF(I)
      PSD(I)=LENGTH/(PI*VEL)*(1.D0+8.D0/3.D0*(1.339D0*LENGTH*F/VEL)**2)/
     +(1.D0+(1.339D0*LENGTH*F/VEL)**2)**1.833333333D0
  220 CONTINUE
      PRINT 104,NV,NPR,NDR
      PRINT 116,ETA1,PHI
      PRINT 119,NONACT,NVACT
      PRINT 120
      PRINT 103,(NA(I),I=1,NONACT)
```

```
      PRINT 106,WL,WT
      WRITE(IU1,107)
      WRITE(IU1,102) (DRV(J),J=1,NV)
      PRINT 109,FMIN,ETA
      PRINT 110,ITMAX,IW
      INC=0
C
C     COMPUTATION OF THE TRANSFORMATION MATRIX  H  WHICH EXPRESSES
C     THE DEFLECTION AND TWIST OF THE 30 PERCENT CHORD POINT FOR THE
C     VARIOUS MID SPAN SECTIONS OF THE CONTROLS,INTERMS OF THE
C     GENERALIZED COORDINATES.
C
      DO  240  I=1,NC2,2
      INC=INC+1
      DO  240  J=1,NM
      H(I,J)=(ZW(I,J)+(CLR(INC)/CTR-1.D0)*ZREF(1,J)-CLR(INC)/CTR*
     *ZREF(2,J))/BTRAN(INC)
      H(I+1,J)=(ZW(I+1,J)-ZW(I,J))/CTRAN(INC)-(ZREF(2,J)-ZREF(1,J))/CTR
  240 CONTINUE
C
C     FORMATION OF NEW ARRAYS WHERE ALL THEIR ELEMENTS RELATE TO
C     ACTIVE PARAMETERS ONLY.
C
      CALL  X2XX(NV,NVACT,X,XX,NA)
      CALL  X2XX(NV,NVACT,EPS,EPSACT,NA)
      CALL  X2XX(NV,NVACT,DRV,DRVACT,NA)
      CALL  X2XX(NV,NVACT,X1,X1ACT,NA)
      CALL  X2XX(NV,NVACT,X2,X2ACT,NA)
      IF(NVACT.EQ.0) GOTO 241
      IFINAL=0
C
C     THE FOLLOWING OPTIMIZATION SUBROUTINE CALL SHOULD BE REPLACED
C     BY A CALL TO GUSPLT WHEN SENSITIVITY PLOTS ARE REQUIRED.
C
      CALL  SOFP(NVACT,X1ACT,XX,X2ACT,FMIN,EPSACT,ETA,ETA1,PHI,DRVACT,
     +ITMAX,IW,FUNCTN,SOLGST,IERR,NV,NA)
C
      CALL  XX2X(NV,NVACT,X,XX,NA)
      PRINT 114,IERR,ITMAX
      PRINT 111,FUNCTN
C
C     PRINTOUT OF OPTIMAL CONTROL GAINS.
C
      PRINT 112
      PRINT 102,(X(J),J=1,NV)
      PRINT 115
  241 CONTINUE
C
C     PRINTOUT OF OPTIMAL GUST RESPONSE OF CONTROLS.
C
      IFINAL=1
      CALL  SOLGST(XX,FUNCTN)
      STOP
  100 FORMAT(4F10.0)
  101 FORMAT(1P,'  LENGTH=',E13.6)
  102 FORMAT(1P,4E14.6)
  103 FORMAT(5I5)
  104 FORMAT(/,1H ,'NV=',I2,'  NPR=',I2,'  NDR=',I2,/)
  106 FORMAT(1P,'  WL=',E13.6,'  WT=',E13.6,/)
```

```
  107 FORMAT('  INITIAL (INPUT) VECTOR DRV(I)',/)
  108 FORMAT(1H ,'    X1(I)            X(I)              X2(I)          EPS(I)',/)
  109 FORMAT(1P,/,' FMIN=',E13.6,' ETA=',E13.6,/)
  110 FORMAT(' ITMAX=',I3,' IW=',I2,/)
  111 FORMAT(1P,' FUNCTN=',E13.6,/)
  112 FORMAT(1H ,'OPTIMUM  VECTOR  X(I)',/)
  114 FORMAT(1H ,'     IERR=',I2,'  ITERATIONS PERFORMED=',I3,/)
  115 FORMAT(//)
  116 FORMAT(1P,' ETA1=',E13.6,' PHI=',E13.6,/)
  119 FORMAT(' NONACT=',I2,' NVACT=',I2,/)
  120 FORMAT(' THE NON ACTIVE PARAMETERS NA(I)',/)
  123 FORMAT(I10,2E10.0)
  130 FORMAT(15A4)
  131 FORMAT(1H ,15A4)
  132 FORMAT(6X,7E10.4)
  133 FORMAT(' DAST M=',F4.2,'Q=',F5.1,'CONTROL NO.',I2,'  HZ')
  135 FORMAT(1H,'M=',F4.2,/)
  140 FORMAT(15A4)
      END
      SUBROUTINE SOLGST(XX,FUNCTN)
      IMPLICIT  REAL*8(A-H,O-Z)
CCCCCCCCCCCCCCCCCCCCCCCCCCCCCCCCCCCCCCCCCCCCCCCCCCCCCCCCCCCCCCCCCCCCCCCC
C                                                                      C
      THE RMS RESPONSE OF THE CONTROL DEFLECTIONS AND/OR RATES ARE     C
C     CALCULATED IN THIS SUBROUTINE USING THE VON KARMAN GUST SPECTRUM C
C                                                                      C
CCCCCCCCCCCCCCCCCCCCCCCCCCCCCCCCCCCCCCCCCCCCCCCCCCCCCCCCCCCCCCCCCCCCCCCC
      COMMON/COSTFN/X(36),PSD(101),CREF,XF(103),Q,VEL,H(12,15),
     *RMASS(15,15),OMEGAN(15),WL,WT,XR(103),Y(103),WX,DRMS(6),DRRMS(6)
      COMMON/COSTFN/NFT,NVACT,IFINAL,NDR,NA(36),NV,LABELX(15,6),NMNC,
     *NCACT,NTE(6)
      REAL*4  XR,Y,FPN
      COMMON/AERF/A0(15,22),A1(15,22),A2(15,22),A3(15,22),A4(15,22)
     +,A5(15,22),A6(15,22)
      COMMON/ICASE/B(4),NM,NC,NG,NL
      DIMENSION  XX(1),QD(10,6),P(6,12,10),DEF(101,6),DEFR(101,6),
     *DEF2(101,6),DEFR2(101,6),BUF(103)
     *,IWK(15,2),IPIVOT(15),NP(6,12),ND(6)
      COMPLEX*16  F,HD(6),BN(6,12),CM(6,15),FC(15,15),FG(15),T(15,15),
     *R(6),AK,DETERM,ZERO
     +,AKB1,AKB2,AKB3,AKB4,FNC(15,6)
      PI=3.14159265400
      P2D=180.D0/PI
      CALL XX2X(NV,NVACT,X,XX,NA)
      NC2=2*NC
C
      CALL CONTRL(NP,P,ND,QD,NC,WR,NTE,X)
C
C     THE EQUATIONS OF MOTION ARE CONSTRUCTED AND SOLVED FOR  NFT
C     VALUES OF FREQUENCIES.
C
      DO 200 JF=1,NFT
      AK=DCMPLX(0.D0,XF(JF)*CREF/VEL)
      F=DCMPLX(0.D0,XF(JF))
      ZERO=DCMPLX(0.D0,0.D0)
      F2=F*F
      AK2=AK*AK
      AKB1=AK/(AK+B(1))
      AKB2=AK/(AK+B(2))
```

```
      AKB3=AK/(AK+B(3))
      AKB4=AK/(AK+B(4))
C
C     THE TRANSFORMATION MATRIX BETWEEN GENERALIZED COORDINATES AND
C     CONTROL ROTATIONS IS CONSTRUCTED NEXT.
C
      DO  300  I=1,NC
      NN=ND(I)
      BD(I)=ZERO
      DO  250  K=1,NN
  250 BD(I)=BD(I)+QD(K,I)*F**(K-1)
      DO  300  J=1,NC2
      BN(I,J)=ZERO
      NP=NP(I,J)
      DO  320  K=1,NN
      IF(P(I,J,K).EQ.0.D0)  GO  TO  320
      BN(I,J)=BN(I,J)+P(I,J,K)*F**(K-1)
  320 CONTINUE
  300 BN(I,J)=BN(I,J)/BD(I)
      DO  340  I=1,NC
      DO  340  J=1,NM
      CM(I,J)=ZERO
      DO  340  K=1,NC2
  340 CM(I,J)=CM(I,J)+BN(I,K)*H(K,J)
C
C     CONSTRUCTION AND SOLUTION OF THE EQUATIONS OF MOTION
C
      DO  360  I=1,NM
      DO  360  J=1,NC
      NMJ=NM+J
      FNC(I,J)=(A0(I,NMJ)+A1(I,NMJ)*AK+A2(I,NMJ)*AK2+A3(I,NMJ)*AKB1+
     *A4(I,NMJ)*AKB2+A5(I,NMJ)*AKB3+A6(I,NMJ)*AKB4)*Q
  360 CONTINUE
      DO  361  I=1,NM
      DO  361  J=1,NM
      FC(I,J)=ZERO
      DO  361  K=1,NC
  361 FC(I,J)=FC(I,J)+FNC(I,K)*CM(K,J)
      DO 380 I=1,NM
      FG(I)=-Q*(1./VEL)*(A0(I,NMNC)+A1(I,NMNC)*AK+A2(I,NMNC)*AK2+
     +A3(I,NMNC)*AKB1+A4(I,NMNC)*AKB2+
     +A5(I,NMNC)*AKB3+A6(I,NMNC)*AKB4)
  380 CONTINUE
      DO 400 I=1,NM
      DO 395 J=1,NM
      T(I,J)=RMASS(I,J)*F2+Q*(A0(I,J)+A1(I,J)*AK+A2(I,J)*AK2+
     +A3(I,J)*AKB1+A4(I,J)*AKB2+A5(I,J)*AKB3+A6(I,J)
     +*AKB4)+FC(I,J)
  395 CONTINUE
       T(I,I)=T(I,I)+RMASS(I,I)*OMEGAN(I)*OMEGAN(I)*4.D0*PI*PI
     +*DCMPLX(1.D0,0.015D0)
  400 CONTINUE
      CALL  CXINVR(T,NM,FG,1,DETERM,IPIVOT,IWK,15,ISCALE)
      DO 420 I=1,NC
      R(I)=ZERO
      DO 420 J=1,NM
  420 R(I)=R(I)+CM(I,J)*FG(J)
      IF(NDR.EQ.1.AND.IFINAL.EQ.0) GO TO 430
      DO  421  I=1,NC
```

```
      DEF(JF,I)=CDABS(R(I))*R2D
  421 DEF2(JF,I)=DEF(JF,I)*DEF(JF,I)
  430 IF(NDR.EQ.0.AND.IFINAL.EQ.0) GO TO 200
      DO  422  I=1,NC
      DEFR(JF,I)=CDABS(R(I)*F)*R2D
  422 DEFR2(JF,I)=DEFR(JF,I)*DEFR(JF,I)
  200 CONTINUE
      IF(NDR.EQ.1.AND.IFINAL.EQ.0) GO TO 440
C
C     COMPUTATION OF RMS RESPONSE OF CONTROL SURFACES
C
      DO  423  I=1,NC
      CALL  INTGLS(NFT,XF,DEF2(1,I),AREA,PSD)
  423 DRMS(I)=DSQRT(AREA)
      FUNCTN=DRMS(1)
      IF(IFINAL.EQ.0) GO TO 480
  440 CONTINUE
      DO  424  I=1,NC
      CALL  INTGLS(NFT,XF,DEFR2(1,I),AREA,PSD)
  424 DRRMS(I)=DSQRT(AREA)
      FUNCTN=DRRMS(1)
      IF(IFINAL.EQ.0) GO TO 480
C
C     PRINT AND PLOT OUTPUTS
C
      PRINT 100
      DO  425  I=1,NFT
      PRINT  110,(XF(I),(DEF(I,J),J=1,NC),PSD(I))
  425 CONTINUE
      PRINT  120,(DRMS(I),I=1,NC)
      PRINT  127
      PRINT  101
      DO  426  I=1,NFT
      PRINT  110,(XF(I),(DEFR(I,J),J=1,NC),PSD(I))
  426 CONTINUE
      PRINT  121,(DRRMS(I),I=1,NC)
      PRINT  127
      PRINT 125
      DO 470 I=1,NFT
      DO  471  J=1,NC
      DEF2(I,J)=DEF2(I,J)*PSD(I)
  471 DEFR2(I,J)=DEFR2(I,J)*PSD(I)
      PRINT  110,(XF(I),(DEF2(I,J),J=1,NC),PSD(I))
  470 CONTINUE
      PRINT  120,(DRMS(I),I=1,NC)
      PRINT  127
      PRINT  126
      DO  427  I=1,NFT
      PRINT  110,(XF(I),(DEFR2(I,J),J=1,NC),PSD(I))
  427 CONTINUE
      PRINT  121,(DRRMS(I),I=1,NC)
      CALL PLOTS(BUF,100,6,10.)
      CALL  SCALE(XR,5.,NFT,1)
      CALL PLOT(10.,2.5,-3)
      DO  900  IP=1,NC
      DO  900  IR=1,2
      IF(IR.EQ.1.AND.DRMS(IP).EQ.0.D0)  GO  TO  900
      IF(IR.EQ.2.AND.DRRMS(IP).EQ.0.D0)  GO  TO  900
      IF(IR.EQ.2)  GO  TO  910
```

```
      DO  901  IIP=1,NFT
  901 Y(IIP)=DEF2(IIP,IP)
      FPN=DRMS(IP)
      GO  TO  950
  910 CONTINUE
      DO  911  IIP=1,NFT
  911 Y(IIP)=DEFR2(IIP,IP)
      FPN=DRRMS(IP)
  950 CONTINUE
      CALL  AXIS(0.,0.,LABELX(1,IP),-36,7.,0.,XR(NFT+1),XR(NFT+2))
      CALL SCALE(Y,5.,NFT,1)
      IF(IR.EQ.1) CALL AXIS(0.,0.,'DEFLN  PSD',10,5.,90.,Y(NFT+1),
     +Y(NFT+2))
      IF(IR.EQ.2) CALL AXIS(0.,0.,'DEFLN  RATE  PSD',16,5.,90.,Y(NFT+1),
     +Y(NFT+2))
      CALL LINE(XP,Y,NFT,1,5,1)
      CALL SYMBOL(5.5,4.75,0.15,1,0.,-1)
      CALL NUMBER(5.75,4.675,0.15,FPN,0.,2)
      CALL PLOT(15.,0.,-3)
  900 CONTINUE
      CALL PLOT(0.,0.,999)
  480 RETURN
  100 FORMAT('   XF(I)         DEFLN(I).......      PSD(I)',//)
  101 FORMAT('   XF(I)         DEFLNR(I).......      PSD(I)',//)
  110 FORMAT(1P,8E13.6)
  120 FORMAT(1P,' DRMS(I)=',6E13.6,/)
  121 FORMAT(1P,' DRRMS(I)=',6E13.6,/)
  125 FORMAT('   XF(I)         DEFLN2(I).......      PSD(I)',//)
  126 FORMAT('   XF(I)         DEFLNR2(I).......      PSD(I)',//)
  127 FORMAT(//)
      END
      SUBROUTINE  GUSPLT(XX,XX1,XX2,DELX,DD,EM)
      IMPLICIT  REAL*8(A-H,O-Z)
CCCCCCCCCCCCCCCCCCCCCCCCCCCCCCCCCCCCCCCCCCCCCCCCCCCCCCCCCCCCCCCCCCCCCCCC
C                                                                      C
C     THIS SUBROUTINE IS NECESSARY ONLY WHEN SENSITIVITY PLOTS ARE     C
C     REQUIRED AROUND GIVEN X(I) CONTROL GAINS AND VARIED BETWEEN      C
C     X1(I) AND X2(I) IN STEPS OF EPS(I). THIS SUBROUTINE REPLACES THE C
C     CALL TO SOFP SUBROUTINE. THE FOLLOWING SUBROUTINE CALLS          C
C     SUBROUTINE  PLT  .  BOTH OF THESE SUBROUTINES HAVE NO CARD       C
C     DATA INPUTS. THE PLOT OUTPUT IS ALSO PRINTED IN SUBROUTINE PLT.  C
C     ONLY ACTIVE X(I) GAINS ARE PLOTTED. MAXIMUM OF 34 INTERVAL       C
C     VARIATIONS OF X(I) ARE ALLOWED FOR.                              C
C                                                                      C
CCCCCCCCCCCCCCCCCCCCCCCCCCCCCCCCCCCCCCCCCCCCCCCCCCCCCCCCCCCCCCCCCCCCCCCC
      COMMON/COSTFN/X(36),PSD(101),CREF,XF(103),Q,VEL,H(12,15),
     *RMASS(15,15),OMEGAN(15),WL,WT,XR(103),Y(103),WR
     *,DRMS(6),DRRMS(6)
      COMMON/COSTFN/NFT,NVACT,IFINAL,NOR,NA(36),NV,LABELX(15,6),NMNC,
     *NCACT,NTE(6)
      DIMENSION  XX(1),XX1(1),XX2(1),DELX(1),D(36,6),DR(36,6),XP(36)
      REAL*4  D,DR,XP,XR,Y
      ISTART=0
      NC=NCACT
      DO  260 I=1,NVACT
      ISTART=ISTART+1
      NP=0
      XT=XX(I)
      XM=XX(I)
```

```
      DO  150  K=1,34
      IF(XM.LT.XX1(I))  GO  TO  150
      XM=XM-DELX(I)
  150 CONTINUE
      XX(I)=XM
      DO  250  K=1,34
      XX(I)=XX(I)+DELX(I)
      IF(XX(I).GT.XX2(I).OR.XX(I).LT.XX1(I))  GO  TO  250
      NP=NP+1
      XP(NP)=XX(I)
      CALL  SOLGST(XX,FUNCTN)
      DO  300  IC=1,NC
      D(NP,IC)=DRMS(IC)
  300 DR(NP,IC)=DRRMS(IC)
  250 CONTINUE
      XX(I)=XT
      DO  251  IC=1,NC
      CALL  PLT(NV,NVACT,NA,XP,D(1,IC),NP,I,1,Q,EM,IC,ISTART,NC)
      ISTART=ISTART+1
      CALL  PLT(NV,NVACT,NA,XP,DR(1,IC),NP,I,2,Q,EM,IC,ISTART,NC)
  251 CONTINUE
  260 CONTINUE
      CALL  PLOT(10.0,0.,999)
      RETURN
      END
      SUBROUTINE  PLT(NV,NVACT,NA,X,Y,NP,IPLT,K,QDP,EMDP,IC,ISTART,NC)
      REAL*8  QDP,EMDP
CCCCCCCCCCCCCCCCCCCCCCCCCCCCCCCCCCCCCCCCCCCCCCCCCCCCCCCCCCCCCCCCCCCCCCCC
C
C     THIS SUBROUTINE IS CALLED BY SUBROUTINE GUSPLT AND IT DOES THE
C     ACTUAL PLOTTING AND PRINTING. FOR FURTHER DETAILS SEE SUBROUTINE
C     GUSPLT.
C
CCCCCCCCCCCCCCCCCCCCCCCCCCCCCCCCCCCCCCCCCCCCCCCCCCCCCCCCCCCCCCCCCCCCCCCC
      DIMENSION  NA(1),X(1),Y(1),LABELX(15),LABELY(3),BUF(100)
      IF(ISTART.EQ.1)  CALL  PLOTS(BUF,100,6,10.0)
      Q=QDP
      EM=EMDP
      YMX=Y(1)
      DO  15  I=2,NP
   15 IF(Y(I).GT.YMX)  YMX=Y(I)
      IF(YMX.EQ.0.D0)  RETURN
      NY=12
      NX=36
      IF(NV.EQ.NVACT)  INDEX=IPLT
      IF(NV.EQ.NVACT)  GO  TO  3
      II=1
      INONAC=0
      DO  10  I=1,NV
      IF(I.NE.NA(II))  GO  TO  2
      INONAC=INONAC+1
      IF(INONAC.LT.(NV-NVACT))  II=II+1
    2 IACTIV=I-INONAC
      IF(IACTIV.EQ.IPLT)  INDEX=I
      IF(IACTIV.EQ.IPLT)  GO  TO  3
   10 CONTINUE
    3 CONTINUE
      REWIND  13
      WRITE(13,100)  INDEX,EM,Q
```

```
      IF(K.EQ.1)  WRITE(13,121) IC
      IF(K.EQ.2)  WRITE(13,123) IC
      REWIND  13
      READ(13,120) (LABELX(J),J=1,9)
      READ(13,120)  LABELY
      NNX=-NX
      IF(ISTART.EQ.1)  CALL  PLOT(10.,2.5,-3)
      CALL  SCALE(X,5.,NP,1)
      CALL  SCALE(Y,5.,NP,1)
      CALL  AXIS(0.,0.,LABELX,NNX,7.,0.,X(NP+1),X(NP+2))
      PRINT 120,LABELX
      PRINT  102,(X(J),J=1,NP)
      PRINT 120,LABELY
      PRINT  102,(Y(J),J=1,NP)
      CALL  AXIS(0.,0.,LABELY,NY,5.,90.,Y(NP+1),Y(NP+2))
      CALL  LINE(X,Y,NP,1,1,1)
      CALL PLOT(15.,0.,-3)
      RETURN
  100 FORMAT('VAR.X(',I2,'),DAST M=',F4.2,'DYN.PRESS=',F5.1)
C
  121 FORMAT('DRMS(',I1,')  PSD')
  123 FORMAT('DRRMS(',I1,') PSD')
  102 FORMAT(4E14.6)
  120 FORMAT(15A4)
      END
      SUBROUTINE  CONTRL(NP,P,ND,OD,NC,WR,NTE,X)
CCCCCCCCCCCCCCCCCCCCCCCCCCCCCCCCCCCCCCCCCCCCCCCCCCCCCCCCCCCCCCCCCCCCCCCC
C                                                                      C
C     L.D.T.T.F. CONTROL LAW FOR ANY NUMBER OF CONTROL SURFACES. CAN   C
C     BE USED FOR BOTH FLUTTER AND GUST PROGRAMS. THE BASIC GAINS      C
C     USED HEREIN ARE APPROPRIATE FOR 20 PERCENT L.E. AND  20 PERCENT  C
C     T.E. CONTROL SYSTEMS WITH THE FORE SENSOR LOCATED AT THE 30      C
C     PERCENT CHORD LOCATION - DIMENSIONS ARE LIMITED TO 6 CONTROLS.   C
C                                                                      C
CCCCCCCCCCCCCCCCCCCCCCCCCCCCCCCCCCCCCCCCCCCCCCCCCCCCCCCCCCCCCCCCCCCCCCCC
      IMPLICIT  REAL*8(A-H,O-Z)
      DIMENSION NP(6,1),P(6,12,1),OD(10,1),E(2,2),NTE(6),X(36),CN(3),
     *CD1(3),CD2(3),TEMP1(5),TEMP2(5),ND(6)
      E(1,1)=-4.D0
      E(1,2)=4.D0
      E(2,1)=4.D0
      E(2,2)=2.8D0
      C21=-1.36D0
      NC2=2*NC
      DO  1  I=1,NC
      DO  1  J=1,NC2
      NP(I,J)=1
      DO  1  K=1,10
      P(I,J,K)=0.D0
    1 CONTINUE
      DO  2 I=1,NC
C
C   CASE OF  T.E.  CONTROL
C
      EH=E(2,1)
      EA=E(2,2)
      IF(NTE(I).EQ.1)  GO  TO  3
C
C   CASE  OF  L.E.  CONTROL
```

```
C
      EH=E(1,1)
      EA=E(1,2)
    3 CONTINUE
      CN(1)=0.D0
      CN(2)=0.D0
C
C     DETERMINATION OF THE DENOMINATOR POLYNOMIAL FOR EACH CONTROL SURF.
C
      CD1(1)=X(6*I-4)**2
      CD1(2)=2.D0*X(6*I-4)*X(6*I-3)
      CD1(3)=1.D0
      CD2(1)=X(6*I-1)**2
      CD2(2)=2.D0*X(6*I-1)*X(6*I)
      CD2(3)=1.D0
      CALL  PROPOL(CD1,3,CD2,3,QD(1,I),ND(I))
C
C     DETERMINATION OF THE NUMERATOR POLYNOMIAL FOR EACH CONTROL SURFACE
C
      CN(3)=X(6*I-5)
      CALL  PROPOL(CD2,3,CN,3,TEMP1,N)
      CN(3)=X(6*I-2)
      CALL  PROPOL(CD1,3,CN,3,TEMP2,N)
      DO  4  K=1,N
      P(I,2*I-1,K)=EH*(TEMP1(K)+TEMP2(K))
      P(I,2*I,K)=EA*(TEMP1(K)+TEMP2(K))+C21*NTE(I)*QD(K,I)
    4 CONTINUE
      NP(I,2*I-1)=N
      NP(I,2*I)=N
    2 CONTINUE
      RETURN
      END
      SUBROUTINE  CONTRL(NP,P,ND,QD,NC,WR,NTE,X)
CCCCCCCCCCCCCCCCCCCCCCCCCCCCCCCCCCCCCCCCCCCCCCCCCCCCCCCCCCCCCCCCCCCCCCCC
C
C     D.T.T.F. CONTROL LAW FOR ANY NUMBER OF CONTROL SURFACES. CAN
C     BE USED FOR BOTH FLUTTER AND GUST PROGRAMS. THE BASIC GAINS
C     USED HEREIN ARE APPROPRIATE FOR 20 PERCENT L.E. AND  20 PERCENT
C     T.E. CONTROL SYSTEMS WITH THE FORE SENSOR LOCATED AT THE 30
C     PERCENT CHORD LOCATION - DIMENSIONS ARE LIMITED TO 6 CONTROLS.
C
CCCCCCCCCCCCCCCCCCCCCCCCCCCCCCCCCCCCCCCCCCCCCCCCCCCCCCCCCCCCCCCCCCCCCCCC
      IMPLICIT  REAL*8(A-H,O-Z)
      DIMENSION NP(6,1),P(6,12,1),QD(13,1),E(2,2),NTE(6),X(36),ND(6)
      E(1,1)=-4.D0
      E(1,2)=4.D0
      E(2,1)=4.D0
      E(2,2)=3.2D0
      C21=-1.86D0
      A=10000.D0
      NC2=2*NC
      DO  1  I=1,NC
      DO  1  J=1,NC2
      NP(I,J)=1
      DO  1  K=1,2
      P(I,J,K)=0.D0
    1 CONTINUE
      DO  2 I=1,NC
      P(I,2*I-1,1)=0.D0
```

```
      P(I,2*I,1)=A*C21*NTE(I)
C
C   CASE OF  T.E.  CONTROL
C
      EH=E(2,1)
      EA=E(2,2)
      IF(NTE(I).EQ.1)  GO  TO  3
C
C   CASE  OF  L.E.  CONTROL
C
      EH=E(1,1)
      EA=E(1,2)
    3 CONTINUE
C
C     DETERMINATION OF  THE NUMERATOR POLYNOMIAL FOR EACH CONTROL  SURFACE
C
      P(I,2*I-1,2)=A*EH*X(I)/WR
      P(I,2*I,2)=A*EA*X(I)/WR
C
C     DETERMINATION OF  THE DENOMINATOR POLYNOMIAL FOR EACH CONTROL SURF.
C
      QD(1,I)=A
      QD(2,I)=1.D0
      NP(I,2*I-1)=2
      NP(I,2*I)=2
      ND(I)=2
    2 CONTINUE
      RETURN
      END
      SUBROUTINE  FIT
      IMPLICIT  REAL*8(A-H,O-Z)
CCCCCCCCCCCCCCCCCCCCCCCCCCCCCCCCCCCCCCCCCCCCCCCCCCCCCCCCCCCCCCCCCCCCCCCCCCCCC
C                                                                          C
C     FITS THE  AERO COEFFICIENTS IN TERMS OF PADE APPROXIMANTS USING      C
C     LEAST SQUARE TECHNIQUE.                                              C
C                                                                          C
C     NAMELIST/FT                                                          C
C     NK - NUMBER OF REDUCED FREQUENCIES K USED FOR INTERPOLATION          C
C                                                                          C
C     AK - ARRAY CONTAINING THE K VALUES(20 MAX) - (FIRST REDUCED K        C
C     MUST BE EQUAL TO ZERO)                                               C
C                                                                          C
C     MAXNK - MAX VALUE OF NK(MAX NK=20 IN PRESENT PROGRAM)                C
C                                                                          C
C     NPRINT - 0 NO PRINTED OUTPUT FROM SUBROUTINE FIT.                    C
C            - 1 PRINTED OUTPUT IS AVAILABLE(FOR DEBUGGING PURPOSES)       C
C                                                                          C
C     NPUNCH - 0 NO PUNCHED OUTPUT FROM SUBROUTINE FIT                     C
C            - 1 PUNCHED OUTPUT(INTERPOLATION COEFFICIENTS).               C
C                                                                          C
C     IRIGID,JRIGID - CURVE FITTING(WITH NO LEAST SQUARES TECHNIQUE)       C
C     OF THE FIRST IRIGID ROWS AND JRIGID COLUMNS OF AERO MATRIX -         C
C     ASSUMED TO CONTAIN RIGID BODY AERO - TO IMPROVE RESULTS.             C
C                                                                          C
C     READ(2,   )  AERO(I,J,K)   FORMAT(2E15.5)                            C
C                                                                          C
CCCCCCCCCCCCCCCCCCCCCCCCCCCCCCCCCCCCCCCCCCCCCCCCCCCCCCCCCCCCCCCCCCCCCCCCCCCCC
      COMMON/AERF/A0(15,22),A1(15,22),A2(15,22),A3(15,22),A4(15,22),
     *A5(15,22),A6(15,22)
```

```
      COMMON/ICASE/B(4),NM,NC,NG,NL
      COMPLEX*16  AERO(15,22,20),COEF
      DIMENSION  AK(20),AK2(20),X(40,6),XT(6,40),Y(40),XTX(6,6),
     *XTY(6),S(6),CLR(4,20),CLI(4,20)
      NAMELIST/FT/NK,AK,MAXNK,NPRINT,NPUNCH,IRIGID,JRIGID
      READ(5,FT)
      WRITE(6,FT)
      MAXNK2=2*MAXNK
      NMNC=NM+NC+NG
      DO  1  K=1,NK
      AK2(K)=AK(K)*AK(K)
      DO  1  J=1,NMNC
      DO  1  I=1,NM
      READ(2,201)  AERO(I,J,K)
    1 CONTINUE
      DO  5  I=1,NL
      B2=B(I)*B(I)
      DO  5  K=1,NK
      CLR(I,K)=AK2(K)/(B2+AK2(K))
      CLI(I,K)=B(I)*AK(K)/(B2+AK2(K))
    5 CONTINUE
      IF(AK(1).NE.0.D0)  PRINT  100
      IF(AK(1).NE.0.D0)  STOP
C
C     DETERMINATION OF THE INTRPLLATION LEAST SQUARE MATRIX  XTX AND
C     THE KNOWN AERO VECTOR  XTY
C
      DO  2  I=1,NM
      DO  2  J=1,NMNC
      IF(I.GT.IRIGID.OR.J.GT.JRIGID)  GO  TO  7
      NKT=NK
      NK=(3+NL)/2+1
    7 CONTINUE
      DO  3  K=2,NK
      X(2*K-3,1)=0.D0
      X(2*K-2,1)=AK(K)
      X(2*K-3,2)=-AK2(K)
      X(2*K-2,2)=0.D0
      Y(2*K-3)=DREAL(AERO(I,J,K)-AERO(I,J,1))
      Y(2*K-2)=DAIMAG(AERO(I,J,K))
      DO  3  L=1,NL
      X(2*K-3,2+L)=CLR(L,K)
      X(2*K-2,2+L)=CLI(L,K)
    3 CONTINUE
      NROWS=2*(NK-1)
      NCOLS=2+NL
      IF(NROWS.LT.NCOLS)  PRINT  110
      IF(NROWS.LT.NCOLS)  STOP
      DO  4  IR=1,NROWS
      DO  4  JR=1,NCOLS
      XT(JR,IR)=X(IR,JR)
    4 CONTINUE
      CALL  MXPROD(XT,X,XTX,NCOLS,NROWS,NCOLS,6,MAXNK2,6)
      CALL  MXPROD(XT,Y,XTY,NCOLS,NROWS,1,6,MAXNK2,6)
C
C     SOLUTION FOR THE UNKNOWN INTERPOLATION COEFFICIENTS
C
      CALL  MXINVR(NCOLS,0,6,XTX)
      CALL  MXPROD(XTX,XTY,S,NCOLS,NCOLS,1,6,6,6)
```

```
      A0(I,J)=AERO(I,J,1)
      A1(I,J)=S(1)
      A2(I,J)=S(2)
      A3(I,J)=S(3)
      IF(NL.LT.2)  GO  TO  10
      A4(I,J)=S(4)
      IF(NL.LT.3)  GO  TO  10
      A5(I,J)=S(5)
      IF(NL.LT.4)  GO  TC  10
      A6(I,J)=S(6)
   10 CONTINUE
      IF(I.LE.IRIGID.AND.J.LE.JRIGID)  NK=NKT
C
C     PRINTED AND/OR PUNCHED OUTPUTS
C
      IF(NPRINT.NE.1.AND.NPUNCH.NE.1)  GO  TC  2
      IF(NPUNCH.NE.1)  GO  TO  9
      PUNCH  600,I,J,A0(I,J),(S(JJ),JJ=1,NCOLS)
    9 CONTINUE
      IF(NPRINT.NE.1)  GO  TO  2
      PRINT  700,I,J
      PRINT  200,A0(I,J),(S(JJ),JJ=1,NCOLS)
      DO  8  IK=1,NK
      COEF=DCMPLX(0.D0,0.D0)
      DO  6  II=1,NL
      COEF=COEF+S(2+II)*DCMPLX(CLR(II,IK),CLI(II,IK))
    6 CONTINUE
      COEF=COEF+AERO(I,J,1)+S(1)*DCMPLX(0.D0,AK(IK))-S(2)*AK2(IK)
      QUOTR=DREAL(AERO(I,J,IK))
      QUOTI=DAIMAG(AERO(I,J,IK))
      IF(QUOTR.EQ.0.D0)  QUOTR=1.D-20
      IF(QUOTI.EQ.0.D0)  QUOTI=1.D-20
      ERR=DREAL(AERO(I,J,IK)-COEF)*100.D0/QUOTR
      ERI=DAIMAG(AERO(I,J,IK)-COEF)*100.D0/QUOTI
      PRINT  210,I,J,IK,AK(IK),AERO(I,J,IK),COEF,ERR,ERI
    8 CONTINUE
    2 CONTINUE
  200 FORMAT(10X' COEFF = '8E12.4)
  210 FORMAT(2X,3I5,4X,7E12.4)
  600 FORMAT(2X,2I2,2X,7E10.4)
  700 FORMAT(20X'  AERO( DEF MODE = ',I2,' PRES MODE = 'I2, ')'/)
      RETURN
  100 FORMAT('  FIRST  REDUCED  FREQUENCY  MUST  BE  EQUAL  TO  ZERO'/)
  110 FORMAT('  THERE  ARE  LESS  EQUATIONS  THAN  UNKNOWNS',/)
  201 FORMAT(2E15.5)
      END
      SUBROUTINE  X2XX(NV,NVACT,X,XX,NA)
      IMPLICIT REAL*8 (A-H,O-Z)
CCCCCCCCCCCCCCCCCCCCCCCCCCCCCCCCCCCCCCCCCCCCCCCCCCCCCCCCCCCCCCCCCCCCCCCC
C                                                                      C
C     THIS  SUBROUTINE REDUCES THE X(I) ARRAY  INTO AN  XX(I) ARRAY    C
C     WHERE THE NON ACTIVE PARAMETERS (NV-NVACT) HAVE BEEN ELIMINATED. C
C     THE POSITION OF THESE NON ACTIVE PARAMETERS ALONG THE X  ARRAY   C
C     IS GIVEN BY THE  NA(I)  ARRAY.                                   C
C                                                                      C
CCCCCCCCCCCCCCCCCCCCCCCCCCCCCCCCCCCCCCCCCCCCCCCCCCCCCCCCCCCCCCCCCCCCCCCC
      DIMENSION X(1),XX(1),NA(1)
      NONACT=NV-NVACT
      NCOUNT=0
```

```
      DO 100 I=1,NV
      IF(NONACT.EQ.NCOUNT) GO TO 115
      DO 110 J=1,NONACT
      IF(I.NE.NA(J)) GO TO 110
      NCOUNT=NCOUNT+1
      GO TO 100
  110 CONTINUE
  115 XX(I-NCOUNT)=X(I)
  100 CONTINUE
      RETURN
      END
      SUBROUTINE  XX2X(NV,NVACT,X,XX,NA)
      IMPLICIT REAL*8 (A-H,O-Z)
CCCCCCCCCCCCCCCCCCCCCCCCCCCCCCCCCCCCCCCCCCCCCCCCCCCCCCCCCCCCCCCCCCCCCCCC
C
C     THIS SUBROUTINE RESTORES THE X(I) ARRAY USING THE REDUCED XX(I)
C     ARRAY AND THE INITIAL VALUES OF THOSE X(I)'S THAT ARE NOT
C     ACTIVE. THIS IS THE INVERSE PROCESS OF SUBROUTINE  X2XX.
C
CCCCCCCCCCCCCCCCCCCCCCCCCCCCCCCCCCCCCCCCCCCCCCCCCCCCCCCCCCCCCCCCCCCCCCCC
      DIMENSION X(1),XX(1),NA(1)
      NONACT=NV-NVACT
      NCOUNT=0
      DO 100 I=1,NV
      IF(NONACT.EQ.NCOUNT) GO TO 115
      DO 110 J=1,NONACT
      IF(I.NE.NA(J)) GO TO 110
      NCOUNT=NCOUNT+1
      GO TO 100
  110 CONTINUE
  115 X(I)=XX(I-NCOUNT)
  100 CONTINUE
      RETURN
      END
      SUBROUTINE CMXPRD(C,A,B,NIA,NJA,NJB)
      IMPLICIT REAL*8 (A-H,O-Z)
CCCCCCCCCCCCCCCCCCCCCCCCCCCCCCCCCCCCCCCCCCCCCCCCCCCCCCCCCCCCCCCCCCCCCCCC
C
C     COMPLEX MATRIX PRODUCT       C=A*B
C
CCCCCCCCCCCCCCCCCCCCCCCCCCCCCCCCCCCCCCCCCCCCCCCCCCCCCCCCCCCCCCCCCCCCCCCC
      COMPLEX*16 A(NIA,NJA),B(NJA,NJB),C(NIA,NJB)
      DO 100 I=1,NIA
      DO 100 J=1,NJB
      C(I,J)=DCMPLX(0.D0,0.D0)
      DO 100 K=1,NJA
  100 C(I,J)=C(I,J)+A(I,K)*B(K,J)
      RETURN
      END
      SUBROUTINE  CMXADD(C,A,B,NI,NJ)
      IMPLICIT REAL*8 (A-H,O-Z)
CCCCCCCCCCCCCCCCCCCCCCCCCCCCCCCCCCCCCCCCCCCCCCCCCCCCCCCCCCCCCCCCCCCCCCCC
C
C     COMPLEX  MATRIX  ADDITION       C=A+B
C
CCCCCCCCCCCCCCCCCCCCCCCCCCCCCCCCCCCCCCCCCCCCCCCCCCCCCCCCCCCCCCCCCCCCCCCC
      COMPLEX*16 A(NI,NJ),B(NI,NJ),C(NI,NJ)
      DO 100 I=1,NI
      DO 100 J=1,NJ
```

```
  100 C(I,J)=A(I,J)+B(I,J)
      RETURN
      END
      SUBROUTINE INTGLS(NN,X,Y,A,W)
      IMPLICIT REAL*8 (A-H,O-Z)
CCCCCCCCCCCCCCCCCCCCCCCCCCCCCCCCCCCCCCCCCCCCCCCCCCCCCCCCCCCCCCCCCCCCCCCC
C
C     INTEGRATION OF  Y*W  VS. X  CURVE USING THE TRAPEZOIDAL RULE.
C     Y,W AND X ARE ARRAYS WITH N ELEMENTS. THE AREA IS DENOTED BY  A
C
CCCCCCCCCCCCCCCCCCCCCCCCCCCCCCCCCCCCCCCCCCCCCCCCCCCCCCCCCCCCCCCCCCCCCCCC
      DIMENSION X(1),Y(1),W(1)
      A=0.D0
      N=NN-1
      DO 1 I=1,N
    1 A=A+(Y(I)*W(I)+Y(I+1)*W(I+1))*(X(I+1)-X(I))
      A=0.5D0*A
      RETURN
      END
      SUBROUTINE SDFP(N,X1,X0,X2,FMIN,EPS,ETA,ETA1,PHI,DRV,ITMAX,IW,FO
     +,EVAL,IERR,NV,NA)
      IMPLICIT REAL*8 (A-H,O-Z)
CCCCCCCCCCCCCCCCCCCCCCCCCCCCCCCCCCCCCCCCCCCCCCCCCCCCCCCCCCCCCCCCCCCCCCCC
C
C     MINIMIZATION SUBROUTINE BASED ON THE STEWART'S ADAPTATION OF
C     THE DAVIDON-FLETCHER-POWELL ALGORITHM. A VARIATION HAD BEEN
C     INCORPORATED HEREIN TO PERMIT THE CONSTRAINT OF THE INDEPENDENT
C     VARIABLES WITHIN A SPECIFIED LOWER AND UPPER BOUNDS.
C
C     N - NUMBER OF INDEPENDENT VARIABLES.
C
C     X1(I) - DENOTES THE LOWEST BOUND OF THE I-TH INDEPENDENT VARIABLE
C
C     X0(I) - DENOTES THE INITIAL VALUE OF THE I-TH INDEPENDENT VARIABL
C
C     X2(I) - DENOTES THE UPPER BOUND OF THE I-TH INDEPENDENT VARIABLE
C
C     FMIN - INPUT APPROXIMATION TO THE FUNCTION MINIMUM.
C
C     EPS(I) - INPUT ARRAY CONTAINING THE DESIRED ABSOLUTE ACCURACY
C     OF THE INDEPENDENT VARIABLES.
C
C     ETA - INPUT PARAMETER CONTAINING AN ESTIMATE OF THE RELATIVE
C     ACCURACY OF THE FUNCTION EVALUATIONS WHICH ARE USED TO DETERMINE
C     THE TYPE OF DIFFERENCE APPROXIMATION TO THE GRADIENT (ABSOLUTE
C     ACCURACY=FUNCTION*ETA )
C
C     ETA1 - RELATIVE ACCURACY OF COMPUTER(ON I.B.M. DOUBLE PRECISION
C     =5.E-13). ABSOLUTE ACCURACY=X*ETA1.
C
C     PHI - RELATIVE SIZE OF 'SUCTION ZONE' WITHIN WHICH THE OPTIMIZED
C     FREE PARAMETER IS SUCKED TO THE CONSTRAINT TO AVOID FALSE
C     CONVERGENCE. ABSOLUTE SIZE OF ZONE=X1(I)*PHI OR X2(I)*PHI
C     DEPENDING ON WHETHER NEAR LOWER OR UPPER CONSTRAINTS.
C
C     DRV - A ONE DIMENSIONAL  INPUT  ARRAY OF AT LEAST LENGTH N
C     CONTAINING INITIAL STEP SIZES FOR DIFFERENCE APPROXIMATIONS
C     TO THE GRADIENT.
C
```

```
C     ITMAX - AN INPUT/OUTPUT INTEGER. ON INPUT,ITMAX CONTAINS THE
C     MAXIMUM ALLOWABLE NUMBER OF OPTIMIZATION ITERATIONS. ON OUTPUT,
C     ITMAX CONTAINS THE NUMBER OF ITERATIONS USED.
C
C     IW - AN INPUT INTEGER CODE FOR PRINTING DURING COMPUTATION.
C       - 0 NO PRINTING EXCEPT FOR SELECTED RESULTS DURING EACH ITERATN
C       - 1 PRINT GRADIENT VECTOR ,AND FUNCTION VALUE BEFORE AND AFTER
C     EACH LINEAR MINIMIZATION.
C       - 2 IN ADDITION TO THE ABOVE,PRINT FUNCTION VALUES CALCULATED
C     DURING THE COURSE OF LINEAR MINIMIZATION.
C       - 3 IN ADDITION TO THE ABOVE PRINT FUNCTION VALUES CALCULATED
C     IN EVALUATING THE GRADIENT.
C
C     FC - FUNCTION MINIMUM ON OUTPUT.
C
C     EVAL - THE NAME OF A USER CODED SUBROUTINE WHICH EVALUATES THE
C     FUNCTION BEING MINIMIZED  . THIS NAME MUST APPEAR IN AN EXTERNAL
C     STATEMENT OF THE CALLING PROGRAM.
C
C     IERR - OUTPUT ERROR CODE.
C           - -1 DISTANCE TO THE MINIMUM IS OPPOSITE THE DIRECTION
C           INDICATED BY THE GRADIENT OF THE FUNCTION.OPTIMUM HAS
C           PROBABLY BEEN REACHED.
C            - 0 NORMAL CONVERGENCE.
C           - 1 DERIVATIVE OF FUNCTION ALONG THE DIRECTION OF LINEAR
C           MINIMIZATION WAS NOT NEGATIVE. USER SHOULD TRY SMALLER
C           VALUES IN THE DRV ARRAY.
C           - 2 NO PROGRESS IN THE LINEAR MINIMIZATION. THE FUNCTION
C           MINIMUM HAS PROBABLY BEEN REACHED. USER SHOULD TRY DIFFERENT
C           INITIAL CONDITIONS FOR XO.
C           - 3 THE LINEAR MINIMIZATION FAILED TO CHANGE THE FUNCTION
C           VALUE. THE FUNCTION MINIMUM HAS PROBABLY BEEN REACHED ON A
C           FLAT SURFACE.USER SHOULD TRY DIFFERENT INITIAL CONDITIONS
C           FOR XO AND SEE IF THE SAME MINIMUM IS REACHED.
C           - 4 FAILURE TO CONVERGE WITHIN ITMAX ITERATIONS.
C
C     NV - TOTAL NUMBER OF PARAMETERS NECESSARY FOR THE DETERMINATION
C     OF THE FUNCTION IN SUBROUTINE EVAL.SOME OF THESE PARAMETERS CAN
C     BE MADE INACTIVE DURING OPTIMIZATION AND THUS LEAD TO A VALUE
C     OF N WHICH IS SMALLER THAN NV.
C
C     NA - INTEGER INPUT ARRAY CONTAINING THE LOCATIONS OF THE NON
C     ACTIVE PARAMETERS IN THE EXPANDED XO ARRAY.
C
C     NOTE  -  THE  ABOVE TWO PARAMETERS ARE USED IN SUBROUTINE EVAL
C     THROUGH THE USE OF SUBROUTINE X2XX AND XX2X.
C
CCCCCCCCCCCCCCCCCCCCCCCCCCCCCCCCCCCCCCCCCCCCCCCCCCCCCCCCCCCCCCCCCCCCCCC
      DIMENSION XO(1),EPS(1),DRV(1),H(60,60),X(60),G(60),Y(60),DEL(60),
     1C(60),E(4),EE(4),F(4)
     2,G1(60)
     3,X1(1),X2(1),TST(60),GEX(60),X1PHI(60),X2PHI(60),X1ETA(60),
     +X2ETA(60)
      DIMENSION NA(1)
      LOGICAL IDENT
C
C     OPTIONAL OUTPUT FORMATS
C
 2000 FORMAT(1H0,'FUNCTION VALUE =',E20.10/' VARIABLES X(I) =',E20.10/
```

```
     1(17X,E20.10))
 2001 FORMAT(1H0,'COMPUTE GRADIENT')
 2002 FORMAT(1H0,'GRADIENT =',6X,E20.10/(17X,E20.10))
 2003 FORMAT(1H0,'DIRECTION OF MINIMIZATIONS'/(4X,E20.10))
 2004 FORMAT(1H0,'LINEAR MINIMIZATION - FUNCTION VALUE =',E20.10)
 2005 FORMAT(1H0,'MINIMUM FUNCTION EVALUATION =',E20.10)
 2006 FORMAT(1H0,'END OF ITERATION ',I3//)
 2007 FORMAT(1P,2X,I3,3X,E14.6,1X,E14.6,1X,I3,2X,E14.6,1X,I3,2X,E14.6)
 2008 FORMAT(' ITERNS      FOPT            GMAX          IGMX     DELMAX
     +IDMX    E(LOWEST)',/)
 2009 FORMAT(4E14.6)
 2010 FORMAT(' INITIAL GRADIENTS VECTOR G(I)',/)
 2011 FORMAT(' FINAL  GRADIENTS  VECTOR G(I)',/)
 2012 FORMAT(' +++++++')
      MXTRIS=25
      IU1=4
      IU2=4
      DO 2 I=1,N
      X1ETA(I)=-DABS(X1(I)*ETA1)
      IF(DABS(X1(I)).LT.1.)  X1ETA(I)=-ETA1
      X2ETA(I)=DABS(X2(I)*ETA1)
      IF(DABS(X2(I)).LT.1.)  X2ETA(I)=ETA1
      X1PHI(I)=DABS(X1(I)*PHI)
      IF(DABS(X1PHI(I)).LE.DABS(EPS(I))) X1PHI(I)=DABS(1.1*EPS(I))
      X2PHI(I)=-DABS(X2(I)*PHI)
      IF(DABS(X2PHI(I)).LE.DABS(EPS(I))) X2PHI(I)=-DABS(1.1*EPS(I))
    2 CONTINUE
C
      EM=.1D-13
      FM=FMIN
      ILIN = 1
      LOWEST=1
      CALL EVAL(X0,F0)
C
C     COMPUTE GRADIENT
C
    4 IF   (IW.GT.2) WRITE(IU2,2001)
      DO 10 I=1,N
      X(I)=X0(I)
    5 X0(I)=X(I)+DRV(I)
      CALL EVAL(X0,FG)
      IF   (IW.GT.2) WRITE(IU2,2000) FG,(X0(J),J=1,N)
    7 G(I)=(FG-F0)/ DRV(I)
   10 X0(I)=X(I)
      CALL XX2X(NV,N,GEX,G,NA)
      PRINT 2010
      PRINT 2009,(GEX(J),J=1,NV)
      WRITE(IU1,2008)
   20 IDENT=.TRUE.
      DO 30 I=1,N
      DO 25 J=1,N
   25 H(I,J)=0.D0
      H(I,I)=1.D0
   30 C(I)=1.D0
      IF   (IW.GT.0) WRITE(IU2,2002) (G(I),I=1,N)
C
C     DETERMINE DIRECTION AND DIRECTIONAL DERIVATIVE
C
   50 D=0.D0
```

```
      FOPT=FO
      EP=1.D0
      DO 60 I=1,N
      DEL(I)=0.D0
      DO 55 J=1,N
   55 DEL(I)=DEL(I)-H(I,J)*G(J)
C
C     IF CONSTRAINTS ARE VIOLATED SET DEL(I)=0.D0
C
      IF(XO(I).EQ.X2(I).AND.DEL(I).GT.0.D0) DEL(I)=0.D0
      IF(XO(I).EQ.X1(I).AND.DEL(I).LT.0.D0) DEL(I)=0.D0
      IF(DEL(I).EQ.0.D0) GO TO 60
      EP=DMIN1(EP,DABS(EPS(I)/DEL(I)))
      D=D+G(I)*DEL(I)
   60 CONTINUE
      EP=EP*.05D0
      IF(D.LT.0.D0) GO TO 70
      IF(.NOT.IDENT)GO TO 20
      IERR = 1
      GO TO 500
   70 IF(FO.GT.FM) GO TO 71
  72  IF(FO)73,74,75
  73  FM=2.D0*FO
      GO TO 71
  74  FM=-1.D0
      GO TO 71
  75  FM=.5D0*FO
  71  CONTINUE
      E(2)=DMIN1(1.D+0,2.D0*(FM-FO)/D)
      IF    (IW.GT.3) WRITE(IO2,2003) (DEL(I),I=1,N)
      IF    (IW.GT.0) WRITE(IO2,2000) FO,(XO(I),I=1,N)
      F(1)=FO
      E(1)=0.D0
      NIT=0
      CALL MX(N,G,GMAX,IGMAX)
      CALL MX(N,DEL,DELMAX,IDMAX)
C
C     PROCEED WITH LINEAR MINIMIZATION
C
      KKK=0
  103 IF(DABS(E(2)).LE.EP)  E(2)=E(2)+1.1D0*EP
      NTRIES=0
      DO 105 I=1,N
  105 X(I)=XO(I)+E(2)*DEL(I)
      CALL EVAL(X,F(2))
      IF    (IW.GT.1) WRITE(IO2,2004) F(2)
      IF(F(2).NE.F(1))GO TO 107
  501 E(2)=2.D0*E(2)
      GO TO 103
  107 CONTINUE
      DENOM=D*E(2)+F(1)-F(2)
      IF(DABS(DENOM).LT.1.D-20) GO TO 501
      ED=.5D0*D*E(2)**2/DENOM
      IF(ED.LE.0.D0)ED=2.D0*E(2)
      IF(F(2).LT.F(1))GO TO 120
      IF(KKK.LT.8.AND.DABS(ED).GT.EP)  E(2)=ED
      KKK=KKK+1
      IF(KKK.LT.8.AND.DABS(ED).GT.EP)  GO TO 103
      F(3)=F(2)
```

```
      F(2)=FD
      E(3)=E(2)
      E(2)=0.D0
      F(1)=-E(3)
      DO 110 I=1,N
  110 X(I)=X0(I)+E(1)*DEL(I)
      CALL EVAL(X,F(1))
      IF    (IW.GT.1) WRITE(IO2,2004) F(1)
      IF(F(1).GE.F(2)) GO TO 150
      FTT1=F(1)
      ETT1=E(1)
      F(1)=F(3)
      E(1)=E(3)
      E(3)=ETT1
      F(3)=FTT1
      GO TO 150
  120 LOWEST=2
      IF(FD.GT.3.D0*E(2))ED=3.D0*E(2)
      IF(DABS(E(2)-ED).LT.EP)ED=E(2)+1.1D0*EP
      IF(DABS(E(2)-ED).LT..05D0*DABS(E(2))) ED=1.1D0*E(2)
      DO 130 I=1,N
  130 X(I)=X0(I)+ED*DEL(I)
      IF(ED.GT.E(2))GO TO 140
      E(3)=E(2)
      E(2)=ED
      F(3)=F(2)
      CALL EVAL (X,F(2))
      IF    (IW.GT.1) WRITE(IO2,2004) F(2)
      GO TO 150
  140 E(3)=ED
      CALL EVAL(X,F(3))
      IF    (IW.GT.1) WRITE(IO2,2004) F(3)
  150 CALL INTP4(E,F,EE,A,B)
  160 LOWEST=1
      NTRIES=NTRIES+1
      DO 165 I=2,3
      IF(F(I).LT.F(LOWEST))LOWEST=I
  165 CONTINUE
      IE=2.D0+DSIGN(1.D0+0,EE(2))
      IF(A.GE.0)IE=4-IE
      IF(A.LE.0.D0.OR. DABS(EE(2)).GT. DABS(3.D0*EE(IE)))EE(2)=3.D0*EE(I
     +E)
      EEE=E(2)+EE(2)
      IF(DABS(EEE-E(LOWEST)).LT.EP) GO TO 250
      IF(DABS(EEE-E(LOWEST)).LT..01D0*DABS(E(LOWEST))) GO TO 250
      IF(NTRIES.GT.MXTRIS)  WRITE(IO1,2012)
      IF(NTRIES.GT.MXTRIS)  GO TO 250
      IF(EE(IE).LT.EE(2))IE=IE+1
      IF(IE.EQ.4)GO TO 180
      DO 170 LL=IE,3
      L=3-LL+IE
      E(L+1)=E(L)
  170 F(L+1)=F(L)
  180 E(IE)=EEE
      DO 190 I=1,N
  190 X(I)=X0(I)+EEE*DEL(I)
      CALL EVAL(X,F(IE))
      IF    (IW.GT.1) WRITE(IO2,2004) F(IE)
      IF(IE.EQ.1)GO TO 150
```

```
      KKK=1
      IF(IE.EQ.4) GO TO 220
      IF(F(1).GT.F(4))GO TO 200
      CALL INTIPM(E,F,EE,A,0)
      IF(E(2)+EE(2).LT.E(4).AND. A.GT.0.D0)GO TO 160
      GO TO 210
  200 KKK=2
      CALL INTIPM(E,F,EE,A,1)
      IF(E(3)+EE(2).GT.E(1).AND. A.GT.0.D0)GO  TO 220
  210 KKK=1
      IF(F(2).LT.F(1).AND. F(2).LE.F(3).OR.F(2).LE.F(1).AND.F(2).LT. F(3
     1))GO TO 150
  220 DO 230 I=1,3
      E(I)=E(I+1)
  230 F(I)=F(I+1)
      GO TO (150,160),KKK
  250 IF    (IW.GT.0) WRITE(IU2,2005) F(LOWEST)
      NIT=NIT+1
C
C END   OF  MINIMIZATION  ALONG  DEL
C
C  IF THERE WAS NO MOTION  RETURN
C
      IF(E(LOWEST).NE.0.0) GO TO 260
      IF(.NOT.IDENT) WRITE(IU1,2007) ILIN,FOPT,GMAX,IGMAX,DELMAX,IDMAX,
     +E(LOWEST)
      IF(.NOT.IDENT) GO TO 20
      IERR = 2
      GO TO 500
  260 IF(F(LOWEST).NE.FO) GO TO 270
      IERR = 3
      GO TO 500
C
C     CHANGE E(LOWEST) IF NECESSARY SO AS NOT TO VIOLATE CONSTRAINTS
C
  270 IF(E(LOWEST).GE.0.D0) GO TO 271
      WRITE(IU1,2007)ILIN,FOPT,GMAX,IGMAX,DELMAX,IDMAX,E(LOWEST)
      IF(.NOT.IDENT) GO TO 20
      IERR=-1
      ITMAX=ILIN
      GO TO 650
  271 FO=F(LOWEST)
      DO 262 I=1,N
      XT=XO(I)+E(LOWEST)*DEL(I)
      TST(I)=0.D0
      IF(XT-X2(I).GT.X2ETA(I))   TST(I)=XT-X2(I)
      IF(XT-X1(I).LT.X1ETA(I))  TST(I)=X1(I)-XT
  262 CONTINUE
      CALL MX(N,TST,TSTMX,IMX)
      IF(TSTMX.EQ.0.D0) GO TO 272
      DELAM=TSTMX/DEL(IMX)
      E(LOWEST)=E(LOWEST)-DABS(DELAM)
  272 CONTINUE
      WRITE(IU1,2007)ILIN,FOPT,GMAX,IGMAX,DELMAX,IDMAX,E(LOWEST)
C
C     CHECK FOR CONVERGENCE AND CREATE A SUCTION ZONE NEAR CONSTRAINTS
C     OF THICKNESS X1(I)*PHI OR X2(I)*PHI
C
      IERR = 0
```

```
      ETEST=DABS(E(LOWEST))
      DO 280 I=1,N
      IR1=10
      IR2=10
      IR3=10
      IF(DABS(ETEST*DEL(I)).LE.DABS(EPS(I))) IR1=0
      IF(XO(I).EQ.X2(I).AND.DEL(I).GT.X2PHI(I))  IR2=0
      IF(XO(I).EQ.X1(I).AND.DEL(I).LT.X1PHI(I))  IR2=0
      IF(IR1.EQ.0.OR.IR2.EQ.0) IR3=0
      IF(IR3.NE.0) IERR=10
      X(I)=XO(I)+E(LOWEST)*DEL(I)
      IF(X(I)-X2(I).GT.X2PHI(I))  X(I)=X2(I)
      IF(X(I)-X1(I).LT.X1PHI(I))  X(I)=X1(I)
  280 CONTINUE
      CALL EVAL(X,FTST)
      IF(FTST.LE.FOPT.OR.NIT.GT.2) GO TO 274
      E(2)=E(LOWEST)
      F(1)=0.D0
      FO=FOPT
      F(1)=FOPT
      KKK=0
      GO TO 103
  274 CONTINUE
      DO 276 I=1,N
      DEL(I)=X(I)-XO(I)
      XO(I)=X(I)
  276 G1(I)=G(I)
      FO=FTST
      IF(IERR.EQ.0.AND.IDENT) GO TO 500
C
C     IF TOO MANY ITERATIONS RETURN
C
      IF   (IW.GT.0) WRITE(102,2006) ILIN
      ILIN=ILIN+1
      IERR = 4
      IF(ILIN.GT.ITMAX) GO TO 500
C
C     CALCULATE NEW GRADIENT
C
  281 IF   (IW.GT.2) WRITE(102,2001)
      DO 300 I=1,N
      X(I)=XO(I)
      IF(FO.EQ.0.D0)GO TO 285
      IF(G(I).EQ.0.D0) GO TO 285
      IF(IDENT) GO TO 285
      ETAM=DMAX1(ETA,DABS(FM*G(I)*XO(I)/FO))
      IF(G(I)**2.GT.C(I)*DABS(FO)*ETAM)GO TO 282
      DRV(I)=2.D0*(DABS(FO)*DABS(G(I) )*ETAM/C(I)**2)**.3333333333D0
      DRV(I)=DRV(I)*(1.D0-DABS(G(I))/(1.5D0*C(I)*DRV(I)+2.D0*DABS(G(I)))
     +)
      GO TO 283
  282 DRV(I)=2.D0*DSQRT(ETAM*DABS(FO)/C(I))
      DRV(I)=DRV(I)*(1.D0-C(I)*DRV(I)/(3.D0*C(I)*DRV(I)+4.D0*DABS(G(I)))
     +)
  283 DRV(I)=DSIGN(DRV(I),G(I))
      IF(.5D0*DABS(C(I)*DRV(I)/G(I)).GT..001D0)GO TO 295
  285 XO(I)=X(I)+DRV(I)
      CALL EVAL (XO,FG)
      IF   (IW.GT.2) WRITE(102,2000) FG,(XO(J),J=1,N)
```

```
  290 G(I)=(FG-FO)/DRV(I)
      GO TO 300
 295  DY=100.D0*DABS(FC*ETAM/G(I))
      DRV(I)=-DABS(G(I))+DSQRT(G(I)**2+200.D0*DABS(FO)*C(I)*ETAM)
      DRV(I)=DRV(I)/C(I)
      DRV(I)=DMIN1(DRV(I),DY)
      XO(I)=X(I)+DRV(I)
      CALL EVAL (XO,FP)
      IF   (IW.GT.2) WRITE(IU2,2000) FP,(XO(J),J=1,N)
      XO(I)=X(I)-DRV(I)
      CALL EVAL(XO,FMI)
      IF   (IW.GT.2) WRITE(IU2,2000) FMI,(XO(J),J=1,N)
      G(I)=.5D0*(FP-FMI)/ DRV(I)
  300 XO(I)=X(I)
C
C     IF ON CONSTRAINTS ,SET G(I)=0.D0
C
      DO 305 I=1,N
      IF(XO(I).EQ.X2(I).AND.G(I).LT.0.D0) G(I)=0.D0
      IF(XO(I).EQ.X1(I).AND.G(I).GT.0.D0) G(I)=0.D0
  305 CONTINUE
C
C     IF MIN ALONG  -DEL  SET H= C(INV)
C
  301 IF(E(LOWEST).LT.0.D0)GO TO 20
      IF(IERR.EQ.0) GO TO 20
C
C     MODIFY H AND REITERATE
C
      IDENT=.FALSE.
      A=0.D0
      DO 310 I=1,N
      Y(I)=G(I)-G1(I)
  310 A=A+Y(I)*DEL(I)
      IF   (IW.GT.0) WRITE(IU2,2002) (G(I),I=1,N)
      AA=A/E(LOWEST)
      C1=1.D0/A- D/AA**2
      C2=2.D0/AA
      B=0.D0
      DO 330 I=1,N
      C(I)=C(I)+C1*Y(I)**2 +C2*Y(I)*G1(I)
      X(I)=0.D0
      DO 320 J=1,N
  320 X(I)=X(I)+H(I,J)*Y(J)
  330 B=B-X(I)*Y(I)
      DO 340 I=1,N
      IF(C(I).LE.0.D0)GO TO 20
      DO 340 J=I,N
      H(I,J)=H(I,J)+DEL(I)*DEL(J)/A +X(I)*X(J)/B
  340 H(J,I)=H(I,J)
      GO TO 50
C
C     RETURN TO CALLING PROGRAM
C
  500 IF   (IW.GT.0) WRITE(IU2,2000) FO,(XO(J),J=1,N)
      ITMAX = ILIN
      IF(IERR.EQ.0.OR.IERR.EQ.4) GO TO 600
      IF(IERR-2)610,620,620
  600 ITERNS=ILIN
```

```
      IF(IERR.EQ.0) ITERNS=ILIN+1
      WRITE(IU1,2007)ITERNS,FU
      GO TO 650
  610 WRITE(IU1,2007)ILIN,FOPT,GMAX,IGMAX,DELMAX,IDMAX
      GO TO 650
  620 WRITE(IU1,2007)ILIN,FOPT,GMAX,IGMAX,DELMAX,IDMAX,F(LOWEST)
      ITERNS=ILIN+1
      WRITE(IU1,2007)ITERNS,F(LOWEST)
  650 PRINT 2011
      CALL XX2X(NV,N,GEX,G,NA)
      PRINT 2009,(GEX(J),J=1,NV)
      RETURN
      END
      SUBROUTINE INTIPM(E,F,EE,A,I)
      IMPLICIT REAL*8 (A-H,O-Z)
CCCCCCCCCCCCCCCCCCCCCCCCCCCCCCCCCCCCCCCCCCCCCCCCCCCCCCCCCCCCCCCCCCCCCCC
C                                                                     C
C     THIS SUBROUTINE FITS A PARABOLA THROUGH THREE DIFFERENT VALUES   C
C     OF THE FUNCTION F(THAT IS THROUGH F(I+1),F(I+1),F(I+3)) THE      C
C     ABSCISSAS OF WHICH ARE GIVEN BY E(I+1),E(I+2),E(I+3). IT THEN    C
C     PROCEEDS TO COMPUTE THE ABSCISSA EM CORRESPONDING TO THE MINIMUM C
C     VALUE OF THE FUNCTION F.                                         C
C                                                                     C
C     NOTE  -  A=COEFFICIENT OF HIGHEST POWER OF PARABOLA.             C
C              EE(2)=EM-E(2)                                           C
C                                                                     C
CCCCCCCCCCCCCCCCCCCCCCCCCCCCCCCCCCCCCCCCCCCCCCCCCCCCCCCCCCCCCCCCCCCCCCC
      DIMENSION E(1),F(1),EE(1)
      EE(3)= E(I+3)-E(I+2)
      EE(1)= E(I+1)-E(I+2)
      DF1=EE(1)*(F(I+3)-F(I+2))
      DF3=EE(3)*(F(I+1)-F(I+2))
      T=0.5D0*(EE(1)*DF1-EE(3)*DF3)
      ACURCY=1.D-09
      ERM=5.D-14
      ERE3=(DABS(E(I+3))+DABS(E(I+2)))*ERM
      ERE1=(DABS(E(I+1))+DABS(E(I+2)))*ERM
      ERF23=(DABS(F(I+3))+DABS(F(I+2)))*ACURCY
      ERF12=(DABS(F(I+1))+DABS(F(I+2)))*ACURCY
      IF(ERF23.LT.2.D0*ACURCY)  ERF23=2.D0*ACURCY
      IF(ERF12.LT.2.D0*ACURCY)  ERF12=2.D0*ACURCY
      ERDF1=ERE1*DABS(F(I+3)-F(I+2))+ERF23*DABS(EE(1))
      ERDF3=ERE3*DABS(F(I+1)-F(I+2))+ERF12*DABS(EE(3))
      ERDF1=ERDF1+ERE1*ERF23
      ERDF3=ERDF3+ERE3*ERF12
      ERB=ERDF1+ERDF3
      ERT=(ERE1*DABS(DF1)+ERDF1*DABS(EE(1))+ERE3*DABS(DF3)+ERDF3*DABS(EE
     +(3)))*0.5D0+DABS(T)*ERM
      ERT=ERT+0.5D0*(ERE1*ERDF1+ERE3*ERDF3)
      ERE13=DABS(EE(1))*ERE3+DABS(EE(3))*ERE1+ERE1*ERE3
      D=ERE13*DABS(EE(1)-EE(3))+DABS(EE(1)*EE(3))*(ERE1+ERE3)+ERE13*(ERE
     +1+ERE3)
      DA=EE(1)*EE(3)*(EE(1)-EE(3))
      D=10.D0*D
      B=10.D0*ERB
      C=10.D0*ERT
      IF(DABS(DF1-DF3).LE.B.OR.DABS(T).LE.C.OR.DABS(DA).LE.D)  GO TO 1
      EE(2)=T/(DF1-DF3)
      A=(DF3-DF1)/DA
```

```
      RETURN
    1 CONTINUE
      EE(2)=0.D0
      IF(F(I+3).LT.F(I+2)) EE(2)=EE(3)
      A=1.D0
      RETURN
      END
      SUBROUTINE  MX(NV,Y,YMAX,IMAX)
      IMPLICIT REAL*8 (A-H,O-Z)
CCCCCCCCCCCCCCCCCCCCCCCCCCCCCCCCCCCCCCCCCCCCCCCCCCCCCCCCCCCCCCCCCCCCCCC
C
C     SUBROUTINE WHICH DETERMINES THE MAXIMUM ABSOLUTE VALUE  AMONG
C     MEMBERS OF ARRAY Y (DENOTED AS YMAX),TOGETHER WITH THE MEMBER
C     LOCATION(DENOTED AS IMAX).
C
CCCCCCCCCCCCCCCCCCCCCCCCCCCCCCCCCCCCCCCCCCCCCCCCCCCCCCCCCCCCCCCCCCCCCCC
      DIMENSION  Y(1)
      YMAX=DABS(Y(1))
      IMAX=1
      IF(NV.EQ.1)  RETURN
      DO 100 I=2,NV
      IF(DABS(Y(I)).LE.YMAX) GO TO 100
      YMAX=DABS(Y(I))
      IMAX=I
  100 CONTINUE
      RETURN
C
C***********************************************************************
C*    END OF QUADRATIC CONVERGENCE PACKAGE(WITHOUT PENALTY FUNCTIONS).
C***********************************************************************
C
      END
      FUNCTION DREAL(Z)
C     THIS SUBROUTINE CAN BE USED WITH EITHER THE SLOW OR FAST,IBM,
C     DOUBLE PRECISION , COMPRESSIBLE AERODYNAMIC COEFFICIENTS PROGRAM .
      IMPLICIT REAL*8(D)
      REAL*8 Z(2)
      DREAL=Z(1)
      RETURN
      ENTRY DAIMAG(Z)
      DAIMAG=Z(2)
         RETURN
         END
      SUBROUTINE PROPOL(A,N,B,M,C,L)
      IMPLICIT  REAL*8(A-H,O-Z)
CCCCCCCCCCCCCCCCCCCCCCCCCCCCCCCCCCCCCCCCCCCCCCCCCCCCCCCCCCCCCCCCCCCCCCC
C
C     A ROUTINE FOR MULTIPLYING POLYNOMIALS  C=A*B  WHERE A,B,C  ARE
C     POLYNOMIALS OF THE FORM
C     A=A(1)+A(2)*X+A(3)*X**2+A(4)*X**3+..........A(N)*X**(N-1)
C     B=B(1)+B(2)*X+B(3)*X**2+B(4)*X**3+..........B(M)*X**(M-1)
C     C=C(1)+C(2)*X+C(3)*X**2+C(4)*X**3+.......C(N+M-1)*X**(N+M-2)
C     AND WHERE        L=N+M-1
C
CCCCCCCCCCCCCCCCCCCCCCCCCCCCCCCCCCCCCCCCCCCCCCCCCCCCCCCCCCCCCCCCCCCCCCC
      DIMENSION C(1),A(1),B(1)
      NM=N+M-1
      DO 1 I=1,NM
    1 C(I)=0.D0
```

```
      DO 2 I=1,N
      DO 2 J=1,M
    2 C(I+J-1)=A(I)*B(J)+C(I+J-1)
      L=NM
      RETURN
      END
      SUBROUTINE CXINVR(A,N,B,M,DET,IPIV,INDX,MAX,ISCALE)
CCCCCCCCCCCCCCCCCCCCCCCCCCCCCCCCCCCCCCCCCCCCCCCCCCCCCCCCCCCCCCCCCCCC
C
C     THIS SUBROUTINE IS IDENTICAL TO SUBROUTINE CXINV EXCEPT FOR
C     MINOR MODIFICATIONS THAT CAUSE IT TO BE FASTER(FOR EXAMPLE,
C     THE PIVOT IS DETERMINED BY AVOIDING THE USE OF CABS() BY USING
C     DABS(REAL)+DABS(IMAG)). FOR DETAILS REGARDING USAGE SEE
C     SUBROUTINE  CXINV.
C
CCCCCCCCCCCCCCCCCCCCCCCCCCCCCCCCCCCCCCCCCCCCCCCCCCCCCCCCCCCCCCCCCCCC
C
      IMPLICIT REAL*8(A-H,O-Z)
      COMPLEX*16 A(MAX,N),B(MAX,M),SWAP,DET,PIV,PIVI,C0,C1,PIVR
      DIMENSION IPIV(N), INDX(MAX,2)
C
C        CONSTANTS, INITIALIZATION
C
      C0=DCMPLX(0.0D0,0.0D0)
      C1=DCMPLX(1.0D0,0.0D0)
      DET = C1
      CADM=1.0D0
      DO 20 J=1,N
   20 IPIV(J) = 0
      DO 500 I=1,N
C
C        SEARCH FOR PIVOT ELEMENT
C
      CAVM=0.0D0
      DO 105 J=1,N
      IF (IPIV(J) .EQ. 1) GO TO 105
      DO 100 K=1,N
      IF (IPIV(K) - 1) 50,100,750
   50 CONTINUE
      DR=DREAL(A(J,K))
      DI=DAIMAG(A(J,K))
      CAVA=DABS(DR)+DABS(DI)
      IF (CAVM .GE. CAVA) GO TO 100
      IROW = J
      ICOL = K
      CAVM = CAVA
  100 CONTINUE
  105 CONTINUE
      IF(CAVM.EQ.0.0D0) GO TO 720
      IPIV(ICOL) = IPIV(ICOL) + 1
C
C        INTERCHANGE ROWS TO PUT PIVOT ELEMENT ON DIAGONAL
C
      IF (IROW .EQ. ICOL) GO TO 230
      DET = -DET
      DO 200 L=1,N
      SWAP = A(IROW,L)
      A(IROW,L) = A(ICOL,L)
      A(ICOL,L) = SWAP
```

```
  200 CONTINUE
      IF (M .LE. 0) GO TO 230
      DO 220 L=1,M
      SWAP = B(IROW,L)
      B(IROW,L) = B(ICOL,L)
      B(ICOL,L) = SWAP
  220 CONTINUE
  230 CONTINUE
      INDX(I,1) = IROW
      INDX(I,2) = ICOL
      PIV = A(ICOL,ICOL)
      CAPV=CDABS(PIV)
      IF(CAPV.EQ.0.0D0) GO TO 720
C
C        DIVIDE PIVOT ROW BY PIVOT ELEMENT
C
      A(ICOL,ICOL) = C1
      PIVR=1.D0/PIV
      DO 350 L=1,N
  350 A(ICOL,L) = A(ICOL,L)*PIVR
      IF (M .LE. 0) GO TO 380
      DO 370 L=1,M
  370 B(ICOL,L) = B(ICOL,L)*PIVR
C
C        REDUCE NON-PIVOT ROWS
C
  380 CONTINUE
      DO 500 L1=1,N
      IF (L1 .EQ. ICOL) GO TO 500
      SWAP = A(L1,ICOL)
      A(L1,ICOL) = C0
      DO 400 L=1,N
  400 A(L1,L) = A(L1,L) - A(ICOL,L)*SWAP
      IF (M .LE. 0) GO TO 500
      DO 450 L=1,M
  450 B(L1,L) = B(L1,L) - B(ICOL,L)*SWAP
  500 CONTINUE
C
C        INTERCHANGE COLUMNS
C
      DO 700 I=1,N
      L = N+1-I
      IF (INDX(L,1) .EQ. INDX(L,2))GO TO 700
      IROW = INDX(L,1)
      ICOL = INDX(L,2)
      DO 690 K=1,N
      SWAP = A(K,IROW)
      A(K,IROW) = A(K,ICOL)
      A(K,ICOL) = SWAP
  690 CONTINUE
  700 CONTINUE
      GO TO 750
  720 DET = C0
      ISCALE = 0
  750 RETURN
      END
C        SUBROUTINE MXINVR _ DOUBLE PRECISION
      SUBROUTINE  MXINVR(N,M,MAX,A)
C
```

```
C        REAL MATRIX INVERSION WITH SOLUTION OF LINEAR EQUATIONS
C
C        CAVM = DABS(A(MAX)),  CAVA = DABS(A(I,J))
C        CADM = DABS(DETERM),  CAPV = DABS(PIVOT)
C
      IMPLICIT REAL*8(A-H,O-Z)
      DIMENSION  A(MAX,1),B(150,1),IPIV(150),INDX(150,2)
      IF(M.NE.0)  GO  TO  1
      DO  2  I=1,N
    2 B(I,1)=0.D0
      GO  TO  10
    1 PRINT  1000
 1000 FORMAT('  NO SOLUTION  OF  LINEAR  EQUATIONS  IS  ALLOWED FOR  IN
     + THIS VERSION OF MXINVR')
      STOP
   10 CONTINUE
C
C        CONSTANTS, INITIALIZATION
C
      C0=0.D0
      C1=1.D0
      DET = C1
      CADM=1.0D0
      DO 20 J=1,N
   20 IPIV(J) = 0
      DO 500 I=1,N
C
C        SEARCH FOR PIVOT ELEMENT
C
      CAVM=0.0D0
      DO 105 J=1,N
      IF (IPIV(J) .EQ. 1) GO TO 105
      DO 100 K=1,N
      IF (IPIV(K) - 1) 50,100,750
   50 CONTINUE
      CAVA=DABS(A(J,K))
      IF (CAVM .GE. CAVA) GO TO 100
      IROW = J
      ICOL = K
      CAVM = CAVA
  100 CONTINUE
  105 CONTINUE
      IF(CAVM.EQ.0.0D0) GO TO 720
      IPIV(ICOL) = IPIV(ICOL) + 1
C
C        INTERCHANGE ROWS TO PUT PIVOT ELEMENT ON DIAGONAL
C
      IF (IROW .EQ. ICOL) GO TO 230
      DET = -DET
      DO 200 L=1,N
      SWAP = A(IROW,L)
      A(IROW,L) = A(ICOL,L)
      A(ICOL,L) = SWAP
  200 CONTINUE
      IF (M .LE. 0) GO TO 230
      DO 220 L=1,M
      SWAP = B(IROW,L)
      B(IROW,L) = B(ICOL,L)
      B(ICOL,L) = SWAP
```

```
  220 CONTINUE
  230 CONTINUE
      INDX(I,1) = IROW
      INDX(I,2) = ICOL
      PIV = A(ICOL,ICOL)
      CAPV=DABS(PIV)
      IF(CAPV.EQ.0.0D0) GO TO 720
C
C           DIVIDE PIVOT ROW BY PIVOT ELEMENT
C
      A(ICOL,ICOL) = C1
      PIVR=1.D0/PIV
      DO 350 L=1,N
  350 A(ICOL,L) = A(ICOL,L)*PIVR
      IF (M .LE. 0) GO TO 380
      DO 370 L=1,M
  370 B(ICOL,L) = B(ICOL,L)*PIVR
C
C           REDUCE NON-PIVOT ROWS
C
  380 CONTINUE
      DO 500 L1=1,N
      IF (L1 .EQ. ICOL) GO TO 500
      SWAP = A(L1,ICOL)
      A(L1,ICOL) = C0
      DO 400 L=1,N
  400 A(L1,L) = A(L1,L) - A(ICOL,L)*SWAP
      IF (M .LE. 0) GO TO 500
      DO 450 L=1,M
  450 B(L1,L) = B(L1,L) - B(ICOL,L)*SWAP
  500 CONTINUE
C
C           INTERCHANGE COLUMNS
C
      DO 700 I=1,N
      L = N+1-I
      IF (INDX(L,1) .EQ. INDX(L,2))GO TO 700
      IROW = INDX(L,1)
      ICOL = INDX(L,2)
      DO 690 K=1,N
      SWAP = A(K,IROW)
      A(K,IROW) = A(K,ICOL)
      A(K,ICOL) = SWAP
  690 CONTINUE
  700 CONTINUE
      GO TO 750
  720 DET = C0
      ISCALE = 0
  750 RETURN
      END
      SUBROUTINE  MXPROD(A,B,C,NIA,NIB,NJB,MAXA,MAXB,MAXC)
      REAL*8 A,B,C,D
      DIMENSION  A(MAXA,1),B(MAXB,1),C(MAXC,1),D(150)
      DO  100 I=1,NIA
      DO  200  J=1,NJB
      D(J)=0.D0
      DO  200  KK=1,NIB
      D(J)=D(J)+A(I,KK)*B(KK,J)
  200 CONTINUE
```

```
      DO  300  J=1,NJM
  300 C(I,J)=D(J)
  100 CONTINUE
      RETURN
      END
      SUBROUTINE  MXADD(A,B,C,NIA,NJ,MAXA,MAXB,MAXC)
      REAL*8  A,B,C
      DIMENSION  A(MAXA,1),B(MAXB,1),C(MAXC,1)
      DO  100 I=1,NIA
      DO  100 J=1,NJ
  100 C(I,J)=A(I,J)+B(I,J)
      RETURN
      END
      SUBROUTINE  MXSUB(A,B,C,NIA,NJ,MAXA,MAXB,MAXC)
      REAL*8  A,B,C
      DIMENSION  A(MAXA,1),B(MAXB,1),C(MAXC,1)
      DO  100 I=1,NIA
      DO  100 J=1,NJ
  100 C(I,J)=A(I,J)-B(I,J)
      RETURN
      END
      SUBROUTINE  MXSCAL(A,B,C,NIB,NJB,MAXA,MAXB,MAXC)
      REAL*8  A,B,C
      DIMENSION  B(MAXB,1),C(MAXC,1)
      DO  100 I=1,NIB
      DO  100 J=1,NJB
  100 C(I,J)=A*B(I,J)
      RETURN
      END
   END OF JOB.  CONDITION CODE WAS     0
```

```
DAST CONFIGURATION AT M=0.9,DATA FOR GUST OPT. CALCULATIONS.
&CASE
NM=          9,NC=          2,NAER=          0,R=  .10000000000000006     ,
  .19999999999999997     ,  .30000000000000003     ,  .39999999999999994     ,
NG=          1,NL=          4
&END
&GST
RMASS=  3.0196000000000007     ,  .0                      ,
  .0                     ,  .0                     ,  .0                     ,
  .0                     ,  .0                     ,  .0                     ,
  .0                     ,  .0                     ,  .0                     ,
  .0                     ,  .0                     ,  .0                     ,
  .0                     ,  .0                     ,  13595.000000000000     ,
  .0                     ,  .0                     ,  .0                     ,
  .0                     ,  .0                     ,  .0                     ,
  .0                     ,  .0                     ,  .0                     ,
  .0                     ,  .0                     ,  .0                     ,
  .0                     ,  .0                     ,  .0                     ,
  .20609999999999998D-01,  .0                     ,  .0                     ,
  .0                     ,  .0                     ,  .0                     ,
  .0                     ,  .0                     ,  .0                     ,
  .0                     ,  .0                     ,  .0                     ,
  .0                     ,  .0                     ,  .0                     ,
  .0                     ,  .33899999999999996D-01,  .0                     ,
  .0                     ,  .0                     ,  .0                     ,
  .0                     ,  .0                     ,  .0                     ,
  .0                     ,  .0                     ,  .0                     ,
  .0                     ,  .0                     ,  .0                     ,
  .0                     ,  .0                     ,  .54629999999999997D-01,
  .0                     ,  .0                     ,  .0                     ,
  .0                     ,  .0                     ,  .0                     ,
  .0                     ,  .0                     ,  .0                     ,
  .0                     ,  .0                     ,  .0                     ,
  .0                     ,  .0                     ,  .0                     ,
  .90800000000000040D-02,  .0                     ,  .0                     ,
  .0                     ,  .0                     ,  .0                     ,
  .0                     ,  .0                     ,  .0                     ,
  .0                     ,  .0                     ,  .0                     ,
  .0                     ,  .0                     ,  .0                     ,
  .0                     ,  .12049999999999999D-01,  .0                     ,
  .0                     ,  .0                     ,  .0                     ,
  .0                     ,  .0                     ,  .0                     ,
  .0                     ,  .0                     ,  .0                     ,
  .0                     ,  .0                     ,  .0                     ,
  .0                     ,  .0                     ,  .16309999999999998D-01,
  .0                     ,  .0                     ,  .0                     ,
  .0                     ,  .0                     ,  .0                     ,
  .0                     ,  .0                     ,  .0                     ,
  .0                     ,  .0                     ,  .0                     ,
  .0                     ,  .0                     ,  .0                     ,
  .15519999999999999D-01,  .0                     ,  .0                     ,
  .0                     ,  .0                     ,  .0                     ,
  .0                     ,  .0                     ,  .0                     ,
  .0                     ,  .0                     ,  .0                     ,
  .0                     ,  .0                     ,  .0                     ,
  .0                     ,  .0                     ,  .0                     ,
  .0                     ,  .0                     ,  .0                     ,
  .0                     ,  .0                     ,  .0                     ,
  .0                     ,  .0                     ,  .0                     ,
  .0                     ,  .0                     ,  .0                     ,
  .0                     ,  .0                     ,  .0                     ,
```

```
  .0                     ,  .0                     ,  .0                     ,
  .0                     ,  .0                     ,  .0                     ,
  .0                     ,  .0                     ,  .0                     ,
  .0                     ,  .0                     ,  .0                     ,
  .0                     ,  .0                     ,  .0                     ,
  .0                     ,  .0                     ,  .0                     ,
  .0                     ,  .0                     ,  .0                     ,
  .0                     ,  .0                     ,  .0                     ,
  .0                     ,  .0                     ,  .0                     ,
  .0                     ,  .0                     ,  .0                     ,
  .0                     ,  .0                     ,  .0                     ,
  .0                     ,  .0                     ,  .0                     ,
  .0                     ,  .0                     ,  .0                     ,
  .0                     ,  .0                     ,  .0                     ,
  .0                     ,  .0                     ,  .0                     ,
  .0                     ,  .0                     ,  .0                     ,
  .0                     ,  .0                     ,  .0                     ,
  .0                     ,  .0                     ,  .0                     ,
  .0                     ,  .0                     ,  .0                     ,
  .0                     ,  .0                     ,  .0                     ,
  .0                     ,  .0                     ,  .0                     ,
  .0                     ,OMEGAN=   .0                    ,
  .0                     ,  9.9410000000000006     ,  31.556999999999986     ,
  34.951000000000005     ,  50.254000000000013     ,  84.307999999999998     ,
  119.80999999999999     ,  127.95000000000000     ,  .0                     ,
  .0                     ,  .0                     ,  .0                     ,
  .0                     ,  .0                     ,VFL=
  11496.000000000000     ,BTRAN=  8.1970000000000006     ,
  8.1970000000000006     ,  .0                     ,  .0                     ,
  .0                     ,  .0                     ,CTRAN=
  6.5569999999999994     ,  6.5569999999999994     ,  .0                     ,
  .0                     ,  .0                     ,  .0                     ,
CREF=  13.542999999999999      ,ZW=  1.0000000000000000      ,
  1.0000000000000000     ,  1.0000000000000000     ,  1.0000000000000000     ,
  .0                     ,  .0                     ,  .0                     ,
  .0                     ,  .0                     ,  .0                     ,
  .0                     ,  .0                     ,  39.719999999999989     ,
  46.280000000000011     ,  39.719999999999989     ,  46.280000000000011     ,
  .0                     ,  .0                     ,  .0                     ,
  .0                     ,  .0                     ,  .0                     ,
  .0                     ,  .0                     ,  .63999999999999999     ,
  .74000000000000005     ,  .63999999999999999     ,  .74000000000000005     ,
  .0                     ,  .0                     ,  .0                     ,
  .0                     ,  .0                     ,  .0                     ,
  .0                     ,  .0                     , -.47999999999999996     ,
  .22999999999999996     , -.47999999999999996     ,  .22999999999999996     ,
  .0                     ,  .0                     ,  .0                     ,
  .0                     ,  .0                     ,  .0                     ,
  .0                     ,  .0                     , -.50999999999999995     ,
  .27999999999999999     , -.50999999999999995     ,  .27999999999999999     ,
  .0                     ,  .0                     ,  .0                     ,
  .0                     ,  .0                     ,  .0                     ,
  .0                     ,  .0                     , -.36000000000000001     ,
 -.45000000000000001D-01, -.36000000000000001     , -.45000000000000001D-01,
  .0                     ,  .0                     ,  .0                     ,
  .0                     ,  .0                     ,  .0                     ,
  .0                     ,  .0                     ,  .36000000000000001     ,
  .10000000000000006     ,  .36000000000000001     ,  .10000000000000006     ,
  .0                     ,  .0                     ,  .0                     ,
  .0                     ,  .0                     ,  .0                     ,
  .0                     ,  .0                     ,  .20000000000000004D-01,
```

```
 .25999999999999995     , .20000000000000004D-01, .25999999999999995     ,
 .0                     , .0                    , .0                     ,
 .0                     , .0                    , .0                     ,
 .0                     , .0                    , -.10000000000000002D-01,
-.22000000000000001     , -.10000000000000002D-01, -.22000000000000001   ,
 .0                     , .0                    , .0                     ,
 .0                     , .0                    , .0                     ,
 .0                     , .0                    , .0                     ,
 .0                     , .0                    , .0                     ,
 .0                     , .0                    , .0                     ,
 .0                     , .0                    , .0                     ,
 .0                     , .0                    , .0                     ,
 .0                     , .0                    , .0                     ,
 .0                     , .0                    , .0                     ,
 .0                     , .0                    , .0                     ,
 .0                     , .0                    , .0                     ,
 .0                     , .0                    , .0                     ,
 .0                     , .0                    , .0                     ,
 .0                     , .0                    , .0                     ,
 .0                     , .0                    , .0                     ,
 .0                     , .0                    , .0                     ,
 .0                     , .0                    , .0                     ,
 .0                     , .0                    , .0                     ,
 .0                     , .0                    , .0                     ,
 .0                     , .0                    , .0                     ,
 .0                     , .0                    , .0                     ,
 .0                     , .0                    , .0                     ,
 .0                     , .0                    , .0                     ,
 .0                     , .0                    , .0                     ,
 .0                     , .0                    , .0                     ,
 .0                     , .0                    ,ZREF=
 1.0000000000000000     , 1.0000000000000000    , -38.199999999999993    ,
-1.2299999999999998     , .0                    , .0                     ,
 .0                     , .0                    , .0                     ,
 .0                     , .0                    , .0                     ,
 .0                     , .0                    , .0                     ,
 .0                     , .0                    , .0                     ,
 .0                     , .0                    , .0                     ,
 .0                     , .0                    , .0                     ,
 .0                     , .0                    , .0                     ,
 .0                     , .0                    , .0                     ,
Q=   5.0000000000000000     ,CLR=   77.920000000000017      ,
 77.920000000000017     , .0                    , .0                     ,
 .0                     , .0                    ,CTR=
 36.969999999999989     ,WR=   100.00000000000000       ,NTF=          1,
          0,          0,          0,          0,          0,NCACT=          1
&END
&FT
NK=          10,AK=   .0                        ,  .50000000000000002D-01,
 .10000000000000006     , .19999999999999997    , .30000000000000003     ,
 .39999999999999994     , .50000000000000000    , .60000000000000006     ,
 .69999999999999997     , .80000000000000003    , .0                     ,
 .0                     , .0                    , .0                     ,
 .0                     , .0                    , .0                     ,
 .0                     , .0                    , .0                     ,
MAXNK=          20,NPRINT=          0,NPUNCH=          0,IRIGID=          2,
JRIGID=          1
&END
```

X1(I)	X(I)	X2(I)	EPS(I)
0.0	4.500000D+00	5.000000D+00	1.000000D-05
6.000000D+01	7.000000D+01	1.500000D+02	1.000000D-05
5.000000D-01	9.000000D-01	1.000000D+00	1.000000D-05
0.0	9.100000D-01	5.000000D+00	1.000000D-05
6.000000D+01	1.200000D+02	1.500000D+02	1.000000D-05
5.000000D-01	6.000000D-01	1.000000D+00	1.000000D-05
0.0	0.0	0.0	0.0
0.0	0.0	0.0	0.0
0.0	0.0	0.0	0.0
0.0	0.0	0.0	0.0
0.0	0.0	0.0	0.0
0.0	0.0	0.0	0.0

LENGTH= 3.000000D+04
NF= 30 FREGIN= 0.500000D+00 FEND= 0.400000D+02

,M=0.90

NV=12 NPR= 0 NDR= 1

ETA1= 5.000000D-13 PHI= 1.000000D-04

NONACT= 6 NVACT= 6

THE NON ACTIVE PARAMETERS NA(I)

7 8 9 10 11
12
WL= 1.000000D+00 WT= 1.000000D+00

INITIAL (INPUT) VECTOR DRV(I)

1.000000D-04	1.000000D-04	1.000000D-04	1.000000D-04
1.000000D-04	1.000000D-04	1.000000D-04	1.000000D-04
1.000000D-04	1.000000D-04	1.000000D-04	1.000000D-04

FMIN= 5.400000D+00 ETA= 1.000000D-09

ITMAX= 8 IW= 0

INITIAL GRADIENTS VECTOR G(I)

-0.762475D-01	0.245235D-01	0.564522D-01	0.670478D-01
0.680202D-03	-0.109930D+00	0.0	0.0
0.0	0.0	0.0	0.0

FINAL GRADIENTS VECTOR G(I)

0.125833D-01	0.228779D-01	-0.549770D+00	0.0
0.292766D-12	0.290509D-12	0.0	0.0
0.0	0.0	0.0	0.0

IERR= 4 ITERATIONS PERFORMED= 9

FUNCTN= 6.371400D+00

OPTIMUM VECTOR X(I)

5.000000D+00	6.000000D+01	6.845296D-01	0.0
1.199568D+02	1.000000D+00	0.0	0.0

0.0 0.0 0.0 0.0

XF(I)	DEFLN(I).......		PSD(I)
3.141593D+00	1.288464D-03	0.0	4.036342D-02
1.141445D+01	1.158425D-01	0.0	4.753116D-03
1.968731D+01	2.516282D-01	0.0	1.917301D-03
2.796017D+01	5.537789D-01	0.0	1.068650D-03
3.623304D+01	6.160991D-01	0.0	6.938318D-04
4.450590D+01	5.347993D-01	0.0	4.925075D-04
5.277876D+01	4.888817D-01	0.0	3.706958D-04
6.105162D+01	4.728004D-01	0.0	2.908210D-04
6.932448D+01	4.767706D-01	0.0	2.353133D-04
7.759734D+01	4.969049D-01	0.0	1.950061D-04
8.587020D+01	5.316543D-01	0.0	1.647114D-04
9.414306D+01	5.771354D-01	0.0	1.413021D-04
1.024159D+02	6.178831D-01	0.0	1.227960D-04
1.106888D+02	6.185298D-01	0.0	1.078842D-04
1.189616D+02	5.527550D-01	0.0	9.567233D-05
1.272345D+02	4.488124D-01	0.0	8.553100D-05
1.355074D+02	3.499800D-01	0.0	7.700648D-05
1.437802D+02	2.721794D-01	0.0	6.976439D-05
1.520531D+02	2.140977D-01	0.0	6.355367D-05
1.603259D+02	1.707177D-01	0.0	5.818261D-05
1.685988D+02	1.376706D-01	0.0	5.350269D-05
1.768717D+02	1.118057D-01	0.0	4.939725D-05
1.851445D+02	9.090681D-02	0.0	4.577362D-05
1.934174D+02	7.329973D-02	0.0	4.255733D-05
2.016902D+02	5.738629D-02	0.0	3.968796D-05
2.099631D+02	6.030754D-02	0.0	3.711608D-05
2.182360D+02	5.602714D-02	0.0	3.480086D-05
2.265088D+02	3.98792[illegible]D-02	0.0	3.270835D-05
2.347817D+02	3.24335[illegible]D-02	0.0	3.081013D-05
2.430546D+02	3.021280D-02	0.0	2.908223D-05
2.513274D+02	3.310507D-02	0.0	2.750433D-05

DRMS(I)= 1.084848D-01 0.0

XF(I)	DEFLNR(I).......		PSD(I)
3.141593D+00	4.047829D-03	0.0	4.036342D-02
1.141445D+01	1.322278D+00	0.0	4.753116D-03
1.968731D+01	4.953883D+00	0.0	1.917301D-03
2.796017D+01	1.548375D+01	0.0	1.068650D-03
3.623304D+01	2.232314D+01	0.0	6.938318D-04
4.450590D+01	2.380172D+01	0.0	4.925075D-04
5.277876D+01	2.580257D+01	0.0	3.706958D-04
6.105162D+01	2.886523D+01	0.0	2.908210D-04
6.932448D+01	3.305188D+01	0.0	2.353133D-04
7.759734D+01	3.855850D+01	0.0	1.950061D-04
8.587020D+01	4.565326D+01	0.0	1.647114D-04
9.414306D+01	5.433330D+01	0.0	1.413021D-04
1.024159D+02	6.328107D+01	0.0	1.227960D-04
1.106888D+02	6.846431D+01	0.0	1.078842D-04
1.189616D+02	6.575664D+01	0.0	9.567233D-05
1.272345D+02	5.710443D+01	0.0	8.553100D-05

1.355074D+02	4.742486D+01	0.0	7.700648D-05
1.437802D+02	3.913402D+01	0.0	6.976439D-05
1.520531D+02	3.255422D+01	0.0	6.355367D-05
1.603259D+02	2.737047D+01	0.0	5.818261D-05
1.685988D+02	2.321110D+01	0.0	5.350269D-05
1.768717D+02	1.977527D+01	0.0	4.939725D-05
1.851445D+02	1.683090D+01	0.0	4.577362D-05
1.934174D+02	1.417744D+01	0.0	4.255733D-05
2.016902D+02	1.157425D+01	0.0	3.968796D-05
2.099631D+02	1.266236D+01	0.0	3.711608D-05
2.182360D+02	1.222714D+01	0.0	3.480086D-05
2.265088D+02	9.033005D+00	0.0	3.270835D-05
2.347817D+02	7.614798D+00	0.0	3.081013D-05
2.430546D+02	7.343357D+00	0.0	2.908223D-05
2.513274D+02	8.320211D+00	0.0	2.750433D-05

DRRMS(I)= 6.371400D+00 0.0

XF(I)	DEFLN2(I).......		PSD(I)
3.141593D+00	6.700890D-08	0.0	4.036342D-02
1.141445D+01	6.378432D-05	0.0	4.753116D-03
1.968731D+01	1.213973D-04	0.0	1.917301D-03
2.796017D+01	3.277239D-04	0.0	1.068650D-03
3.623304D+01	2.633634D-04	0.0	6.938318D-04
4.450590D+01	1.408622D-04	0.0	4.925075D-04
5.277876D+01	8.859827D-05	0.0	3.706958D-04
6.105162D+01	6.501018D-05	0.0	2.908210D-04
6.932448D+01	5.348912D-05	0.0	2.353133D-04
7.759734D+01	4.814983D-05	0.0	1.950061D-04
8.587020D+01	4.655672D-05	0.0	1.647114D-04
9.414306D+01	4.706565D-05	0.0	1.413021D-04
1.024159D+02	4.688100D-05	0.0	1.227960D-04
1.106888D+02	4.127425D-05	0.0	1.078842D-04
1.189616D+02	2.923154D-05	0.0	9.567233D-05
1.272345D+02	1.722873D-05	0.0	8.553100D-05
1.355074D+02	9.432214D-06	0.0	7.700648D-05
1.437802D+02	5.168260D-06	0.0	6.976439D-05
1.520531D+02	2.913162D-06	0.0	6.355367D-05
1.603259D+02	1.695705D-06	0.0	5.818261D-05
1.685988D+02	1.014047D-06	0.0	5.350269D-05
1.768717D+02	6.174916D-07	0.0	4.939725D-05
1.851445D+02	3.782754D-07	0.0	4.577362D-05
1.934174D+02	2.286541D-07	0.0	4.255733D-05
2.016902D+02	1.306999D-07	0.0	3.968796D-05
2.099631D+02	1.349912D-07	0.0	3.711608D-05
2.182360D+02	1.092413D-07	0.0	3.480086D-05
2.265088D+02	5.201792D-08	0.0	3.270835D-05
2.347817D+02	3.241022D-08	0.0	3.081013D-05
2.430546D+02	2.654664D-08	0.0	2.908223D-05
2.513274D+02	3.014324D-08	0.0	2.750433D-05

DRMS(I)= 1.084848D-01 0.0

XF(I)	DEFLNR2(I).......		PSD(I)
3.141593D+00	6.613514D-07	0.0	4.036342D-02

1.141445D+01	8.310443D-03	0.0	4.783116D-03
1.968731D+01	4.705241D-02	0.0	1.917301D-03
2.796017D+01	2.562052D-01	0.0	1.068650D-03
3.623304D+01	3.457521D-01	0.0	6.938318D-04
4.450590D+01	2.790163D-01	0.0	4.925075D-04
5.277876D+01	2.467991D-01	0.0	3.706958D-04
6.105162D+01	2.423124D-01	0.0	2.908210D-04
6.932448D+01	2.570625D-01	0.0	2.353133D-04
7.759734D+01	2.899269D-01	0.0	1.950061D-04
8.587020D+01	3.432949D-01	0.0	1.647114D-04
9.414306D+01	4.171388D-01	0.0	1.413021D-04
1.024159D+02	4.917358D-01	0.0	1.227960D-04
1.106888D+02	5.056924D-01	0.0	1.078842D-04
1.189616D+02	4.136810D-01	0.0	9.567233D-05
1.272345D+02	2.789094D-01	0.0	8.553100D-05
1.355074D+02	1.731966D-01	0.0	7.700648D-05
1.437802D+02	1.068422D-01	0.0	6.976439D-05
1.520531D+02	6.735272D-02	0.0	6.355367D-05
1.603259D+02	4.358708D-02	0.0	5.818261D-05
1.685988D+02	2.882484D-02	0.0	5.350269D-05
1.768717D+02	1.931735D-02	0.0	4.939725D-05
1.851445D+02	1.296671D-02	0.0	4.577362D-05
1.934174D+02	8.554017D-03	0.0	4.255733D-05
2.016902D+02	5.316734D-03	0.0	3.968796D-05
2.099631D+02	5.951019D-03	0.0	3.711608D-05
2.182360D+02	5.202829D-03	0.0	3.480086D-05
2.265088D+02	2.668844D-03	0.0	3.270835D-05
2.347817D+02	1.786530D-03	0.0	3.081013D-05
2.430546D+02	1.568257D-03	0.0	2.908223D-05
2.513274D+02	1.904012D-03	0.0	2.750433D-05

DRRMS(I)= 6.371400D+00 0.0

ITERNS	FOPT	GMAX	IGMX	DELMAX	IDMX	F(LOWEST)
1	6.636445D+00	1.099297D-01	6	1.099297D-01	6	2.097215D+00
2	6.608625D+00	2.473027D-01	3	9.769578D-02	6	1.734505D+00
3	6.580560D+00	1.422296D-01	3	1.539202D-01	1	1.479236D+00
4	6.554190D+00	3.780755D-02	4	1.493344D-01	4	3.022319D+00
5	6.537558D+00	1.579243D-01	3	2.471685D-02	3	3.195800D+00
6	6.531153D+00	4.176370D-02	4	6.229736D-02	4	2.492477D-01
7	6.530286D+00	2.344989D-02	2	2.577852D-02	2	1.705048D+02
8	6.471205D+00	5.497702D-01	3	3.352684D-02	2	1.390840D+02
9	6.371400D+00					

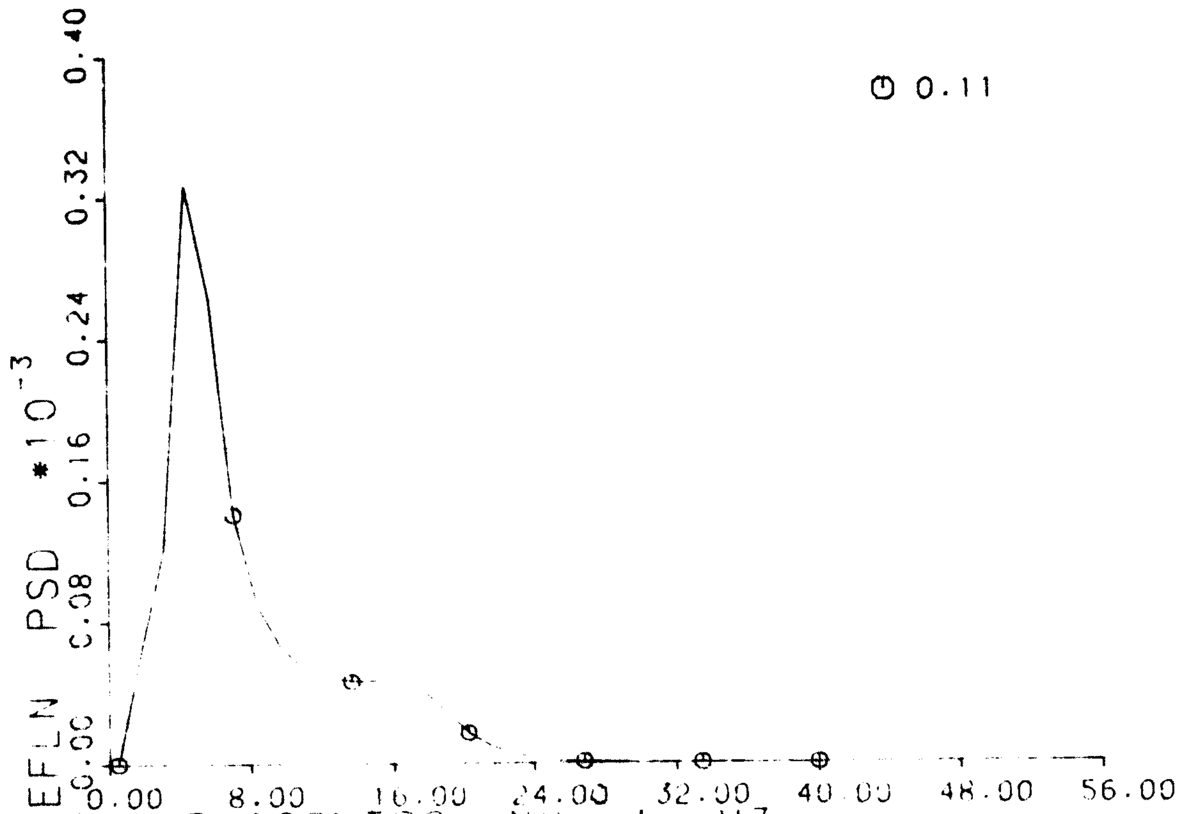

DAST,M=0.900= 5.0CONTROL NO. 1 HZ

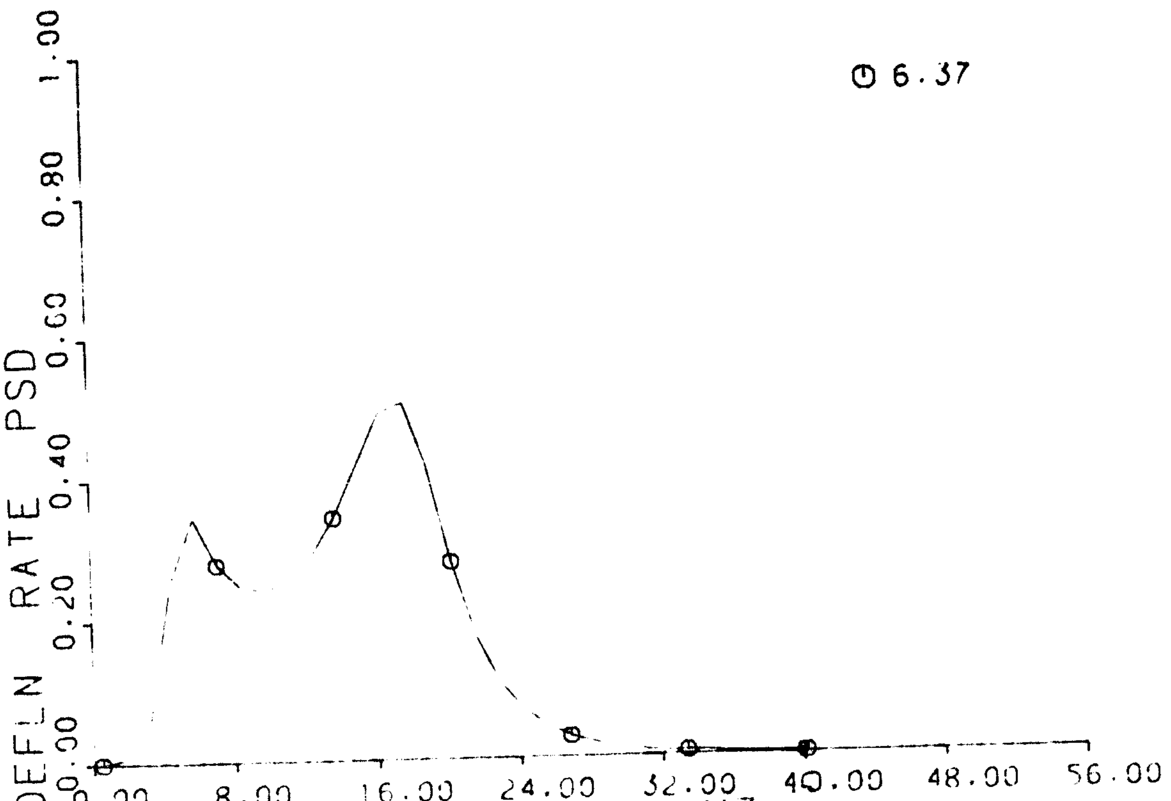

DAST, M=0.900= 5.0CONTROL NO. 1 HZ

APPENDIX G

INPUT/OUTPUT EXAMPLE FOR GUST SENSITIVITY PROGRAM

The source listing of the program is identical to that of the gust optimization program. The operating instructions given in Appendix B indicate which cards need be deleted or replaced together with the required changes in the data.

The example chosen relates to the same DAST configuration (M=0.9) chosen for the gust optimization example. All the data required (except for the aerodynamic coefficients which are identical to the ones used in the previous examples) appears in the output. The control law used is based on the L.D.T.T.F. and it employs only three control variables. The sensitivity of these 3 variables is tested herein. Note that the array NA(I) involves 9 control variables.

The variation of DRMS(I) (= $\delta_{i,rms}$) and DRRMS(I) (= $\delta_{i,rms}$) with the control variables is printed in the output and is supplemented by plots illustrating this variation.

It is important to note the following points:

1) Reference to X(I) in the plotted output implies reference to the active X(I) array.

2) In studying the sensitivity of the resonse to the various control parameters, one should remember the constraints imposed on the control variables during optimization. This is important since a control variable lying on a constraint will not necessarily exhibit a minimum type variation during the sensitivity studies.

Note that all the control deflections are given in degrees per unit gust velocity. The plotted output shows labels which appear to be displaced. These displacements reflect transient difficulties encountered using a new plotter and they do not originate from the programs used.

```
DAST CONFIGURATION AT M=0.9,DATA FOR GUST SENS CALCULATIONS.
&CASE
NM=          9,NC=          2,NAER=          0,B= .10000000000000006    ,
  .19999999999999997    , .30000000000000003    , .39999999999999994    ,
NG=          1,NL=          4
&END
&GST
RMASS=  3.0195000000000007    , .0                   ,
  .0                    , .0                    , .0                    ,
  .0                    , .0                    , .0                    ,
  .0                    , .0                    , .0                    ,
  .0                    , .0                    , .0                    ,
  .0                    , .0                    , 13695.000000000000    ,
  .0                    , .0                    , .0                    ,
  .0                    , .0                    , .0                    ,
  .0                    , .0                    , .0                    ,
  .0                    , .0                    , .0                    ,
  .0                    , .0                    , .0                    ,
  .20605999999999998D-01, .0                    , .0                    ,
  .0                    , .0                    , .0                    ,
  .0                    , .0                    , .0                    ,
  .0                    , .0                    , .0                    ,
  .0                    , .0                    , .0                    ,
  .0                    , .33895999999999996D-01, .0                    ,
  .0                    , .0                    , .0                    ,
  .0                    , .0                    , .0                    ,
  .0                    , .0                    , .0                    ,
  .0                    , .0                    , .0                    ,
  .0                    , .0                    , .54629999999999997D-01,
  .0                    , .0                    , .0                    ,
  .0                    , .0                    , .0                    ,
  .0                    , .0                    , .0                    ,
  .0                    , .0                    , .0                    ,
  .0                    , .0                    , .0                    ,
  .90800000000000040D-02, .0                    , .0                    ,
  .0                    , .0                    , .0                    ,
  .0                    , .0                    , .0                    ,
  .0                    , .0                    , .0                    ,
  .0                    , .0                    , .0                    ,
  .0                    , .12049999999999999D-01, .0                    ,
  .0                    , .0                    , .0                    ,
  .0                    , .0                    , .0                    ,
  .0                    , .0                    , .0                    ,
  .0                    , .0                    , .0                    ,
  .0                    , .0                    , .16309999999999998D-01,
  .0                    , .0                    , .0                    ,
  .0                    , .0                    , .0                    ,
  .0                    , .0                    , .0                    ,
  .0                    , .0                    , .0                    ,
  .0                    , .0                    , .0                    ,
  .15519999999999999D-01, .0                    , .0                    ,
  .0                    , .0                    , .0                    ,
  .0                    , .0                    , .0                    ,
  .0                    , .0                    , .0                    ,
  .0                    , .0                    , .0                    ,
  .0                    , .0                    , .0                    ,
  .0                    , .0                    , .0                    ,
  .0                    , .0                    , .0                    ,
  .0                    , .0                    , .0                    ,
  .0                    , .0                    , .0                    ,
  .0                    , .0                    , .0                    ,
```

```
 .0                       ,  .0                       ,  .0                       ,
 .0                       ,  .0                       ,  .0                       ,
 .0                       ,  .0                       ,  .0                       ,
 .0                       ,  .0                       ,  .0                       ,
 .0                       ,  .0                       ,  .0                       ,
 .0                       ,  .0                       ,  .0                       ,
 .0                       ,  .0                       ,  .0                       ,
 .0                       ,  .0                       ,  .0                       ,
 .0                       ,  .0                       ,  .0                       ,
 .0                       ,  .0                       ,  .0                       ,
 .0                       ,  .0                       ,  .0                       ,
 .0                       ,  .0                       ,  .0                       ,
 .0                       ,  .0                       ,  .0                       ,
 .0                       ,  .0                       ,  .0                       ,
 .0                       ,  .0                       ,  .0                       ,
 .0                       ,  .0                       ,  .0                       ,
 .0                       ,  .0                       ,  .0                       ,
 .0                       ,  .0                       ,  .0                       ,
 .0                       ,  .0                       ,  .0                       ,
 .0                       ,  .0                       ,  .0                       ,
 .0                       ,  .0                       ,  .0                       ,
 .0                       ,OMEGAN=  .0                   ,
 .0                       ,  9.5410000000000006       ,  31.556999999999986       ,
 34.981000000000006       ,  50.254000000000013       ,  84.307999999999998       ,
 119.80999999999999       ,  127.98000000000000       ,  .0                       ,
 .0                       ,  .0                       ,  .0                       ,
 .0                       ,  .0                       ,VEL=
 11496.000000000000       ,BTRAN=  8.1970000000000006     ,
 8.1970000000000006       ,  .0                       ,  .0                       ,
 .0                       ,  .0                       ,CTRAN=
 6.5565999999999994       ,  6.5565999999999994       ,  .0                       ,
 .0                       ,  .0                       ,  .0                       ,
CREF=  13.542999999999999     ,ZW=  1.0000000000000000     ,
 1.0000000000000000       ,  1.0000000000000000       ,  1.0000000000000000       ,
 .0                       ,  .0                       ,  .0                       ,
 .0                       ,  .0                       ,  .0                       ,
 .0                       ,  .0                       ,  39.719999999999989       ,
 46.280000000000011       ,  39.719999999999989       ,  46.280000000000011       ,
 .0                       ,  .0                       ,  .0                       ,
 .0                       ,  .0                       ,  .0                       ,
 .0                       ,  .0                       ,  .63999999999999999       ,
 .74000000000000005       ,  .63999999999999999       ,  .74000000000000005       ,
 .0                       ,  .0                       ,  .0                       ,
 .0                       ,  .0                       ,  .0                       ,
 .0                       ,  .0                       , -.47999999999999996       ,
 .22999999999999996       , -.47999999999999996       ,  .22999999999999996       ,
 .0                       ,  .0                       ,  .0                       ,
 .0                       ,  .0                       ,  .0                       ,
 .0                       ,  .0                       , -.50999999999999995       ,
 .27999999999999999       , -.50999999999999995       ,  .27999999999999999       ,
 .0                       ,  .0                       ,  .0                       ,
 .0                       ,  .0                       ,  .0                       ,
 .0                       ,  .0                       , -.36000000000000001       ,
-.45000000000000001D-01, -.36000000000000001       , -.45000000000000001D-01,
 .0                       ,  .0                       ,  .0                       ,
 .0                       ,  .0                       ,  .0                       ,
 .0                       ,  .0                       ,  .36000000000000001       ,
 .10000000000000006       ,  .36000000000000001       ,  .10000000000000006       ,
 .0                       ,  .0                       ,  .0                       ,
 .0                       ,  .0                       ,  .0                       ,
 .0                       ,  .0                       ,  .20000000000000004D-01,
```

```
 .25999999999999998      , .20000000000000004D-01, .25999999999999995    ,
 .0                      , .0                    , .0                    ,
 .0                      , .0                    , .0                    ,
 .0                      , .0                    , -.10000000000000002D-01,
-.22000000000000001      , -.10000000000000002D-01, -.22000000000000001  ,
 .0                      , .0                    , .0                    ,
 .0                      , .0                    , .0                    ,
 .0                      , .0                    , .0                    ,
 .0                      , .0                    , .0                    ,
 .0                      , .0                    , .0                    ,
 .0                      , .0                    , .0                    ,
 .0                      , .0                    , .0                    ,
 .0                      , .0                    , .0                    ,
 .0                      , .0                    , .0                    ,
 .0                      , .0                    , .0                    ,
 .0                      , .0                    , .0                    ,
 .0                      , .0                    , .0                    ,
 .0                      , .0                    , .0                    ,
 .0                      , .0                    , .0                    ,
 .0                      , .0                    , .0                    ,
 .0                      , .0                    , .0                    ,
 .0                      , .0                    , .0                    ,
 .0                      , .0                    , .0                    ,
 .0                      , .0                    , .0                    ,
 .0                      , .0                    , .0                    ,
 .0                      , .0                    , .0                    ,
 .0                      , .0                    , .0                    ,
 .0                      , .0                    , .0                    ,
 .0                      , .0                    , .0                    ,
 .0                      , .0                    , .0                    ,
 .0                      , .0                    , .0                    ,
 .0                      , .0                    ,ZREF=
 1.0000000000000000      , 1.0000000000000000    , -38.199999999999993   ,
-1.2299999999999998      , .0                    , .0                    ,
 .0                      , .0                    , .0                    ,
 .0                      , .0                    , .0                    ,
 .0                      , .0                    , .0                    ,
 .0                      , .0                    , .0                    ,
 .0                      , .0                    , .0                    ,
 .0                      , .0                    , .0                    ,
 .0                      , .0                    , .0                    ,
 .0                      , .0                    , .0                    ,
Q=  5.0000000000000000     ,CLA=  77.920000000000017    ,
 77.920000000000017      , .0                    , .0                    ,
 .0                      , .0                    ,CIR=
 36.569999999999989      ,WR=  100.00000000000000     ,NTE=         1,
        0,          0,          0,          0,          0,NCACT=          1
&END
&FI
NK=         10,AK=  .0                           ,  .50000000000000002D-01,
 .10000000000000006      , .15999999999999997    , .30000000000000003    ,
 .39999999999999994      , .50000000000000000    , .60000000000000006    ,
 .69999999999999997      , .80000000000000003    , .0                    ,
 .0                      , .0                    , .0                    ,
 .0                      , .0                    , .0                    ,
 .0                      , .0                    , .0                    ,
MAXNK=         20,NPRINT=          0,NPUNCH=          0,IRIGID=          2,
JRIGID=         1
&END
```

```
     X1(I)            X(I)             X2(I)            EPS(I)

  3.000000D+00     5.000000D+00     6.000000D+00     5.000000D-01
  5.000000D+01     6.000000D+01     7.000000D+01     5.000000D+00
  7.000000D-01     9.000000D-01     1.000000D+00     5.000000D-02
  0.0              0.0              0.0              0.0
  6.000000D+01     1.200000D+02     1.500000D+02     1.000000D-05
  5.000000D-01     6.000000D-01     1.000000D+00     1.000000D-05
  0.0              0.0              0.0              0.0
  0.0              0.0              0.0              0.0
  0.0              0.0              0.0              0.0
  0.0              0.0              0.0              0.0
  0.0              0.0              0.0              0.0
  0.0              0.0              0.0              0.0
  LENGTH= 3.000000D+04
 NF= 30 FBEGIN= 0.500000D+00 FEND= 0.400000D+02

.M=0.90


 NV=12  NFF= 0  NDF= 1

 ETA1= 5.000000D-13 PHI= 1.000000D-04

 NCNACT= 9 NVACT= 3

 THE NON ACTIVE PARAMETERS NA(I)

    4     5     6     7     8
    9    10    11    12
  WL= 1.000000D+00   WT= 1.000000D+00

  INITIAL (INPUT) VECTOR DRV(I)

  1.000000D-04   1.000000D-04   1.000000D-04   1.000000D-04
  1.000000D-04   1.000000D-04   1.000000D-04   1.000000D-04
  1.000000D-04   1.000000D-04   1.000000D-04   1.000000D-04

 FMIN= 5.400000D+00 ETA= 1.000000D-09

 ITMAX=  8 IW= 0

VAR.X( 1).CAST M=0.90DYN.PRESS=  5.0
  0.300000E+01   0.350000E+01   0.400000E+01   0.450000E+01
  0.500000E+01   0.550000E+01   0.600000E+01
DRMS(I)  FSD
  0.810798E-01   0.849950E-01   0.891183E-01   0.932783E-01
  0.974055E-01   0.101469E+00   0.105451E+00
VAR.X( 1).CAST M=0.90DYN.PRESS=  5.0
  0.300000E+01   0.350000E+01   0.400000E+01   0.450000E+01
  0.500000E+01   0.550000E+01   0.600000E+01
DRRMS(I) FSD
  0.653673E+01   0.642680E+01   0.636840E+01   0.633686E+01
  0.632062E+01   0.631363E+01   0.631239E+01
VAR.X( 2).CAST M=0.90DYN.PRESS=  5.0
  0.500000E+02   0.550000E+02   0.600000E+02   0.650000E+02
  0.700000E+02
DRMS(I)  FSD
  0.102940E+00   0.997592E-01   0.974055E-01   0.956903E-01
  0.944999E-01
```

```
VAR.X( 2).DAST M=0.90DYN.PRESS=   5.0
  0.500000E+02   0.550000E+02   0.600000E+02   0.650000E+02
  0.700000E+02
DRRMS(1) FSD
  0.613022E+01   0.622211E+01   0.632062E+01   0.642682E+01
  0.654043E+01
VAR.X( 3).DAST M=0.90DYN.PRESS=   5.0
  0.750000E+00   0.800000E+00   0.850000E+00   0.900000E+00
  0.950000E+00   0.100000E+01
DRRMS(1)  FSD
  0.104474E+00   0.101834E+00   0.994928E-01   0.974055E-01
  0.958358E-01   0.938838E-01
```

```
VAR.X( 3).DAST M=0.90DYN.PRESS=   5.0
  0.750000E+00   0.800000E+00   0.850000E+00   0.900000E+00
  0.950000E+00   0.100000E+01
DRRMS(1) FSD
  0.634409E+01   0.633059E+01   0.632344E+01   0.632062E+01
  0.632194E+01   0.632689E+01
    IERR= 0  ITERATIONS PERFORMED=  8


 OPTIMUM  VECTOR  X(I)

  8.000000D+00   6.000000D+01   9.000000D-01   0.0
  1.200000D+02   6.000000D-01   0.0            0.0
  0.0            0.0            0.0            0.0
```

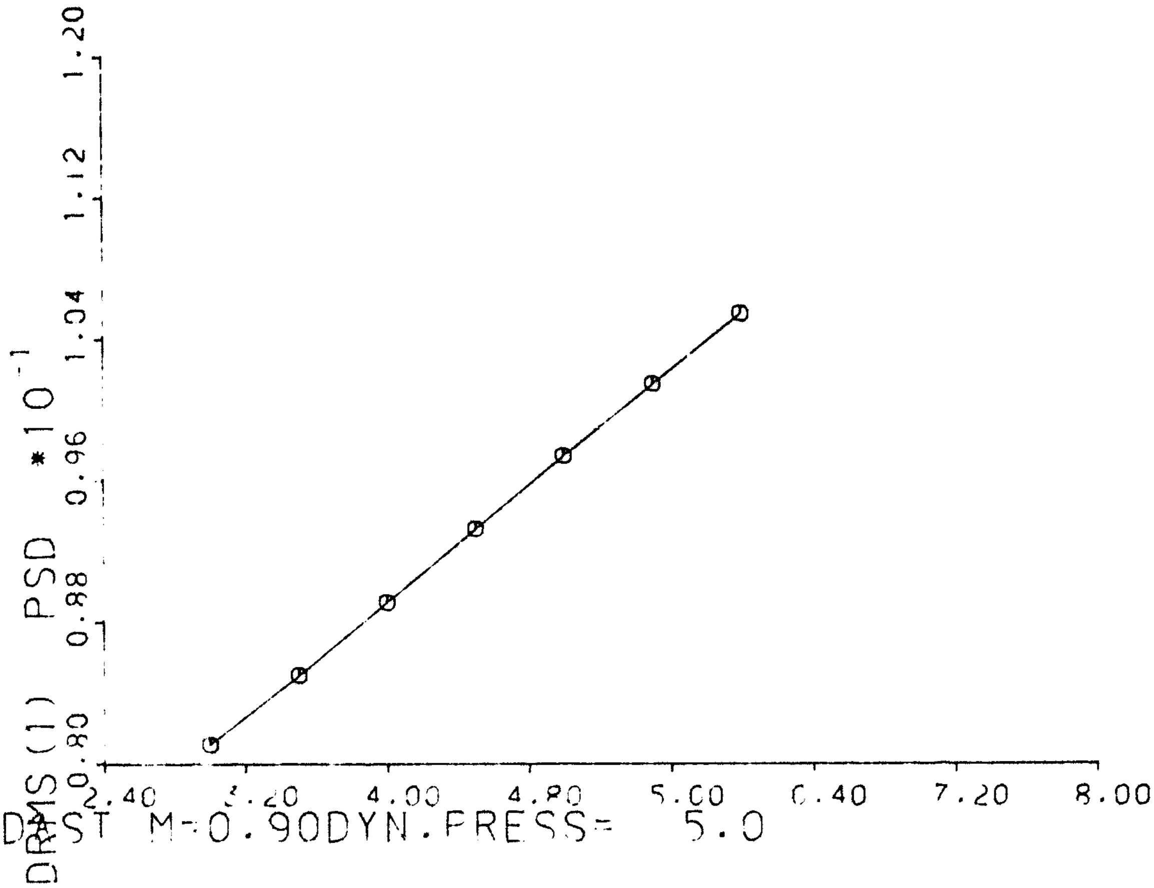

AR.X(1).DAST M=0.90DYN.PRESS= 5.0

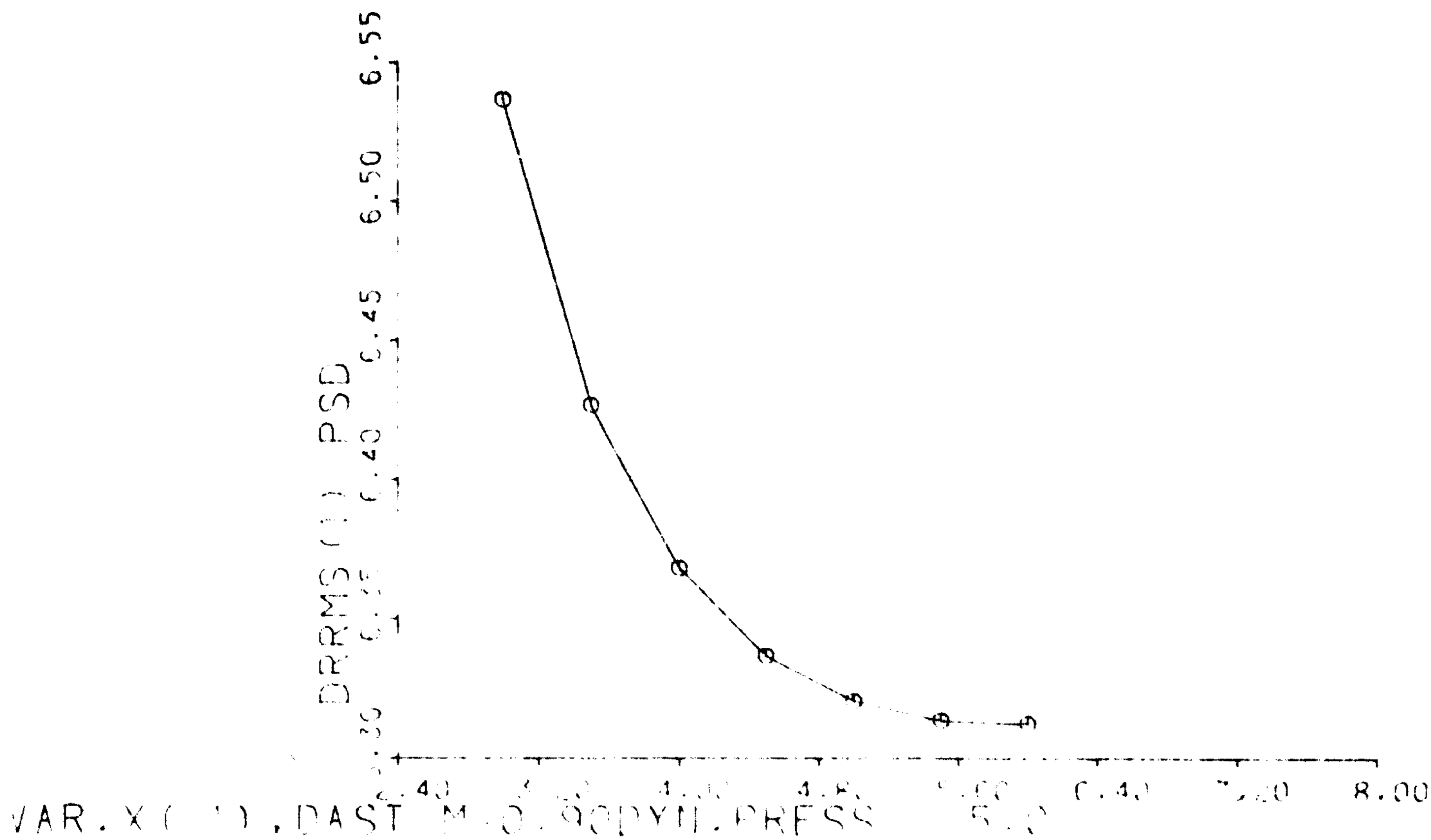
6.55
6.50
8.00

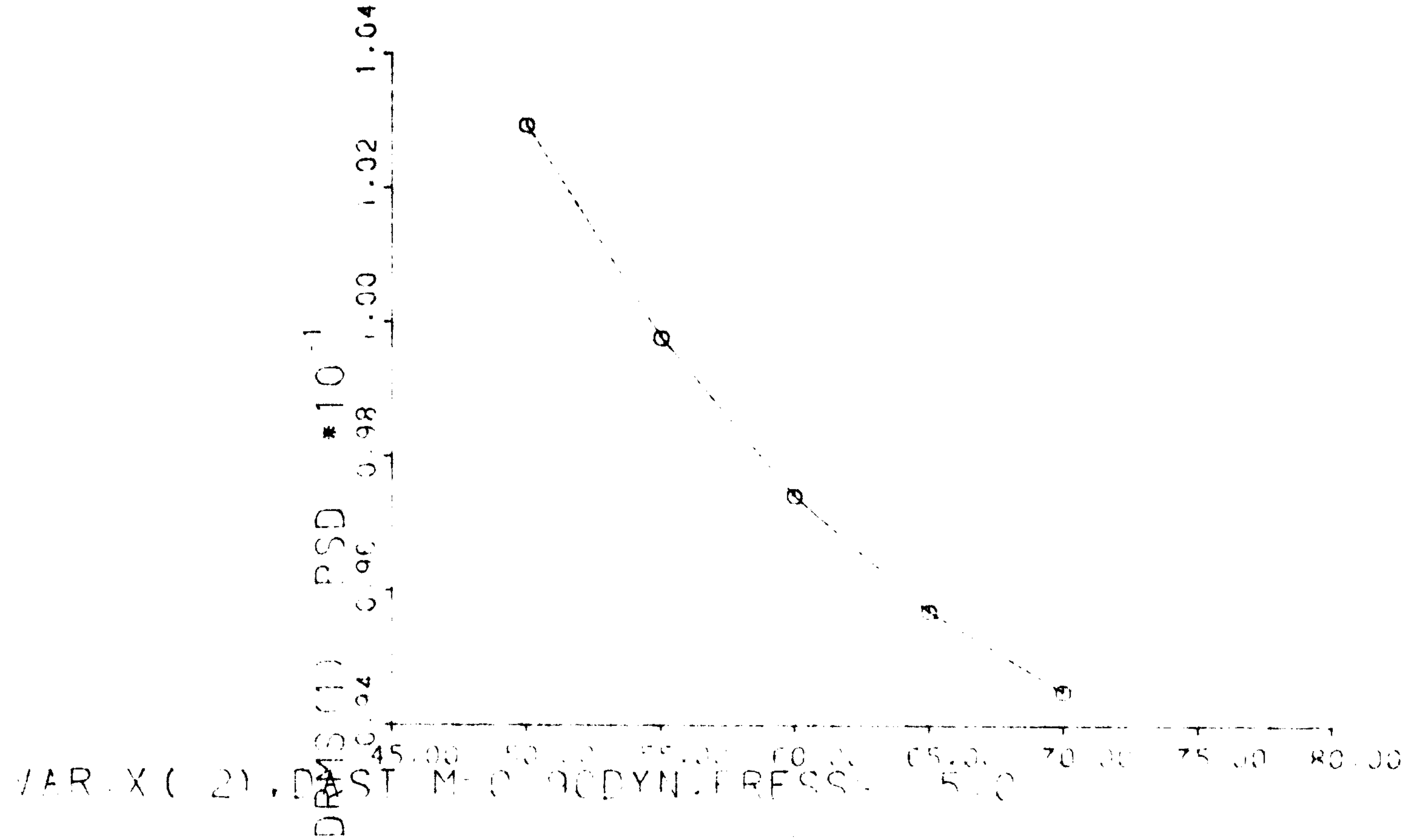
1.04
1.02
1.00
0.98
0.96
0.94
45.00
70.00
80.00
DRMS (1) RSD *10^{-1}
VAR X(2),DAST M-0.90DYN.PRESS.

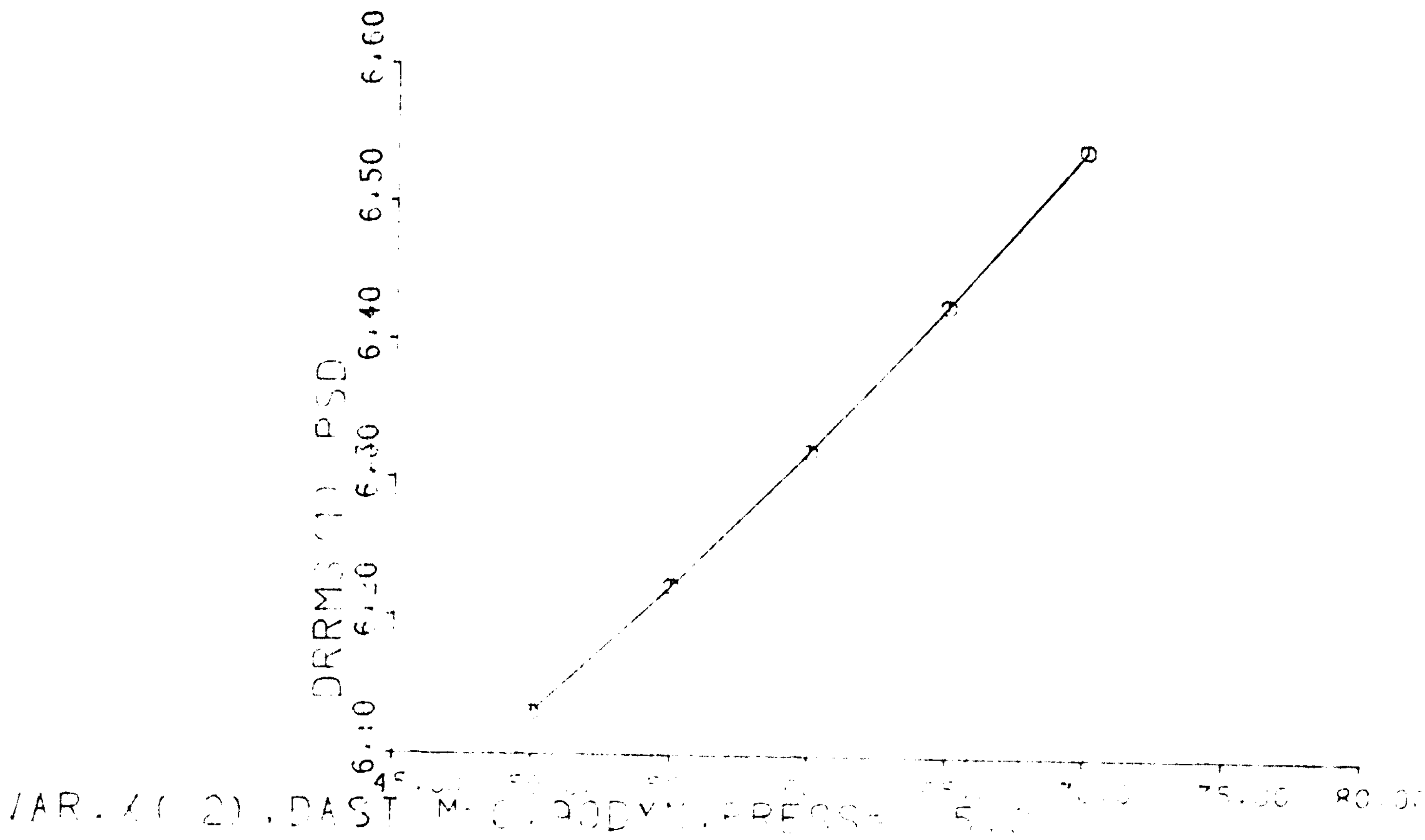
6.60
6.50
6.40
6.30

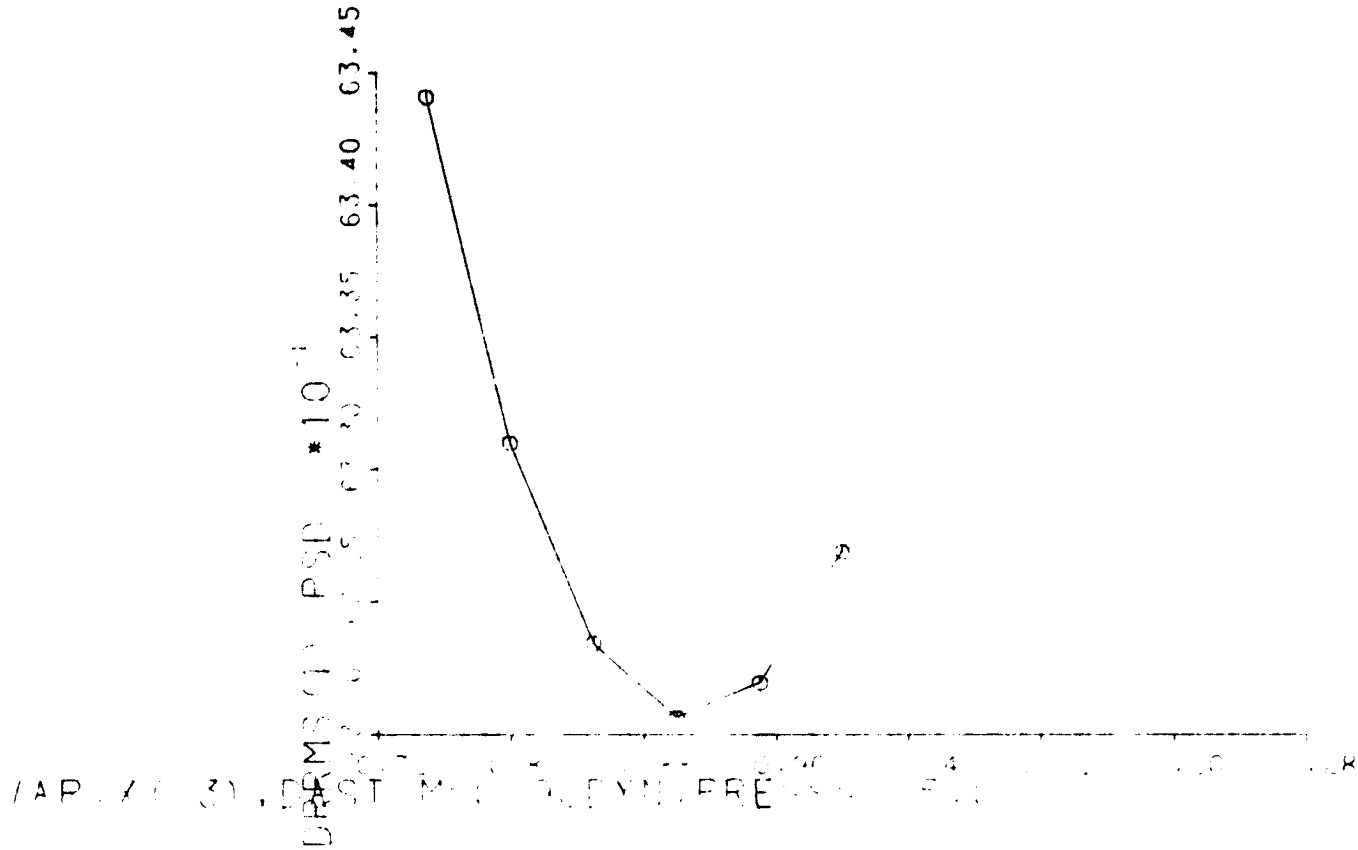
63.45
63.40